University of Strathclyde

Department of Chemical and Process Engineering

Development of Improved Aircraft De-Icing Fluids

By

Yuchen Wang

A thesis presented in fulfilment of the requirements

for the degree of Doctor of Philosophy

May 2013

Declaration of Authenticity

This thesis is the result of the author's original research. It has been composed by the author and has not been previously submitted for examination which has led to the award of a degree.

Signed:

Date:

Acknowledgements

I wish to thank Kilfrost Limited (Newcastle Upon Tyne, UK) and its staff, and Department of Chemical and Process Engineering of University of Strathclyde (Glasgow, UK), particularly in providing the necessary financial and technical support for this research.

This thesis would not have been possible without the support of the people around me.

First and foremost, I would like to express my sincerest gratitude to my primary supervisor, Prof Carl Schaschke, who gave me the opportunity to carry out this study and has supported me throughout my stay in the UK, with great patience and motivation. I would like to thank my second supervisor, Dr Nicholas Hudson, for his enthusiasm and immense knowledge in rheology. His guidance has been invaluable to me in the research and writing this thesis.

I am extremely grateful to Prof Richard Pethrick for his help and support in all the time of the research. I would not have been able to write this thesis without his advice and unsurpassed knowledge in polymer science.

I would like to thank the staff and my fellow postgraduate students in the Department of Chemical and Process Engineering and the Department of Pure and Applied Chemistry.

My sincere gratitude also goes to my friends in Glasgow and in China for their support and encouragement. I am most grateful to Dr Yin Deqiang for the motivation and inspiration he has offered to me.

Above all, I would like to thank my parents, Mr Wang Shaoguo and Ms Wang Xia, for their unequivocal support, for which my mere expression of thanks does not suffice.

For any errors or inadequacies that may remain in this work, I assume full responsibility.

Glossary

Term	Definition	Unit
A	Area	m^2
a	Tube diameter	m
b	Monomer length	m
c	Polymer concentration	g dL^{-1}
c_r	Scaling factor of Rouse motion	—
c_t	Threshold concentration	g dL^{-1}
F	Applied force	N
h_1	Degree of complexation	—
i	Degree of ionization	—
K	Mark-Houwink coefficient	mL g^{-1}
k	Boltzmann constant	m^2 kg s^{-2}
K_1	Equilibrium constant	—
l_k	Kuhn segment length	m
l_p	Persistence length	m
M	Molar mass	kg mol^{-1}
M_c	Critical molar mass of entanglement	kg mol^{-1}
M_d	Molar mass of a rigid entity formed by entanglement segments	kg mol^{-1}
M_k	Molar mass of a Kuhn unit	kg mol^{-1}
Mw	Molecular weight	MDa
N	Total mode number within a polymer chain	—
N_c	Number of entanglement units within a molecule	—
N_d	Number of the rigid units formed along a molecule	—
N_e	Number of segments between entanglement points	—
P	Pressure	Pa
p	Mode number	—

R	Universal gas constant	J mol^{-1} K^{-1}
t	Flow time	s
T	Temperature	K or °C
u	Velocity	m s^{-1}
z_1	Scaling factor of 'slip-coil' motion	—
z_2	Scaling factor of reptation motion	—
α	Mark-Houwink coefficient	—
γ	Shear rate	s^{-1}
δ	Phase lag	—
δ^*	Boundary layer displacement thickness	mm
ΔG	Change of energy of the system	J mol^{-1}
ΔS	Change of entropy	J mol^{-1} K^{-1}
ζ	Bead friction coefficient of Rouse motion	s m^{-1} mol^{-1}
η	Viscosity	Pa s
η_0	Zero shear rate viscosity of solution	Pa s
η_{rel}	Relative viscosity	—
η_s	Solvent viscosity	Pa s
η_{sp}	Specific viscosity	—
η^*	Complex viscosity	Pa s
μ	Dynamic viscosity	Pa s
ρ	Density	kg m^{-3}
σ	Standard deviation	—
τ	Shear stress	Pa
τ_b	Reptation motion relaxation time	s
τ_d	Terminal relaxation time	s
τ_r	Rouse relaxation time	s
ω	Frequency	rad s^{-1}

Abstract

In this study the potential of utilizing poly(acrylic acid) (PAA) and polyvinylpyrrolidone (PVP) blends as improved thickening agents of aircraft de-/anti-icing fluids is investigated. Current fluid thickeners commonly comprise PAA homo- or co-polymers and two examples are investigated in terms of their structure, characteristics, size and the rheological profile as aqueous and solutions in a typical glycol based deicing fluid. The rheological properties of these polymer thickeners are found to be sensitive to composition, electrolyte concentration, and pH as well as temperature. The rheological and aerodynamic performances of thickened water/glycol mixtures were evaluated under the conditions typically experienced by de-icing fluids. A model is also developed to simulate the rheological behaviour of the polymer solutions. The model involves consideration of reptation, relaxation of the chains by slippage or loop relaxation, and normal Rouse dynamics is appropriately adapted to reflect the structural changes of the polymer molecules and the consequent pseudoplastic behaviour. The model has helped with development of an understanding of the way in which these polymer systems create the rheological characteristics which are necessary for the action of the fluids in protecting the aircraft during the period it is at the stand and also in the initial stages of taxiing and take-off. For the purpose of developing improved thickening materials with proper de-icing ability and reduced gel formation tendency, various PVP-PAA blends are formulated and rheologically examined together with wind tunnel testing. The gels have a tendency to form insoluble deposits which are capable of jamming the ailerons and flaps during flight. The influences of multiple mono- and di-valent cations, with which de-icing fluids are commonly diluted was investigated. The PVP-PAA blends achieve the characteristic rheological properties through a different set of interactions from those of pure PAA and are shown to be less sensitive to electrolyte effects. This study has identified a new potential de-icing fluid system.

Contents

Chapter 1. Literature Survey

1.1. Ground Application of Aircraft De-Icing

Ice is a major challenge to all aircraft operations, particularly during winter conditions. In fact, all forms of aqueous condensate, including ice, snow, and frost, adhering to aircraft control surfaces, wings, or propellers, are considered adverse to safe flights. Aircraft are designed on the basis of low drag coefficients for wings and ailerons and ice destroys the smooth air flows across the aerodynamically critical surfaces of an airplane (Figure 1.1), increases drag while decreasing the ability of aerofoil to create lift [1]. Ice contamination on the surface of an aircraft is the beginning of a vicious circle. When a certain amount of ice is deposited on those critical surfaces, extra power is needed to provide additional speed and the airplane is forced to adopt an increased attack angle to gain the additional lift required for take-off. Adopting the higher attack angle exposes the underside of the wings and fuselage to more ice. Furthermore, the accumulation of ice goes far beyond the wings, ailerons or propellers. It can build on the surfaces of vents, intakes, landing gears or even antenna where no heat will reach, causing aircraft to stall at a much-higher-than-normal speed and lower angles of attack. All these factors will severely compromise the flight, causing airplane to roll or pitch uncontrollably, and make it difficult to recover. Therefore the ground application of de-icing on an aircraft becomes an obvious requirement, especially in Northern Hemisphere, during the most severe winter flight operations.

The process of ground de-icing operation is typically performed after loading of the plane. At many airports the aircraft may be moved to a specially designed site where the de-/anti-icing fluids are applied to its levelled surfaces to remove ice structures until the pilot perceives no sign of ice on the wings [2]. Such an operation is commonly required when active frost is forming when the surface temperature of the aeroplane is at or below 0°C and the dew point. In certain circumstances, due to the “cold-soaked” effect which

refers to the condition when the wings are loaded with very cold fuel, clear icing may occur even the ambient temperature is between -2°C and +15°C [3]. Other icing conditions include freezing drizzle, freezing fog, hail, ice pellets, slush, rime ice, and snow.

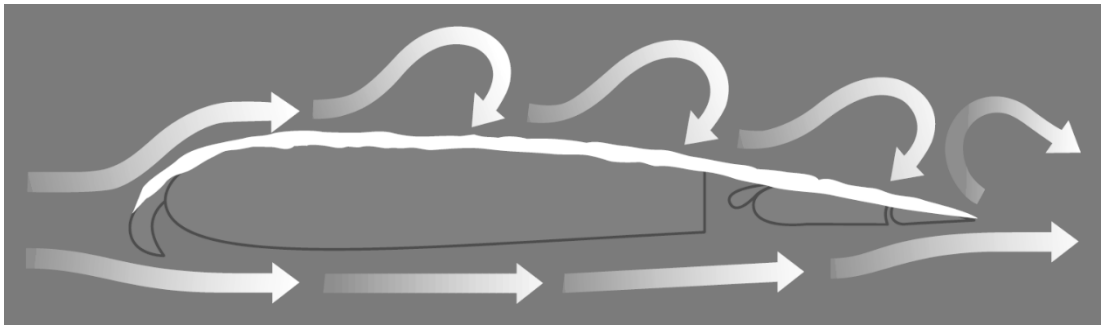

Figure 1.1 Effect of frost, ice, or snow on wing surface airflow [4].

1.2. De-/Anti-Icing Fluids

The invention of de-/anti-icing fluids for aircraft can be dated well back to the mid-20th century [5, 6]. The fluids typically are composed of water blended with ethylene glycol or propylene glycol and the ratio of the mixtures can range from 50:50 to 20:80 wt/wt%. Other additives may include corrosion inhibitors, surfactants, pH regulators and coloured, UV sensitive dyes. When the fluids are applied to ice, they effectively reduce the melting point of ice and remove frost, snow, or ice attached to aircraft surfaces. Meanwhile the fluids form a layer coating on the surfaces to provide protection against further ice accumulation until take-off [7-9], serving the purpose of anti-icing.

The Society of Automotive Engineers published standards which has classified de-icing or anti-icing fluids into four types [10, 11]. Type I fluids have a low viscosity and are generally considered unthickened. They are normally composed of 20:80 wt/wt water/glycol mixtures and are applied hot (55-80°C) at high pressure to remove ice which has accumulated on the aircraft surfaces while the aircraft is on the ground [12, 13]. However, the period of time for which ice formation is prevented (commonly referred as “hold-over time”) is relatively short, approximately 3 minutes in freezing rain

and 20 minutes in frost-forming conditions. They mainly prevent refreezing when no precipitation occurs [2, 8, 11, 14]. They are usually dyed in orange to aid in identification and application.

In cases which require a longer protection time such as high humidity or long standby, a two-step de-icing process is often used which involves the initial use of a type I fluid followed by application of other types of fluids. Thickened de-icing or anti-icing fluids, which have a typical blending ratio of 50:50 water/glycol, are generally classified as Type II or Type IV fluids. Such fluids contain polymeric thickening agents to achieve longer periods of time for protection against ice formation [9, 15, 16]. The thickened fluid is typically applied on the aircraft surfaces after ice has been removed, hence allowing further ice build-up to occur on the film coating and not on the aircraft surfaces. The coating layer should be efficiently removed during take-off as the air flow is increased across the wings. The difference between Type II and Type IV fluids lies mainly in the amount of time provided for protection against frost, snow, or ice building up on the surfaces of aircraft. This term of protection time is commonly referred as "hold-over time". Type II fluids typically provide 30 minutes of hold-over time while Type IV fluids usually have a guideline of 80 minutes[3, 17]. Colour-wise, Type II fluids are generally dyed light yellow while Type IV fluids are typically green.

Type III fluids were originally developed for slower, usually commuter, airplanes as a compromise between Type I and Type II fluids and the major target of such type of fluids is business and regional aviation market. They are also dyed light yellow in general.

For general application of de-/anti-icing fluids, Type I fluids are recommended for operation from the freezing point of the fluid plus 10°C and Type II, III and IV fluids plus 7°C [3]. Changes in the ratio of the glycol to water mix allow the operational temperature to be progressively lowered. The de-icing fluids will usually be applied hot and precautions have to be taken to avoid water loss [18-20]. Whilst ethylene glycol in principal has the right physical characteristics for use as in de-icing fluids, it is however

potentially harmful to humans and animals and has significant influences on the environment. Propylene glycol has lower toxicity and is usually used as a base for most formulations [21-27]. Aqueous mixtures of propylene glycol containing 60% glycol have a melting point of -60°C. However at the lowest temperatures its viscosity is too high and it may not be usable. Below -32°C ethylene glycol is still usually used, however the use of 1,3-propylene glycol as a more environmentally acceptable fluid has been proposed [20]. Choice of fluid type depends on the hold-over time which can depend on operating conditions. Whilst de-icing will mainly involve the upper areas of the wing and fuselage, de-icing under wings areas and in particular flaps may be necessary.

The production of de-/anti-icing fluids must meet standard requirements which includes appropriate compositions of glycol-water mixture to meet the freeing point requirements, neutral pH, and rheological properties. The usual quality controls are the refractive indices, pH values, and viscosities under specific conditions [28-32].

The simple mixtures of glycol and water form the basis of type I fluids but are not easily retained on the aircraft surface and hence only provide protection for short periods of time. To achieve longer hold-over times Type II, III and IV fluids have a higher viscosity to develop a stable fluid layer on the surface to be protected. However during the initial stages of take-off this thin surface layer should be rapidly depleted and ideally be completely removed prior to rotation. The performances of hold-over time and the "removability" of de-/anti-icing fluids can be evaluated in a laboratory environment by standard ISO tests [10, 11, 33-35] which include, namely, a Wet Spray Endurance Test (WSET) and a Boundary Layer Displacement Thickness (BLDT) measurement. The test methods have been developed and refined over the years by the eminent works of several research groups [36-45] and will be elaborated in the following chapter. The two properties; WSET and BLDT are critical to the safe flight operation and are closely associated with several factors which include density, surface tension, and most importantly, the viscosity of the fluids.

1.3. Shear-Thinning Fluids and Polymer Thickeners

1.3.1. Viscosity and Types of Fluids

"Fluid" is a term used to define a substance which continuously flows under an applied shear stress. Viscosity is a measure of resistance to flow of a fluid and commonly described as its "thickness" or "internal friction". Generally, in any flow, layers move at different velocities and the viscosity of fluid arises from shear stress between the layers (Figure 1.2) assuming the shear stress (τ) at the stationary boundary is zero. The applied forces, *F*, is proportional to the area (A) and velocity gradient (u/y) in the fluid.

$$F = \mu A \frac{u}{y} \tag{1.1}$$

where μ is the dynamic viscosity, which is the tangential force per unit area required to move one horizontal layer with respect to the other at unit velocity when maintained a unit distance apart by the fluid, and u is the velocity.

The above equation can be expressed in terms of shear stress,

$$\tau = \frac{F}{A} \tag{1.2}$$

If equation (1.2) is expressed in differential form for a straight, parallel and uniform flow, the shear stress between layers is proportional to the velocity gradient in the direction perpendicular to the layers.

$$\tau = \mu \frac{\partial u}{\partial y} \tag{1.3}$$

This equation is usually expressed in the following form,

$$\tau = \eta \dot{\gamma} \tag{1.4}$$

where $\dot{\gamma}$ is shear rate (velocity gradient), and η is the coefficient of shear viscosity, commonly referred to as viscosity.

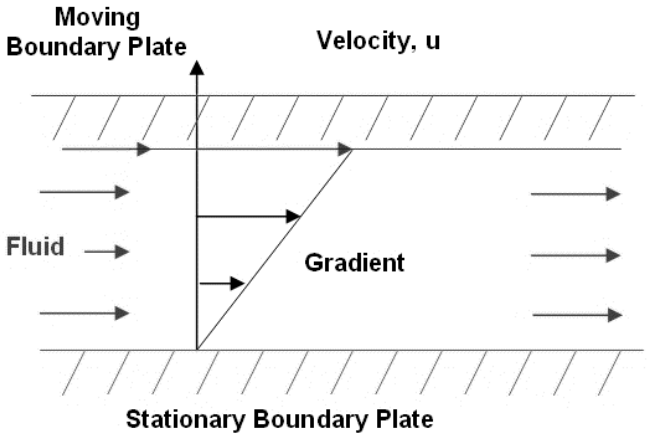

Figure 1.2 Schematic plot of laminar shear of fluid between two plates.

Newton's law of viscosity (equation 1.3) only applies to some materials. Depending on the relationship between shear stress and the shear rate, fluids are generally characterizing in two categories:

- Newtonian fluids (named after Isaac Newton), where shear rate is linearly proportional to the shear stress;
- Non-Newtonian fluids, where shear rate is not directly proportional to the shear stress.

For Non-Newtonian fluids, the relationship between shear stress and shear rate (also its derivatives) in more complicated. If the viscosity of the fluid does not depend on the period of time during which the material is being sheared, such fluids can be characterized as one of the following:

- Bingham plastic (named after Eugene C. Bingham) is a kind of material that does not flow under shear stress until a certain value is reached commonly referred as "yield stress". Beyond this point the shear stress increases linearly with shear rate in the same way as Newtonian fluids [46]. Typical examples include toothpaste and mayonnaise.
- Shear-thinning fluid (also known as "pseudoplastic fluid") is a kind of material whose viscosity decreases with increasing shear stress. Shear thinning property

is often found in molten polymers, polymer solutions and other materials, such as lava, tomato ketchup and blood, of which the microstructures within are randomly distributed before external shear is applied and are forced to align more tidily resulting in a decreasing internal resistance to flow [47-49]. Shear thinning can commonly be observed in polymer systems as a consequence of the shear rate exceeding the time required for the polymer to respond to the external forces; this will be explained further in the section of thixotropy.

- Shear-thickening fluid (also known as "dilatant fluid") is a kind of material whose viscosity increases with increasing shear stress. Corn-starch and water mixture is a typical sample of such fluid of which shear thickening behaviour occurs when a colloidal suspension is agitated causing its stable state transiting to a state of flocculation [50, 51]. Typically fluids which are aligned as a consequence of shear and exhibit a larger hydrodynamic volume or adopt an extended more ordered structure shear thicken.

A schematic plot of the relationships between shear stress and shear rate for the above non-Newtonian fluids (in comparison with Newtonian fluid) is shown in Figure 1.3. However, the viscosity of the fluid can be time-dependent, in which case the fluids will also have the following properties:

- Thixotropy is a property of a shear thinning fluid whose viscosity will further decrease when shaken, agitated, or otherwise stressed over time. This is due to the microstructural elements within the fluid taking a finite time to rearrange their alignments and therefore the fluid reaching an equilibrium viscosity [52].

- Anti-thixotropy (or rheopexy), compared to thixotropy, is a rare property of a non-Newtonian fluid which shows a time-dependent increase in viscosity with agitation over time or with cumulative shear stress. A rheopectic fluid, such as certain lubricants, becomes more viscous (or even solidified) when shaken over time which, similarly to shear-thickening fluids, corresponds to the result of

increase in interlayer friction of the material [53, 54].

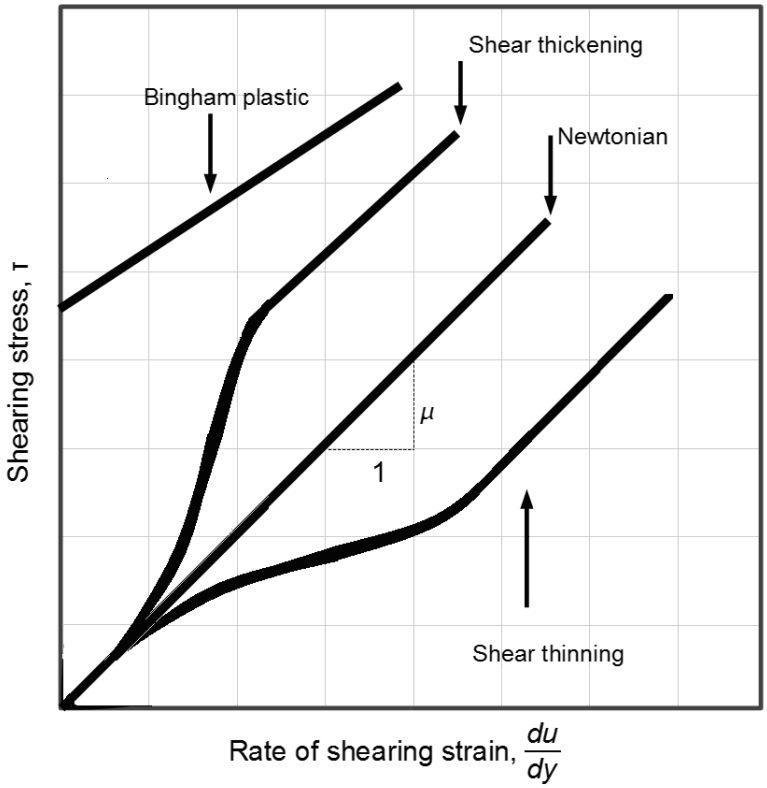

Figure 1.3 Viscous regimes chart.

1.3.2. Polymer Thickeners and Poly(acrylic acid)

It has been mentioned in the previous sections that thickened de-/anti-icing fluids are required to have a sufficiently high viscosity to maintain a stable thin film on the surfaces of aircraft which suppresses ice formation during the period the aircraft taxies before reaching the hold position prior to take-off. During the short period between the aircraft's release from the hold position at the end of the runway to the point at which it reaches rotational speed, when the aircraft begins to lift from the runway, the thin film must be cleanly removed from the wings and fuselage. The fluid layer has to be sufficiently stable to provide the necessary cover when the aircraft is taxiing, but must

be easily released as the air shear increases during the period up to rotation. To achieve such desired shear thinning characteristics small amounts of high molecular weight polymers, commonly referred as “thickeners”, are added to the base glycol mixtures [9, 15, 16, 20]. By adjusting the molecular weight and concentration these thickened fluids with appropriate glycol mixtures are able to provide the desired hold over and shear thinning characteristics for effective use as de-icing fluids and achieve the desired performance when subjected to simulation of the conditions found during take-off.

Poly(acrylic acid) (PAA) is the generic name of a high molecular weight synthetic polymer of acrylic acid (Figure 1.4) and is a water soluble polyelectrolyte system which has wide applications as a fluid thickener, as well as a dispersing, suspending, and emulsifying agent in pharmaceuticals, water treatments, cosmetics, production of ceramics as binders, and controlled release of biologically active agents [55-67]. In very dilute solution, a large portion of the carboxylic acid groups of PAA will be ionized and will repel one another, so that the macromolecule can adopt a loose conformation forming pseudo-isolated polymer chains [68-73]. As a consequence of the negative charge repulsion on the carboxyl group, the end-to-end distance and the volume occupied by the polymer coil will be large, and will depend on the pH of the medium (Figure 1.5). With increasing polymer concentration, the extent of dissociation of the carboxyls will decrease, leading to apparent changes in polymer sizes, which is in turn influenced by pH and added salt concentration. These effects have been investigated for aqueous solutions [15, 74].

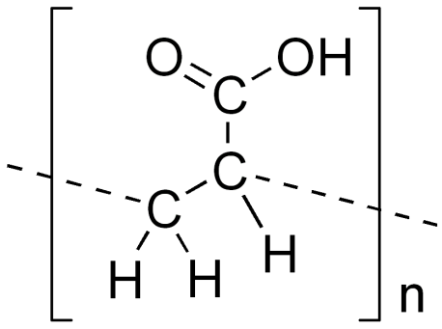

Figure 1.4 Poly(acrylic acid)

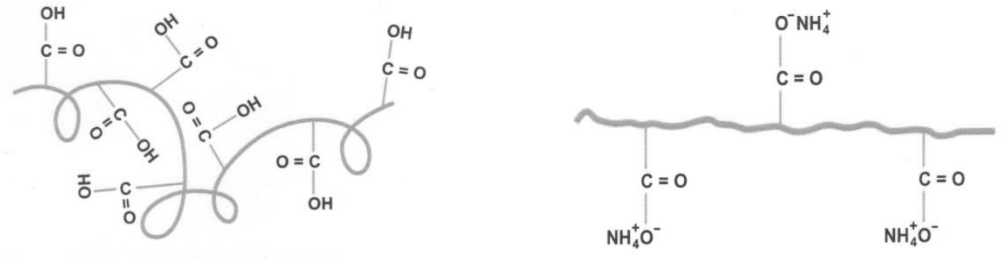

Figure 1.5 Schematic depicting molecule of PAA in relaxed state and uncoiled state [75].

1.3.3. PAA and Gelation

PAA is widely used in de-icing fluids to impart pseudoplastic characteristics at temperatures of the order of zero centigrade [6, 9, 15, 20, 22, 24, 26, 27]. PAA, like many polyelectrolytes, is able to form gel structures at high concentrations and has been associated with problems with jamming flight control systems when residues build-up in aerodynamically quiet areas. This problem has been encountered with Type IV fluids when the evaporation of water and glycol in the formulations creates powder-like residues which remain in balance bays, under wing and rear spar stabilizer areas [4, 18, 76, 77]. In moist conditions these deposited gels can absorb moisture and re-swell, expanding in volume by several orders of magnitude, freeze, potentially restricting movement of flight control surfaces, with the possible result of a malfunction of critical control equipment (Figure 1.6) [76].

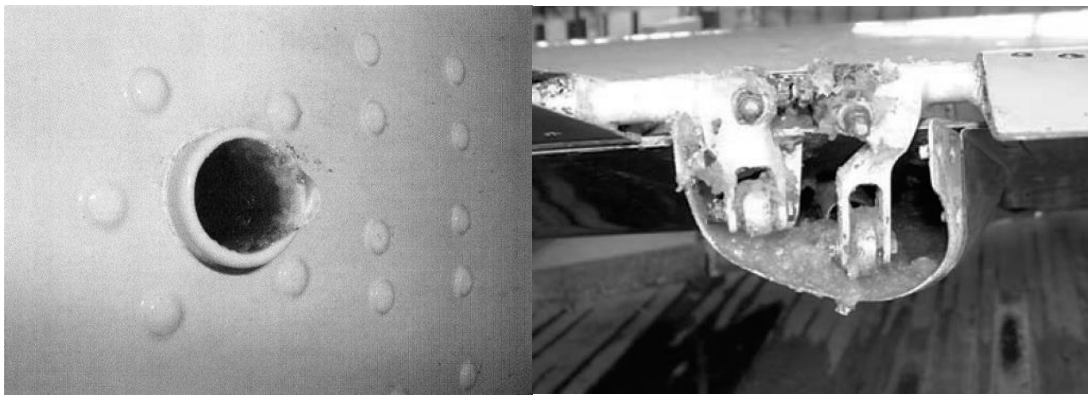

Figure 1.6 Anti-icing fluid residue gels [76].

1.4. Summary and Aim of Study

This chapter provided a brief introduction of aircraft ground de-icing operation and the utilization of de-/anti-icing fluids. Current fluids, Type II and Type IV in particular, have been widely used in the aviation industry and served particular purposes for years. However, in the light of recent events involving potential build-up of gel residues, improved polymer thickening agents with enhanced properties are required. Therefore the aim of this study is to be able to understand the way in which the molecular architecture of PAA creates the desirable pseudoplastic characteristics so as to be able to design systems which do not suffer from insoluble gel formation. In this thesis the following studies will be reported.

- Characterization of the current polymer thickeners (PAA-based co-polymer and homo-polymer) in terms of the molecular structure and rheological behaviour
- A mathematical model to explore the possible relationships between molecular structure and pseudoplastic behaviour of PAA polymer
- Influence of electrolyte on the rheological properties of PAA-thickened glycol-water mixtures
- Possibility of utilizing PAA-PVP blends as improved thickening agents of glycol-water mixtures
- Influence of multiple cations on the thickened fluids and impact of hard water dilution

1.5. References

1. AOPA *Aircraft Icing*. Safety Advisor - Weather No. 1, 2008.
2. Stanley, M.E. and Smith, K.W., *Deicing*, USPTO, Editor 2003, Clearwater, Inc.: U.S.
3. Blau, K. *Recommendations for De-icing/Anti-icing Aeroplanes on the Ground*. 2011.
4. Kotker, D., *Deicing/Anti-Icing Fluids*, in *Aero*1999, Boeing Commercial Airplanes Group: Seattle, WA, USA.
5. Mackenzie, W.E., *Anti-Icing Fluid for Use in Freezing Rain*, USPTO, Editor 1960: U.S.
6. Cohen, L., *New Thickener for Glycerine.* Soap and Chemical Specialties, 1956. **32**(10).
7. Lemma, S., *Anti-icing fluids*, USPTO, Editor 1998, The B.F. Goodrich Company: U.S.
8. Meyer, G.R. and Smith, D.C., *Deicing fluids*, USPTO, Editor 1991, The Dow Chemical Company (Midland, MI): U.S.
9. Jenkins, R.D., Bassett, D.R., Lightfoot, R.H., and Boluk, M.Y., *Aircraft anti-icing fluids*, USPTO, Editor 1995, Union Carbide Chemicals & Plastics Technology Corporation: U.S.
10. SAE, *SAE AMS1428 Fluid, Aircraft Deicing/Anti-Icing, Non-Newtonian (Pseudoplastic), SAE Types II, III, and IV*, 2010, SAE International.
11. SAE, *SAE AMS1424 Deicing/Anti-Icing Fluid, Aircraft, SAE Type I*, 1993, SAE International.
12. Paredes, X., Pensado, A.S., Comuñas, M.a.J.P., and Fernández, J., *How Pressure Affects the Dynamic Viscosities of Two Poly(propylene glycol) Dimethyl Ether Lubricants.* Journal of Chemical & Engineering Data, 2010. **55**(9): pp. 4088-4094.
13. Ritter, S., *what's that stuff?* Chemical & Engineering News Archive, 2001. **79**(1): pp. 30.
14. Frank Ma and Comeau, D., *Aircraft de-icing and anti-icing composition*, USPTO, Editor 1990, Union Carbide Corporation: U.S.
15. Coffey, D.A., Nieh, E.C.Y., and Armstrong, R.A., *Aircraft deicing fluid with thermal and pH-stable wetting agent* USPTO, Editor 1995, Texaco Inc.: U.S.
16. Jenkins, R.D., Bassett, D.R., Lightfoot, R.H., and Boluk, M.Y., *Aircraft anti-icing fluids thickened by associative polymers*, USPTO, Editor 1997, Union Carbide Chemicals & Plastics Technology Corporation: U.S.
17. Simonot, M., Mischka, G., Holland, N., Fieandt, J., Pontinen, J., Gerritsen, A., Krause, H., Bedrzycki, W., Bostrom, H.-E., and Buhler, R. *Recommedations for De-icing*

/Anti-icing of aircraft on the ground. 2004.

18. Cal, A. *Training Recommendations and Background Information for De-Icing /Anti-Icing of Aircraft on the Ground* 2008.

19. Seiler, M. and Bernhardt, S., *Deicing agent and/or anti-icing agent*, USPTO, Editor 2011, Evonik Degussa GmbH: U.S.

20. Ross, F., *Aircraft De-/Anti-Icer*, USPTO, Editor 2011, Kilfrost Limited: U.S.

21. Patocka, J. and Hon, Z., *Ethylene glycol, hazardous substance in the household.* Acta medica (Hradec Kralove) / Universitas Carolina, Facultas Medica Hradec Kralove, 2010. **53**(1): pp. 19-23.

22. Switzenbaum, M.S., Veltman, S., Mericas, D., Wagoner, B., and Schoenberg, T., *Best management practices for airport deicing stormwater.* Chemosphere, 2001. **43**(8): pp. 1051-1062.

23. Shupack, D.P. and Anderson, T.A., *Mineralization of propylene glycol in root zone soil.* Water Air and Soil Pollution, 2000. **118**(1-2): pp. 53-64.

24. Kent, R.A., Andersen, D., Caux, P.Y., and Teed, S., *Canadian Water Quality Guidelines for glycols - An ecotoxicological review of glycols and associated aircraft anti-icing and deicing fluids.* Environmental Toxicology, 1999. **14**(5): pp. 481-522.

25. Bausmith, D.S. and Neufeld, R.D., *Soil biodegradation of propylene glycol based aircraft deicing fluids.* Water Environment Research, 1999. **71**(4): pp. 459-464.

26. Cancilla, D.A., Martinez, J., and Van Aggelen, G.C., *Detection of aircraft deicing/antiicing fluid additives in a perched water monitoring well at an international airport.* Environmental Science & Technology, 1998. **32**(23): pp. 3834-3835.

27. Klecka, G.M., Carpenter, C.L., and Landenberger, B.D., *Biodegradation of Aircraft Deicing Fluids in Soil at Low-Temperatures.* Ecotoxicology and Environmental Safety, 1993. **25**(3): pp. 280-295.

28. ASTM, *ASTM D1331 - 11 Standard Test Methods for Surface and Interfacial Tension of Solutions of Surface-Active Agents*, 2011, ASTM International: West Conshohocken, PA.

29. ASTM, *ASTM D1193 - 06(2011) Standard Specification for Reagent Water*, 2011, ASTM International: West Conshohocken, PA.

30. ASTM, *ASTM D2196 - 10 Standard Test Methods for Rheological Properties of Non-Newtonian Materials by Rotational (Brookfield type) Viscometer*, 2010, ASTM International: West Conshohocken, PA.

31. ASTM, *ASTM D1747 - 09 Standard Test Method for Refractive Index of Viscous*

Materials, 2009, ASTM International: West Conshohocken, PA.

32. ASTM, *ASTM E70 - 07 Standard Test Method for pH of Aqueous Solutions With the Glass Electrode*, 2007, ASTM International: West Conshohocken, PA.

33. SAE, *SAE AS5901B Water Spray and High Humidity Endurance Test Methods for SAE AMS1424 and SAE AMS1428 Aircraft Deicing/Anti-icing Fluids*, 2010, SAE International.

34. SAE, *SAE AS5900B Standard Test Method for Aerodynamic Acceptance of SAE AMS 1424 and SAE AMS 1428 Aircraft Deicing/Anti-icing Fluids*, 2007, SAE International.

35. SAE, *SAE AMS4037 Aluminum Alloy, Sheet and Plate 4.4Cu - 1.5Mg - 0.60Mn (2024--T3 Flat Sheet, -T351 Plate) Solution Heat Treated*, 1940, SAE International.

36. Ekblad, J. and Edwards, Y., *Precision of method for determining resistance of bituminous mixtures to de-icing fluids.* Materials and Structures, 2008. **41**(9): pp. 1551-1562.

37. Beisswenger, A., Laforte, J.L., Tremblay, M.M., and Perron, J., *Investigation of a New Reference Fluid for Use in Aerodynamic Acceptance Evaluation of Aircraft Ground Deicing and Anti-icing Fluid*, in *prepared for the Federal Aviation Administration*2007.

38. Tong, T.V.K., Louchez, P.R., and Zouzou, A., *Introductory analysis of draining and freezing of de-icing fluids.* Cold Regions Science and Technology, 1997. **25**(3): pp. 207-214.

39. Louchez, P., *Fluid Behaviour Simulation: Modelling of Water Diffusion in Ground Aircraft De/Anti-Icing Fluids for Numerical Prediction of Laboratory Holdover Time*, 1997, Transportation Development Centre of Canada: Montreal, Quebc Canada. pp. 1-60.

40. Louchez, P.R., Laforte, J.L., Bouchard, G., and Farzaneh, M., *Laboratory Evaluation of Aircraft Ground De Antiicing Products*, in *Proceedings of the Fourth*, Chung, J.S., Karal, K., and Koteryama, W., Editors. 1994, International Society Offshore& Polar Engineers: Cupertino. pp. 479-483.

41. Louchez, P., Laforte, J.L., and Bouchard, G., *Boundary Layer Evaluation of Anti-Icing Fluids for Commuter Aircraft*, 1994, UQAC.

42. Louchez, P., Laforte, J.L., and Bernardin, S., *A proposal of standard evaluation of aerodynamic performance of de-icing and anti-icing fluids applied on commuter type aircraft*, 1994, Universite du Quebec a Chicoutimi.

43. Laforte, J.L., Louchez, P., and Bernardin, S., *Experimental Holdover Time Evaluation and Prediction of Type III Anti-Icing Fluid*, 1994, Federal Aviation Administration

Technical Center: US Department of Transportation.

44. Laforte, J.L., Louchez, P.R., and Bouchard, G., *Cold and Humid Environment Simulation for De-Anti-Icing Fluids Evaluation.* Cold Regions Science and Technology, 1992. **20**(2): pp. 195-206.

45. Laforte, J.L., Louchez, P., Bouchard, G., and Ma, F., *A Facility to Evaluate Performance of Aircraft Ground De-Antiicing Fluids Subjected to Freezing Rain.* Cold Regions Science and Technology, 1990. **18**(2): pp. 161-171.

46. Bingham, E.C., *Fluidity and Plasticity* 2007: Read Books.

47. Osswald, T.A., *Polymer Processing Fundamentals* 1998: Hanser.

48. Barnes, H.A., Hutton, J.F., and Walters, K., *An Introduction to Rheology* 1989: Elsevier Sci.

49. Brandrup, J., Immergut, E.H., and Grulke, E.A., *Polymer handbook* 2003, NY: Wiley-Interscience.

50. Painter, P.C. and Coleman, M.M., *Fundamentals of Polymer Science: An Introductory Text, Second Edition* 1997: Crc Press.

51. Morrison, I.D. and Ross, S., *Colloidal Dispersions: Suspensions, Emulsions, and Foams* 2002: Wiley.

52. Barnes, H.A., *Thixotropy—a review.* Journal of Non-Newtonian Fluid Mechanics, 1997. **70**(1–2): pp. 1-33.

53. Mezger, T.G., *The Rheology Handbook: For Users of Rotational and Oscillatory Rheometers* 2006: Vincentz Network.

54. Briant, J., Denis, J., and Parc, G., *Rheolgical Properties of Lubricants* 1989: Éditions Technip.

55. Staikos, G., Sotiropoulou, M., Bokias, G., Bossard, F., Oberdisse, J., and Balnois, E., *Hydrogen-Bonded Interpolymer Complexes Soluble at Low pH*, in *Hydrogen-bonded interpolymer complexes: formation, structure and applications*, Khutoryanskiy, V.V. and Staikos, G., Editors. 2009, World Scientific. pp. 23-53.

56. Volk, N., Vollmer, D., Schmidt, M., Oppermann, W., and Huber, K., *Conformation and Phase Diagrams of Flexible Polyelectrolytes - Polyelectrolytes with Defined Molecular Architecture II*, in *Advances in Polymer Science*, Schmidt, M., Editor 2004, Springer Berlin / Heidelberg. pp. 29-65.

57. Prime, R.B., *Thermosets*, in *Thermal characterization of polymeric materials*, Turi, E.A., Editor 1997, Academic Press. pp. 173-174.

58. Bertini, V. and Pocci, M., *Functional Polymers for Selective Flocculation of Minerals*, in *Desk reference of functional polymers: syntheses and applications*, Arshady, R.,

Editor 1997, American Chemical Society.

59. Munk, P., *Tertiary Structure — Arrangement of Larger Segments*, in *Introduction to Macromolecular Science*, Munk, P., Editor 1989, John Wiley & Sons: New York. pp. 60-61.

60. Chu, J.S., Yu, D.M., Amidon, G.L., Weiner, N.D., and Goldberg, A.H., *Viscoelastic Properties of Polyacrylic-Acid Gels in Mixed-Solvents.* Pharmaceutical Research, 1992. **9**(12): pp. 1659-1663.

61. Lin, S.Y., Amidon, G.L., Weiner, N.D., and Goldberg, A.H., *Viscoelasticity of Anionic Polymers and Their Mucociliary Transport on the Frog Palate.* Pharmaceutical Research, 1993. **10**(3): pp. 411-417.

62. Jones, D.S., Muldocin, B.C.O., Woolfson, A.D., and Sanderson, F.D., *An examination of the rheological and mucoadhesive properties of poly(acrylic acid) organogels designed as platforms for local drug delivery to the oral cavity.* Journal of Pharmaceutical Sciences, 2007. **96**(10): pp. 2632-2646.

63. Bhosale, P.S. and Berg, J.C., *Poly(acrylic acid) as a rheology modifier for dense alumina dispersions in high ionic strength environments.* Colloids and Surfaces a-Physicochemical and Engineering Aspects, 2010. **362**(1-3): pp. 71-76.

64. Winnik, M.A. and Yekta, A., *Associative polymers in aqueous solution.* Current Opinion in Colloid & Interface Science, 1997. **2**(4): pp. 424-436.

65. Glass, J., *A perspective on the history of and current research in surfactant-modified, water-soluble polymers.* Journal of Coatings Technology, 2001. **73**(913): pp. 79-98.

66. Viota, J.L., Delgado, A.V., Arias, J.L., and Duran, J.D.G., *Study of the magnetorheological response of aqueous magnetite suspensions stabilized by acrylic acid polymers.* Journal of Colloid and Interface Science, 2008. **324**(1-2): pp. 199-204.

67. Bromberg, L., Temchenko, M., Alakhov, V., and Hatton, T.A., *Bioadhesive properties and rheology of polyether-modified poly(acrylic acid) hydrogels.* International Journal of Pharmaceutics, 2004. **282**(1-2): pp. 45-60.

68. Wang, J., Li, L., Ke, H.L., Liu, P., Zheng, L., Guo, X.H., and Lincoln, S.F., *Rheology control by modulating hydrophobic and inclusive associations of side-groups in poly (acrylic acid).* Asia-Pacific Journal of Chemical Engineering, 2009. **4**(5): pp. 537-543.

69. Miquelard-Garnier, G., Demoures, S., Creton, C., and Hourdet, D., *Synthesis and rheological behavior of new hydrophobically modified hydrogels with tunable properties.* Macromolecules, 2006. **39**(23): pp. 8128-8139.

70. Guo, X.H., Abdala, A.A., May, B.L., Lincoln, S.F., Khan, S.A., and Prud'homme, R.K., *Rheology control by modulating hydrophobic and inclusion associations in modified poly(acrylic acid) solutions.* Polymer, 2006. **47**(9): pp. 2976-2983.

71. Bossard, F., Sotiropoulou, M., and Staikos, G., *Thickening effect in soluble hydrogen-bonding interpolymer complexes. Influence of pH and molecular parameters.* Journal of Rheology, 2004. **48**(4): pp. 927-936.

72. Bromberg, L., Temchenko, M., and Colby, R.H., *Interactions among hydrophobically modified polyelectrolytes and surfactants of the same charge.* Langmuir, 2000. **16**(6): pp. 2609-2614.

73. Foerster, S., Schmidt, M., and Antonietti, M., *Experimental and theoretical investigation of the electrostatic persistence length of flexible polyelectrolytes at various ionic strengths.* The Journal of Physical Chemistry, 1992. **96**(10): pp. 4008-4014.

74. Tunc, S., Duman, O., and Uysal, R., *Electrokinetic and rheological behaviors of sepiolite suspensions in the presence of poly(acrylic acid sodium salt)s, polyacrylamides, and poly(ethylene glycol)s of different molecular weights.* Journal of Applied Polymer Science, 2008. **109**(3): pp. 1850-1860.

75. Lubrizol Advanced Materials, I., *Minimizing Influence of Salts In Presence of Carbopol Polymers*, in *TDS-54*2002: Cleveland, Ohio.

76. Hille, J., *Deicing and Anti-Icing Fluid Residues*, in *Aero*2007, Boeing Commercial Airplanes Group: Seattle, WA, USA. pp. 14-21.

77. DOW, J.P., *Understanding the stall-recovery procedure for turboprop airplanes in icing conditions*, in *Flight Safety Digest*2005, Flight Safety Foundation, Inc. pp. 1-17.

Chapter 2. Experimental Methods

2.1. Introduction

Several experiments were conducted initially for the purpose of characterisation of the polymers used in terms of their structure, molecular weights, and acid numbers. The main investigation which was concerned with the design of alternative de-icing fluids and involved the study of polymer solutions, rheological performances, hold-over times, and aerodynamic performances.

2.1.1. Infrared Spectroscopy and Nuclear Magnetic Resonance Spectroscopy

Routine spectrophotometric analyses such as ultraviolet (UV), infrared (IR), or nuclear magnetic resonance (NMR) spectroscopy can provide information about functional groups in a polymer. IR spectroscopy exploits the fact that when a beam of infrared light passes though the material, absorptions will occur at specific frequencies; and such resonant frequencies match the ones at which the bonds or functional groups that vibrate. By examining the transmitted light, it reveals the amount of energy absorbed at each frequency. When the absorbance spectrum is generated, analysis of the position, shape, and intensity of the peaks exhibited in the spectrum will reveal the molecular structure of the material sample in detail [1-3]. On the other hand, NMR spectroscopy uses magnetic properties of certain atomic nuclei to determine physical or chemical properties of atoms or the molecules in which they are contained. When placed in a magnetic field, NMR active nuclei (in this case, ^{1}H) absorb electromagnetic radiation at a frequency characteristic of the isotope. The resonant frequency, energy of the absorption, and the intensity of the signal are proportional to the strength of the magnetic field [4, 5]. Such technique is frequently used to investigate the properties of organic molecules.

2.1.2. Intrinsic Viscosity and Molecular Weight Determination

In this study, two polymer samples were supplied by Kilfrost Ltd, namely poly(acrylic acid) based co-polymer, Carbomer A, and poly(acrylic acid) based homo-polymer, Carbomer B. It was claimed that these two polymers have the molecular weights of approximately 4 and 5 MDa. There are several widely-used techniques, which can be used to determine the molar mass of a polymer, including mass spectrometry, vapour pressure osmometry, low-angle laser light scattering in conjunction with size exclusion chromatography (gel permeation chromatography, in particular). In this study, intrinsic viscosity measurements were used as these provide information on the hydrodynamic size of the polymer. Gel permeation chromatography using aqueous solvents was not available at the University of Strathclyde.

Intrinsic viscosity is measured from the flow time of a solution through a glass capillary. The concept of capillary viscometry is rather simple: the flow time of either solvent or solution through a thin capillary is proportional to the viscosity of the fluid, and inverse-proportional to the density.

$$t_{\text{solvent}} \propto \frac{\eta_{\text{solvent}}}{\rho_{\text{solvent}}} \tag{2.1}$$

$$t_{\text{solution}} \propto \frac{\eta_{\text{solution}}}{\rho_{\text{solution}}} \tag{2.2}$$

Therefore the relative viscosity is defined to be the ratio of the viscosity of solution over the one of solvent, i.e.

$$\eta_{\text{rel}} = \frac{\eta_{\text{solution}}}{\eta_{\text{solvent}}} \tag{2.3}$$

For most polymer solutions, at very dilute condition, it is reasonable to assume that densities of solvent and solution are approximately the same so the ratio of flow time is proportional to the ratio of their viscosities. The relative viscosity becomes a simple ratio of time:

$$\eta_{\text{rel}} = \frac{t_{\text{solution}}}{t_{\text{solvent}}} \tag{2.4}$$

Another term – specific viscosity – is also defined as the fractional change in viscosity (again, the approximation implemented previously is adapted here):

$$\eta_{\text{sp}} = \frac{t_{\text{solution}} - t_{\text{solvent}}}{t_{\text{solvent}}} \tag{2.5}$$

Both relative viscosity and specific viscosity depend on the polymer concentration. Therefore in order to extract the influence of the polymer molecules on solution, one must extrapolate to the condition when the polymer concentration, *c*, equals zero. In theory, the term 'intrinsic viscosity' is the extrapolation of the above two viscosities at zero polymer concentration:

$$[\eta] = \lim_{c \to 0} \frac{\eta_{\text{sp}}}{c} \equiv \lim_{c \to 0} \frac{\ln \eta_{\text{rel}}}{c} \tag{2.6}$$

A more practical way to acquire the value of $[\eta]$ is to plot both η_{sp}/c and $(\ln \eta_{\text{rel}})/c$ against polymer concentration, *c*, and extrapolate an intercept of both function to the y-axis (or the mean value of both intercepts). Based on the principle of the Mark-Houwink equation [6, 7], intrinsic viscosity and molecular weight are, intra-connected:

$$[\eta] = KM^{\alpha} \tag{2.7}$$

In this equation, *K* and α are the Mark-Houwink coefficients, whose values depend on the particular polymer-solvent system and the temperature. The specific values of these coefficients depend on the polymer type and the molecular weight concentration range. For an ideally flexible polymer in a "theta" solvent, α has a value of 0.5; and as the rigidity of the polymer chain is increased, so the value will tend towards 1 or greater. The value of *K* is characteristic of the chemical structure of the polymer and will change with the solvent being used in the study. Implicit in Equation 2.7 is the connectivity between the size of the polymer molecule in solution – its hydrodynamic volume and the molecular weight. Values for a wide range of polymers are available [6, 7].

2.1.3. Monomer Equivalent Weight Determination

The determination of monomer equivalent weight in this study is essentially an acid-base reaction. An organic acid such as poly(acrylic acid) is acidic enough to partially ionise and release hydrogen cations. Therefore a neutralization titration procedure using a strong base, sodium hydroxide, was conducted. The polymer equivalent weights of both polymers were obtained through the consumption of base.

2.1.4. Rheology

In this study, several techniques were incorporated to generate the rheological profiles of the fluids. The primary purpose of these rheological measurements is to determine the viscosities at specific conditions.

i. **Continuous flow test – shear stress (shear rate) ramp**, in which at fixed temperature, continuously changing shear stresses (or shear rates) are applied to the material, and consequent shear rates (or shear stresses required to achieve such shear rates) are measured and shear viscosities of materials are therefore calculated. Under steady shear flow, the network formed within fluid will be inevitably broken, which will give rise to shear thinning. The typical shear rates it generated can well represent the shearing conditions that fluids experienced during on-site de-icing operations.

ii. **Steady shear flow test – temperature ramp**. This test is performed at fixed shear stresses, while temperature is continuously changing. As with the shear stress ramp, shear rates are measured, and shear viscosities are calculated. It is of particular importance to observe the temperature dependence of the viscosity of these fluids.

iii. **Creep test**. In this test procedure, a constant stress, σ, is imposed on the fluid. Under the influence of external shear, the fluid progressively experiences the stages of immediate elastic response, delayed elastic response, and steady-state

viscous response (Figure 2.1). After a long period of time, the slope of the deformation-time curve (deformation rate) will become constant. The ratio of the applied stress over the deformation rate is usually defined as viscosity at this specific shear rate. The constant viscosity at low shear rates is defined as the zero-shear viscosity.

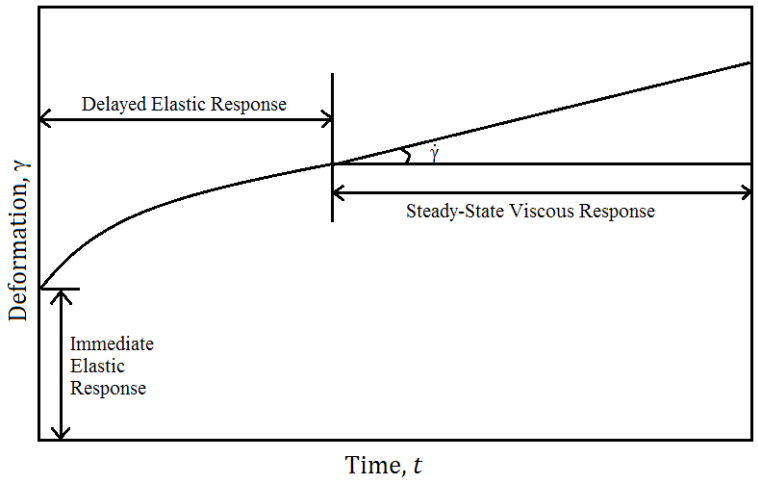

Figure 2.1 Schematic plot of an ideal creep curve.

iv. **Oscillatory measurement**. This test procedure applies when deformation behaviour of fluids needs to be investigated at very low strains whilst maintaining their rest structure. During the test procedure, a sinusoidal stress (strain) is imposed on the fluids, and the consequent sinusoidal strain (stress) is measured. For an elastic material the response signal will be completely in phase with the applied stimulus; for a viscous material, the response will be 90° out of phase (Figure 2.2). The principle of such technique is to measure the phase lag (δ) and the amplitudes of the input and response signals and calculate the amplitudes of the elastic and viscous components. If stress is applied at a frequency, ω, and amplitude, σ_0, the magnitude of the stress at time t is

$$\sigma = \sigma_0 \cos(\omega t) \tag{2.8}$$

The response of the strain is

$$\gamma = \gamma_0 \cos(\omega t - \delta) \tag{2.9}$$

$$\gamma = \gamma_0 \cos(\omega t)\cos(\delta) + \gamma_0 \sin(\omega t)\sin(\delta) \tag{2.10}$$

$\gamma_0\cos(\delta)$ is the amplitude of the strain component in phase with the stress and can be considered to be related to the elastic response of the fluid. The elastic modulus (or storage modulus) is defined as

$$G' = \sigma_0 \frac{\cos(\delta)}{\gamma_0} \tag{2.11}$$

For the component 90° out of phase it is considered to be related to the viscous response of the fluid. The viscous modulus (or loss modulus) is defined as

$$G'' = \sigma_0 \frac{\sin(\delta)}{\gamma_0} \tag{2.12}$$

Therefore a frequency-dependent viscosity function, the complex viscosity, is determined, and the size of which is given by

$$|\eta^*| = \sqrt{\left(\frac{G''}{\omega}\right)^2 + \left(\frac{G'}{\omega}\right)^2} \tag{2.13}$$

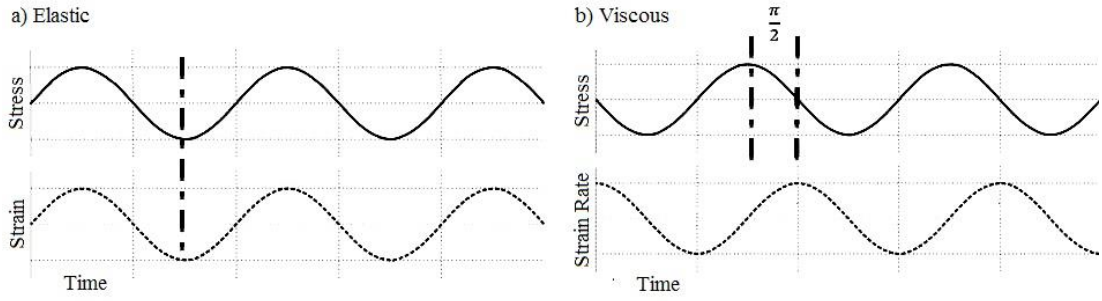

Figure 2.2 Schematic plot of in or out phase response for elastic or viscous material.

2.1.5. Boundary Layer Displacement Thickness Measurement

For the purpose of retaining the desired film during taxiing and the safety during take-

off, it is required for all aircraft ground de-/anti-icing fluids to have acceptable aerodynamic flow-off characteristics. According to previous studies [8-10] and industrial standards [11-17], such aerodynamic acceptance is based on the air and fluid BLDT (boundary layer displacement thickness) on a flat plate measured after experiencing the free stream velocity/time history of a representative aircraft take-off. Acceptability of the fluid is determined by comparing BLDT measurements of the candidate fluid with a datum established from the values of a reference fluid BLDT and the BLDT over the dry (clean) plate. The testing facility is set up according to Figure 2.3.

The BLDT is evaluated from the measurement of the two pressure differences ($P_1 - P_2$) and ($P_2 - P_3$), recorded as functions of time during all the test runs, where P_1 is the total pressure measured as the static pressure in the settling chamber immediately upstream of the test duct, P_2 is the inlet static pressure measured in the middle of the ceiling of the duct entrance (Station 2), P_3 is the outlet static pressure measured in the middle of the ceiling of the duct exit (Station 3). The average BLDT (δ_{ave}^*) over the test duct perimeter is evaluated using the following relation.

$$\delta_{ave}^* = \frac{1}{c}\left[S_3 - S_2\sqrt{\frac{(P_1-P_2)}{(P_1-P_2)+(P_2-P_3)}}\right] \tag{2.14}$$

Where c is the duct perimeter at Station 3, S_2 is the duct cross-sectional area at Station 2, S_3 is the duct cross-sectional area at Station 3.

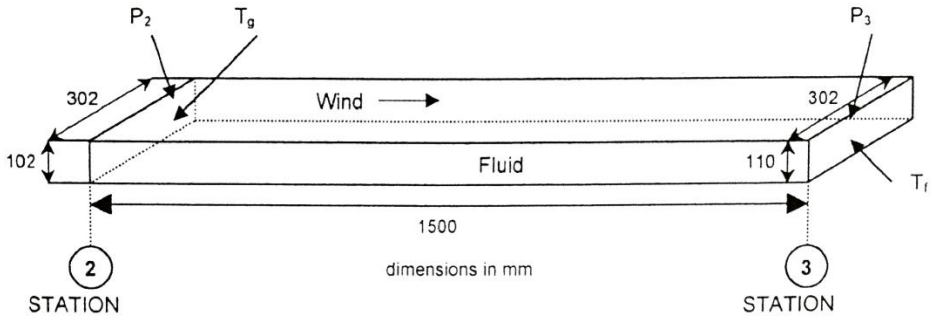

Figure 2.3 Schematic plot of BLDT test duct with dimensions.

When no fluid is present on the bottom flat plate, all four test section walls of the duct

are in the same dry state and the previous Equation 2.14 yields the value of the BLDT on a dry wall:

$$\delta_{\mathrm{d}}^{*} = \delta_{\mathrm{ave}}^{*} \tag{2.15}$$

On the other hand, when the test duct floor is covered with a layer of de-icing/anti-icing fluid and the top and sides are not, the BLDT is not constant over the perimeter at Station 3. It assumes a value δ_{f}^{*} on the lower surface and another value δ_{d}^{*} on the dry sides and top walls. Expressing the previously determined $\delta_{\mathrm{ave}}^{*}$ as perimeter-weighted average of δ_{d}^{*} and δ_{f}^{*}, the following relation can be obtained:

$$\delta_{\mathrm{f}}^{*} = \frac{c}{b}\left[\delta_{\mathrm{ave}}^{*} - \left(\frac{c-b}{c}\right)\delta_{\mathrm{d}}^{*}\right] \tag{2.16}$$

Where b is the width of the bottom flat plate. This relation is used to derive the BLDT over a wet surface, δ_{f}^{*}, from the measurement of $\delta_{\mathrm{ave}}^{*}$ carried out as explained with fluid on the test duct lower surface, provided an expression for δ_{d}^{*} has been previously determined by a number of "dry" runs carried out without any fluid in the test section.

2.1.6. Wet Spray Endurance Test

The primary purpose of this test is to evaluate the anti-icing performance of an aircraft deicing or anti-icing fluid, in an environmental test chamber. It describes how to determine the laboratory anti-icing performance of SAE Type I, Type II, Type III, and Type IV fluids; and the results can be considered representing the "hold-over time" which is one of the critical specifications of the fluids. The procedure of this test complies with previous studies and industrial standards [11, 13, 16, 18-20].

The test fluids to be evaluated are applied to a test plate exposed to a freezing condition, and their anti-icing performance is evaluated by measuring the minimum exposure time before a specified degree of freezing occurs. The test involves pouring the un-chilled fluid onto an inclined test plate at approximately -5.0°C and applying a cooled water spray in air at approximately -5.0°C. The water spray endurance is recorded as the time for ice

formation to reach the failure zone defined as the area 25 mm below the upper edge of the test plate and 5 mm in from either side of the test plate or the formation of slush on 10% of the plate surface (Figure 2.4), when water spray intensity corresponds to approximately 5.0 g dm^{-2} h^{-1} weight increment of the testing area.

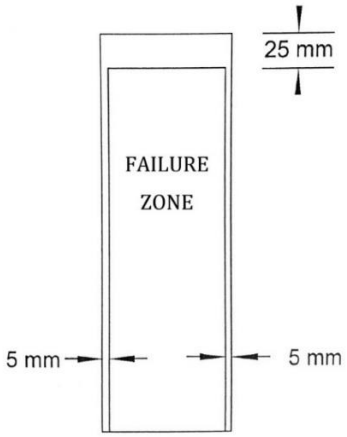

Figure 2.4 WSET test failure zone.

2.2. Experiments and Equipments

2.2.1. FTIR Spectroscopy

Infrared spectra were obtained using two spectrometers; the ATR spectra were obtained using the Agilent technology 4500 Series Portable FTIR Spherical Diamond ATR. Each spectrum consisted of 128 scans with a resolution of 8 wavenumbers and 2-3 μm depth penetration. The transmittance IR spectra were obtained using a Perkin Elmer 100 FTIR spetrometer. Prior to the sample analysis a background spectrum of the empty chamber was run. 32 scans were recorded per spectrum at a resolution of 4 wavenumbers. Spectra were obtained using ATR and also in transmission as a mull in Nujol (low molecular weight paraffin). Polymer concentration may vary from sample to sample. Measurements for each Carbomer were triplicated.

2.2.2. FT-NMR Spectroscopy

Solutions of the polymer were prepared in two solvents; deuterated dimethyl sulphoxide (DMSO) and deuterated water (D_2O). The polymer is sparingly soluble in both solvents and the polymers were left to disperse for periods of 24 hours and 3 weeks for DMSO and for 8 days in D_2O. Clear solutions were obtained in both solvents. ^1H FT-NMR were obtained at a frequency of 400 MHz using a Buker AV3 400 and the signal was obtained using 32 scans at 25°C.

2.2.3. Intrinsic Viscosity Measurement

The PAA polymers, Carbomer A and Carbomer B, were supplied with nominated molecular weights of 4 and 5 MDa. Previous studies have suggested that a PAA polymer, Carbopol 934P, with molecular weight of 3 MDa, was examined in terms of viscometric properties [21, 22], and the values of Mark-Houwink coefficients were provided [23, 24]. Both PAA polymers were dispersed in distilled water and allowed 5 days to completely dissolve. Initial concentrations of solutions were 0.0891 g dL^{-1} and 0.0952 g dL^{-1} respectively. These solutions were further diluted with distilled water to a series samples with different concentrations. 0.012 M of neutral electrolyte, sodium chloride, was added to each sample. The sample concentrations are listed below (Table 2.1):

Table 2.1 Sample polymer concentration for intrinsic viscosity measurements

Series Carbomer A	**Polymer Concentration (g dL^{-1})**	**Series Carbomer B**	**Polymer Concentration (g dL^{-1})**
1	0	1	0
2	0.0036	2	0.0119
3	0.0053	3	0.0238
4	0.0071	4	0.0381
5	0.0089	5	0.0571

6	0.0134	6	0.0761
7	0.0178	7	0.0952
8	0.0891		

The apparatus used in this series of experiments was a 0C suspended level (Ubbelohde) viscometer (Figure 2.5). The viscometer needed to be cleaned prior to use, by washing with nitric acid and rinsed with deionized water. The flow time of the fluid passing time lines (Marked D in Figure 2.5) was recorded and repeated 3 times. The solution was raised by application of a vacuum to B with the inlet A close with a plug. Once the solution has risen above the upper timing mark D the vacuum and the plug A were removed. A suspended plug of solution is then created in the bulb. The time for the liquid to fall between the two marks was measured. The side tube equalizes the pressure either side of the fluid sample and hence avoids the effects of pressure on the flow inherently in the non-suspended level viscometers. Average values were used in calculations.

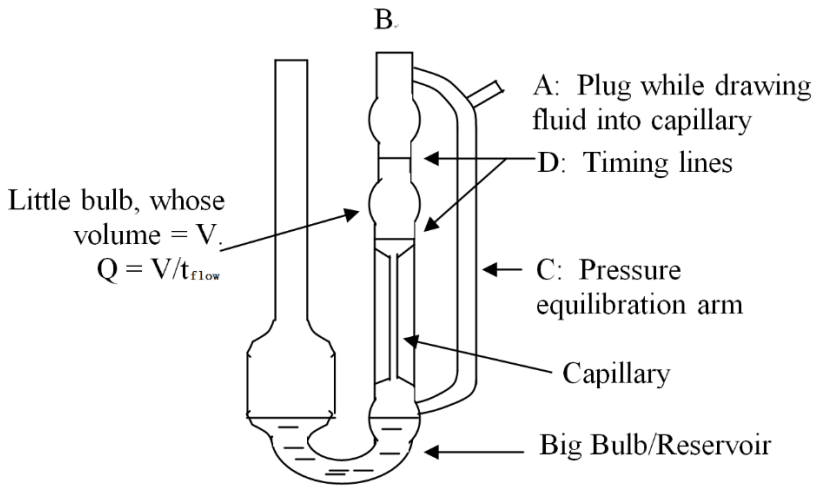

Figure 2.5 Schematic plot of suspended level viscometer.

2.2.4. Neutralization Titration

A series of neutralization titration experiments were conducted to determine the polymer equivalent weight for both Carbomer A and Carbomer B. They were dispersed

in distilled deionized water and gently stirred until completely dissolved. The polymer concentration for both Carbomers in 0.1 g dL^{-1}; the electrolyte level was adjusted to 0.012 M sodium chloride. 0.1 M Sodium hydroxide solution was used as neutralising agent. Due to their limited acidity and ability to ionise, both Carbomer solutions were titrated until a pH of 10.0 was reached at 20°C. The pH value was monitored by a probe pH meter.

2.2.5. Rheology

Rheological properties have been the major aspect of polymer characterisation and one of the most critical aspects of material evaluation throughout the entire program. Rotational rheometers have been used for all rheological experiments, including both parallel plate and cone-and-plate geometries (Figure 2.6). Creep tests and part of the steady shear measurements were carried out on an AR1000N rheometer (TA Instruments, Crawley, UK) using a 4-cm parallel plate geometry fitted with a solvent trap. Temperature ramp and part of the shear stress (shear rate) ramp tests, and oscillatory measurements were carried out on a Carri-Med CSL^2500 rheometer. Geometries used include 4-cm parallel plate with solvent trap, 6-cm 0.5° cone and plate, and 4-cm 4° cone and plate. Temperature was controlled by using the Peltier effect, with a water bath maintained at 20°C or an anti-freezing bath as a heat/cooling source. For details of each rheological experiment, please refer to each experiment section of the relevant chapter.

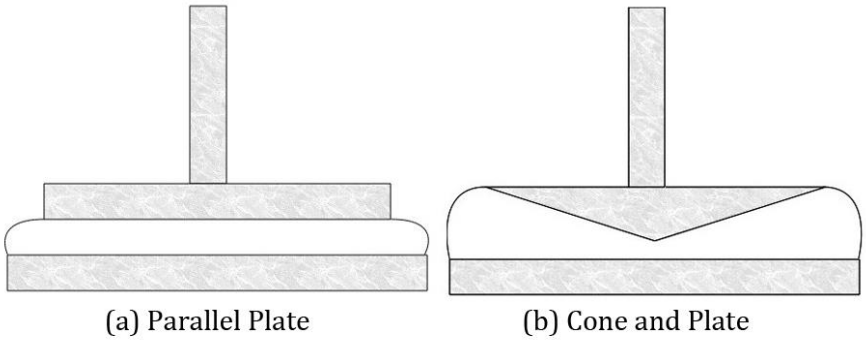

Figure 2.6 Schematic Plot of rotational rheometers, (a) parallel plate, (b) cone and plate.

2.2.6. BLDT Measurement

BLDT measurements were performed in a horizontal duct placed in an environment chamber for temperature (and/or humidity) control. The schematic plot of the duct is shown in Figure 2.3. The test duct floor is required to be horizontal, while the ceiling should slope upward linearly 8 mm from Station 2 to Station 3. All duct inner surfaces are required to be hydraulically smooth, which can be confirmed by a dry run prior to all other tests with a dry BLDT value of no greater than 3.0 mm at the air velocity of approximately 65 m s^{-1}.

Test fluids were prepared in 3 different specifications: 100% original fluid, 75% vol/vol dilution with demineralized water, and 50% vol/vol dilution with demineralized water. All samples were pre-cooled to testing temperature and applied as a coating on the floor of the duct to a thickness of 1.5 mm using a doctor blade and this simulates the coating which would be deposited by spray application. The temperature of the test facility was thermostatically controlled and tests were carried out at approximately 0°C, -5°C, -10°C and -15°C unless otherwise specified. At the start of each run, air velocity was increased from stationary at a linear rate to 65 m s^{-1} over a period of 25 seconds (Figure 2.7).

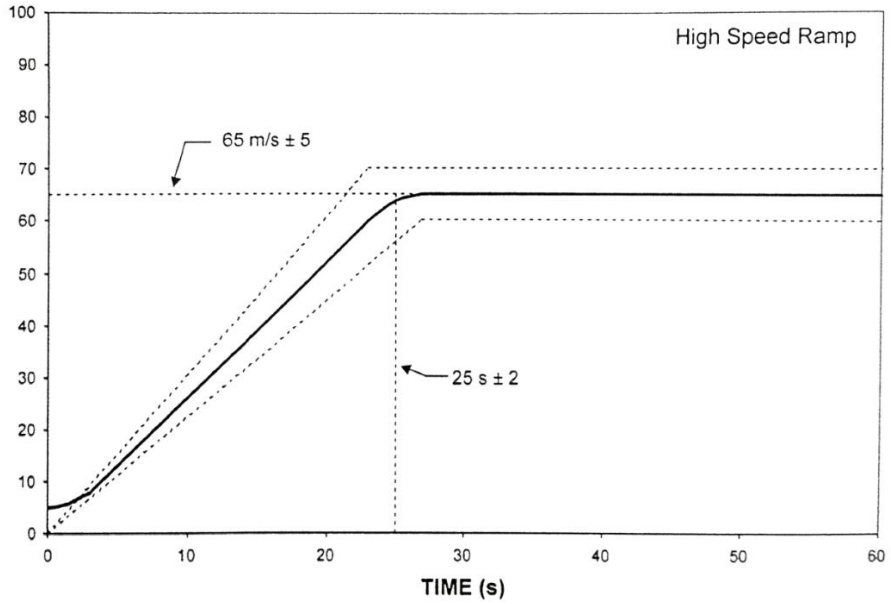

Figure 2.7 Air velocity acceleration simulation.

2.2.7. WSET Measurement

The WSET facility consists of a 10° inclined test plate and a water spray nozzle, both located in an environment chamber (Figure 2.8).

Each test fluid is prepared in 4 different sample specifications: 100% original fluid; 100% original fluid, shear processed using lab blender to simulate the potential degradation occurring during on-site spray operation; 75% vol/vol dilution with AEA hard water (which, by specification, contains Ca^{2+} 400±5 mg L^{-1} and Mg^{2+} 280±5 mg L^{-1}), shear processed; 50% vol/vol dilution with AEA hard water, shear processed. In practice, the neat solution will be diluted during application by proportions which will lie between 0 – 50%. The specified dilutions simulate the operations which would be carried out in practice, the neat de-icing fluids being diluted before being applied to the aircraft.

All test samples are applied to the test plate after the required ambient temperature, -5°C, was reached and then allowed 5 minutes to be cooled. Then start timing and water spray simultaneously. Observe the test panels and, when the ice front touches the failure zone, record the time of this event.

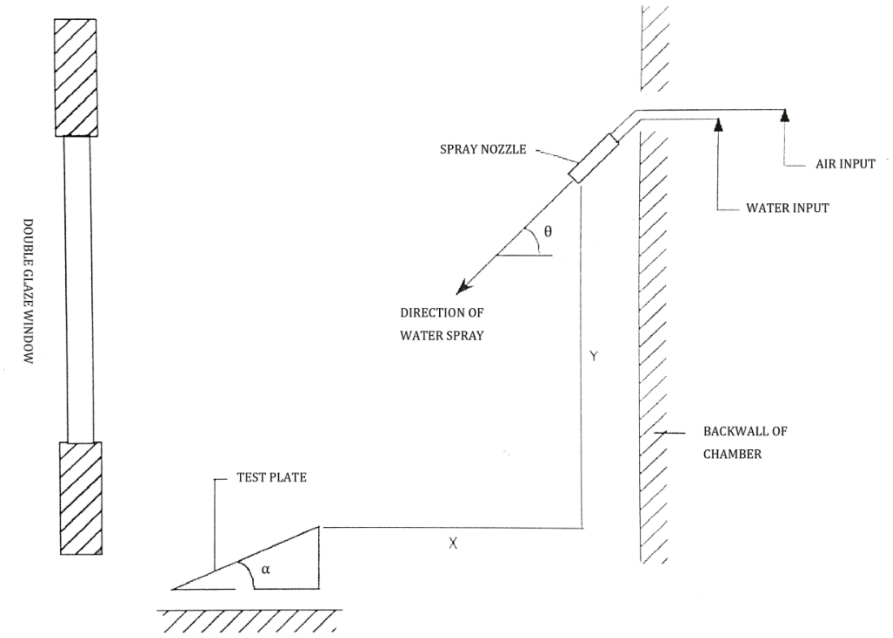

Figure 2.8 Schematic plot of a WSET set-up.

2.3. References

1. Atkins, P. and De Paula, J., *Elements of Physical Chemistry* 2009: W. H. Freeman.
2. Harwood, L.M. and Moody, C.J., *Experimental Organic Chemistry: Principles and Practice* 1989: Blackwell Scientific Publications.
3. White, R., *Chromatography/Fourier Transform Infrared Spectroscopy and Its Applications* 1990: M. Dekker.
4. Keeler, J., *Understanding NMR Spectroscopy* 2011: John Wiley & Sons.
5. Traficante, D.D., *Two-dimensional NMR methods for establishing molecular connectivity. A chemist's guide to experiment selection, performance, and interpretation.*, in *Concepts in Magnetic Resonance*, Martin, G.E. and Zektzer, A.S., Editors. 1991, John Wiley & Sons, Inc. pp. 49-50.
6. Kwei, T.K., *Macromolecules in Solution*, in *Maromolecules - An Introduction To Polymer Science*, Bovey, F.A. and Winslow, F.H., Editors. 1979, Academic Press, Inc. (London) Ltd.: London. pp. 305-310.
7. Hiemenz, P.C. and Lodge, T.P., *Condenation or Step-Growth Polymerization*, in *Polymer Chemistry*, Hiemenz, P.C., Editor 2007, CRC Press: Boca Raton. pp. 338-339.
8. Louchez, P., Laforte, J.L., and Bernardin, S., *A proposal of standard evaluation of aerodynamic performance of de-icing and anti-icing fluids applied on commuter type aircraft*, 1994, Universite du Quebec a Chicoutimi.
9. Louchez, P., Laforte, J.L., and Bouchard, G., *Boundary Layer Evaluation of Anti-Icing Fluids for Commuter Aircraft*, 1994, UQAC.
10. Beisswenger, A., Laforte, J.L., Tremblay, M.M., and Perron, J., *Investigation of a New Reference Fluid for Use in Aerodynamic Acceptance Evaluation of Aircraft Ground Deicing and Anti-icing Fluid*, in *prepared for the Federal Aviation Administration*2007.
11. SAE, *SAE AMS1424 Deicing/Anti-Icing Fluid, Aircraft, SAE Type I*, 1993, SAE International.
12. N/A, *Militry Specification - Anti-Icing and Deicing-Defrosting Fluids*, Naval Air Engineering Center, S.E.S.D.S., Editor 1989: Lkaehurst, NJ.
13. ASTM, *ASTM D1193 - 06(2011) Standard Specification for Reagent Water*, 2011, ASTM International: West Conshohocken, PA.
14. ASTM, *ASTM D1331 - 11 Standard Test Methods for Surface and Interfacial Tension of Solutions of Surface-Active Agents*, 2011, ASTM International: West

Conshohocken, PA.

15. SAE, *SAE AS5900B Standard Test Method for Aerodynamic Acceptance of SAE AMS 1424 and SAE AMS 1428 Aircraft Deicing/Anti-icing Fluids*, 2007, SAE International.

16. SAE, *SAE AMS1428 Fluid, Aircraft Deicing/Anti-Icing, Non-Newtonian (Pseudoplastic), SAE Types II, III, and IV*, 2010, SAE International.

17. Renton Division Aerodynamics Engineering, *Aerodynamic Acceptance Test for Aircraft Ground Deicing/Anti-icing Fluids*, 1992, Boeing: Chicago, IL.

18. SAE, *SAE AS5901B Water Spray and High Humidity Endurance Test Methods for SAE AMS1424 and SAE AMS1428 Aircraft Deicing/Anti-icing Fluids*, 2010, SAE International.

19. SAE, *SAE AMS4037 Aluminum Alloy, Sheet and Plate 4.4Cu - 1.5Mg - 0.60Mn (2024--T3 Flat Sheet, -T351 Plate) Solution Heat Treated*, 1940, SAE International.

20. ISO, *ISO 9001:2008 Quality management systems -- Requirements*, 2009, ISO: Geneva.

21. Nikolaeva, O., Budtova, T., Bobrova, N., and Bronnikov, S., *Influence of the Interpolymer Complex Formation Between Poly(Acrylic Acid) and Cellulose Ethers on the Properties of Their Mixtures and Films.* Journal of Macromolecular Science, Part B, 2001. **40**(3-4): pp. 539-552.

22. Chu, J.S., Yu, D.M., Amidon, G.L., Weiner, N.D., and Goldberg, A.H., *Viscoelastic Properties of Polyacrylic-Acid Gels in Mixed-Solvents.* Pharmaceutical Research, 1992. **9**(12): pp. 1659-1663.

23. Tsvetkov, V.N., Lyubina, S.Y., and Barskaya, T.V., *The flow birefringence and viscosity of poly (acrylic acid) solutions.* Polymer Science U.S.S.R., 1964. **6**(5): pp. 886-892.

24. Brandrup, J., Immergut, E.H., and Grulke, E.A., *Polymer handbook* 2003: Wiley-Interscience.

Chapter 3. Preliminary Polymer Characterisation

3.1. Background

Two different polymers, Carbomer A as a poly(acrylic acid) (PAA) based co-polymer and Carbomer B as a PAA based homo-polymer, were initially supplied by Kilfrost Ltd. MSDSs and technical data sheets indicate that these polymers were manufactured by Lubrizol (Brussels, Belgium) as flocculated solid particles approximately 0.2 μm in diameter, with nominal molecular weights of 4 and 5 MDa, respectively. Limited information for both polymers was available. As explained previously (Chapter 1), de-/anti-icing fluids rely on these materials to provide desirable rheological and aerodynamic properties. It is important to understand the fundamental characteristics of these polymers, especially in terms of their polymeric structures, mechanism of rheological behaviour and the principle behind them.

PAA is commercially available in a range of molecular weights and branched chain content. Commercial PAA is a copolymer which if branched can contain vinyl pentaerythritol. During the drying process PAA can form anhydride crosslinks which can increase the rigidity of the chain backbone but also will increase the molecular weight by cross-linking lower molecular weight chains. In order to probe the structure of these polymers several examinations and measurements were carried out for a preliminary characterisation of both polymers.

3.2. Polymer Characterisation

3.2.1. FTIR Spectroscopy

The FTIR spectra have shown consistent peak locations throughout all runs (Figure 3.1 and Figure 3.2). The spectra obtained were compared in Figure 3.3. Because the hydroxyl

groups on the acrylic acid will be expected to be bonded to other hydroxyl groups and also to carbonyl groups it would be expected that the absorption would be broad and not necessarily exhibit a distinct peak. Since the study is in Nujol mull the intensity of the C-H stretch at 2940 cm^{-1} which is used to normalise the spectra will vary with the amount of PAA present. As a consequence it is not possible to make an absolute comparison of the two polymer systems. However the feature at ~1720 cm^{-1} is consistent with the stretch of the C=O of the carboxylic acid. It is not however possible to make any comments on the composition of the polymers. The spectra are consistent with the main constituent being acrylic acid and there is little obvious difference between the two polymers.

A study of the spectra as function of the concentration of PAA in the Nujol mull indicated changes in the profile of the -OH characteristic absorption in the 3400 cm^{-1} region. These changes are consistent with the solvent, Nujol, increasing the distance between the -OH groups and changing the band intensity related to free and bound (interacting) -OH groups. The breadth of the peak reflects the nature of the hydrogen bonding with neighbouring groups.

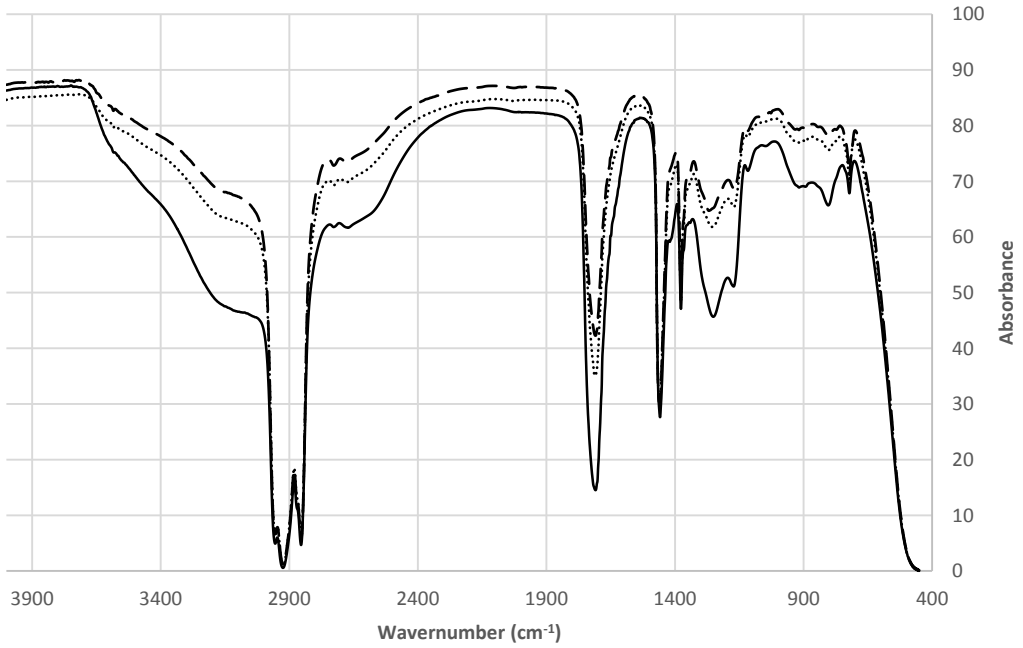

Figure 3.1 FTIR results for Carbomer A. Lines represent separate runs.

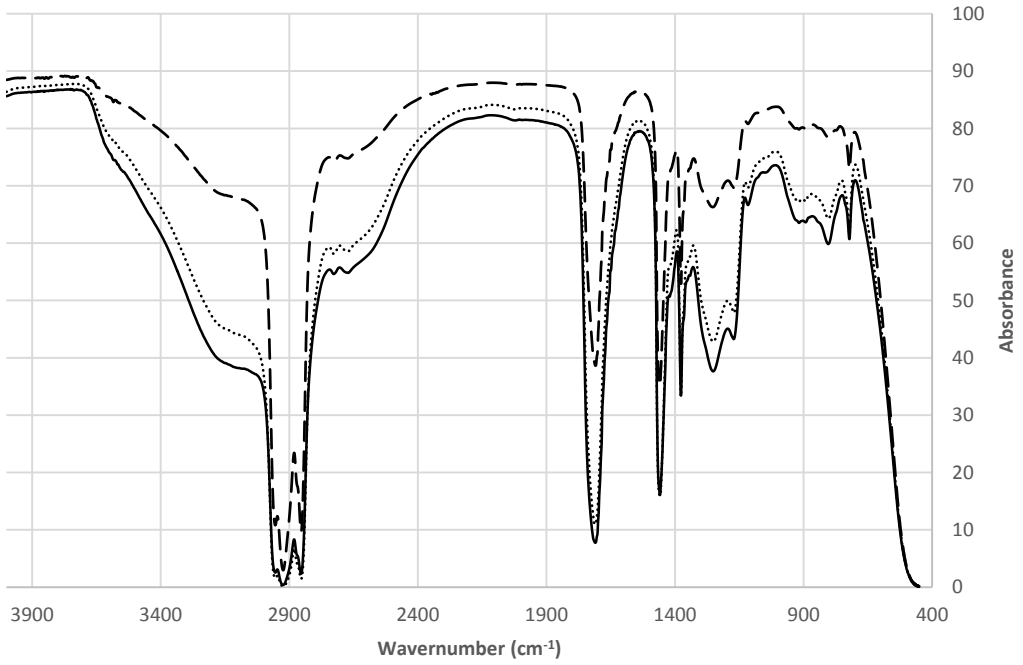

Figure 3.2 FTIR results for Carbomer B. Lines represent separate runs.

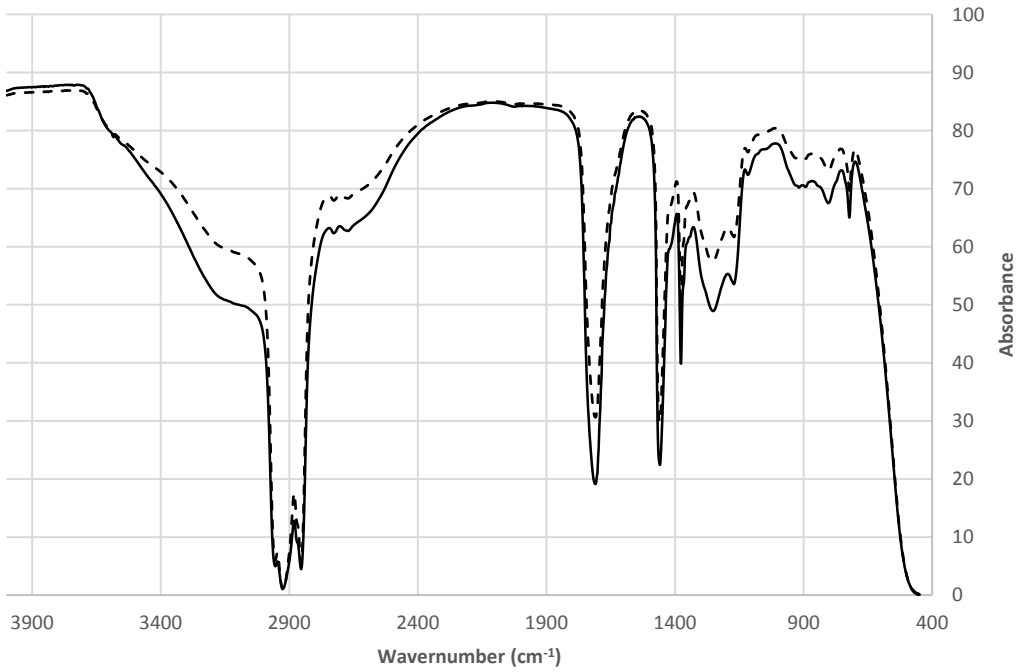

Figure 3.3 Comparison of FTIR spectroscopy for Carbomer A and Carbomer B.
Lines are (––) Carbomer A, (—) Carbomer B.

3.2.2. FT-NMR Spectroscopy

The spectra obtained are presented below. To aid assignment of the spectra, theoretical peak shifts for model structural elements of PAA were calculated using ChemDraw. A simulation was created using 20 monomer units, with 8 methyl ester and 2 anhydride units in the chain. The simulation is shown in Figure 3.4. The polymers are very high molecular weight materials so it would not be expected to detect resonances which might be assigned to end groups. Inspection of the predicted shifts indicates that CH_2 groups which are associated with the acrylic acid occur at 1.75 ppm and the associated C-H resonance occurs at 2.35 ppm. Formation of the anhydride would shift the CH_2 resonance to 1.88 ppm but also a possible resonance at 1.63 ppm indicative of the splitting of the degeneracy of the two protons by the ring formation.

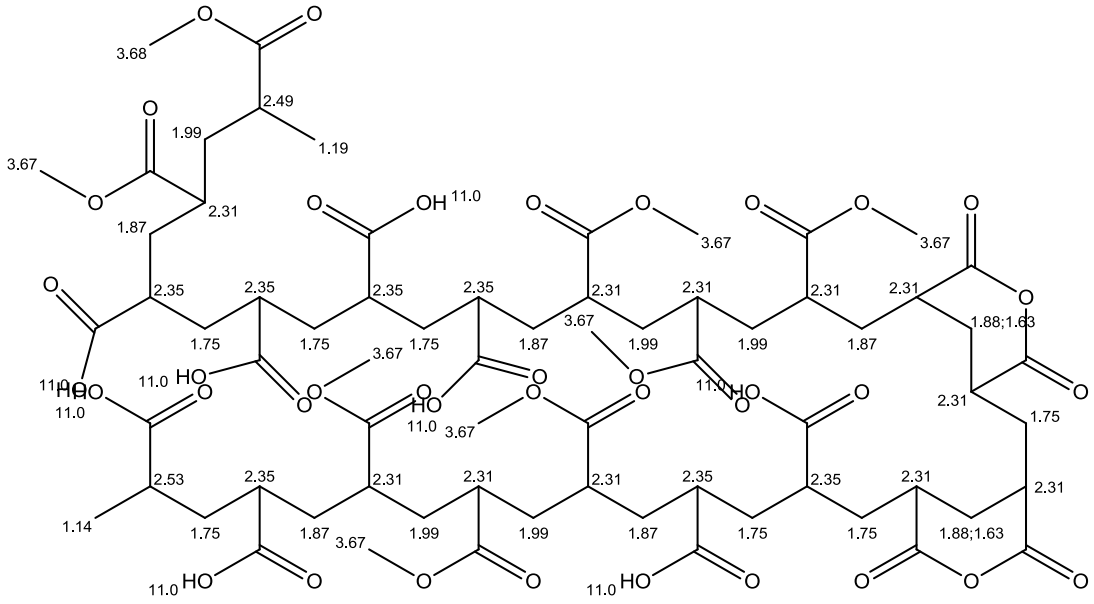

Figure 3.4 ChemDraw simulation of the NMR spectra of a theoretical poly(acrylic acid) copolymer.

The C-H resonance is shifted to 2.31 ppm, which is identical to that for the methyl ester. The -OCH_3 group in the methyl ester has a resonance at 3.67. The -OH proton resonance is located at 11.0 but its shift depends strongly on the solvent used and can be located significantly away from the predicted value.

The ^{1}H spectrum for the Carbomer A obtained after 24 hours dissolution in DMSO is shown in Figure 3.5. In addition to the predicted shifts for the acrylic acid and the anhydride groups, a characteristic peak at 3.30 ppm is observed which is assigned to the methyl ester. This spectrum suggests that the copolymer is a mixture of acrylic acid, the anhydride and the methyl ester. The ratio of OH / C-H / C-H_2 is 1:1:1. The ratio of O-CH_3 / C-H / C-H_2 is 1:3:3, suggesting the ratio of O-CH_3 / anhydride is 1:1. These gave a ratio of OH / O-CH_3 / anhydride of 3:1:1.

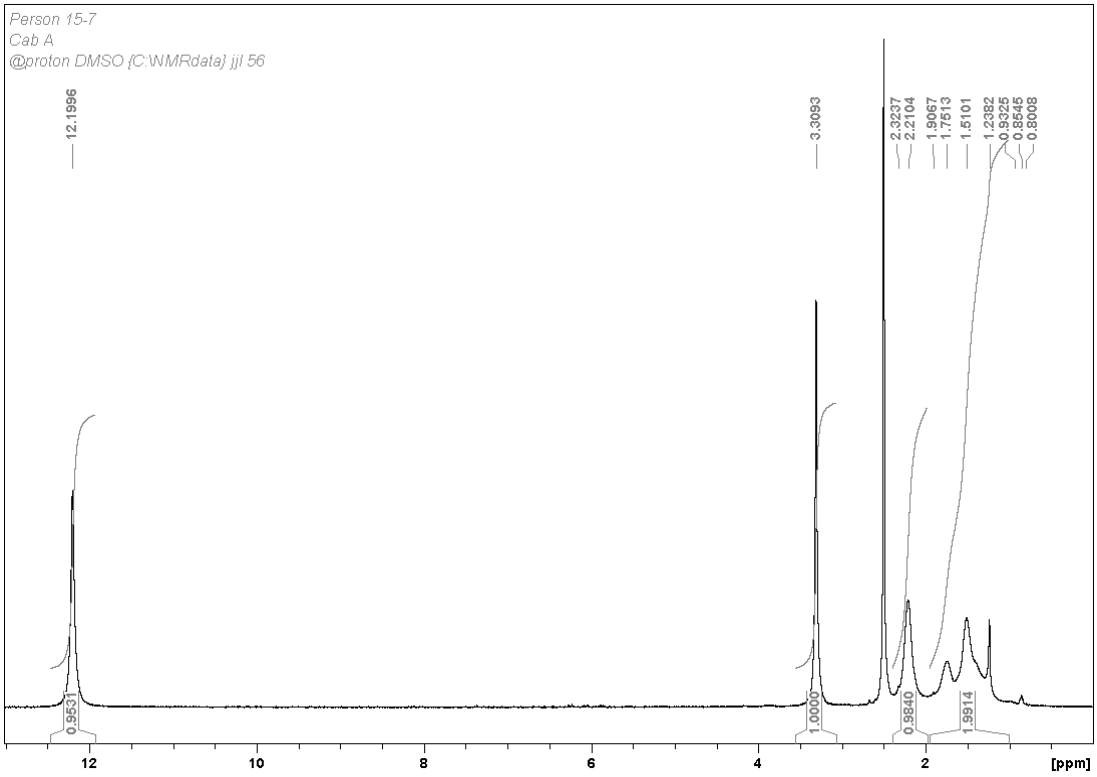

Figure 3.5 ^{1}H NMR spectra of Carbomer A in DMSO after 24 hours dissolution.

Another spectrum for Carbomer A was obtained after 3 weeks dissolution (Figure 3.6). The repeat of the ^{1}H NMR after 3 weeks was carried out to establish whether the initial spectrum was of a completely dissolved material or whether only partial dissolution had occurred. Analysis of the spectrum indicates that the ratio of OH / C-H / C-H_2 is 1:1:1. The ratio of O-CH_3 / C-H / C-H_2 is also 1:2:2, suggesting the ratio of O-CH_3 / anhydride is 2:1. These gave a ratio of OH / O-CH_3 / anhydride 4:2:1. The change in the spectrum could be a result in a change in the polymer composition due to more dissolution of polymer in

the solvent or methylation of the acrylic acid by the DMSO. The literature shows that DMSO can be used with methylating agents for the conversion of -OH functions to -OCH_3. However, it has not been possible to find direct reference to this reaction.

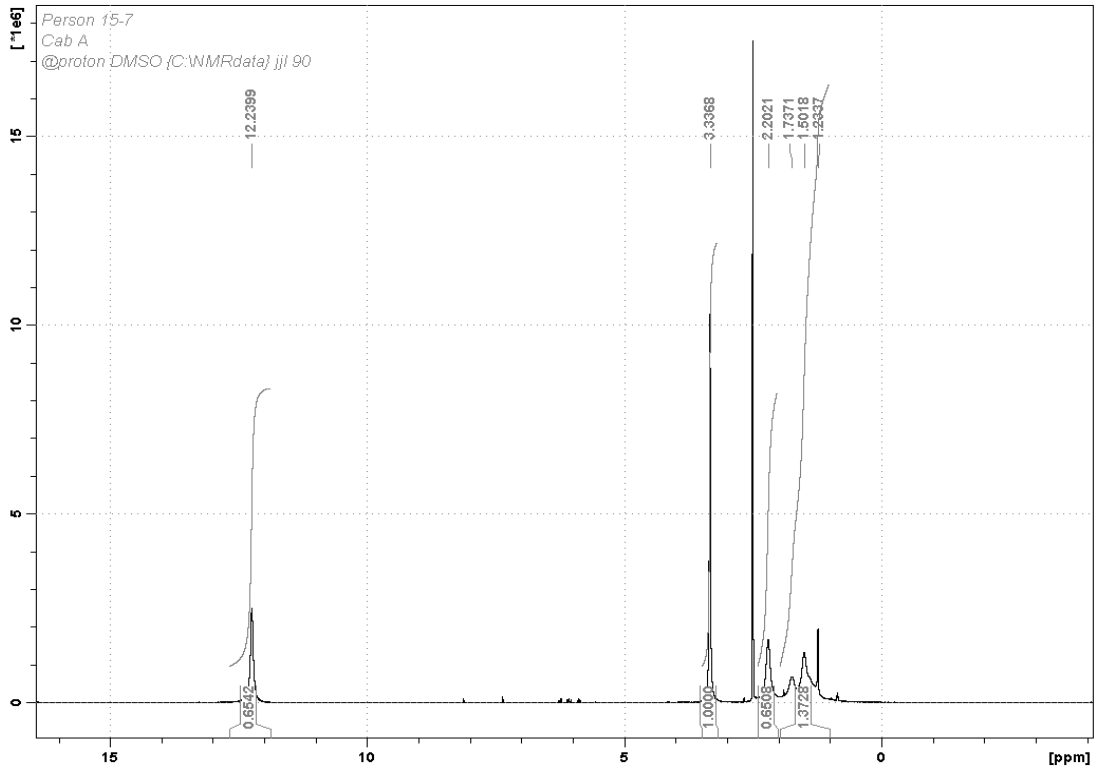

Figure 3.6 ^{1}H NMR spectra of Carbomer A in DMSO after 3 weeks dissolution.

Measurements were also conducted on Carbomer B and the spectra are shown in Figure 3.7 and Figure 3.8. Analysis of the spectrum indicated that it was very similar to Carbomer A dissolved in DMSO. The ratio of OH / C-H / C-H_2 is approximately 1:1:1. The ratio of O-CH_3 / C-H / C-H_2 is 1:3:3, suggesting the ratio of O-CH_3 / anhydride is 1:1. These gave a ratio of OH / O-CH_3 / anhydride 3:1:1. The spectrum after three weeks shows a very large increase in the intensity of the methyl peak.

The implication was that the extended period in DMSO was achieving methylation of the acrylic acid and hence the analysis in terms of the polymer being composed of three types of monomer was incorrect.

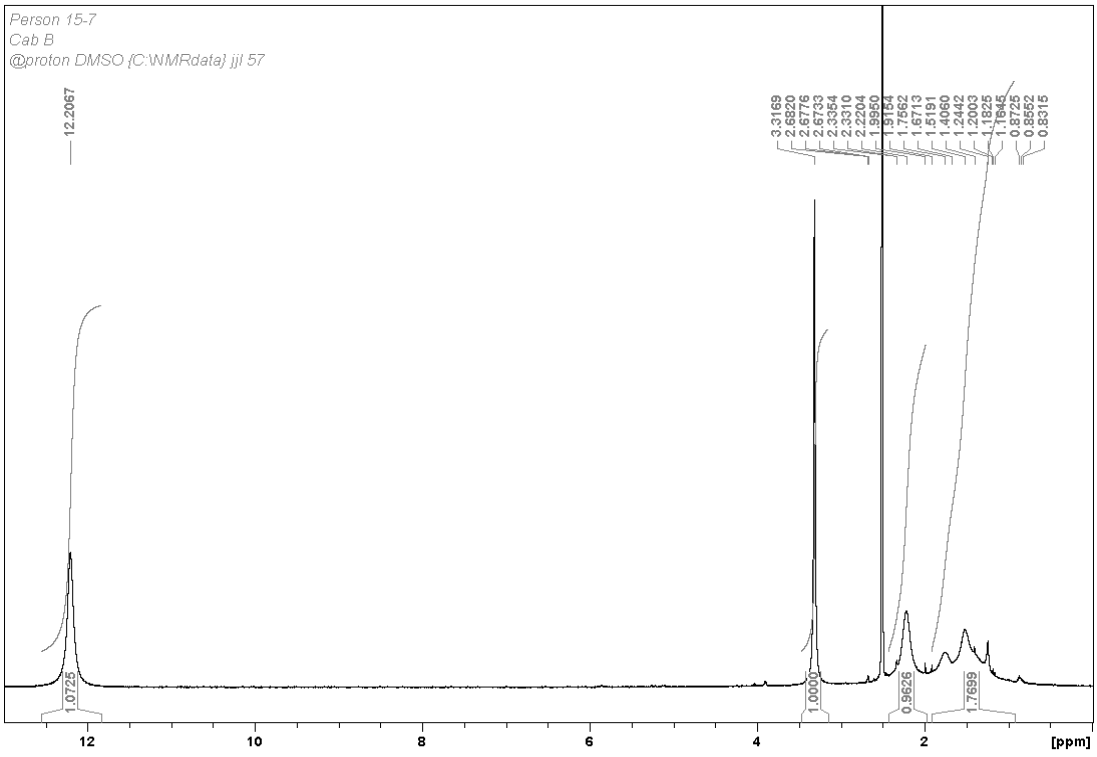

Figure 3.7 ^{1}H NMR spectra of Carbomer B in DMSO after 24 hours dissolution.

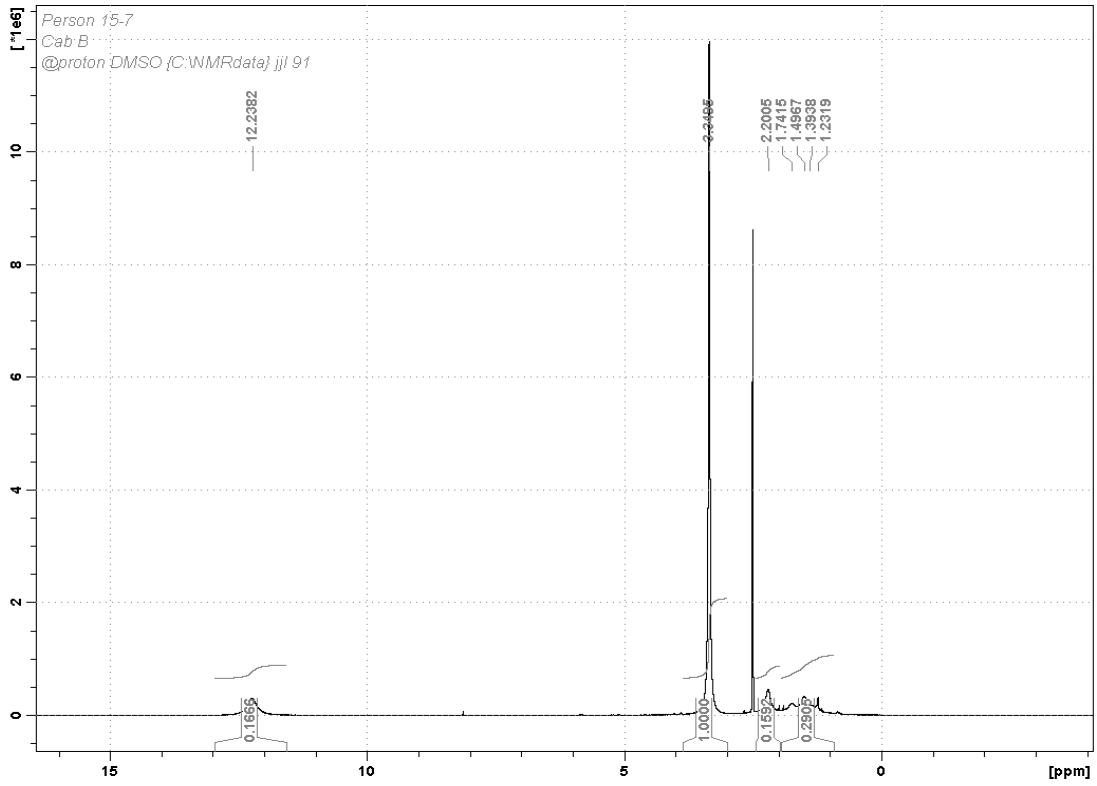

Figure 3.8 ^{1}H NMR spectra of Carbomer B in DMSO after 3 weeks dissolution.

Measurements of the ^{1}H NMR were performed in D_2O. In order to suppress the effects of water on the spectrum the pre-saturation pulse sequence (specifically, "ZPGR") was used. This pulse sequence suppresses the solvent relaxation time and allows observation of resonance which would otherwise be masked by the solvent. The solvent peak however can be broadened, as in the case of Carbomer A spectrum (Figure 3.9), if the frequency selected for the water resonance is not exact. The broadening of the peak also gives a slight asymmetry to the resonance. In the case of Carbomer B (Figure 3.10) a better match was achieved but the FT process has produced a small differentiation of the peak on the high field side. Both spectra indicate that there is not methyl peak present confirming that the polymers are purely acrylic acid polymer. In interpretation of the spectrum we have to be cautious as during the eight days required to achieve dissolution anhydride units could be hydrolysed back to the acid. Because of the pulse sequence used the -OH resonance is also suppressed.

The spectrum for Carbomer B is also very similar to that for Carbomer A there being slight differences in the intensity distribution. The spectra are characterised by peaks at; 2.30 ppm, 1.84 ppm which is a weak shoulder on the side of the peak at 1.64 and there is also a peak at 1.26 ppm.

Computer simulations were carried out of various sequence structures (Figure 3.11). A sequence of 5 acrylic acid with an anhydride group predicts peaks at 2.35 ppm associated with the C-H next to the acrylic acid, 1,75 ppm for the CH_2 bridging peak. This does not however explain the peak at 1.26 ppm which is a minor shoulder on the main peak.

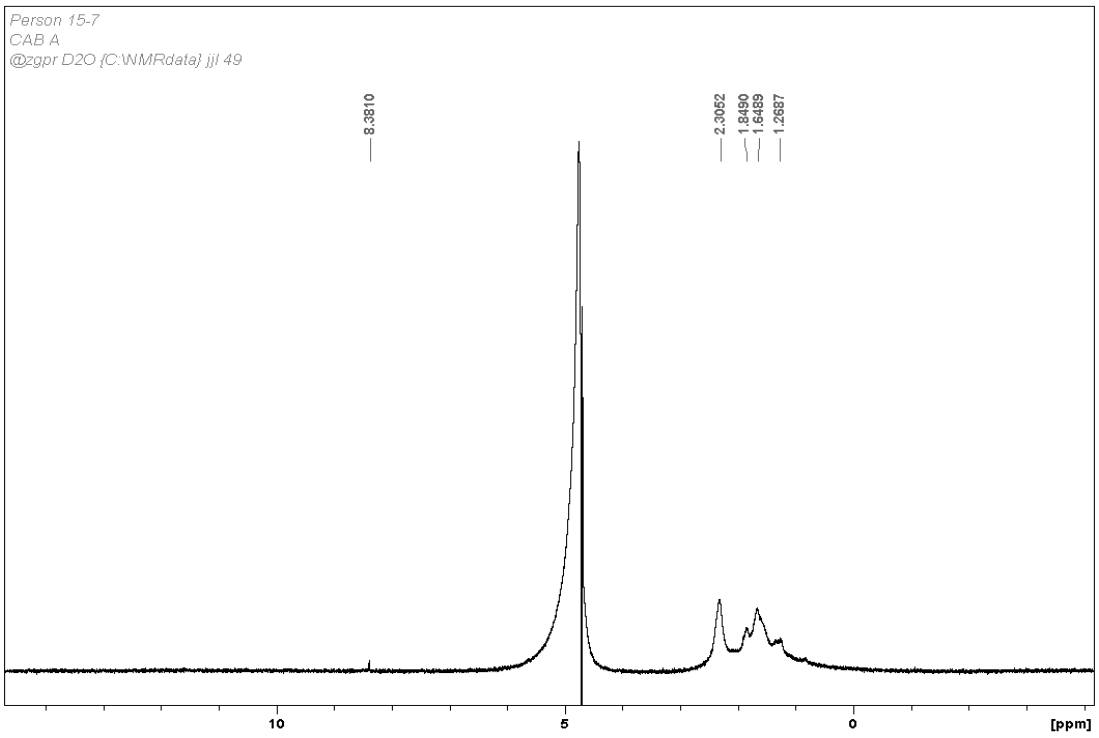

Figure 3.9 D_2O NMR spectrum of Carbomer A after 8 days dissolution.

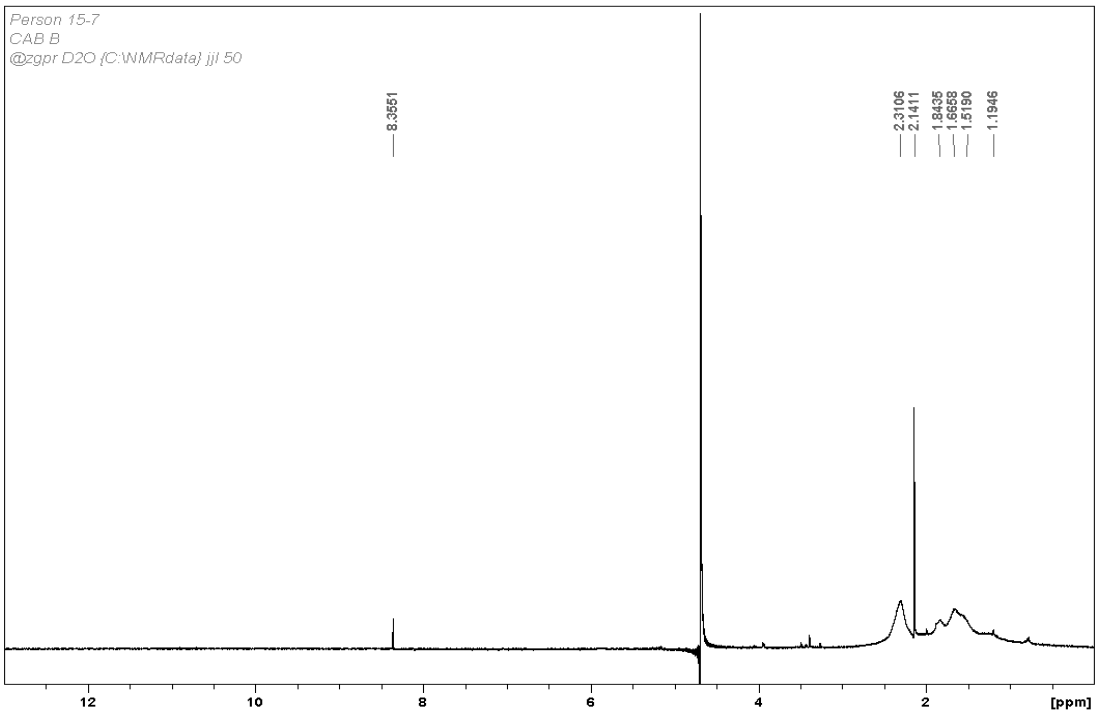

Figure 3.10 D_2O NMR spectrum of Carbomer B after 8 days dissolution.

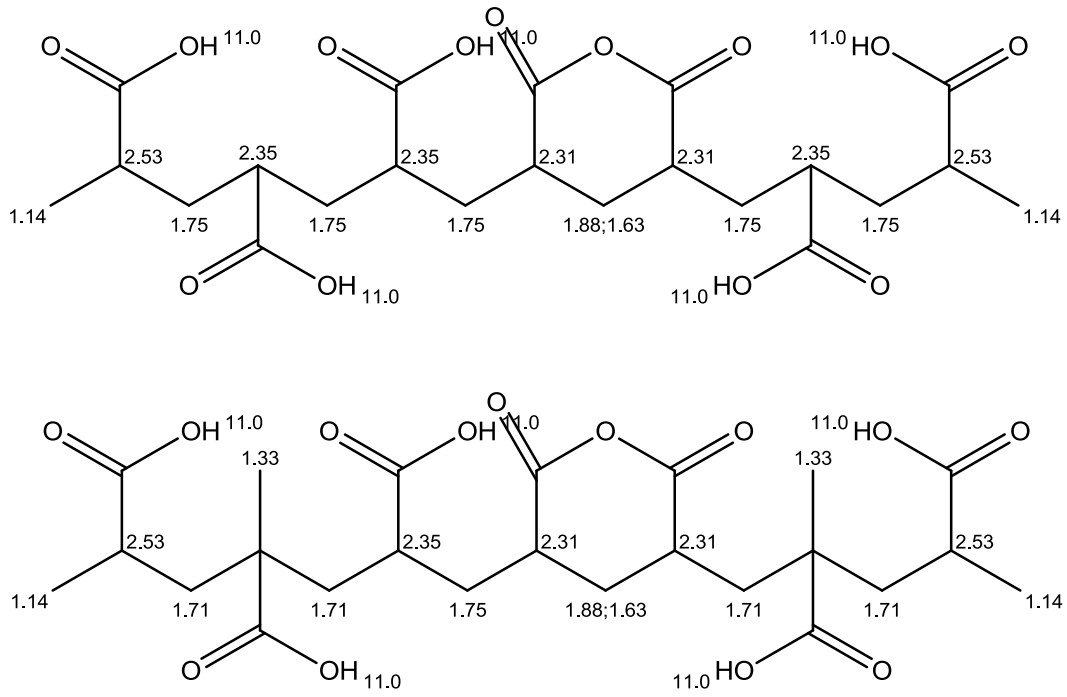

Figure 3.11 Computer simulation of the possible Carbomer structures.

If instead of acrylic acid a certain amount of methacrylic acid is incorporated then a peak would be predicted at 1.33 ppm which is close to the observed resonance at 1.26 ppm. This would suggest that a small amount of methacrylic acid has been incorporated into the polymer. The anhydride gives two peaks for the bridging CH_2 at 1.88 and 1.63 ppm, the splitting being due to the restriction in the conformation of the ring on forming the anhydride. The weak peak observed at 1.84 ppm is consistent with the anhydride formation. The approximate ratios of the peaks are indicated in Table 3.1. This implies that Carbomer B has a slightly higher level of methacrylic acid and also anhydride links. The anhydride links, although shown in the simulation to be within a single chain, will also be between chains and are presumably one of the mechanisms for achieving a high molecular weight polymer.

The peaks overlap and hence there is a significant level in uncertainty in the fractions calculated. The very weak peaks in the region of 3.5 ppm in Carbomer B are indicative of the pentaerythritol unit and indicate that this polymer is very lightly cross-linked. The intensity of this peak indicates that the pentaerythritol units are present in the order of

less than 3 wt%. Quantification of the peak intensities is only approximate as their intensities can be influenced by differences in chain mobility.

The anhydride units can create crosslinks between PAA chains which will effectively increase the molecular weight of the PAA but will also convert it from a linear to a branched chain polymer structure. Branched chains will also be created by the incorporation of pentaerythritol into the PAA.

Table 3.1 Analysis of the peak intensities for Carbomer A and B

Polymer	**Carbomer A**	**Carbomer B**	**Designation**
Resonance (ppm)	Intensity (fraction)		
1.84	0.21±0.04	0.24±0.04	Anhydride
1.64	0.76±0.05	0.72±0.05	Acrylic acid
1.26	0.03±0.02	0.04±0.03	Methacrylic acid

3.2.3. Intrinsic Viscosity and Molecular Weight Determination

Through intrinsic viscosity measurements, the hydrodynamic volume of the polymer can be determined; and hence the molecular weight [1, 2]. The intrinsic viscosity, $[\eta]$, is the extrapolation to infinite dilution of the viscosity increment. For polyelectrolytes the hydrodynamic volume depends on the media in which the polymer is dispersed [3]. In a medium of high dielectric constant, polyelectrolytes are often ionised and the molecules assume extended configurations as a result of electrostatic interactions between charged groups. The total electrostatic repulsion depends on the number of charged groups and on the ions present in solution. The former is usually expressed in terms of the degree of ionization, *i*. The ions present in solution are the counter ions created by the dissociation of the polymer and ions which may be added to the solution, usually an inorganic or organic salt. The ionic strength, μ, of the solution can then be defined as $\mu = \frac{1}{2}\sum_{\mathrm{j}}(c_{\mathrm{m}})_{\mathrm{j}} m_{\mathrm{j}}^2$,

where $(C_m)_j$ is the molarity and m_j the charge on the j^{th} ion. Salts with low molar mass suppress the electrostatic repulsion of charged groups. At sufficiently high concentration, c_e, the repulsion is reduced to such an extent that the configuration and the solution properties are similar to those on a non-ionic polymer, and the behaviour of the chains becomes governed by excluded volume factors. The Mark-Houwink coefficients, K and α, are constants that depend on the polymer, the temperature, and the solvent used. Chu et al. [4] and Tsvetkov et al. [5] have reported studies of the measurement of the intrinsic viscosity of PAA with added salt. The values of K and α were shown to depend on the salt concentration. For PAA in solutions with NaBr at 25°C, values of $K \times 10^3$ and α, respectively, of 124 and 0.50 at c_{NaBr} = 1.5M, of 25.4 and 0.75 at 0.1M, and of 13.6 and 0.89 at 0.01M have been reported [6]. At high ionic strength, the value of α approaches the ideal random coil coefficient of 0.5, however at these high values the polymer is approaching a condition where precipitation can occur due to salting out. For this study we follow the procedure outlined by Tsvetskov et al. [5], in which the PAA was neutralized by the addition of an appropriate quantity of sodium hydroxide, and sodium chloride was used as the neutral electrolyte (concentration 0.012M). The appropriate values of the coefficients of the Mark-Houwink equation are $K = 11.9 \times 10^{-3}$ mL g^{-1} and $\alpha = 0.8596$ [4]. The high value for α is consistent with the chain being in an extended conformation under these conditions. The intrinsic viscosity values were obtained using Figure 3.12 and Figure 3.13.

$$[\eta]_A = 54.70 \pm 0.90$$

$$[\eta]_B = 10.37 \pm 0.22$$

Estimates of molecular weights are obtained using the above values in the Mark-Houwink equation.

$$Mw_A = 3.86 \times 10^6 \frac{g}{mol}$$

$$Mw_B = 5.60 \times 10^5 \frac{g}{mol}$$

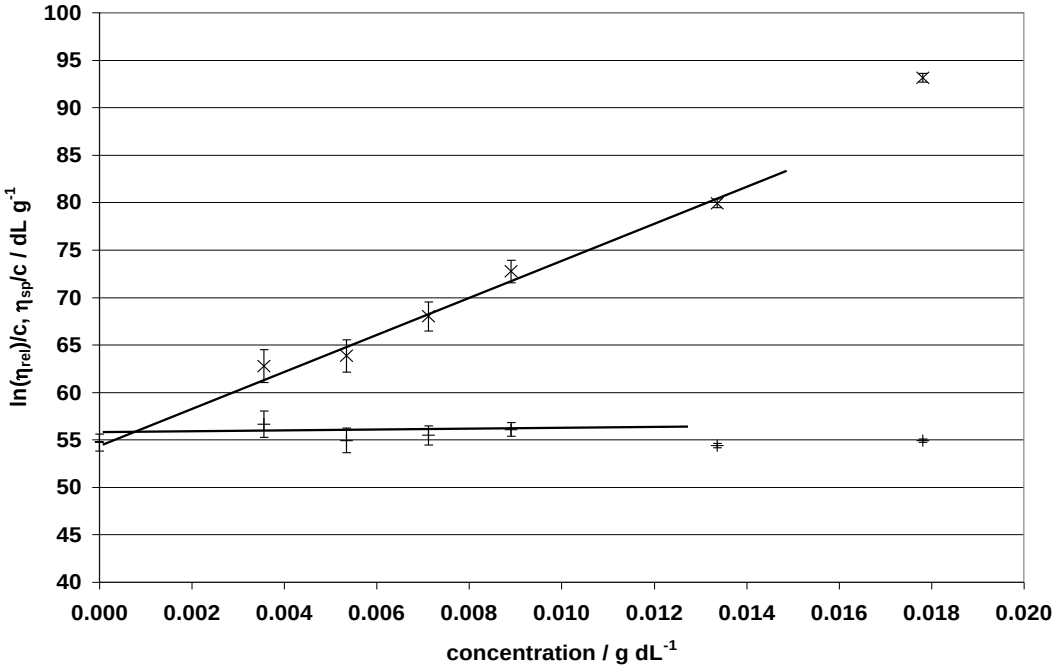

Figure 3.12 Determination of intrinsic viscosity at 20°C in deionised water for Carbomer A. Symbols are: (+) $\ln(\eta_{rel})/c$; (×) η_{sp}/c.

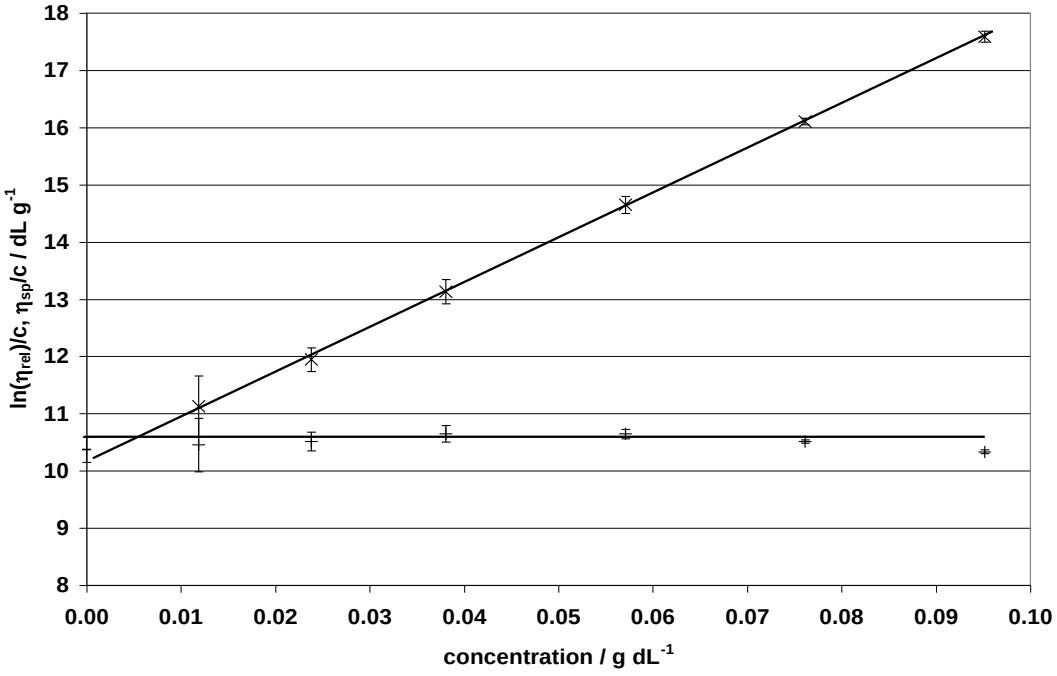

Figure 3.13 Determination of intrinsic viscosity at 20°C in deionised water for Carbomer B. Symbols are: (+) $\ln(\eta_{rel})/c$; (×) η_{sp}/c.

The molecular weight of Carbomer A is approximately the same as the supplier's nominated value, 4MDa. However the value of Carbomer B is significantly smaller than the 5MDa nominated value. These values indicate that the polymers are cross-linked through the formation of anhydride linkages, or possibly hydrophobically modified by incorporation of methyl acrylic acid or a proportion of pentaerythritol units. It is worth noticing that the intrinsic viscosity and hence hydrodynamic volume of a branched polymer arising from the formation of anhydride cross-links will be lower than that of the equivalent linear polymer [7]. As a consequence the values of *Mw* obtained above must be considered to represent lower limiting values, and that for Carbomer B, a more highly branched polymer, is artificially low.

The intrinsic viscosities of solutions produced using the slow dissolution method and the higher shear approach were compared and were found to be comparable indicating that viscosity changes occurring during dissolution are probably associated with changes in the extent to which PAA forms clusters rather than degradation of the polymer.

3.2.4. Monomer Equivalent Weight Determination

The concentration of both Carbomer A and B solution is 0.1 g dL^{-1}; the electrolyte level had been adjusted to 0.012M by adding sodium chloride (solid state) to the solution [5]. The pH values of the original solution before neutralization were 2.97 for Carbomer A and 2.94 for Carbomer B, after the electrolyte level adjustment. Plot pH values against weight ratio (weight of sodium hydroxide over weight of polymer); the results are shown in Figure 3.14 and Figure 3.15.

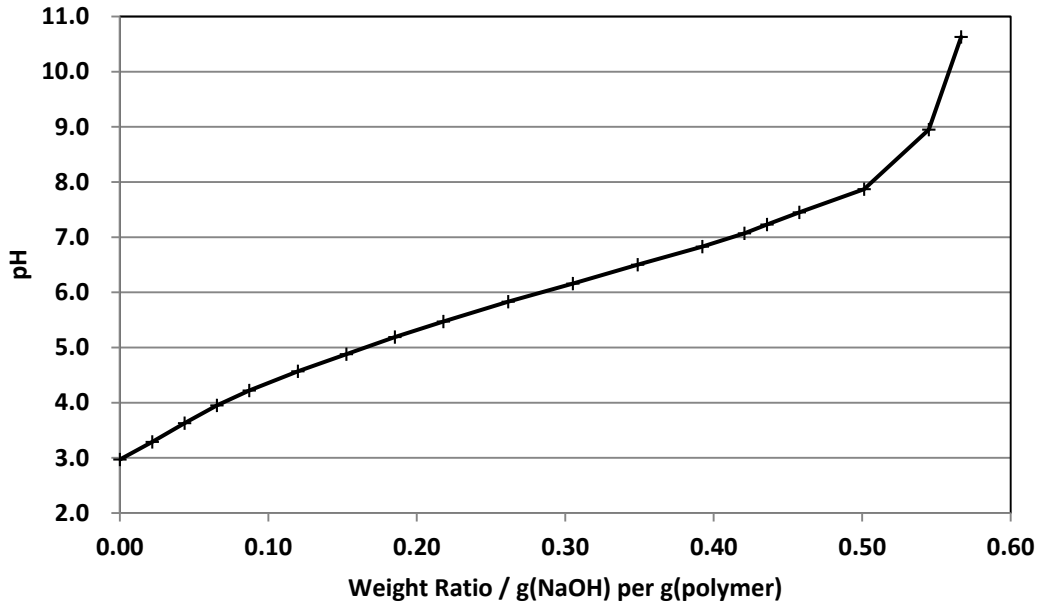

Figure 3.14 pH changes for Carbomer A in neutralization titration.

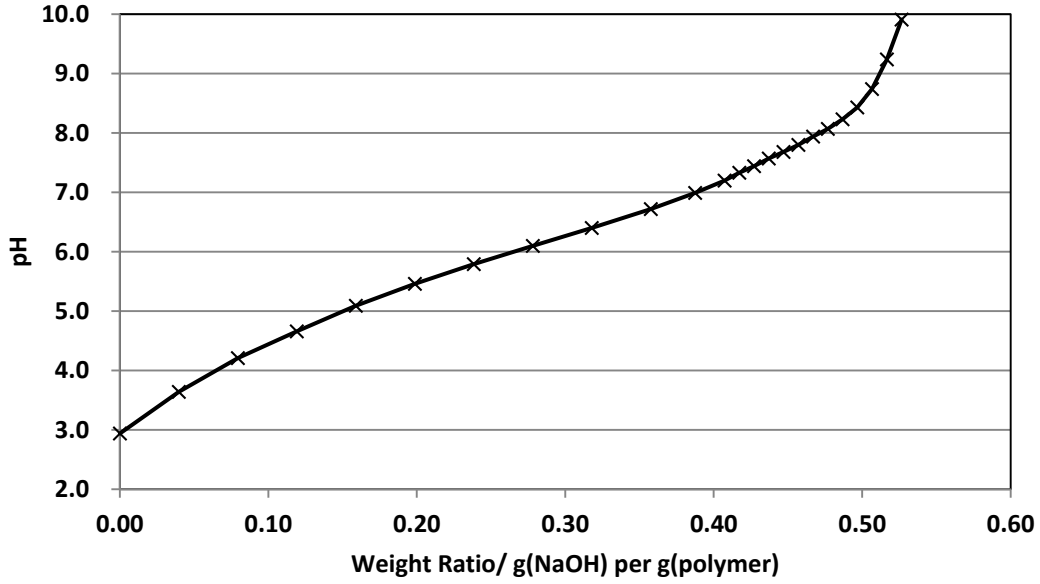

Figure 3.15 pH changes for Carbomer B in neutralization titration.

Because of their weak abilities to ionise in water, both polymers were neutralized until pH values of solutions reach 10.0. For Carbomer A, after the point (0.50, 7.87) the slope of the curve exhibited a significant increment. Therefore this point has been assumed as the neutral point at which all carboxylic acid groups have been ionised. Based on such

assumption the equivalent mass of Carbomer A is calculated to be 79.99. For Carbomer B, the breaking point is identified to be (0.49, 8.23); and the equivalent mass of Carbomer B is 81.63. Both values are greater than that of acrylic acid monomer which is 72. As pointed out by Volk et al. [8] the effective molecular weight can be influenced by association with the electrolyte and the pH. These values indicate that the polymers are cross-linked through the formation of anhydride linkages or possibly hydrophobically modified by incorporation of methyl acrylic acid or a proportion of vinyl ester. The proportions of the latter must be very low as these were not detected by NMR.

3.3. Rheological Measurements

3.3.1. Materials and Methods

Both Carbomer A and Carbomer B were initially dissolved in distilled water at a significantly higher concentration and allowed 5 days while gently stirring to achieve homogeneity. After complete dissolution, they were diluted with distilled water to a series of different concentration (Table 3.2). Electrolyte level for all sample solutions was adjusted to 0.012M of sodium chloride. Initially all samples were not neutralized and a series of creep tests were performed; another set of tests were then performed on the first 5 samples of each polymer group which were neutralized to pH 7 using 1 M potassium hydroxide solution for parallel comparison.

Creep tests were performed using AR1000N rheometer (TA Instruments, Crawley, UK) using a 4-cm parallel plate geometry fitted with a solvent trap at 20°C. The zero shear viscosities were estimated from creep measurements, by steadily reducing the applied stress, and determining the resultant shear rate in the dissipative part of the response curve. The results were extrapolated back to a shear rate of 10^{-6} s^{-1}.

Each solution was also tested on the same rheometer with the same geometry fitting at a temperature of 20°C over a shear rate range of 1 to 1000 s^{-1}, values being increased

logarithmically over a 30 minute period. The AR1000N rheometer is a stress-controlled rheometer. Shear rate controlling is achieved by adjusting the applied stress and measuring the torque feedback to reach required shear rate.

Table 3.2 Sample polymer concentration for rheological measurements

Series Carbomer A	**Polymer Concentration (g dL^{-1})**	**Series Carbomer B**	**Polymer Concentration (g dL^{-1})**
A-1	0.2145	B-1	0.4369
A-2	0.1608	B-2	0.3276
A-3	0.1072	B-3	0.2184
A-4	0.0804	B-4	0.1638
A-5	0.0536	B-5	0.1092
A-6	0.0268	B-6	0.0546
A-7	0.0134		

3.3.2. Results and Discussion

Through creep tests, the steady state viscosities at zero shear rate, which in this case is an arbitrary value of 10^{-6} s^{-1}, were extrapolated and shown below (Figure 3.16 and Figure 3.17). Whilst for the very dilute solutions the viscosity is almost independent of shear rate, at the higher concentrations significant shear thinning is observed. Combining these data with the viscosity measurements obtained using the Ubbelohde viscometer produces a plot of the relative viscosity against concentration (Figure 3.18). For Carbomer A, in the low concentration range, the viscosities estimated from the creep experiments are slightly higher than those measured from the Ubbelohde viscometer experiments; the shear rate is less well defined in the capillary viscometer and a lower value would be consistent with shear-thinning. In both systems, a clear concentration

can be identified at which the rheological behaviour changes from that associated with the 'isolated' polymer chain to one in which polymer-polymer interactions have to be considered. It is also clear from the data presented in Figure 3.16 and Figure 3.17 that these solutions are able to exhibit marked shear thinning, and in the context of their application as thickeners this shear rate dependence could be very important in understanding their action in applications where changes are occurring in the shear stresses, such as on an aircraft in the initial stages of take-off.

For the ideal polymer chain, increasing the concentration changes the viscosity behaviour as the isolated polymer chains start to interact. Plotting the relative viscosity against concentration clearly indicates that there is a threshold concentration, c_t, at which polymer–polymer interactions start to play a dominant role. For Carbomer A this occurs at 2.117×10^{-2} g dL^{-1} and for Carbomer B at 8.021×10^{-2} g dL^{-1}. If the polymers have similar architecture then the product $c_t[\eta]$ should be constant. The value for Carbomer A is 1.167 and for Carbomer B is 0.832. For linear non-ionic polymers, a value of between 1 and 2 for the product $c[\eta]$ usually indicates the onset of polymer-polymer interactions. However, if the polymer is more branched, the hydrodynamic volume of the molecules does not simply scale as molecular weight. The differences in the values of $c[\eta]$ for Carbomer A and Carbomer B are a reflection of a more highly branched structure in Carbomer B compared with Carbomer A, and support the conclusions from the previous intrinsic viscosity analysis. Branched chain structures can be created through anhydride formation or incorporation of vinyl pentaerythritol and these will be difficult to observe spectroscopically.

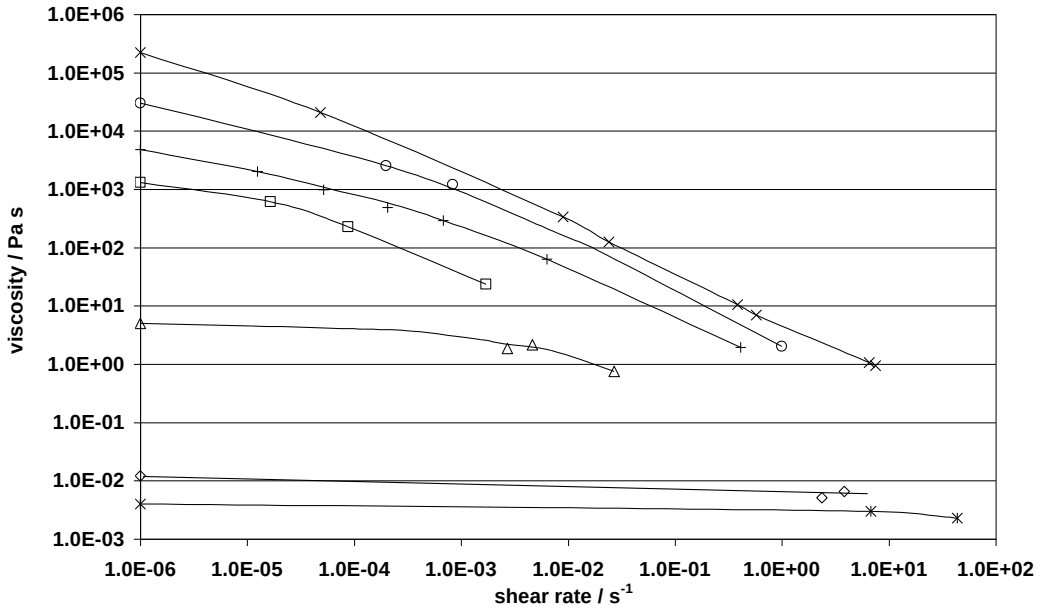

Figure 3.16 Viscosity/shear rate plots for Carbomer A. Symbols are (×) A-1, c=0.2415 g/dL, (○) A-2, 0.1608 g/dL, (+) A-3, 0.1072 g/dL, (□) A4, 0.0804 g/dL, (△) A-5, 0.0536 g/dl, (◊) A-6, 0.0268 g/dL, (*) A-7, 0.0134 g/dL.

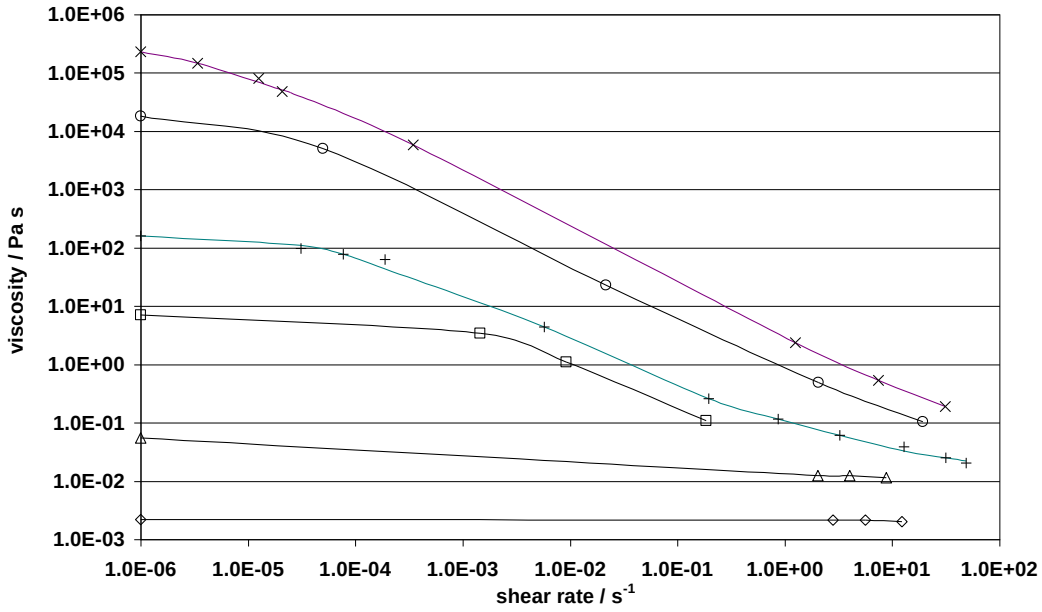

Figure 3.17 Viscosity/shear rate plots for Carbomer B. Symbols are (×) B-1, *c*=0.4369 g/dL, (○) B-2, 0.3276 g/dL, (+) B-3, 0.2184 g/dL, (□) B-4, 0.1638 g/dL, (△) B-5, 0.1092 g/dl, (◊) B-6, 0.0546 g/dL.

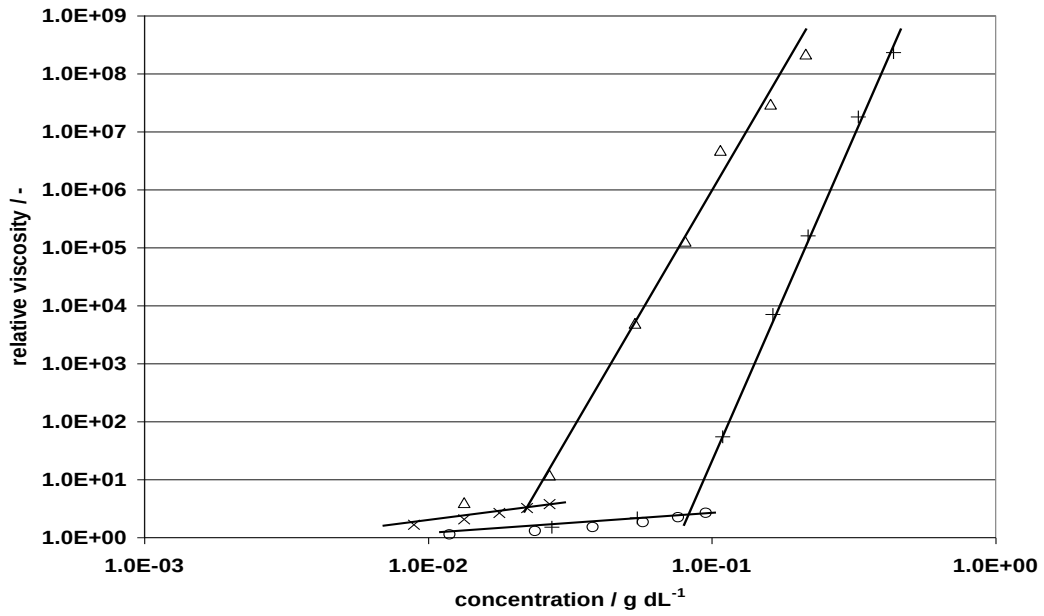

Figure 3.18 Plot of the relative viscosity against concentration for Carbomer A and Carbomer B. Symbols are: (△, +) extrapolated 10^{-6} s^{-1} shear rate values; (×,○) Ubbelohde viscometer measured values.

Redrawing Figure 3.16 and Figure 3.17 as Figure 3.19 and Figure 3.20, in which the independent variable (abscissa) is the shear stress, enables an estimate to be made of any dynamic yield stress present in the fluid. The existence of a yield stress in pseudoplastic materials, such as concentrated suspensions, pastes, foams and composites (i.e. fluids containing particles of colloidal size) has been well documented [9]. Whether a polymer solution can exhibit a yield stress has been the subject of much discussion [10], but what has emerged is that, at very low levels of shear, these fluids can exhibit very high levels of viscosity; then, over a limited range of shear stress, the viscosity can fall dramatically. This has been compared to yield in solids, and so a new idea of a "yield stress" has evolved – a "static" one where a finite stress has to be developed in order for the fluid to flow, and a "dynamic" one in which the increasing stress in a slowly flowing fluid causes the viscosity to fall rapidly.

It is difficult from the plots to determine precise points at which the viscosity/stress curves change slope, however there is a clear progression in the case of both polymer

systems. For Carbomer A, the curve for a concentration of 0.2415 g dL^{-1} changes slope at a viscosity of approx. 10^4 Pa s and a stress of approx. 1 – 2 Pa. Reducing the concentration to 0.1608 g dL^{-1} reduces the critical points to a value of viscosity of 1.5×10^3 Pa s and a stress of approx. 0.9 – 1.5 Pa. Decreasing the concentration further to 0.1072 g dL^{-1} further deceases the critical viscosity to 2×10^2 Pa s and a stress of 0.3 – 0.45 Pa. Further decrease of the polymer concentration to 0.0804 g dL^{-1} leads to the reverse and an increased value of 5×10^2 Pa s but with a stress level of 0.02 – 0.03 Pa. At a concentration of 0.0536 g dL^{-1} the viscosity is approx. 1.5 Pa s and the stress 0.015 Pa. The lower concentrations do not show a change of viscosity with increasing stress level.

These shear thinning characteristics parallel the observations (Figure 3.16 and Figure 3.17) of the shear rate behaviour and are indicative of the complex deformation of the polymers during shear. In the context of the de-icing fluids, as air flow increases over the aerofoil the levels of stress will increase, and as a consequence the probability for the fluid to be removed from the wing will be increased.

For Carbomer B, the points at which changes occur are more clearly defined. At a concentration of 0.4369 g dL^{-1} and a viscosity of 8×10^4 Pa s the stress level is 2 – 3 Pa. Reducing the concentration to a value of 0.3276 g dL^{-1} reduces the break point to a viscosity of approx. 8×10^3 Pa s and a stress of 0.2 – 0.4 Pa. Further reduction of the concentration to 0.2184 g dL^{-1} shows that over the range measured it is always in a shear thinning condition. Lowering the concentration to 0.1638 g dL^{-1} reveals a break point at a viscosity of 5 Pa s and a stress level of 0.008 – 0.012 Pa.

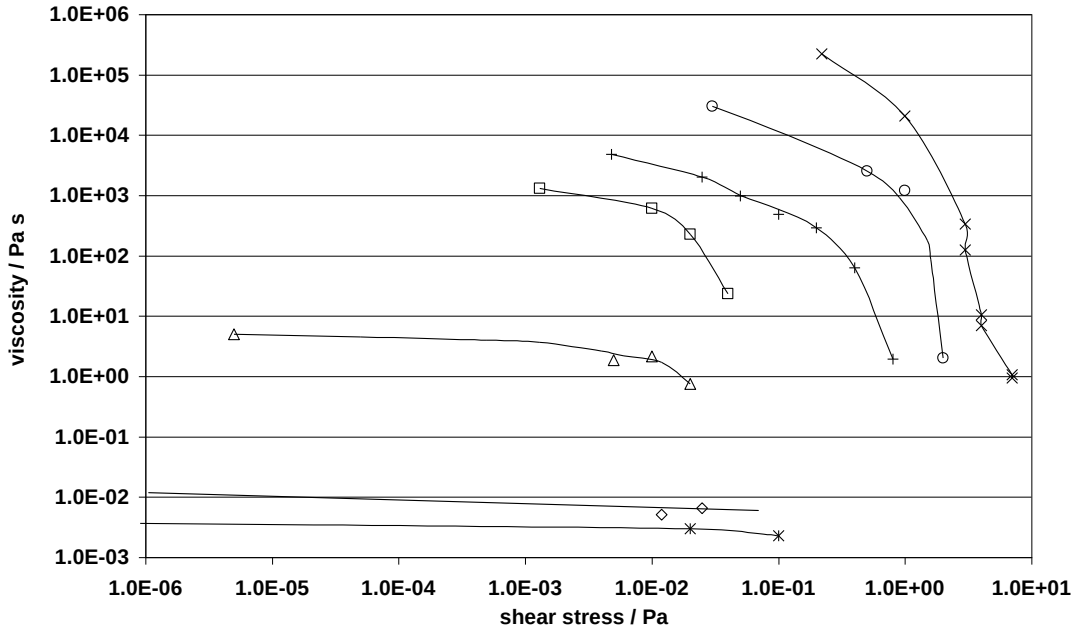

Figure 3.19 Viscosity/shear stress plots for Carbomer A. Symbols are (×) A-1, c=0.2415 g/dL, (○) A-2, 0.1608 g/dL, (+) A-3, 0.1072 g/dL, (□) A4, 0.0804 g/dL, (△) A-5, 0.0536 g/dl, (◊) A-6, 0.0268 g/dL, (*) A-7, 0.0134 g/dL.

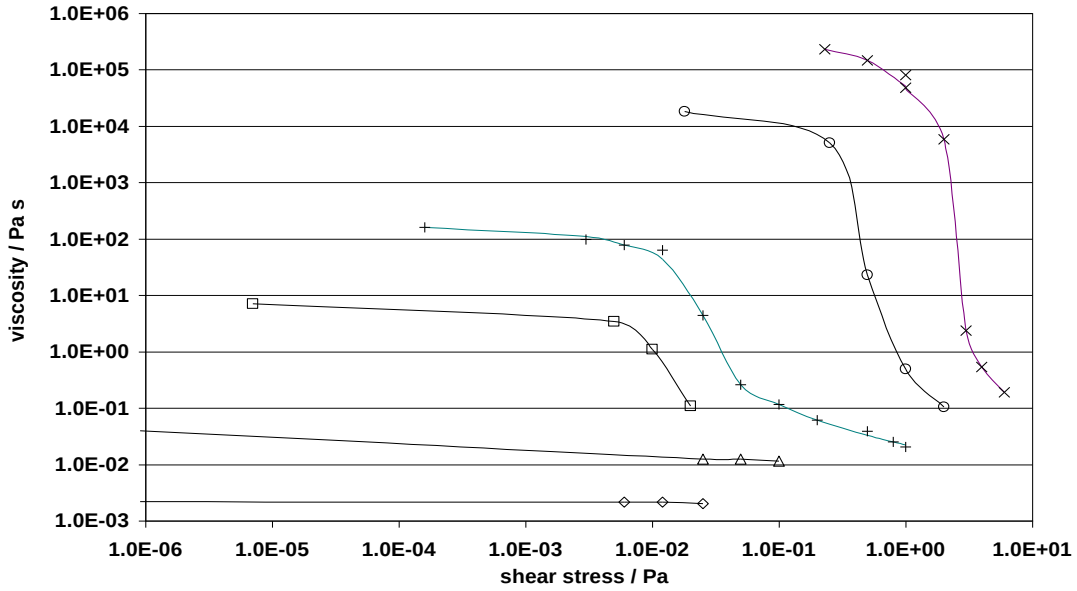

Figure 3.20 Viscosity/shear stress plots for Carbomer B. Symbols are (×) B-1, c=0.4369 g/dL, (○) B-2, 0.3276 g/dL, (+) B-3, 0.2184 g/dL, (□) B-4, 0.1638 g/dL, (△) B-5, 0.1092 g/dl, (◊) B-6, 0.0546 g/dL.

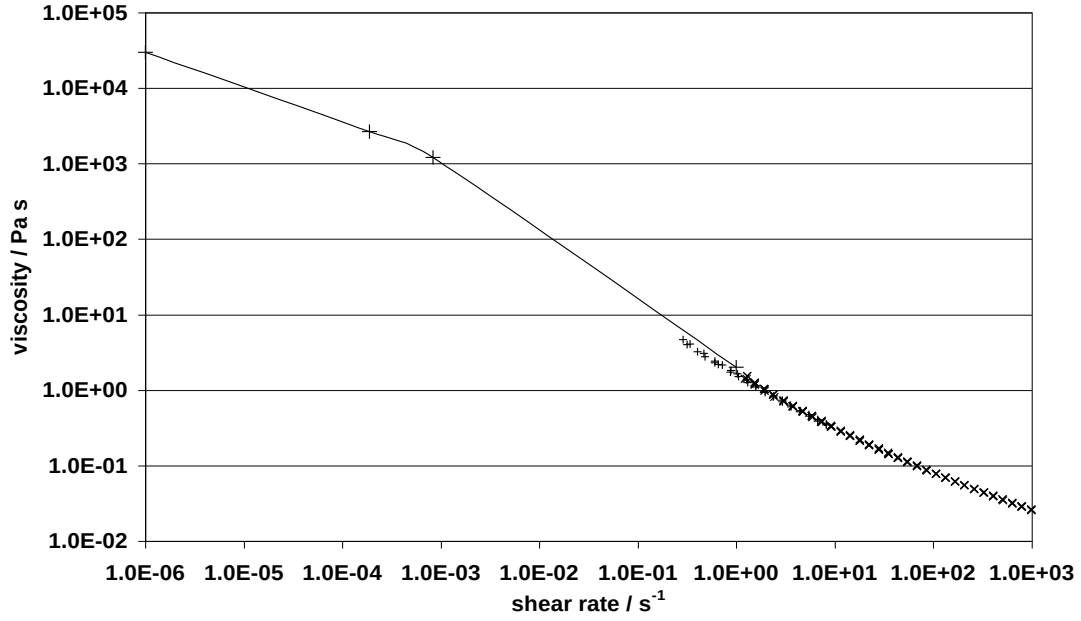

Figure 3.21 Shear rate dependence of the viscosity for Carbomer A at 0.1608 g/dL at 20°C. Symbols are: (+) viscosity measured via creep tests; (×) viscosity measured via steady shear flow tests.

Comparison of the data for the two polymers indicates that there are significant differences between these materials in terms of their ability to form an extended network structure which leads to an enhanced viscosity. If the polymers had similar architectures then it would be expected that the variation of the break points would scale as the molecular weight.

Steady shear tests provided information on rheological behaviours in an extended range of shear rate. Combining steady shear and creep data, a typical curve is shown for Carbomer A at a concentration of 0.1608 g dL^{-1} (Figure 3.21). Solutions at other PAA concentrations also exhibited the same shear-thinning behaviour at higher ranges of shear rate.

Once the sample solutions have been neutralized to pH 7, the rheological behaviours of both polymer systems changed significantly. It is known that the size of the PAA will be influenced by the pH and this in turn will influence the viscosity. In the case of non-

polyelectrolytes, increasing the concentration of the polymer in solution leads to a point where dramatic changes in the viscosity occur which can be associated with the onset of entanglement and the rheology becomes controlled by reptation processes. In the case of polyelectrolyte systems, polymer-polymer interactions can lead to significant effect on the rheological characteristics of the materials. The polymer molecules were initially knotted together tightly via hydrogen bonding. As they are partially neutralized with an appropriate base, the molecules are stretched and expanded when electrostatic forces become dominant over the normal inter-molecular interactions and in dilute solution the chain is forced to adopt a highly extended structure. This allows more polymer-polymer interactions to occur and causes the formation of a gel type of network structure and the viscosity of solutions increases dramatically. The results shown below (Figure 3.22 and Figure 3.23) are examples of the changes in viscosity of polymer solutions after partial neutralization. A solution with 0.4369 g dL^{-1} of Carbomer B (B-1) became very viscous and air bubbles were trapped in the solution during neutralization which resulted in a condition that was not suitable for rheological measurements. For such a viscous material, it is difficult to neutralize the solution and achieve homogeneity through addition of concentrated potassium hydroxide solution. Large bubbles trapped in the fluid will also be problematic.

The intrinsic viscosity and titration data indicate that these polymers have different architectures and that Carbomer B can be more highly branched than Carbomer A. From Figure 3.24 it is clear that at same polymer concentrations, approx. 0.11, 0.16, and 0.21 g dL^{-1}, viscosity of Carbomer A is generally higher than Carbomer B. Assume that the molecular weight of Carbomer B is higher compared to Carbomer A (5MDa to 4MDa, nominated), Carbomer B is clearly more sensitive to electrolyte addition. The fact that electrolyte effectively shields bindings of neighbouring carboxylic groups and causes decrease in viscosity may suggest that Carbomer B is more highly branched material. The impact of electrolyte on both Carbomer solutions will be further investigated and discussed in Chapter 5.

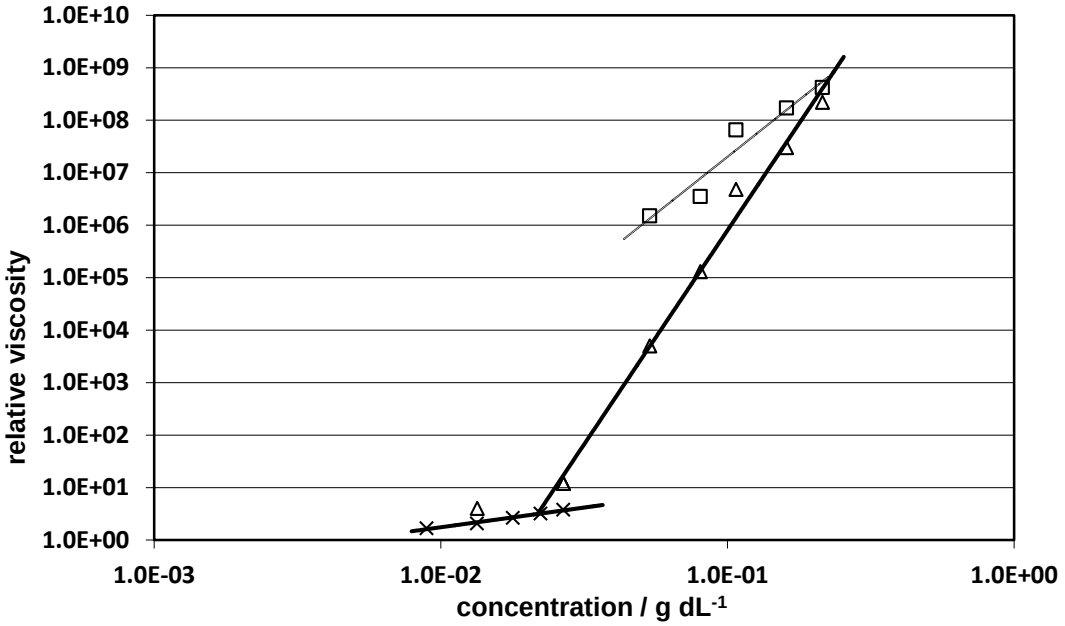

Figure 3.22 Plot of the relative viscosity against concentration for Carbomer A. Symbols are: (△) extrapolated 10^{-6} s^{-1} shear rate values, un-neutralized; (□) extrapolated 10^{-6} s^{-1} shear rate values, neutralized; (×) Ubbelohde viscometer measured values.

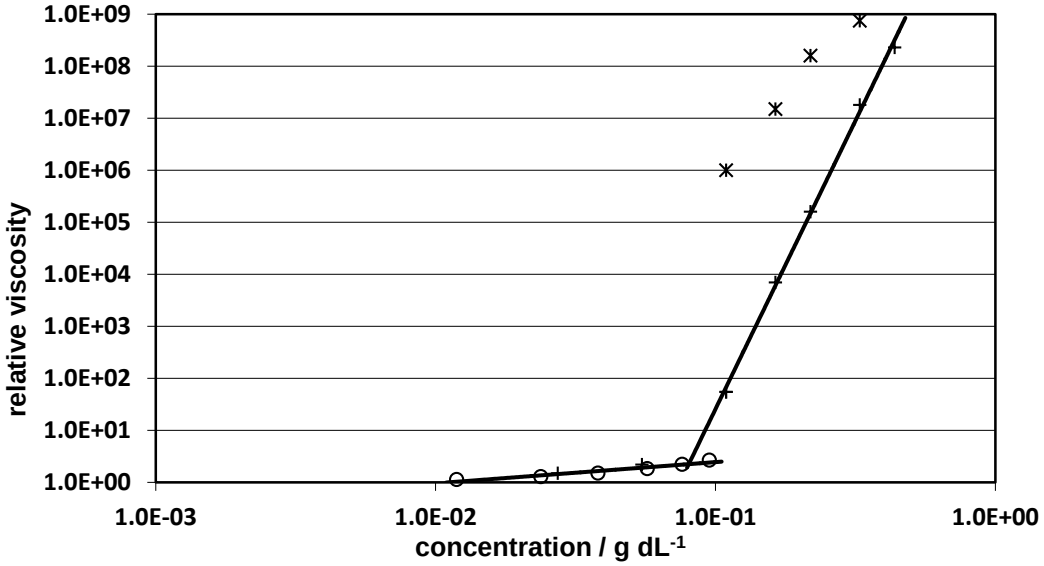

Figure 3.23 Plot of the relative viscosity against concentration for Carbomer B. Symbols are: (+) extrapolated 10^{-6} s^{-1} shear rate values, un-neutralized; (*) extrapolated 10^{-6} s^{-1} shear rate values, neutralized; (○) Ubbelohde viscometer measured values.

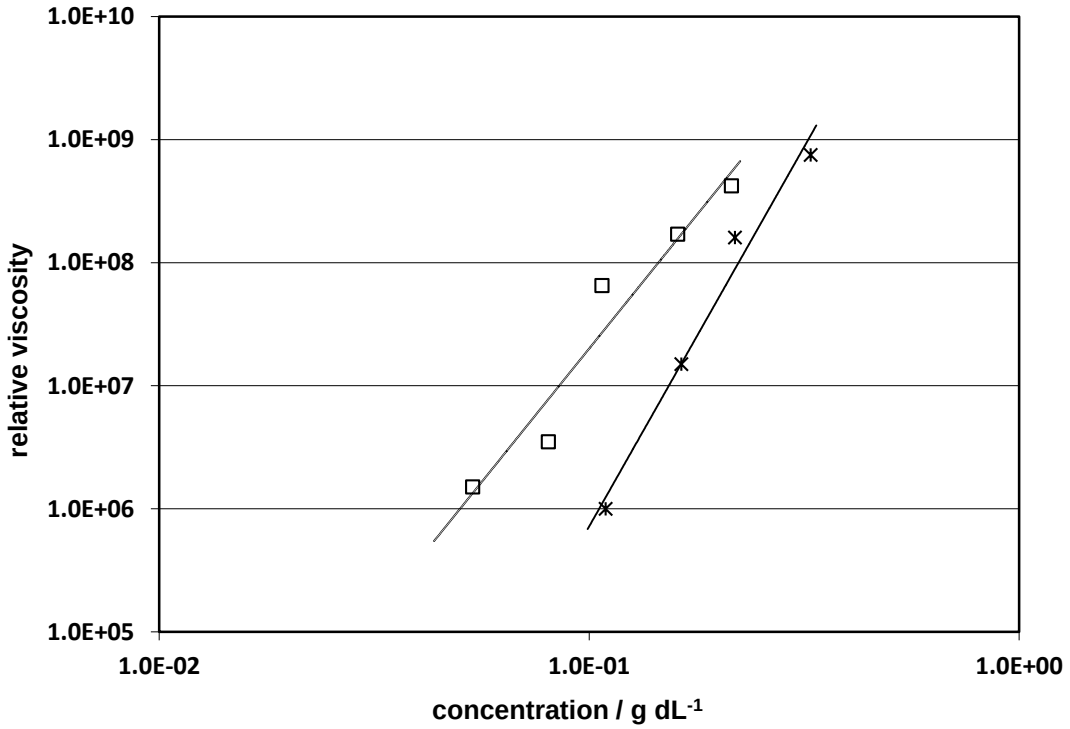

Figure 3.24 Plot of the relative viscosity extrapolated to 10^{-6} s^{-1} shear rate against concentration for Carbomer A and Carbomer B neutralized. Symbols are: (□) Carbomer A; (*) Carbomer B.

3.4. Conclusions

This set of study provided important information about the current polymer thickeners. Both Carbomers are PAA based polymers with high molecular weights of 4 and 5 MDa. Due to the size of the polymer molecule, both Carbomers are able to develop polymer-polymer interactions at concentrations below 1 g dL^{-1} and effectively thicken their aqueous solutions. The rheological properties of the polymers in aqueous solutions, particularly the shear-thinning behaviour, have been investigated and enable us to further investigate their performances in the solvent of propylene glycol-water mixture under the conditions typically experienced by aircraft de-icing fluids.

3.5. References

1. Pethrick, R.A., *Polymer Science and Technology for Engineers and Scientists* 2010, Chichester, UK: John Wiley & Sons.

2. Brandrup, J., Immergut, E.H., and Grulke, E.A., *Polymer handbook* 2003, NY: Wiley-Interscience.

3. Bohdanecky, M. and Kovar, J., *Viscosity of Polymer Solutions*, in *Polymer science library*, Jenkins, A.D., Editor 1979, Elsevier Scientific Pub. Co.: Amsterdam.

4. Chu, J.S., Yu, D.M., Amidon, G.L., Weiner, N.D., and Goldberg, A.H., *Viscoelastic Properties of Polyacrylic-Acid Gels in Mixed-Solvents.* Pharmaceutical Research, 1992. **9**(12): pp. 1659-1663.

5. Tsvetkov, V.N., Lyubina, S.Y., and Barskaya, T.V., *The flow birefringence and viscosity of poly (acrylic acid) solutions.* Polymer Science U.S.S.R., 1964. **6**(5): pp. 886-892.

6. Takahashi, A. and Nagasawa, M., *Excluded Volume of Polyelectrolyte in Salt Solutions.* Journal of the American Chemical Society, 1964. **86**(4): pp. 543-548.

7. Doi, M. and Edwards, S.F., *The theory of polymer dynamics* 1988, Oxford, UK: Clarendon Press.

8. Volk, N., Vollmer, D., Schmidt, M., Oppermann, W., and Huber, K., *Conformation and Phase Diagrams of Flexible Polyelectrolytes - Polyelectrolytes with Defined Molecular Architecture II*, in *Advances in Polymer Science*, Schmidt, M., Editor 2004, Springer Berlin / Heidelberg. pp. 29-65.

9. Nguyen, Q.D. and Boger, D.V., *Measuring the Flow Properties of Yield Stress Fluids.* Annual Review of Fluid Mechanics, 1992. **24**(1): pp. 47-88.

10. Barnes, H.A. and Walters, K., *The yield stress myth?* Rheologica Acta, 1985. **24**(4): pp. 323-326.

Chapter 4. Modelling the Viscosity Curves

4.1. Theory Introduction

A polymer in solution can typically be described by Rouse theory [1] in which the relaxation times are dictated by the solvent and the molecular weight of the polymer. However the Rouse theory is unable to predict the very slow relaxation times observed with PAA, and additional contributions to the relaxation behaviour have to be added in order to describe the observed behaviour. For non-electrolyte polymers the polymer-polymer interactions are usually described in terms of Doi-Edwards reptation theory [2]. Studies of concentrated polymer solutions have shown that, in dilute solution and for small strain, the stress relaxation occurs in two steps: the relaxation of chain segments between fixed entanglement points, and the relaxation of the entanglement points via reptation motion [3, 4]. However in the nonlinear, large strain region there appears a new relaxation process which lies between the other two processes, the breathing relaxation. This breathing motion is envisaged as the retraction of extended chains after the application of a shear stress.

In the case of polyelectrolytes, there is the possibility of chain interaction occurring between neighbouring chains, effectively increasing the molecular weight and hence hydrodynamic volume of the relaxing entity. Hudson et al. [5] have proposed a model in which a pair of polymer molecules form a ladder-type of structure which contains loops which are distributed along the ladder in a random manner. The loops will be able to execute relaxation behaviour which will be rather like the Doi breathing chain model [3] and in which the chains are constrained by the entanglements. In the context of the polymer electrolyte, entanglement is both a consequence of the high molecular weight and the occurrence of hydrogen bonding interactions between neighbouring chains. In the Hudson et al. theory [5], the molecular weight is assumed to be that of the isolated chain. In the present model we allow for the interactions to produce an effective molecule

which is a multiple of the isolated polymer chain. It is also recognised that the molecular weight distribution must be included in the calculation of the Rouse and reptation contributions for a realistic modelling of the dynamic characteristics of the polymer. In the approach adopted here it is assumed that the contributions to the overall viscosity are additive and therefore the effects of the molecular weight distribution can be simulated by the calculation of the contribution from the individual polymer species. The Rouse motions will reflect the motion of short elements of chains which are constrained by the entanglements and hydrogen bonding interactions which form the complexed relaxing polymer entity.

4.2. Modelling Process

4.2.1. Rouse Theory with Molar Mass Distribution

The viscoelastic behaviour of a dilute polymer solution has been well described by Rouse theory [1], in which a number of parameters are influencing the rheological properties of a fluid: (1) the size of the polymer chains which is reflected by the average molecular weight and the molecular weight distribution; (2) the flexibility of the polymer backbones; (3) the interactions between individual segments within a polymer molecule or with other molecules which involves the chain topography (extent of chain branching) and polymer concentration; (4) the interactions between the polymer and solvent. For an ideally flexible mono-dispersed polymer in an ideal solvent, the relaxation behaviour can be satisfactorily described by two parameters; the excluded volume integral, β, and the statistical or Kuhn segment length, l_k, which is related to the persistence length l_p [6, 7].

From the intrinsic viscosity the molar mass of the polymer as an isolated species was determined using the Mark-Houwink-Kuhn-Sakurada equation. The effect of molar mass distribution was included in the form of the distribution function:

$$f(x) = \frac{1}{x\sqrt{2\pi\sigma^2}} e^{-\frac{(\ln x - \mu)^2}{2\sigma^2}} \tag{4.1}$$

where σ is the standard deviation, and μ is the mean, respectively, of the distribution variable's natural logarithm. The variable, x, is the number of repeat units in the chain. The Rouse first normal mode (the slowest internal motion of the chains), τ_1, can be defined as:

$$\tau_1 = \frac{\sum_{i=1}^{N} 6\eta_0 f_i M_i}{\sum_{i=1}^{N} \pi^2 \rho R T f_i} \tag{4.2}$$

where ρ is the solution density, η_0 is the zero shear rate viscosity of the solution, M is the molar mass, R is the universal gas constant, T is the absolute temperature, and N is the total mode number within a polymer chain.

Following the approach of Doi [2, 4], the Rouse contribution to the viscosity describes the relaxation of the polymer chain between entanglements or, in the case of polyelectrolytes, between points of clustering, and will make a frequency-shear rate dependent contribution,

$$\eta_1(\omega) = \eta_s + \frac{6(\eta_0 - \eta_s)}{\pi^2} \sum_{p=1}^{N} \frac{p^2}{p^4 + \omega^2 {\tau_r}^2} \tag{4.3}$$

where η_s is the solvent viscosity, p is the mode number, ω is the frequency, and τ_r is the Rouse relaxation time.

4.2.2. Reptation and Entanglement-Clustering

The reptation model is based on the concept that, for high molar mass polymers, their motion is constrained by entanglements, and these constraints points form a "tube". The average number of entanglements stays constant, although the polymer chain moves so as to break and make new entanglements. The formation of the entanglements leads to the viscosity shown, a rapid increase with molar mass, similar to that observed in Figure 3.18. Entanglement depends on the hydrodynamic volume of the polymer and rises to approximately the third power of the size for an ideal flexible chain. The relaxation

contribution to the viscosity has the form:

$$\eta_1(\omega) = \eta_s + \frac{6(\eta_0-\eta_s)}{\pi^2}\sum_{p=1}^{N}\frac{p^2}{p^4+\omega^2{\tau_r}^2} + \frac{8(\eta_e-\eta_0)}{\pi^2}\sum_{p=1}^{N_e}\frac{p^2}{p^4+\omega^2{\tau_d}^2} \quad (4.4)$$

where η_e is the critical viscosity when entanglement motion reaches equilibrium, N_e is the number of segments between entanglement points, and τ_d is the terminal relaxation time, given by $\tau_d = \frac{1}{\pi^2}\frac{\zeta a^2 N_e}{kT}N^3$, where a is the tube diameter ($a^2 = N_e b^2$), b is the monomer length (in this case, the Kuhn length), ζ is the bead friction coefficient of Rouse motion, and k is the Boltzmann constant.

Whilst this equation describes the behaviour of a polymer melt, it is not necessarily appropriate for a system with nonlinear characteristics [4]. Doi has shown that for concentrated solutions an additional contribution associated with a contour length relaxation must be added, and has the form $\tau_b = \frac{\zeta b^2 N^2 {N_e}^2}{3\pi^2 kT}$. In this case, N is the total number of Kuhn units, N_e is the number of Kuhn units between entanglement points, $N_e = \frac{M_c}{M_k}$, M_c is the critical molar mass of entanglement, and M_k is the molar mass of a Kuhn unit. This form of the equation refers to the process of retraction of a segment of the chain which has been affinely deformed when a system has been subjected to a step shear event. This breathing motion can in the case of a polyelectrolyte be likened to the motions of the loops created by the hydrogen bonding interactions between neighbouring chains. It has previously been shown that this type of solution exhibits elogational flow and relaxation behaviour in this region may be envisaged as chains moving in and out of the dynamic clusters as flow occurs. A number of alternative models of this type of chain motion exist, all lead to equation for τ_b of a similar form [8-11]. Typically, the value for M_c will be of the order of $20 - 30 \times 10^3$, and depends on the polymer type [12]. In the Rouse theory it is assumed that the friction coefficient is equal to the solution viscosity, however in the case of a polyelectrolyte this may not necessarily be correct as electrostatic interactions which expand the chain will also have a significant effect on the local chain mobility, and it is therefore appropriate to make η_s an adjustable

variable. It may be argued that for the polymer chain effectively shielded by the addition of the electrolyte, the chain will behave in a similar fashion to the ideal, flexible chain but with chain motion which has been significantly slowed down relative to its flexible counterpart. In the theory, adjusting the rate of Rouse-like motion will be achieved using a scaling factor.

In a polyelectrolyte, the Kuhn length may be significantly increased as a consequence of electrostatic repulsion opening the chain dimensions. The viscosity then has the form:

$$\eta_1(\omega) = \eta_s + \frac{6(\eta_0-\eta_s)}{\pi^2}\sum_{p=1}^{N}\frac{p^2}{p^4+\omega^2{\tau_r}^2} + \frac{1}{2}\cdot\frac{8(\eta_e-\eta_0)}{\pi^2}\sum_{p=1}^{N_e}\frac{p^2}{p^4+\omega^2{\tau_b}^2} + \frac{1}{2}\cdot \frac{8(\eta_e-\eta_0)}{\pi^2}\sum_{p=1}^{N_e}\frac{p^2}{p^4+\omega^2{\tau_d}^2} \quad (4.5)$$

This theory, however, assumes that the polymeric entity undergoing relaxation is a single polymer chain and does not allow for the dynamic (hydrogen bonding) interactions which are found in polyelectrolytes.

4.2.3. Complexation

The problem of dynamic complexation has been considered by Hudson et al. [5], who assumed that a fraction g (<1) of the molecules are complexed. The distribution then takes the form $f'(x) = f(x) - g \cdot h(x)$. Assuming that the original molar mass distribution given by Equation 4.1 is normalized, so that $\sum_{x=1}^{\infty} f(x) = 1$, then $h(x)$, the degree of occupancy of the complex by a molecule of chain length x, is also normalized so that $\sum_{x=1}^{\infty} h(x) = 1$.

The change in the energy of the system when complexation occurs is $\Delta G_1 = \Delta G_1^0 \sum_{x=1}^{\infty} n^0(x)$, where $n^0(x)$ is the number of base moles of polymer with chain length x in the complex, and $\Delta G_1^0 = RT \ln K_1$, where R is the gas constant, T is the absolute temperature, and K_1 is the reaction or equilibrium constant. When the base pair is formed there will also be a change in the entropy $\Delta G_2 = -T\Delta S_2$, where ΔS_2 is the entropy change associated with the complex formation. The number of ways the free chains can be

arranged in the complex is related to the entropy via the Boltzmann equation. The distribution is therefore written as $f'(x) = f(x)/(1 + rgK)$, where $r = \sum_x h(x)/x$. To allow for the effects of complexation, two changes have been made to Equation 4.5. A variable has been introduced which allows a proportion of the molecules to have a molar mass which is a multiple of the uncomplexed molar mass, and this will also have an effect on the distribution parameter σ. The 'slip-coil-breathing' motion also contributes to the overall viscosity profile.

$$\eta_1(\omega) = \eta_s + \frac{6(\eta_0-\eta_s)}{\pi^2}\sum_{p=1}^{N_c}\frac{p^2}{p^4+\omega^2{\tau_r}^2} + \frac{1}{2}z_1\frac{8(\eta_e-\eta_0)}{\pi^2}\sum_{p=1}^{N_e}\frac{p^2}{p^4+\omega^2{\tau_b}^2} + \frac{1}{2}z_2\left[\frac{8(\eta_e-\eta_0)\cdot h_1}{\pi^2}\sum_{p=1}^{N_d}\frac{p^2}{p^4+\omega^2{\tau_{d1}}^2} + \frac{8(\eta_e-\eta_0)\cdot h_2}{\pi^2}\sum_{p=1}^{N_e}\frac{p^2}{p^4+\omega^2{\tau_{d2}}^2}\right] \quad (4.6)$$

N_c (= M/M_c) is the number of entanglement units within a polymer molecule, and N_d (= M/M_d) is the number of the rigid units formed along a polymer molecule. In this case, it is assumed that the critical molar mass, M_c, is 30,000, and 5 entanglement segments form a 'rod-like' entity. The molar mass, M_d, is therefore 150,000. z_1 and z_2 are the scaling factors used to adjust the contribution of 'slip-coil' and reptation motions (z_1 = 1- z_2), whilst h_1 and h_2 are the degrees of complexation (h_1 = 1- h_2). Accordingly, $\tau_{d1} = \frac{1}{\pi^2}\frac{\zeta a^2 N_e}{kT}[N\cdot(1+h_1)]^3$, and τ_{d2} remains unchanged as the uncomplexed terms.

4.2.4. Fitting the Model

The contribution of Rouse relaxation motion assumes that the friction force on the motion of the chain element is due to the viscosity of the solvent. This assumption is valid for dilute solutions of flexible polymers in a good solvent. Modification of the Rouse theory to allow for interaction between the solvent and the polymer has been proposed in terms of the Zimm and Wang theory [13]. Introduction of solvent/polymer interactions effectively slows the rate at which chain dynamics occurs and results in a shift of the Rouse relaxation to lower frequency. In the case of PAA, the carboxyl groups are not only able to undergo strong interaction with water, which will form a sheath around the

polymer chain, but are also partially ionized and hence internal rotation can produce significant changes in the potential; surface-controlling the chain dynamics. To allow for all these factors, we introduce a scaling parameter, c_r, to allow the Rouse contribution to be adjusted to fit the experimental data. The Rouse contribution adds to the overall contribution to the relaxation behaviour, but will predominately influence the relaxation at higher frequencies than those used in this study. The Rouse relaxation time is therefore adjusted to $\tau_r = \frac{6\eta_0 M_c}{\pi^2 \rho RT} c_r$.

During the fitting process, all the complex viscosity data were obtained from oscillatory measurements. To ensure the strain imposed were low enough, a strain amplitude ramp test at fixed frequency was perform prior to each complex viscosity measurement to determine the linear viscoelastic region (at the point where the values of the moduli are no longer constant and appear to decrease with increasing strain). An example is shown in Figure 4.1, and the strain amplitude chosen for frequency sweep was 0.011. Using the modified form of the theory, Equation 4.6, a fit to the experimental data was obtained (Figure 4.2) using the equilibrium viscosity as $\eta_e = 10^5$ Pa s, and the terminal viscosity η_0 = 0.031 Pa s, which were determined from the creep measurements and extrapolated using Sisko model based on data from continuous flow measurements (Chapter 3). The coefficients $z_1 = 0.008$ and $h_1 = 0.9$ reflect the extent to which complexation is occurring in the system. The molar mass of the polymer used is 4×10^6 g mol^{-1}, and values of the coefficients which define the size of the relaxation element, and the effective size of the polymer at entanglement, are as follows: $N_c = 173$; $N_e = 34$; $N_d = 34$. The shift factor for the Rouse relaxation is $c_r = 10^4$, which implies that the interaction with the solvent, and the added retardation effects of the hydrogen bonding and charges, have a large effect on the rate at which chain rotation occurs. A good fit between experiment and theory is obtained, and the equation is found to be sensitive to small changes in the value of z_1 and h_1 which reflect the extent of complexation between the PAA polymers in the system. Such sensitivity is further explored and the detailed program has been composed using

Mathcad and listed in Appendix A.

If we examine the various components in Equation 4.6, the reptation contribution, whilst being important in achieving the high values of the viscosity at low shear rates, makes an insignificant contribution the shear dependence in the region of 0.1 – 100 rad s^{-1}. The Rouse motion similarly provides the shear dependence above 100 rad s^{-1} but is not a dominating factor in the overall shear dependence. The main contribution comes from the breathing process proposed by Doi [4], modified to include the effects of complexation. In the context of the polyelectrolytes, this implies that under the influence of shear in the region of 0.1 – 100 rad s^{-1}, the motion of the loops and semi-pinned elements of the polymer chain are important in achieving the desired shear rate characteristics for the solutions to perform adequately as de-icing fluids. The theory is surprisingly sensitive to small changes in the values of z_1 and h_1, which are the principal fitting parameters used in the theory. The parameter c_r, whilst it adjusts the shear dependence at high shear rates to have the correct form, has little effect in the region of interest.

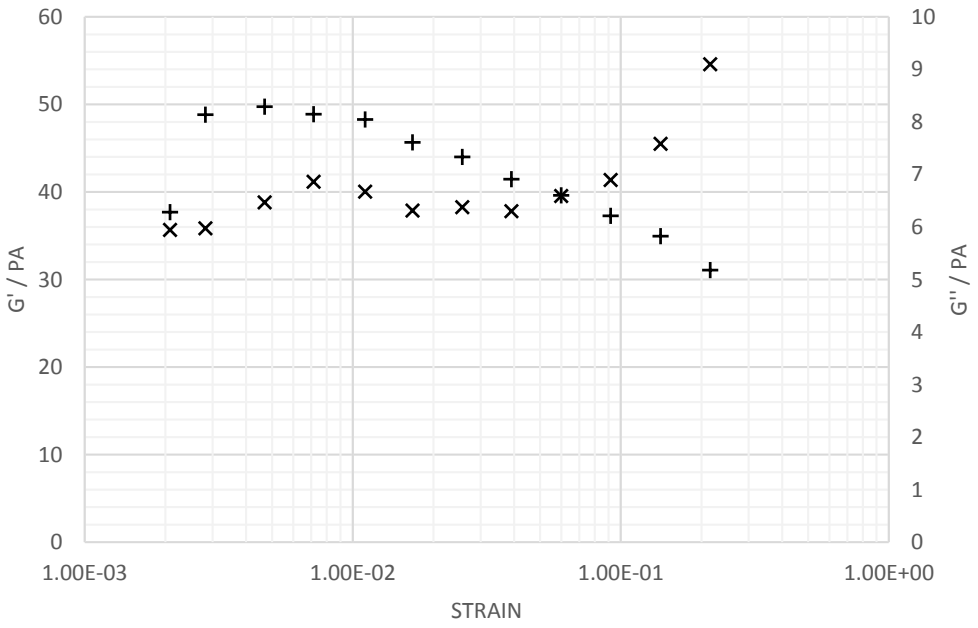

Figure 4.1 Strain amplitude ramp test for a solution sheared for 30s. (+) G'; (×) G''.

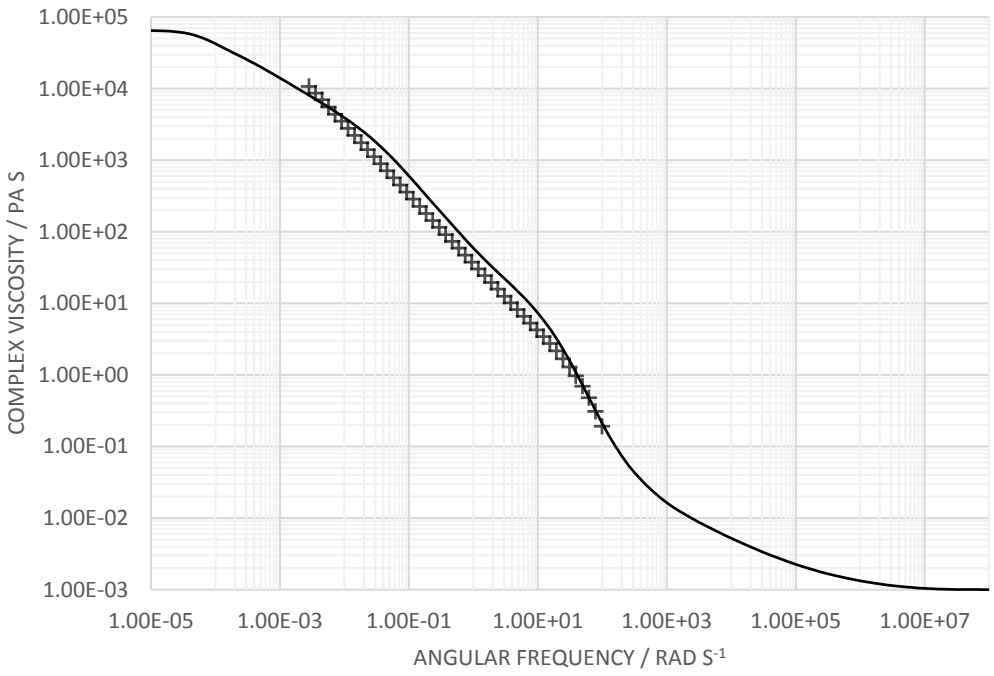

Figure 4.2 Viscosity as a function of frequency for a solution sheared for 30s fitted to the model. (×) Experimental data; (–) model prediction.

4.3. Effects of Shear on the Polymer Solutions

In Chapter 3, the solutions were produced by a method of slow dissolution which was allowed to take place over a period of five days. In practice, dissolution is usually achieved using high shear mixing, and the possibility of degradation of the polymer arises. In this section, a study was undertaken in which solutions were produced using a Silverson high shear mixer, and the rheology was examined periodically to determine the nature of the solution being generated. For this study the following solution preparation procedure was followed.

The head of a Silverson high speed mixer was located ¼ of the height from the bottom of a 2L beaker. 1L of deionized water was poured into the beaker, then 12.5 g of Carbomer A powder was slowly added to a vortex created using a speed of 4800 rpm, in order to disperse without aggregation. The suspension was mixed for 5 min, with 50 mL samples

being taken at 30 s, 1 min, 2 min, and 5 min. The high speed mixing of the sample was continued for a further 80 min at the rate of 3600 rpm, samples being taken at 25 min, 60 min, and 85 min from the start of mixing. Each 50 mL sample was further diluted by adding 150 mL of deionized water, and a magnetic stirrer was used to obtain a homogeneous mixture. This process is assumed to be sufficiently mild to avoid degradation and produced homogeneous solutions with a concentration of approximately 0.30 g dL^{-1}.

All the samples were neutralised to pH 7 using 2M sodium hydroxide aqueous solution, and an appropriate amount of sodium chloride was added to adjust the electrolyte level to a value of 0.012M. Shear rate measurements were carried out over the range 0.1 to 100 s^{-1}, increasing values logarithmically over 10 minutes, and then decreasing under the same conditions. The variations of the viscosity against both shear rate (Figure 4.3) and shear stress (Figure 4.4) are shown.

After the first minute, the continuous shearing of the solution induces a dramatic reduction in viscosity levels, and the initial values of the viscosity after 85 min have dropped by almost two orders of magnitude at 0.1 s^{-1} of shear rate. In order to explore the origin of the changes being observed, a study was undertaken using oscillatory shear on one of the solutions which had been subjected to shear of 4800 rpm for 5 min and then 3600 rpm for 55 min. The viscosity against frequency is shown in Figure 4.5.

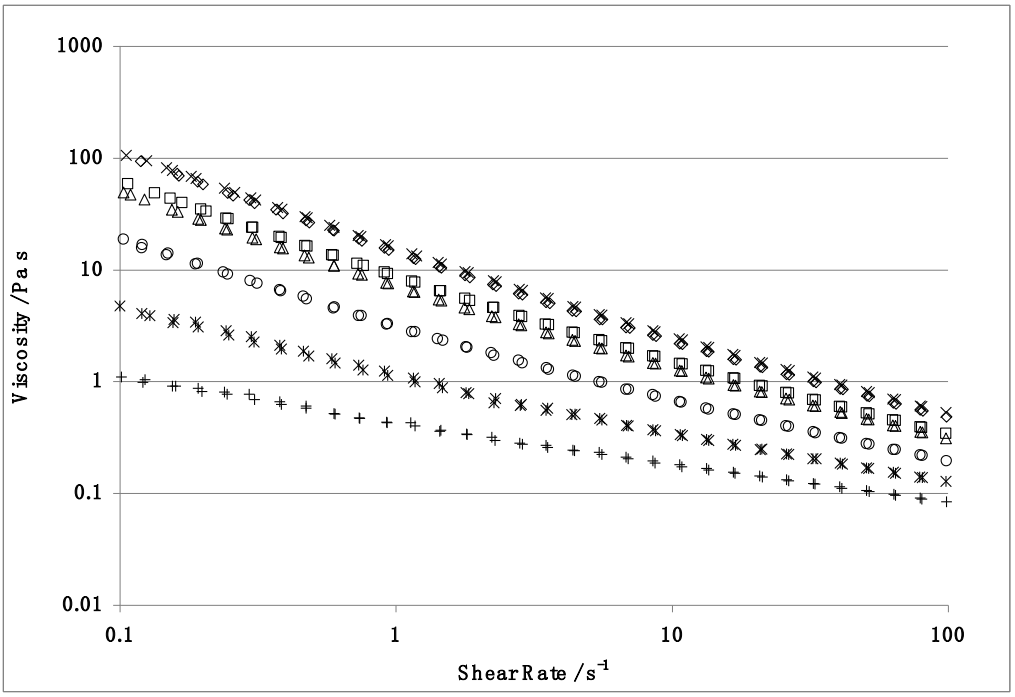

Figure 4.3 Effect of shear mixing on the shear rate behaviour of a Carbomer A solution subjected to high shear mixing. Symbols are: (◊) sheared at 4800 rpm for 30 s, (×) 1 min, (□) 2 min, (△) 5 min; (○) sheared at 4800 rpm for 5 min then at 3600 rpm for further 20 min, (*) 55 min, and (+) 80 min.

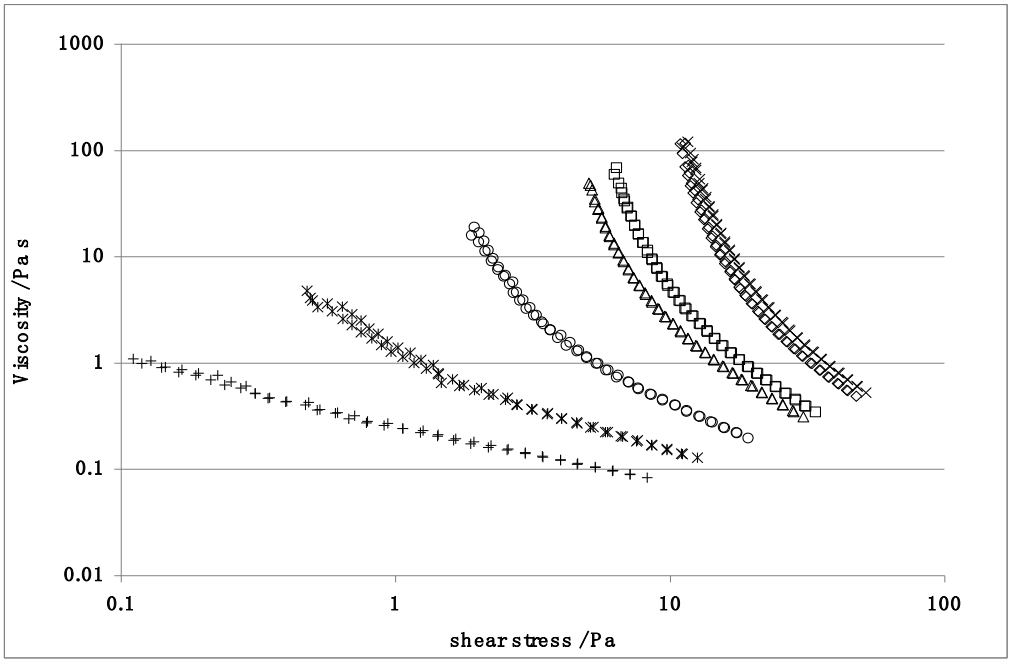

Figure 4.4 Effect of shear mixing on the shear stress behaviour of a Carbomer A solution subjected to high shear mixing. Symbols are: (◊) sheared at 4800 rpm for 30 s, (×) 1 min, (□) 2 min, (△) 5 min; (○) sheared at 4800 rpm for 5 min then at 3600 rpm for further 20 min, (*) 55 min, and (+) 80 min.

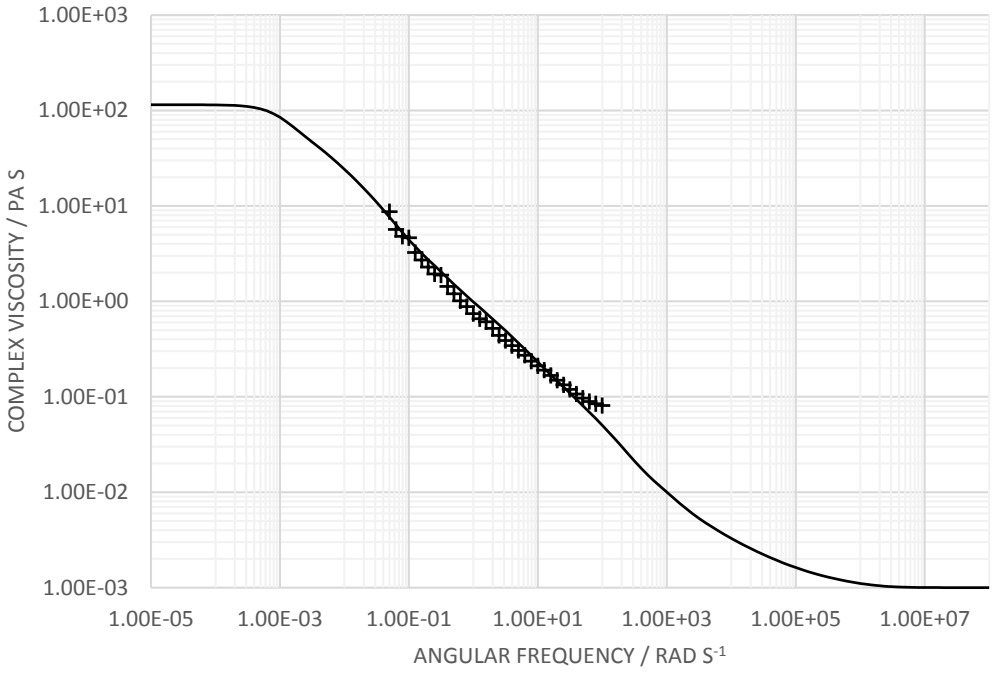

Figure 4.5 The model fitted to data of viscosity against frequency for a solution sheared for 60 min. (+) Experimental data; (–) model prediction.

The model presented above was used to explore the nature of the dynamic processes which influence the polymer in this solution. Creep data (Chapter 3) indicate that the value of η_0 has dropped from 10^5 to 185 Pa s. It is assumed that the friction factor associated with the Rouse mode should not be changed by the application of the high shear to the mixture, and the value of c_r maintains its value of 10^4. To obtain a good fit of the data the average molar mass of the polymer has to be reduced to 1×10^6 g mol^{-1}, and there are corresponding changes to two of the parameters (N_c = 43; N_d = 8), consistent with the PAA having a reduced chain length, however the value for the entanglement is retained at N_e = 34. The high shear may be expected to stretch the chains and this will favour the extent to which PAA interacts with other polymers; the value of z_1 has to be increased from 0.008 to 0.015. Studies of the extensional viscosity [17] imply that under the action of shear the PAA chains may be stretched, and this allows more favourable interaction between chains. The modelling, however, also suggests that there has been degradation of the polymer chains during the exposure to high shear; the degradation of

high molar mass polymer chains in a high shear field is well known [13-17].

The application of high shear to achieve the dissolution of the polymer significantly changes the interaction between polymer chains, as reflected in the '*z*' parameter, but also is reflected in the changes in N_c and N_d. Degradation of the polymer is also inferred by the reduction in the effective molar mass from 4×10^6 g mol^{-1} to 1×10^6 g mol^{-1}. The high molar mass in these polymers in part is attributed to the formation of anhydride linkages between polymers and under the influence of shear these may undergo degradation.

4.4. Conclusions

The solution properties of PAA have been successfully modelled in terms of a combination of processes which involve consideration of reptation, relaxation of the chains by slippage or loop relaxation and normal Rouse dynamics slowed down as a consequence of local interaction between chain elements and the solvent. The simple theory for flexible polymers has been modified to include the possibility of complex formation by association between neighbouring polymer molecules. The theory is sensitive to small changes in these parameters which themselves are probing the extent of polymer-polymer interactions prior to gel formation.

Subjecting the solutions to high shear induces changes in the extent to which PAA chains interact with one another, but the PAA may also be undergoing degradation as a consequence of the high shear fields. The model proposed is shown to be able to fit both the behaviour of the initially highly viscous solutions and those exhibiting a significantly reduced viscosity as a consequence of being subjected to high shear. The theoretical model is sensitive to the molar mass of the polymer, and the two interaction parameters. More extensive high shear rate data would be required to explore the validity of the Rouse description, however the scaling of the viscosity by the addition of an increased friction factor provides a reasonable description of the short range motions.

4.5. References

1. Rouse, P.E., *A Theory of the Linear Viscoelastic Properties of Dilute Solutions of Coiling Polymers.* Journal of Chemical Physics, 1953. **21**(7): pp. 1272-1280.

2. Doi, M. and Edwards, S.F., *Dynamics of concentrated polymer systems. Part 1.-Brownian motion in the equilibrium state.* Journal of the Chemical Society, Faraday Transactions 2: Molecular and Chemical Physics, 1978. **74**: pp. 1789-1801.

3. Rahalker, R.R., Lamb, J., Harrison, G., Barlow, A.J., Hawthorn, W., Semlyen, J.A., North, A.M., and Pethrick, R.A., *Viscoelastic Studies of Linear Polydimethylsiloxanes.* Proceedings of the Royal Society of London Series a-Mathematical Physical and Engineering Sciences, 1984. **394**(1806): pp. 207-222.

4. Doi, M., *Molecular Rheology of Concentrated Polymer Systems.1.* Journal of Polymer Science Part B-Polymer Physics, 1980. **18**(5): pp. 1005-1020.

5. Hudson, N.E., Ferguson, J., and Warren, B.C.H., *Polymer Complexation Effects in Extensional Flows.* Journal of Non-Newtonian Fluid Mechanics, 1988. **30**(2-3): pp. 251-266.

6. Fujita, H., *Polymer solutions* 1990: Elsevier.

7. Yamakawa, H., *Modern theory of polymer solutions* 1971: Harper & Row.

8. Mead, D.W., Larson, R.G., and Doi, M., *A Molecular Theory for Fast Flows of Entangled Polymers.* Macromolecules, 1998. **31**(22): pp. 7895-7914.

9. Yaoita, T., Isaki, T., Masubuchi, Y., Watanabe, H., Ianniruberto, G., and Marrucci, G., *Primitive Chain Network Simulation of Elongational Flows of Entangled Linear Chains: Role of Finite Chain Extensibility.* Macromolecules, 2011. **44**(24): pp. 9675-9682.

10. Marrucci, G., Bhargava, S., and Cooper, S.L., *Models of shear-thickening behavior in physically crosslinked networks.* Macromolecules, 1993. **26**(24): pp. 6483-6488.

11. Viovy, J.L., *Tube Relaxation - A Quantitative Molecular-Model for the Viscoelastic Plateau of Entangled Polymeric Media.* Journal of Polymer Science Part B-Polymer Physics, 1985. **23**(12): pp. 2423-2442.

12. Pethrick, R.A., *Polymer Science and Technology for Engineers and Scientists* 2010, Chichester, UK: John Wiley & Sons.

13. Wang, F.W. and Zimm, B.H., *Approximate theory of the viscoelasticity of chain-molecule solutions not infinitely dilute.* Journal of Polymer Science: Polymer Physics Edition, 1974. **12**(8): pp. 1619-1637.

14. Dostál, J., Kašpárková, V., Zatloukal, M., Muras, J., and Šimek, L., *Influence of the*

repeated extrusion on the degradation of polyethylene. Structural changes in low density polyethylene. European Polymer Journal, 2008. **44**(8): pp. 2652-2658.

15. Jou, D., Casas-Vázquez, J., and Criado-Sancho, M., *Thermodynamics of polymer solutions under flow: Phase separation and polymer degradation*, 1995, Springer Berlin / Heidelberg. pp. 207-266.

16. Odell, J.A., Keller, A., and Muller, A.J., *Thermomechanical degradation of macromolecules.* Colloid & Polymer Science, 1992. **270**(4): pp. 307-324.

17. Nguyen, T. and Kausch, H.-H., *Mechanochemical degradation in transient elongational flow*, 1992, Springer Berlin / Heidelberg. pp. 73-182.

Chapter 5. Rheology of Carbomer Thickened Fluids

5.1. Introduction

In previous chapters, work has been done to characterise both PAA-based polymers, Carbomer A and Carbomer B. With the polymer structure, molecular weight, and their rheological properties being initially examined, a polymer concentration-viscosity profile of polymer/water solutions at room temperature has been built up (Chapter 3). The effects of high rate shearing during the polymer dispersion process was also investigated (Chapter 4); and with a mathematical model set up to describe the rheological behaviour of the fluids, a logical explanation was provided for such effects. In order to develop a new thickening agent which is expected to deliver the similar, desirable performances as the current ones, it is important to first examine and characterise the behaviour of current fluids rheologically, and aerodynamically, under the conditions typically experienced by the fluids during application.

The de-icing fluids normally consist of propylene glycol/water mixtures for the purpose of depressing the freezing point. PAA provides the desired rheological properties which enable the fluids to settle on the aircraft surface under low shear conditions, such as standing or taxiing, and to easily flow off when the air shear increases during take-off [1-4]. The fluids are usually produced with pH approximately 7 for environmental concerns [5-8]; and inert electrolyte, such as sodium chloride, is added to suppress the viscosity to achieve easy dispersion and ability to achieve removal of the film when the air velocity is increased [9-12].

As a polyelectrolyte, the inter-polymer interactions of PAA in aqueous solutions can be controlled by changing polymer concentration, degree of ionisation, or adding salts and surfactant. At high dilution, a larger portion of carboxylic acid groups of PAA will be ionized and repel each other so it forms a pseudo-isolated polymer dispersion. As the

polymer concentration increases, the extent to which the carboxylic groups on the macromolecular chain are dissociated will decrease with change and this will also change the polymer size. Changes in pH will also influence the conformation and size of the polymer molecules. For a polyelectrolyte system, the change in polymer interactions will lead to significant changes in the rheological characteristics of the materials. [13-17]

In this chapter results will be presented from a series of experiments designed to investigate the influence of electrolyte on the rheological properties of PAA-thickened glycol/water mixtures. In previous chapters it has been shown that it is possible to describe the shear-dependent viscosity of PAA in water in terms of a theoretical model which includes descriptions of Rouse-like behaviour, combined with reptation and breathing motions combined with the possibility of complexation between neighbouring molecules. In this chapter it is aimed to explore the application of this model to the description of a typical de-icing formulation. Measurements of the performance of these fluids in a wind tunnel were carried out to explore the possible correlation between the measured rheological characteristics and the performance of the fluids in a simulated real situation.

5.2. Experimental

5.2.1. Materials and Sample Preparations

Two poly(acrylic acid) polymers, Carbomer A and Carbomer B, were supplied by Lubrizol (Brussels, Belgium) as flocculated solid particles. The diameter is approximately 0.2 μm. The nominal molecular weights are 4 MDa and 5 MDa. To achieve quick dissolution, polymers were first treated with a Silverson high shear mixer type L4R. The Silverson mixer was equipped with a general purpose head, which was immersed in a 1 L beaker filled with 600 g of de-ionized water. Polymer was then dispersed into the water slowly with the mixer rotation speed of 4800 rpm (rotation speeds determined by stroboscope).

After 5 minutes the rotation speed was reduced to 3600 rpm, and the dispersion was further sheared for a longer period of 55 minutes. This produced a 'gel-like' dispersion with a polymer concentration of 1.22 g dL^{-1}. The dispersion was then mixed with a 1,2-propylene glycol/de-ionized water mixture to achieve a solution with total polymer concentration of 0.30 g dL^{-1}. The mixing ratio of glycol/water is 50:50 by weight. 5.0M sodium chloride solution was added progressively to the solution and a series of samples were produced. Each sample solution was neutralized to a pH of approximately 7.0, using 5.0M potassium hydroxide aqueous solution. The electrolyte levels of each sample are presented in Table 5.1.

Table 5.1 Electrolyte level of Carbomer sample solutions

Sample	**Polymer / *Mw***	**g NaCl/ 100 g Solution**
A1	Carbomer A / 4MDa	0
A2	Carbomer A / 4MDa	0.030
A3	Carbomer A / 4MDa	0.045
A4	Carbomer A / 4MDa	0.061
A5	Carbomer A / 4MDa	0.076
A6	Carbomer A / 4MDa	0.091
A7	Carbomer A / 4MDa	0.122
B1	Carbomer B / 5MDa	0
B2	Carbomer B / 5MDa	0.030
B3	Carbomer B / 5MDa	0.061
B4	Carbomer B / 5MDa	0.091
B5	Carbomer B / 5MDa	0.122

5.2.2. Rheology

Viscosities were measured using both a temperature ramp at fixed stress, and a steady shear stress ramp at various temperatures. These were carried out using a shear stress-controlled Carri-Med CSL²500 rheometer (TA Instruments, Crawley, UK) using a 4-cm parallel plate fitted with a solvent trap. Temperature was controlled by using the Peltier effect and an anti-freezing bath maintained at 0°C, enabling test temperatures between 15°C and –15°C. Temperature ramp tests were carried out at a rate of 1.0°C per two minutes from 15°C to –15°C, and then from –15°C to 15°C, at shear stresses of 5 and 10 Pa (simulating conditions on taxiing or at a stand under light wind). As part of the preliminary test, the size of the gap between parallel plates has been adjusted to a series of values to ensure no effect of interfacial slip has occurred to cause influence on the results of measurements. Steady shear stress tests were carried out at 10°C, 5°C, 0°C, -5°C, and -10°C at between 0.5 to 50 Pa with a ten-fold increase in stress per 10 minutes, and subsequent decrease. Oscillatory tests were carried out at 20°C, 10°C, 0°C, and -10°C and set to measure the complex viscosity of fluid in the frequency range of 250 rad s^{-1} to 2.50E-03 rad s^{-1} using a 6-cm 0.5 degree cone and plate geometry fitting.

5.2.3. Wind Tunnel Testing and BLDT Measurement

Wind tunnel testing was carried out to determine the removal capability of the fluid from a flat surface. The wind tunnel consists of a duct through which temperature-controlled air is blown. The effectiveness of the removal of the fluid is evaluated using pressure sensors to determine the boundary layer displacement thickness (BLDT) which is a measure of the remaining film thickness on the surface during its continuous removal by the increasing flow of air. The acceleration of the air flow mimics the passage of air over the wind during the initial stages of take-off.

In this test, sample A4 (Carbomer A solution with electrolyte concentration of 0.061 g NaCl per 100 g solution) was selected based on the fact that it has the similar viscosity

level in the designated temperature range compared to the commercial material. The BLDT values were measured for its 100% fluid, 75 vol% dilution with deionized water, 50 vol% dilution with deionized water. Samples of test fluid were initially applied as a coating on the floor of the duct to a thickness of 1.5 mm using a doctor blade and this simulates the coating which would be deposited by spray application. The temperature of the test facility was thermostatically controlled and tests were carried out at approximately 0°C, -5°C, -10°C and -15°C (not applicable for 50 vol% dilution due to freezing). At the start of each run, air velocity was increased from stationary at a linear rate to 65 m s^{-1} over a period of 25 seconds. Tests at each temperature were triplicated.

5.3. Results and Discussion

5.3.1. Carbomer A

5.3.1.1. Temperature Ramp Test

Temperature ramp tests confirmed that partially neutralized PAA had a significant thickening effect on the glycol/water mixture (Figure 5.1). At 15°C and shear stress of 5 Pa (simulating conditions on taxiing or at a stand under light wind), Carbomer A thickened fluid with no electrolyte addition has the viscosity of approximately 9.37 Pa s, which is more than 1,100 times higher than the one of solvent itself (the water/glycol mixture has a viscosity of approx. 0.0078 Pa s at 15°C, rising to approx. 0.046 Pa s at -15°C). With the same shear stress applied, as temperature decreases to –15°C, the viscosity increased 5 times to approximately 48.64 Pa s. Such increase in viscosity coincides with the behaviour of most randomly coiled polymers. Decreasing temperature populates the more extended conformations which have lower energy, and hence the formation of larger networks.

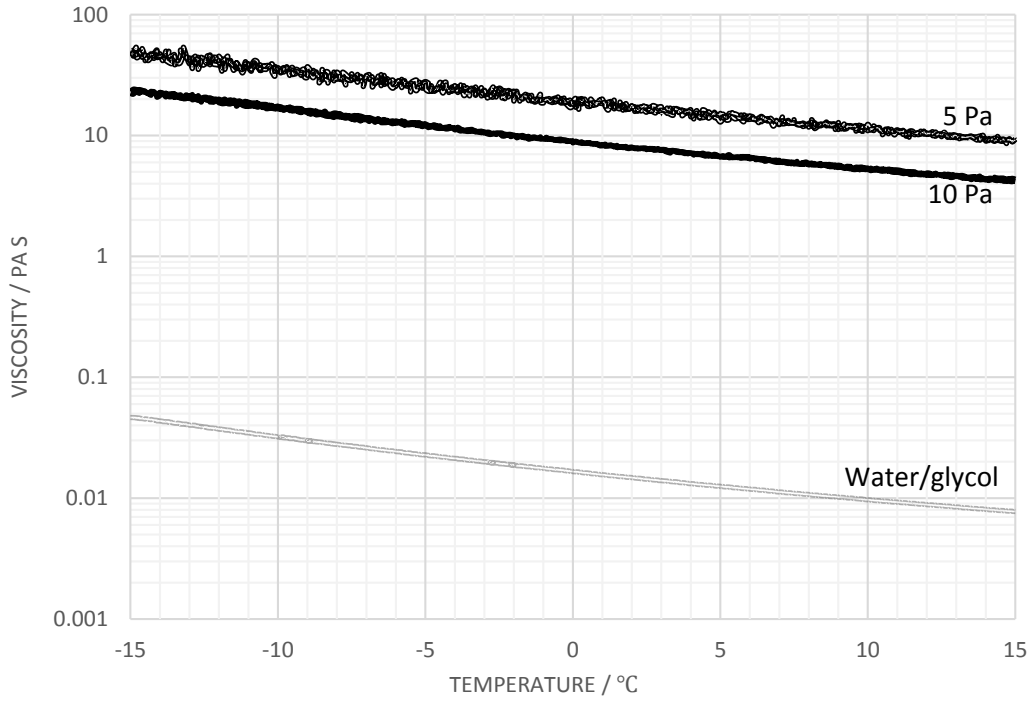

Figure 5.1 Viscosity variation with temperature plots for sample A1 at Carbomer A concentration of 0.30 g/dL, shear stress 5 and 10 Pa. Water/glycol 50:50 wt/wt.

The addition of electrolyte, sodium chloride in this case, will alter the interactions between the carboxylic groups of PAA by randomly blocking the neighbouring groups from binding with each other and preventing the polymer from forming large polymeric entities with an resultant in the decrease in viscosity. The following figures (Figure 5.2 and Figure 5.3) demonstrate the gradual reduction of viscosity across the testing temperature range as the electrolyte level is progressively elevated. Temperature ramp data for individual sample please refer to Appendix B.

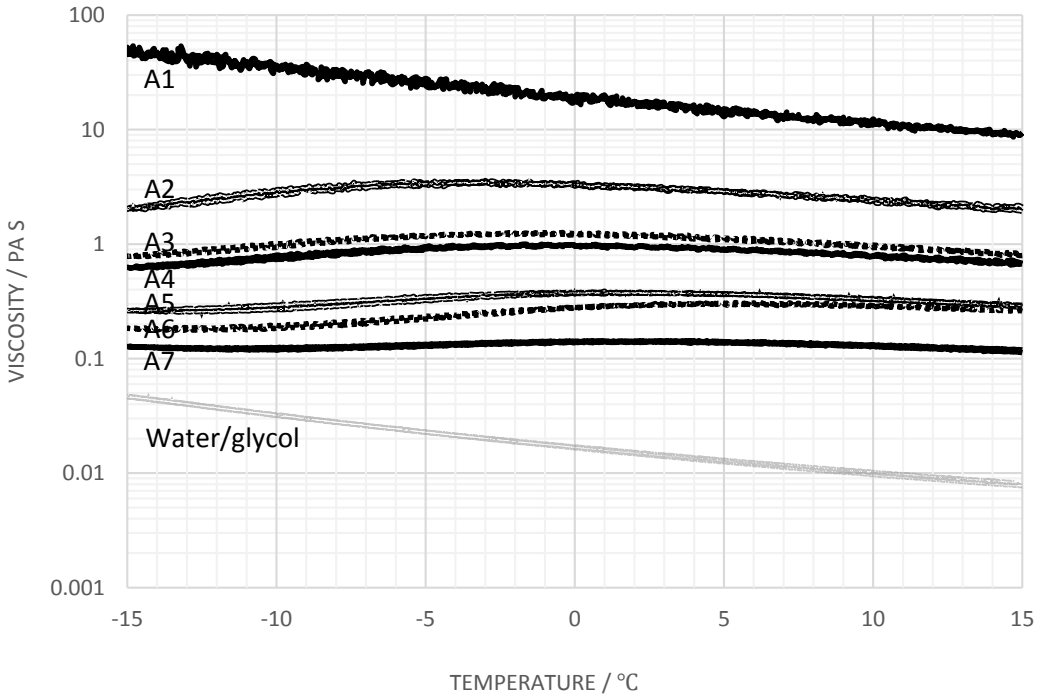

Figure 5.2 Viscosity variation with temperature plots for Carbomer A series, shear stress 5 Pa.

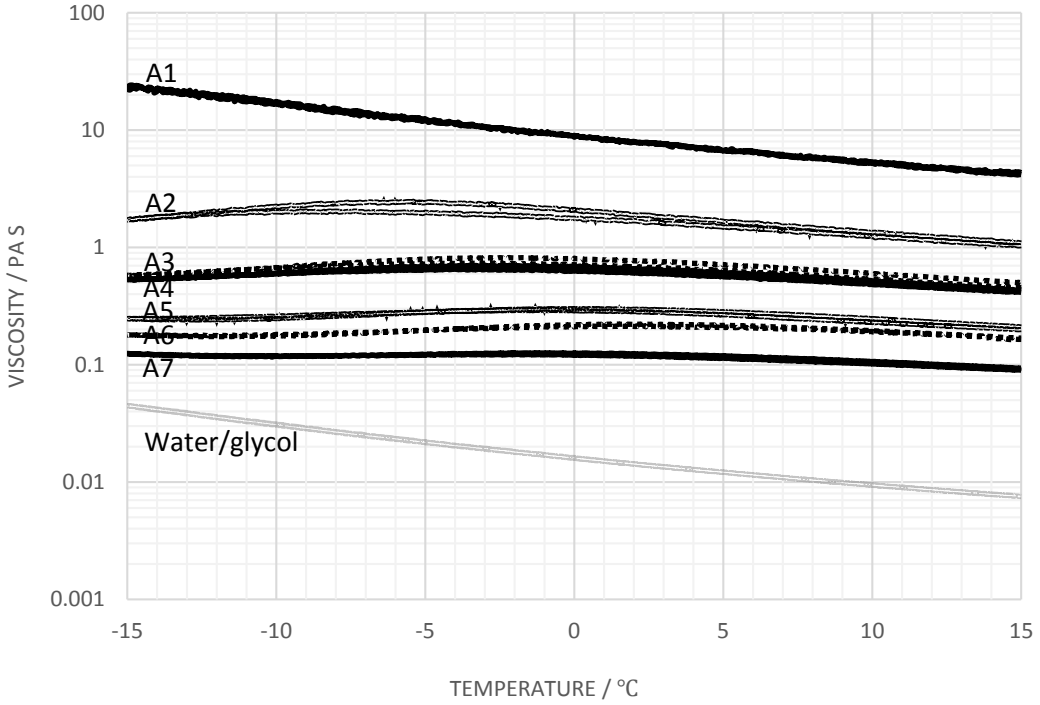

Figure 5.3 Viscosity variation with temperature plots for Carbomer A series, shear stress 10 Pa.

For the solution with highest level of electrolyte in this series, A7 (c_{NaCl}=0.122 g NaCl / 100 g solution), the viscosity at 15°C of temperature and 5 Pa of shear stress is approximately 0.12 Pa s, and at -15°C it is approximately 0.13 Pa s (Figure 5.4), with a viscosity 'peak' observed at around 2.3°C. Unlike the solutions with no electrolyte added, the temperature changes the equilibrium constant associated with binding of the salt with the carboxylic acid will vary as will the conformation of the polymer. Because of the decreasing temperature, sodium chloride tends to salt out and is less effective at blocking the interaction between the carboxylic acid groups. The observed peak may be interpreted as being the result of the increasing carboxyl-carboxyl group interactions and formation of polymeric structures which will precipitate from solution. Ultimately at low temperature the polymer will precipitate as a gel. There will be a reduction in the viscosity as globular structures are formed prior to gel formation. When the balance of interactions tends towards polymer-polymer interactions a stable phase-separated gel state is formed. Collapse of the polymer chain to pre-form a globular structure prior to phase separation leads to the observed reduction in the viscosity as the solution is cooled below 2.3°C. This type of behaviour will be observed with all the polymer systems studied, the temperature at which the collapse occurs will depend subtly upon the balance of the various interactions.

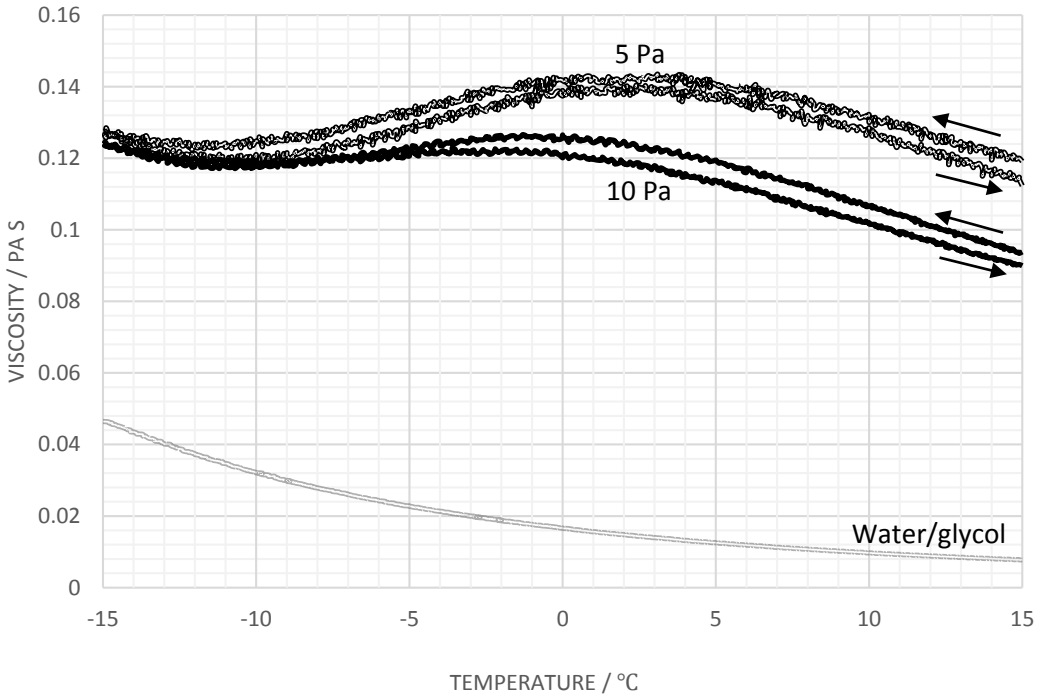

Figure 5.4 Viscosity variation with temperature plots for A7, applied shear stresses 5 and 10 Pa.

Similar behaviours were also exhibited for other samples with electrolyte addition, also with applied shear stress of 10 Pa (Figure 5.3). Again, the viscosity levels at any value of temperature do not depend upon whether the fluid is being heated or cooled (little or no hysteresis). In comparison to the solution without electrolyte, the fluids containing salt exhibit apparent constant viscosity over the temperature range studied. While viscosities remain reasonably steady, compared to the constant increase of the original fluid as decreasing temperature, location of viscosity 'peak' has also been shifted. For sample A2, c_{NaCl} = 0.030 g (NaCl) / 100 g (solution), the 'peak' exhibited at around -3.6°C with shear stress of 5 Pa and at -6.9°C at 10 Pa; A3, c_{NaCl} = 0.045, peaked at -1.3°C at 5 Pa and -2.9°C at 10 Pa; A4, c_{NaCl} = 0.061, at -0.9°C at 5 Pa and -3.2°C at 10 Pa (Figure 5.5); A5, c_{NaCl} = 0.076, at 1.6°C at 5 Pa and -0.5°C at 10 Pa; A6, c_{NaCl} = 0.091, at 5.6°C at 5 Pa and 1.9°C at 10 Pa; for A7 at 5 Pa viscosity peak shifted to 1.9°C, and -1.6°C at 10 Pa. Generally, the temperature, at where the viscosity peak occurs, increases with electrolyte level. However it becomes lower with higher shear stresses. The addition of electrolyte is of particular interests for the de-icing applications. While viscosity can be suppressed to a

desired level, the characteristic of 'visco-staticity' gives the solution good rinsability at low temperature.

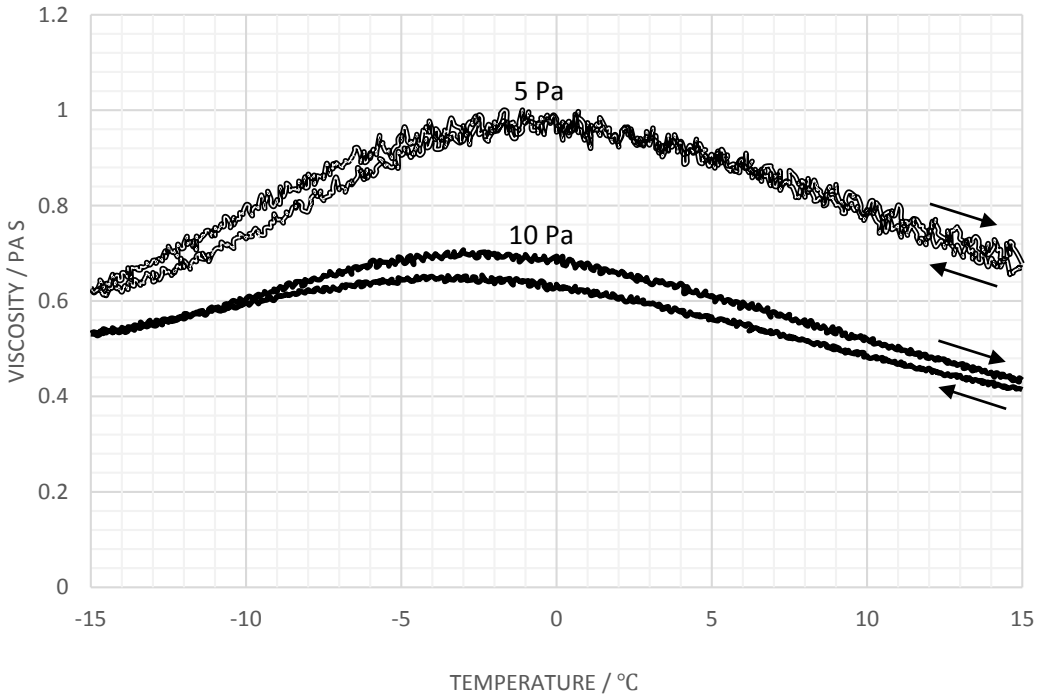

Figure 5.5 Viscosity variation with temperature plots for A4, applied shear stresses 5 and 10 Pa.

The viscosity of a commercially available Type II fluid, ABC-2000, is also measured at 5 Pa of shear stress between 15 and -15°C for the purpose of referencing (Figure 5.6). Across the measuring temperature range, the viscosity of the sample remains steady within the range of 0.6 to 0.7 Pa s with little thixotropic behaviour. The viscosity profile of sample A4, with c_{NaCl} = 0.061 g (NaCl) / 100 g (solution), resembled most closely.

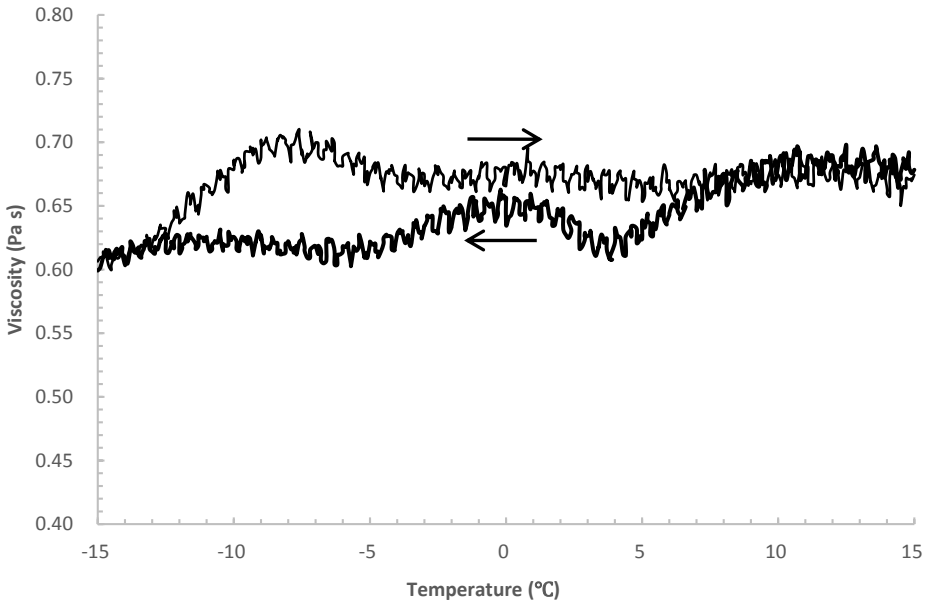

Figure 5.6 Viscosity variation with temperature plots for ABC-2000, applied shear stress 5 Pa.

5.3.1.2. Steady Shear Flow Test

Another important feature of the PAA-thickened solutions is its shear-thinning characteristic, which is important for its application as de-icing fluids. In the context of de-icing, the film must be stable up to the hold point (at the end of the runway prior to take-off). This is essentially achieved by having a sufficiently high value of the viscosity. For the layer to be shear cleaned it is essential to understand how the viscosity changes with increasing shear rate. Electrolyte addition does not change this behaviour. The following figures (Figure 5.7) showed that solutions remain shear-thinning at various temperatures. At high shear stress condition, when polymer molecules are more orderly aligned, solution viscosity increases with decreasing temperature. At lower shear conditions, viscosities at (or around) 'peak' temperature generally have higher values.

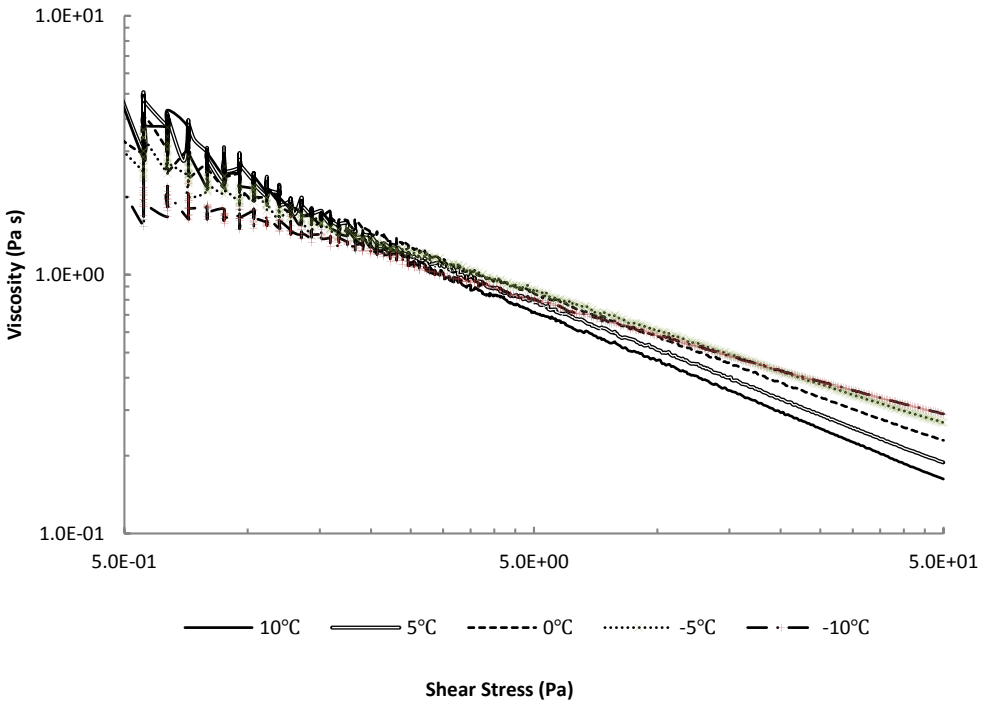

Figure 5.7 Viscosity variation with applied shear stress for A4 at different temperatures.

When comparing various samples experiencing the same stress sweep at the same temperature, the viscosity level decreases as increasing electrolyte level. In the stress-viscosity plot of Carbomer A series at 0°C (Figure 5.8), at the lower end of the stress/viscosity plot, the viscosity of solution dropped approximately an order in magnitude when the electrolyte level was doubled (A2 compared to A4, A3 compared to A6); even at the higher end, the viscosity still decreased to half of its original value when electrolyte concentration was doubled. It also demonstrated clearly that the slope of viscosity decrement is rising as the shear stresses has been progressively reduced and the electrolyte concentration increased. This may be as well interpreted as the shielding effect provided by the electrolyte which prevent carboxylic groups from binding with each other and forming large polymeric networks.

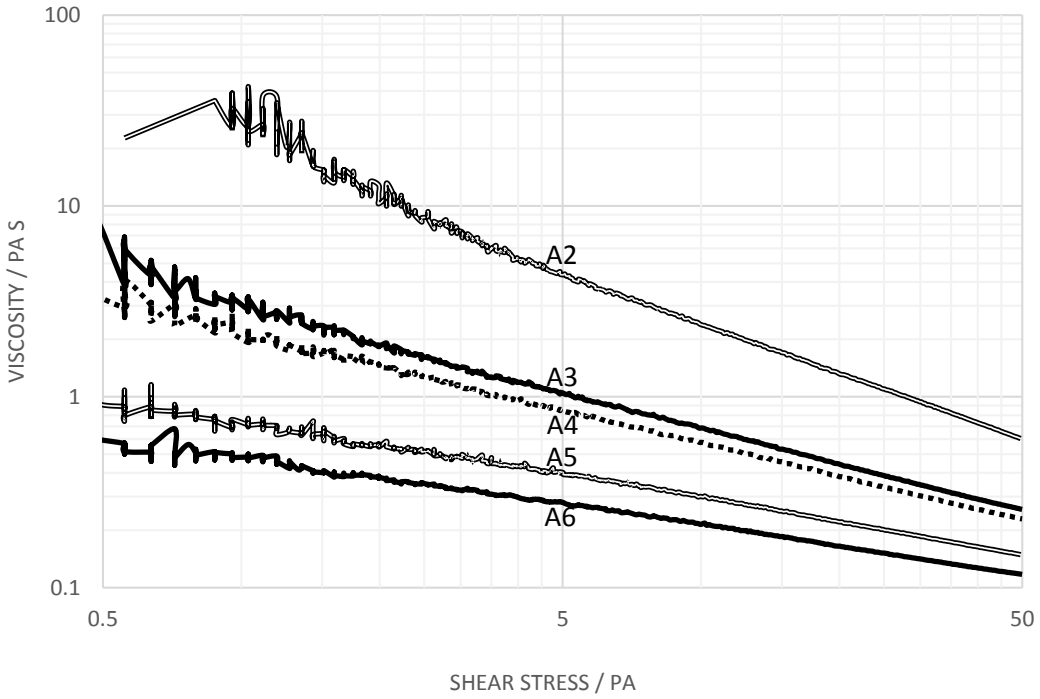

Figure 5.8 Viscosity variation with applied shear stress plots for Carbomer A series, A2, c_{NaCl} = 0.030 g (NaCl) / 100 g (solution); A3, c_{NaCl} = 0.045; A4, c_{NaCl} = 0.061; A5, c_{NaCl} = 0.076; A6, c_{NaCl} = 0.091; temperature 0°C.

5.3.2. Carbomer B

Previous study (Chapter 3) indicates that Carbomer B has a more highly branched structure. Its glycol/water mixture-based solution as prepared is acidic at pH 3.61 at 20°C. When neutralized to pH around 7 using 5.0M potassium hydroxide solution, the viscosity of Carbomer B solution increased significantly. Figure 5.9 shows the temperature/viscosity plot for a pH 7 sample solution B1 with no electrolyte addition. The applied shear stresses are 50 and 100 Pa, for the reason that no sufficient torque feedback of the rheometer could be generated to produce precise data using such technique at 5 and 10 Pa of shear stress. In terms of temperature/viscosity peak, it differs from Carbomer A sample A1 and exhibits one between 0 and -15°C, without electrolyte addition. This may suggest that at low temperature, the polymer molecules tend to form

an extended structure of low energy state. Additionally, the hysteresis exhibited between the curves of decreasing and increasing temperature suggests that the polymer is forming pseudo gel-like structures which are sensitive to thermal and shear stress history. When no electrolyte is presented in the system, inter-molecular interactions randomly formed through hydrogen bonding; and as temperature decreases it takes longer period of time for the polymer network to accommodate the thermodynamic changes, which may explain the fact that the viscosity is generally lower when temperature decreases compared to the opposite direction of temperature change.

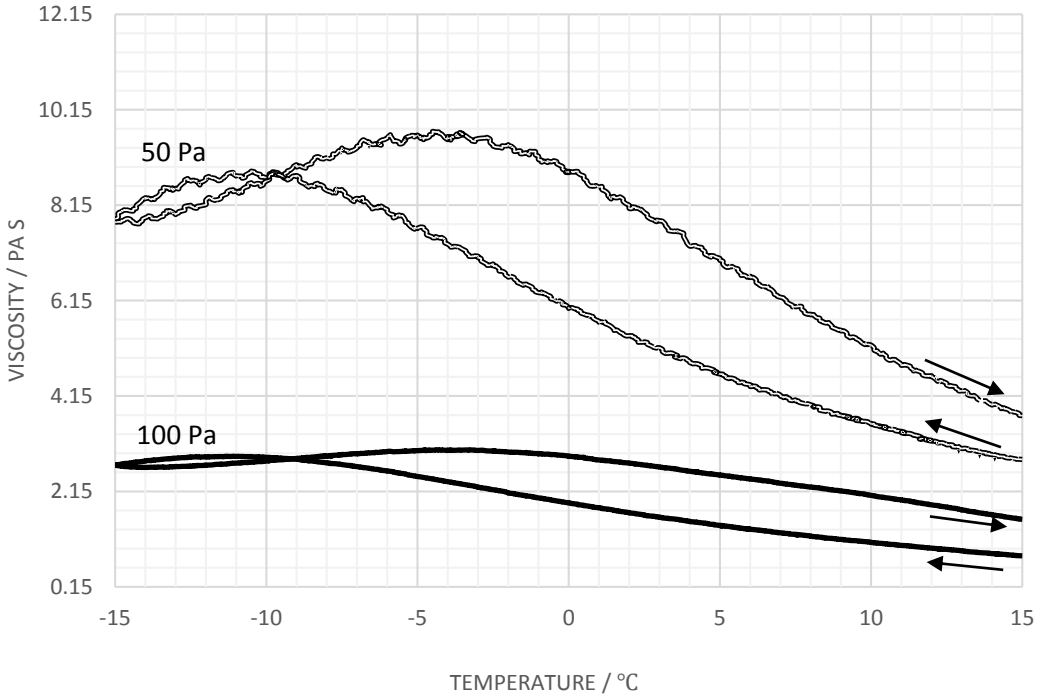

Figure 5.9 Viscosity variation with temperature plots for B1, applied shear stresses 50 and 100 Pa.

With electrolyte addition, an immediate viscosity drop was observed. With sodium chloride concentration of 0.030 g (NaCl) / 100 g (solution), which is the same concentration as Carbomer A sample A2, the viscosity decreased to approximately 0.26 Pa s at 15°C and 0.45 Pa s at -15°C, when applied 5 Pa of shear stress. Compared to A2's 2 Pa s at the same condition and its viscosity peaked at approximately 3.5 Pa s at -3°C, Carbomer B is much more sensitive to electrolyte in terms of viscosity level (Figure 5.10).

The inclusion of more highly branched molecules occupy lower hydrodynamic volume when electrolyte shields the carboxylic group interactions and the probability to form network with neighbouring molecules is lower. The 'peak' behaviour has been altered by the presence of electrolyte, possibly being shifted to a lower temperature range. However, the chain branches will also inhibit extended elements of the chain interacting with neighbouring polymer molecules and this will also contribute to differences in the observed behaviour. (Figure 5.11 and Figure 5.12).

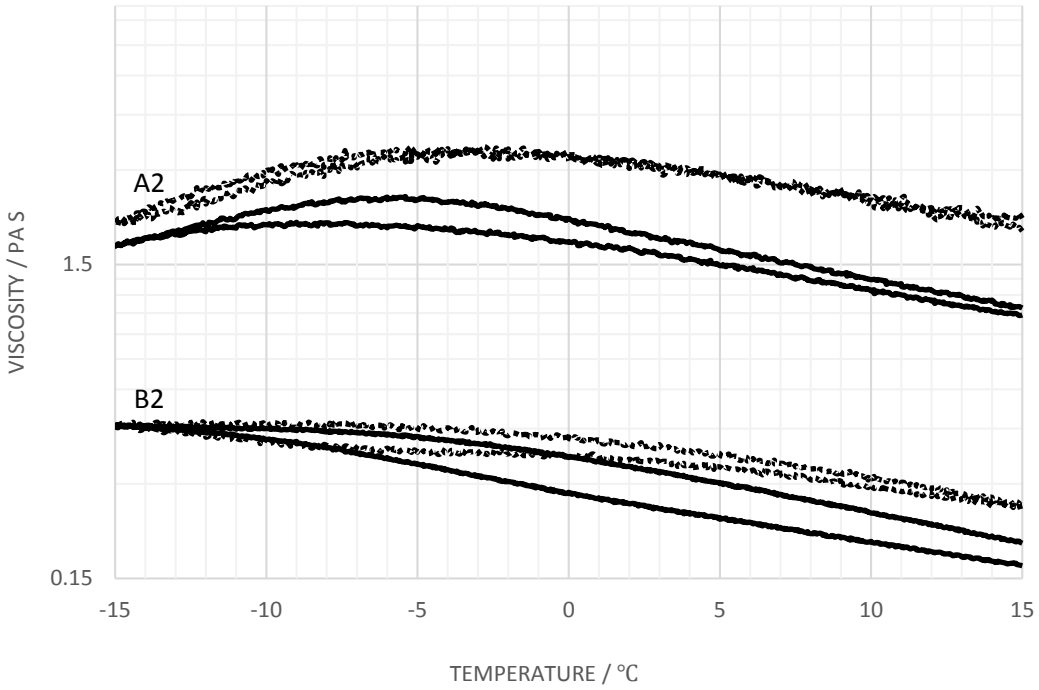

Figure 5.10 Viscosity variation with temperature plots for B2, in comparison with A2; applied shear stresses (…) 5 Pa, (–) 10 Pa.

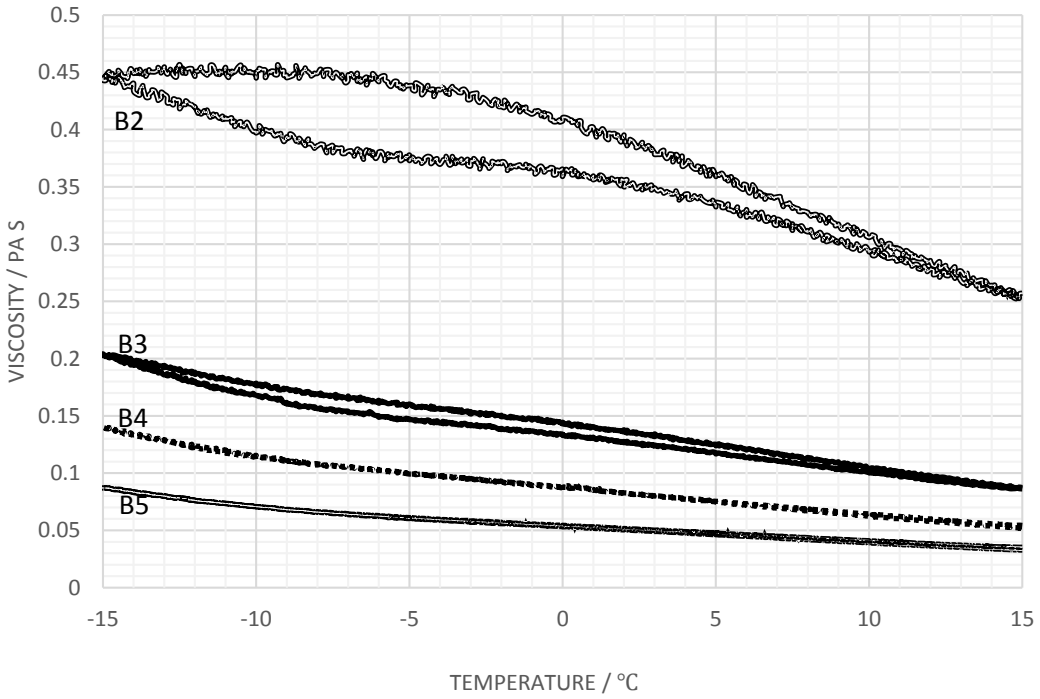

Figure 5.11 Viscosity variation with temperature plots for Carbomer B series, shear stress 5 Pa.

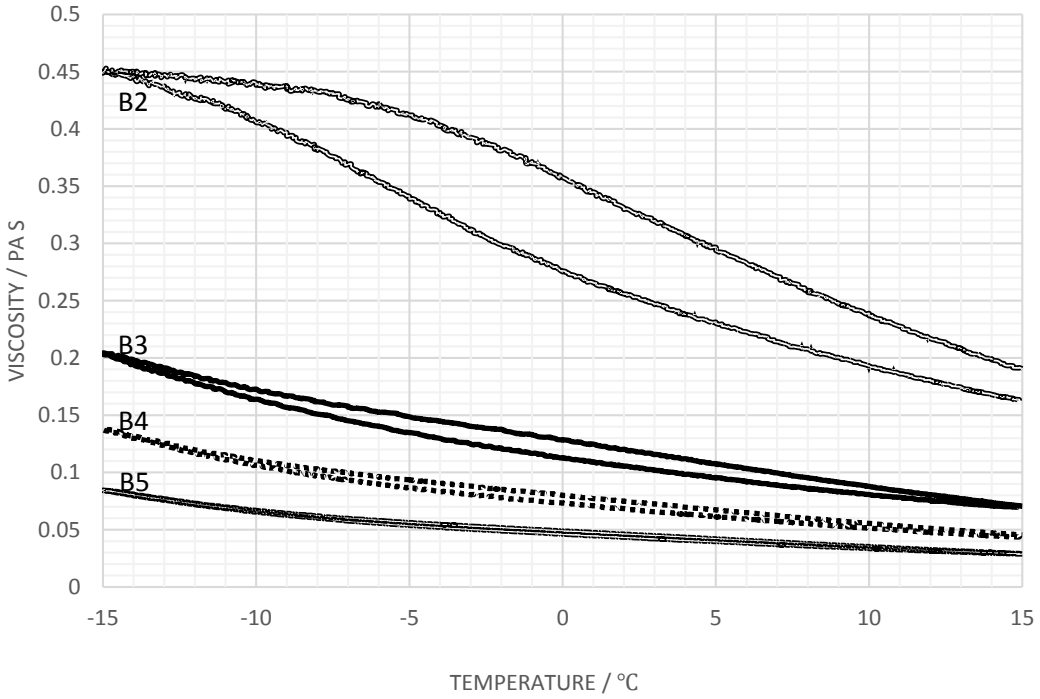

Figure 5.12 Viscosity variation with temperature plots for Carbomer B series, shear stress 10 Pa.

The rheological behaviour of both Carbomers indicates that, even in dilute solution c.a. 0.30 g dL^{-1}, significant intra- and inter-chain interactions are occurring which can be mediated by the addition of salt. The salt is able to interact with the carboxylic acid groups and partially block these intra- and inter-chain interactions. The extent of these interactions will vary with temperature, and leads to a peak in the viscosity-temperature plots which is observed in the linear polymer systems, but disappears in the more branched Carbomer B system.

5.3.3. Modelling

From previous section 5.3.1, sample A4 was selected as the candidate material as it has a similar viscosity profile from temperature ramp test at 5 Pa of shear stress to that of the reference solution. After a series of oscillatory tests were performed, the complex viscosities of A4 were obtained at various temperatures (Figure 5.13). At the higher frequency end, the complex viscosities exhibited increment as decreasing temperature, which is expected; it increased from 0.1048 Pa s at 20°C to 0.2341 Pa s at -10°C. At the lower frequency range, on the other hand, the complex viscosities at 10°C and 0°C are generally higher compared to the one at -10°C. Such a phenomenon is similar to the temperature/viscosity 'peak' which was observed before in the temperature ramp tests. In an attempt to interpret this abnormal change in complex viscosity profile, the mathematical model described in Chapter 4 was fitted to simulate the frequency viscosity relationship at various temperatures.

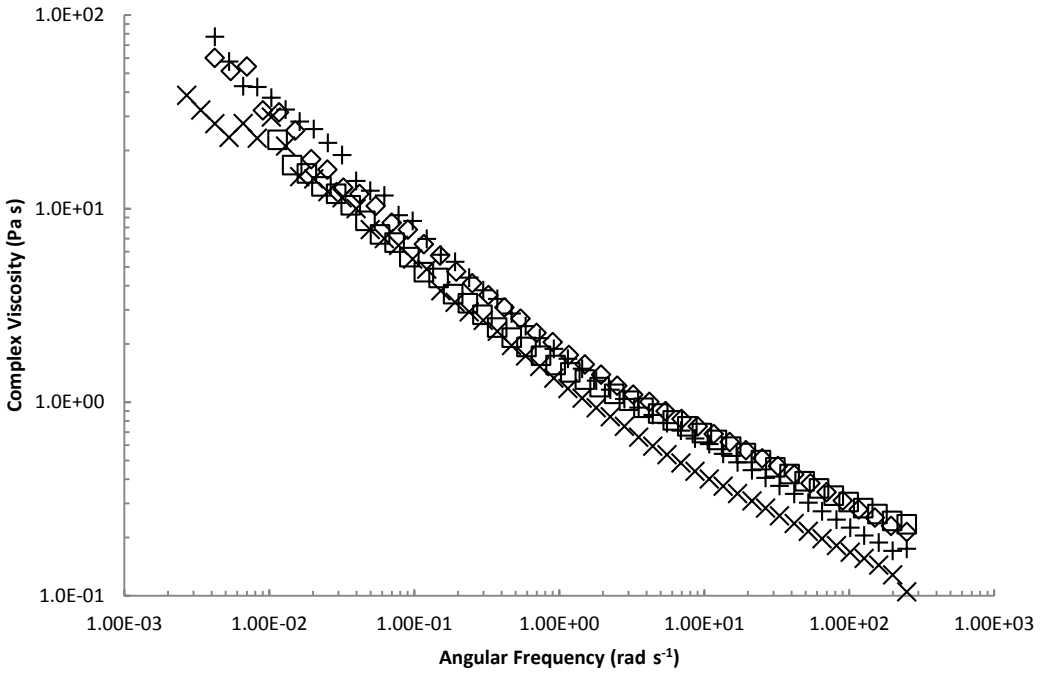

Figure 5.13 Complex viscosity of A4, c_{NaCl} = 0.061 g (NaCl) / g (solution). Lines are temperatures: (×) 20°C; (+) 10°C; (◊) 0°C; (□) -10°C.

As has previously being established, the overall modelling of the viscosity profile is based on three theories; each having their own individual contributions corresponding to different frequency ranges. Rouse theory describes the motions of polymers in solution [18]; and the polymer interactions of non-polyelectrolytes are usually described by Doi-Edwards theory [19-21]. In addition to the polymer entanglements of chain segments relaxation and the reptation motion within the non-linear, large strain region, a train-and-loop concept was also introduced [22] and the contributions of all the relaxation processes to the overall viscosity are additive.

$$\eta_1(\omega) = \eta_s + \frac{6(\eta_m - \eta_s)}{\pi^2}\sum_{p=1}^{N_c}\frac{p^2}{p^4 + \omega^2\tau_r^2} + \frac{1}{2}z_1\frac{6(\eta_e - \eta_m)}{\pi^2}\sum_{p=1}^{N_e}\frac{p^2}{p^4 + \omega^2\tau_b^2} + \frac{1}{2}z_2\left[\frac{8(\eta_e - \eta_0)\cdot h_1}{\pi^2}\sum_{p=1}^{N_d}\frac{p^2}{p^4 + \omega^2\tau_{d1}^2} + \frac{8(\eta_e - \eta_0)\cdot h_2}{\pi^2}\sum_{p=1}^{N_e}\frac{p^2}{p^4 + \omega^2\tau_{d2}^2}\right]$$

where η_s is the solvent viscosity. For the propylene glycol/water mixture used in the fluid

samples, the viscosities at different temperatures were measured using a rheometer. η_m is the terminal viscosity corresponding to the Rouse relaxation process. Based on the fact that the Rouse relaxation time is inversely proportional to the absolute temperature, the terminal viscosity should increase as temperature decreases. η_e is the equilibrium viscosity at extremely low strain region. For such material, temperature ramp tests exhibited a special viscosity profile in which at around -1°C it reached its maximum viscosity within the temperature range. Therefore it is assumed that the value of η_e at 0°C is higher than the ones at 20°C, 10°C, and -10°C. The key parameters are listed as following:

Table 5.2 Viscosities parameters for modelling

Temperature (°C)	20	10	0	-10
$\boldsymbol{\eta_s}$ **(Pa s)**	6.82E-03	9.72E-03	1.63E-02	3.14E-02
$\boldsymbol{\eta_m}$ **(Pa s)**	0.35	0.5	0.56	0.72
$\boldsymbol{\eta_e}$ **(Pa s)**	500	1200	1800	1500

The effective molecular weight of polymer was assumed to be 1 MDa in the previous modelling process. With the same material being processed using the same procedure, it is assumed that the effective molecular weight remains unchanged; and therefore the numbers of total modes within a polymer chain, Kuhn units and entanglement units remain unchanged. For model fitting results shown in Figure 5.14, the differences between this material and the one used in the fitting in Chapter 4 are the solvent, propylene glycol/water mixture and deionized water, and electrolyte concentration, 0.061 g NaCl per 100 g solution (approx. 0.0105M) and 0.012M. Without any knowledge of the effects which change of solvent might have on the polymer interactions, it is reasonable to assume that the degree of complexation, h_1, and consequently, h_2, do not change. With decreasing electrolyte concentration, the coefficient of 'breathing' process

needs to increase from 0.015 to 0.018 to fit with experiment data. This may suggest that due to the weaker shielding effect provided by electrolyte against bonding of neighbouring carboxylic acid groups, polymer chains adopt a more extended structure and the extent of polymer chains forming the 'loop' structures has increased.

As the temperature decreases, the polymer populates the lower energy conformations which are essentially more extended. It creates more polymer-polymer interactions between the non-ionized carboxylic acid groups which causes a rise in viscosity. At the same time the electrolyte will become less soluble and 'salting-out' can occur which will also decrease the screening of the polymer chain, and results in it being less efficient in blocking the formation of hydrogen bonds between neighbouring carboxylic acid groups. In this process, the changes in complex viscosity are likely due to the balance of two motions which contribute to the term in opposite directions. At 20°C, the viscosity drops almost linearly (on the log/log plot) and it is not obvious how the balance of the various contributions give rise to the observed behaviour. At 10°C (Figure 5.15), the degree of complexation and the breathing coefficient are reduced to 0.86 and 0.01, respectively. This suggests that the less dynamic complexation has occurred and less coiled 'loops' are forming within the polymer chains due to the lowering of system energy. When the temperature continues to decrease, at 0°C (Figure 5.16), there are rises in both h_1 and z_1 terms (0.92 and 0.012, respectively). During the temperature ramp tests (Section 5.3.1.1), an observation of a peak in viscosity at approximately -0.9°C has been made, which suggests that the process of electrolyte salting out is causing increase in carboxyl interactions. This observation supports the theory in which both parameters are rising. Then as the temperature is continuously lowered, decrease in ionic concentration finally leads to a state where polymer chains are so entangled that they are forming species that will eventually precipitate from solution and form gel. Prior to this phase-separated state, collapse of the polymer chain to pre-form a globular structure explains the observed reduction in the viscosity in the temperature ramp tests. At -10°C (Figure 5.17), h_1 is reduced to 0.9 due to the formation of those globular structures. However, z_1 has

increased to 0.016 which suggests the extent of polymer chains forming loops is rising.

The analysis indicates that the desirable peak in the viscosity of PAA is achieved by a complex interplay of several factors. As the temperature is lowered the ability for the salt to complex with the carboxylic acid groups of the polymer is decreased, and this ultimately leads to the formation of globular gel particles and precipitation of the polymer. Changes in the degree of shielding of the interaction between groups will influence the chain mobility but also the extent to which inter- and intra-polymer interactions lead to complexation. These changes will influence the extent to which ladder and loop structures are created, and hence the overall hydrodynamic volume of the polymer.

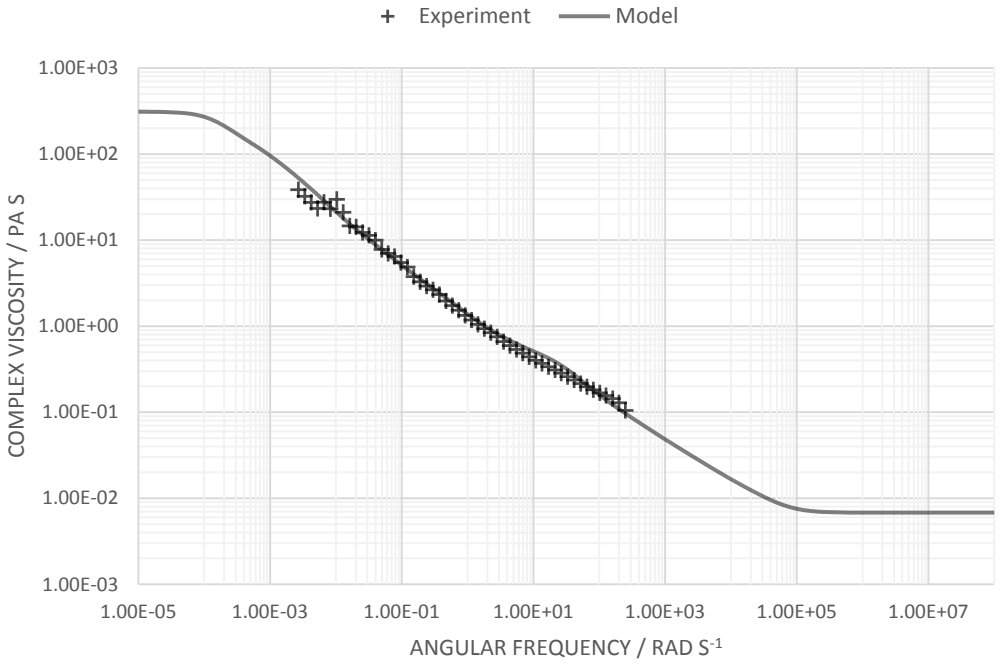

Figure 5.14 Model fitting for Carbomer A solution A4 (c_{NaCl} = 0.061 g per 100 g solution) at 20°C.

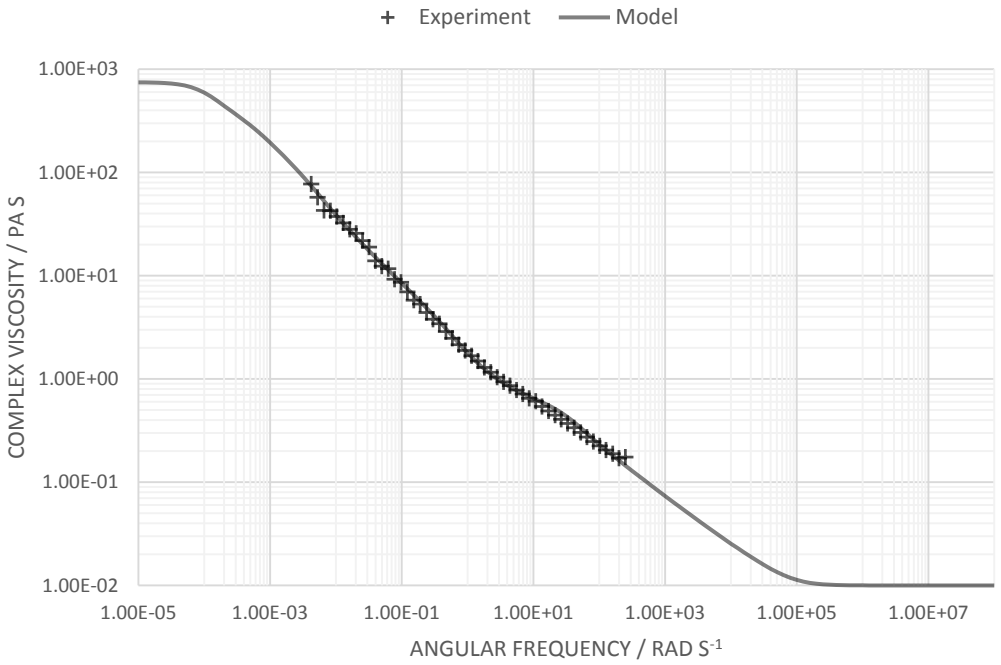

Figure 5.15 Model fitting for Carbomer A solution A4 at 10°C.

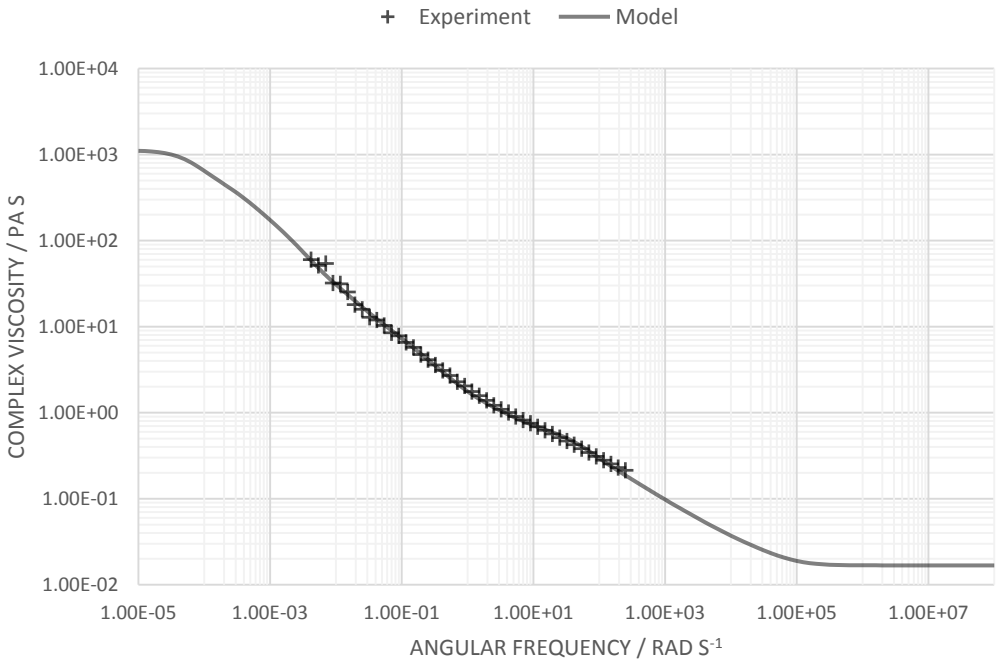

Figure 5.16 Model fitting for Carbomer A solution A4 at 0°C.

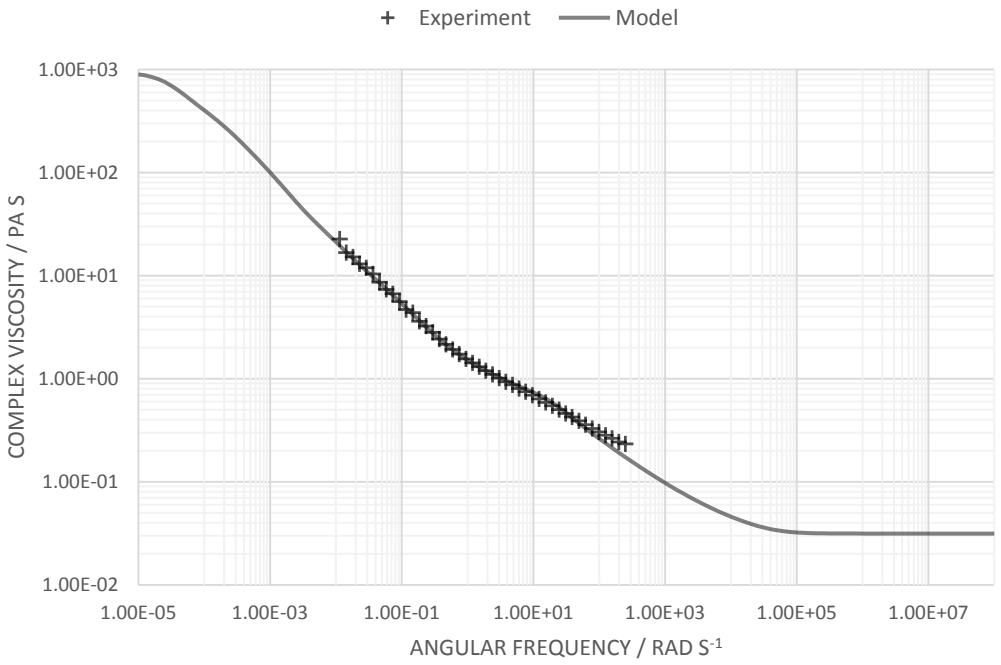

Figure 5.17 Model fitting for Carbomer A solution A4 at -10°C.

5.3.4. Wind Tunnel Evaluation of Carbomer Fluids

For a fluid to possess suitable characteristics to perform as a type II, III or IV fluid it is important that the film which is created during the deicing process should be removed in the period up to rotation. From previous temperature ramp tests it has shown that sample A4 (electrolyte concentration of 0.061 g NaCl per 100g solution) has the preferred range in viscosity, compared to the commercial fluid. It is worth testing its performance in the wind tunnel which may give an insight into its behaviour on the aircraft surface. And this is an important criteria when evaluating deicing fluids. The BLDT of sample A4 is shown in Figure 5.18.

The values of the BLDT are measured in terms of the film thickness around 30 seconds, which is the rotation time for most small to medium-sized aircraft. Acceptable values for fluids are that the BLDT should be lower than 11.3 mm at -20°C and below 8.75 mm at 0°C [23]. The performance of the sample fluid at 100% lies approximately on the limiting line and remains stable across the temperature range. The BLDT values measured around

-10°C are slightly higher compared to the ones at other temperatures. This collaborates with the observation of a peak in viscosity during temperature ramp tests. Such a peak was also shifted to lower temperature when higher shear stress was applied to the fluid. In wind tunnel tests, high air velocity results in higher shear stress than 10 Pa, therefore it is reasonable to assume that a viscosity peak will exhibit at temperatures below -3.2°C (A4 at 10 Pa shear stress); and it would be normal for the fluid to have a higher BLDT value at around -10°C. After dilution, the random coil structure of the polymer chains will swell and form a more extended structure. With the extent of complex entanglements of polymer chains being reduced, the increased value of the BLDT is now in parallel with the increased viscosity as the temperature is lowered (Figure 5.19). As the solution is diluted with water, the values will decrease, but the lowest usable temperature will also increase.

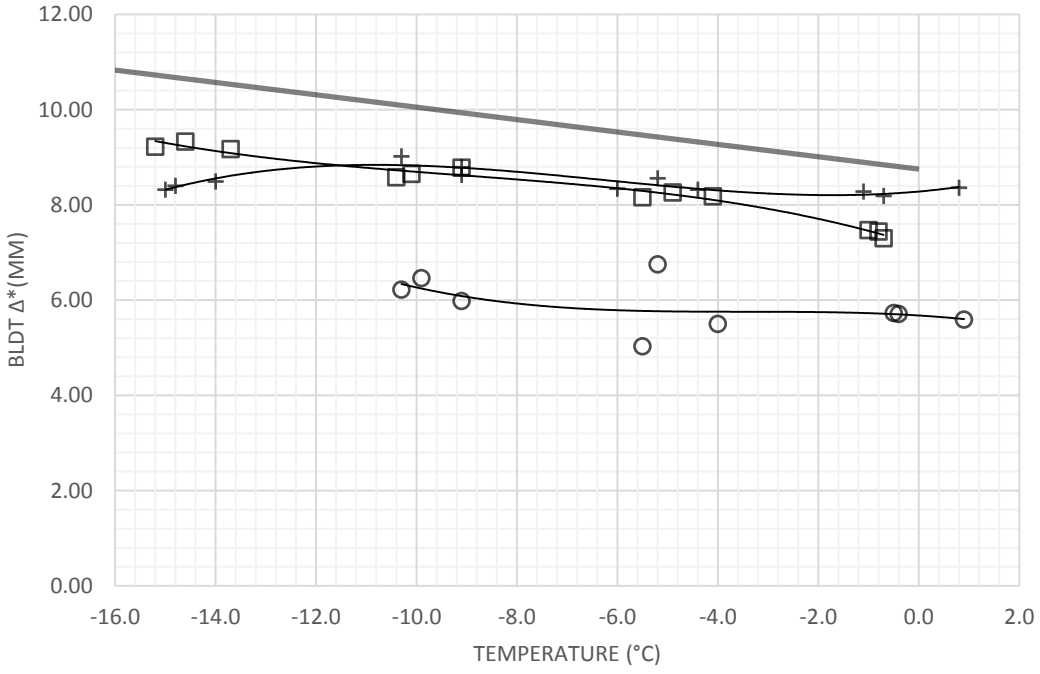

Figure 5.18 BLDT for A4, c_{NaCl} = 0.061 (g NaCl per 100 g solution). (+) Undiluted, (□) 75% concentration wt/wt %, (○) 50% concentration wt/wt %, (–) acceptance.

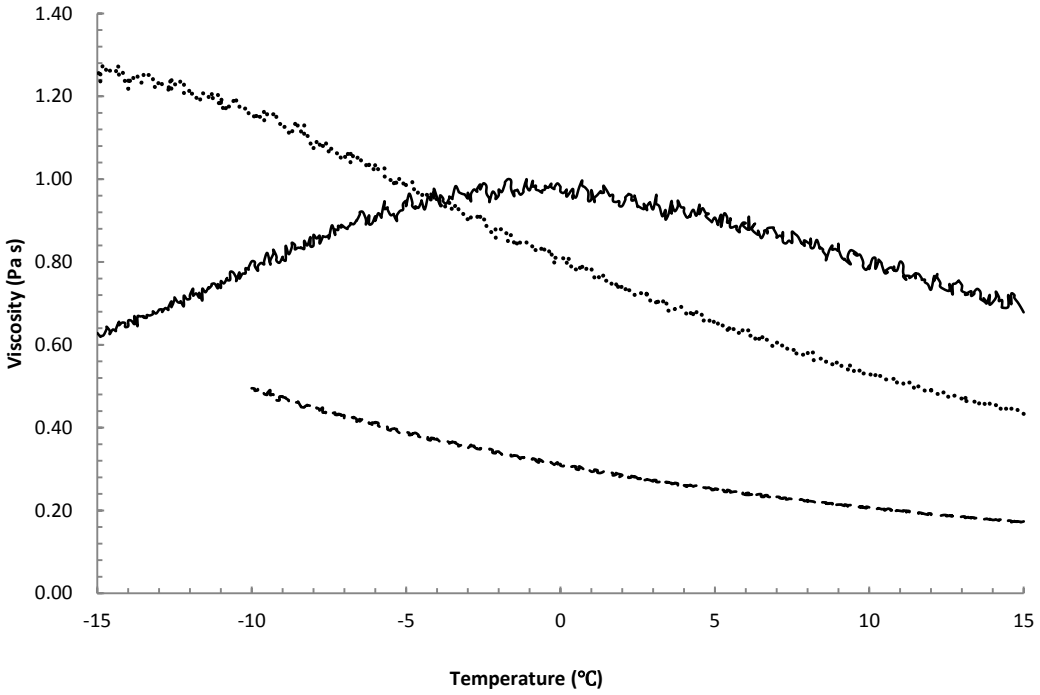

Figure 5.19 Viscosity variation with temperature plots for A4 at 5 Pa applied shear stress. Lines are (—) Undiluted, (…) 75% concentration wt/wt %, (---) 50% concentration wt/wt %.

The ability to achieve the required values of BLDT are clearly closely connected to the observation of the peak in the viscosity which is, in turn, related to the complex array of interactions which exist between and within the molecules for the PAA. The ability for the salt to shield the carboxylic acid interactions is critical to achieving both the desired level of the viscosity, the creation of a peak in the viscosity in the temperature ramp measurements, and the oscillatory shear response which determines the ability for the fluid to be released from the wing during the initial stages of take-off.

5.4. Conclusions

This set of the study has examined the impact of electrolyte addition on the rheological behaviours of the Carbomer A and Carbomer B in a propylene glycol/water mixture at different temperatures. The effect of electrolyte suppressing viscosity is mainly due to its ability to block the bonding of neighbouring carboxylic acid groups. The electrolyte also has an effect on the location of peaks observed in viscosity. With the help of the mathematical model established in the previous chapter, this observed changes can be interpreted as the conformation and structure changes of the polymer chains which will ultimately lead to gel formation. Wind tunnel tests have successfully confirmed that there is consistency between BLDT and viscosity values. For a polymer solution behaving similarly to a commercial fluid in rheological tests, it is likely that it will be acceptable in wind tunnel tests. This study has established a series of criteria to evaluate a polymer-thickened fluid which has the potential of being used as an aircraft de-icing fluid; and such criteria will be utilised in the following chapters to investigate the possibility of formulating new fluids thickened by polyvinylpyrrolidone-PAA blends.

5.5. References

1. Coffey, D.A., Nieh, E.C.Y., and Armstrong, R.A., Aircraft deicing fluid with thermal and pH-stable wetting agent USPTO, Editor 1995, Texaco Inc.: U.S.

2. Jenkins, R.D., Bassett, D.R., Lightfoot, R.H., and Boluk, M.Y., Aircraft anti-icing fluids thickened by associative polymers, USPTO, Editor 1997, Union Carbide Chemicals & Plastics Technology Corporation: U.S.

3. Jenkins, R.D., Bassett, D.R., Lightfoot, R.H., and Boluk, M.Y., Aircraft anti-icing fluids, USPTO, Editor 1995, Union Carbide Chemicals & Plastics Technology Corporation: U.S.

4. Ross, F., Aircraft De-/Anti-Icer, USPTO, Editor 2011, Kilfrost Limited: U.S.

5. Switzenbaum, M.S., Veltman, S., Mericas, D., Wagoner, B., and Schoenberg, T., Best management practices for airport deicing stormwater. Chemosphere, 2001. 43(8): pp. 1051-1062.

6. Kent, R.A., Andersen, D., Caux, P.Y., and Teed, S., Canadian Water Quality Guidelines for glycols - An ecotoxicological review of glycols and associated aircraft anti-icing and deicing fluids. Environmental Toxicology, 1999. 14(5): pp. 481-522.

7. Cancilla, D.A., Martinez, J., and Van Aggelen, G.C., Detection of aircraft deicing/antiicing fluid additives in a perched water monitoring well at an international airport. Environmental Science & Technology, 1998. 32(23): pp. 3834-3835.

8. Klecka, G.M., Carpenter, C.L., and Landenberger, B.D., Biodegradation of Aircraft Deicing Fluids in Soil at Low-Temperatures. Ecotoxicology and Environmental Safety, 1993. 25(3): pp. 280-295.

9. ASTM, ASTM D1193 - 06(2011) Standard Specification for Reagent Water, 2011, ASTM International: West Conshohocken, PA.

10. SAE, SAE AMS1428 Fluid, Aircraft Deicing/Anti-Icing, Non-Newtonian (Pseudoplastic), SAE Types II, III, and IV, 2010, SAE International.

11. ASTM, ASTM E70 - 07 Standard Test Method for pH of Aqueous Solutions With the Glass Electrode, 2007, ASTM International: West Conshohocken, PA.

12. SAE, SAE AMS1424 Deicing/Anti-Icing Fluid, Aircraft, SAE Type I, 1993, SAE International.

13. Staikos, G., Sotiropoulou, M., Bokias, G., Bossard, F., Oberdisse, J., and Balnois, E., Hydrogen-Bonded Interpolymer Complexes Soluble at Low pH, in Hydrogen-bonded interpolymer complexes: formation, structure and applications,

Khutoryanskiy, V.V. and Staikos, G., Editors. 2009, World Scientific. pp. 23-53.

14. Volk, N., Vollmer, D., Schmidt, M., Oppermann, W., and Huber, K., Conformation and Phase Diagrams of Flexible Polyelectrolytes - Polyelectrolytes with Defined Molecular Architecture II, in Advances in Polymer Science, Schmidt, M., Editor 2004, Springer Berlin / Heidelberg. pp. 29-65.

15. Prime, R.B., Thermosets, in Thermal characterization of polymeric materials, Turi, E.A., Editor 1997, Academic Press. pp. 173-174.

16. Bertini, V. and Pocci, M., Functional Polymers for Selective Flocculation of Minerals, in Desk reference of functional polymers: syntheses and applications, Arshady, R., Editor 1997, American Chemical Society.

17. Munk, P., Tertiary Structure — Arrangement of Larger Segments, in Introduction to Macromolecular Science, Munk, P., Editor 1989, John Wiley & Sons: New York. pp. 60-61.

18. Rouse, P.E., A Theory of the Linear Viscoelastic Properties of Dilute Solutions of Coiling Polymers. Journal of Chemical Physics, 1953. 21(7): pp. 1272-1280.

19. Doi, M. and Edwards, S.F., Dynamics of concentrated polymer systems. Part 1.-Brownian motion in the equilibrium state. Journal of the Chemical Society, Faraday Transactions 2: Molecular and Chemical Physics, 1978. 74: pp. 1789-1801.

20. Rahalker, R.R., Lamb, J., Harrison, G., Barlow, A.J., Hawthorn, W., Semlyen, J.A., North, A.M., and Pethrick, R.A., Viscoelastic Studies of Linear Polydimethylsiloxanes. Proceedings of the Royal Society of London Series a-Mathematical Physical and Engineering Sciences, 1984. 394(1806): pp. 207-222.

21. Doi, M., Molecular Rheology of Concentrated Polymer Systems.1. Journal of Polymer Science Part B-Polymer Physics, 1980. 18(5): pp. 1005-1020.

22. Hudson, N.E., Ferguson, J., and Warren, B.C.H., Polymer Complexation Effects in Extensional Flows. Journal of Non-Newtonian Fluid Mechanics, 1988. 30(2-3): pp. 251-266.

23. SAE, SAE AS5900B Standard Test Method for Aerodynamic Acceptance of SAE AMS 1424 and SAE AMS 1428 Aircraft Deicing/Anti-icing Fluids, 2007, SAE International.

Chapter 6. Rheology of Carbomer A – PVP Fluids

6.1. Introduction

In the previous chapter, a study has been carried out to characterise the rheological behaviour of Carbomer-thickened fluids. The complex nature of polymer-polymer interactions has altered the simple rheological property of a propylene glycol/water mixture. With the addition of electrolyte, the viscosity profile was even further complicated. Electrolytes allow an almost constant viscosity to be created which is independent of temperature over the designated temperature range, in spite of the fact that salting out of the electrolyte can create gels which may potentially become insoluble.

Polyvinylpyrrolidone (PVP) is a widely used polymer and has been used since the 1950s as a blood plasma expander for trauma victims and also used in many pharmaceutical tablet and liquid formulations [1-3]. The potential use of PVP in conjunction with various salts as a run way de-icing medium has been proposed [4] . In the typical PAA formulation, salt is added to control the viscosity making the product sensitive to changes in ionic strength as a consequence of dilution with water during application or in the subsequent evaporation of solvent. Conceptually, partial replacement of PAA by PVP would allow achievement of the pseudoplastic characteristics through hydrogen bonding between the PVP and PAA. PAA gel formation can be associated with a change in the balance of electrostatic screening interactions with mono-valent salt ions and the creation of insoluble hydrogen-bonded precipitates. Creating of deposits in which the hydrogen-bonded structure can be readily re-swollen would reduce gel formation and the build-up of insoluble gel building up on the control surfaces [5]. In Chapter 8 we will investigate the effects of calcium ions in the formation of insoluble gel particles in PAA solutions. Reducing the sensitivity of the solution properties to added electrolyte and the introduction of an easily dissolvable element into the gel should, in principle, reduce the gel formation problem. It is also proposed that the addition of PVP will effectively block

the interaction between PAA and calcium ions and thus reduce the possibility of forming insoluble gel.

Previous studies have shown that PVP/PAA miscible blends can be formed at any molar ratio and are sensitive to low pH [6]. The hydrogen bond is not affected by the addition of salts of low molecular weight carboxylic acids, which only interact with the cations without forming hydrogen bonds with the carboxyl groups on the PAA chain. Reversibility of the complex formed between PVP/PAA has been shown for pH values above 4.5 and the interaction between PAA and PVP at pH 7 is minimal [7]. On the other hand, the molar ratio of PVP/PAA complexes has always to be greater 1.5:1, to form a stable complex [8]. The stability of the complex depends on pH and as it is raised there is a tendency for the mutual interactions to be reduced [8-11]. To avoid the creation of insoluble deposits the ratio of the two polymers is held below the critical value for gel formation, hence allowing the benefits of dynamic interaction enhancing the rheology without promoting gel formation.

Reported in this chapter is a study of the rheological behaviour of Carbomer A/propylene glycol/water mixtures with four high molecular weight PVP species which potentially can exhibit similar rheological characteristics to those of the standard de-icing fluids. To assess the performance of selected mixtures, BLDT and WSET measurements were also conducted.

6.2. Experimental

6.2.1. Materials and Sample Preparation

Carbomer A, a poly(acrylic acid) based co-polymer, was supplied by Lubrizol (Brussels, Belgium) as flocculated solid particles with diameter of approximately 0.2 μm and nominal molar mass of 4 MDa. Characterisation of this material has been undertaken and has been reported in Chapter 3and Chapter 5, including FTIR and FT-NMR analyses,

intrinsic viscosity measurements, acid number determination, and rheological measurements. To achieve quick dissolution, the solid polymer was dispersed using a Silverson L4R high shear mixer with its head placed in a 1 L beaker containing 600 g of de-ionized water and operated at 4800 rpm for 5 minutes; on completion the rotation speed was reduced to 3600 rpm and stirring continued for a further 55 minutes. A 'gel-like' dispersion was produced with a polymer concentration of 1.22 g dL^{-1}.

Four PVP polymers were used in this study, and their characteristics are listed below (Table 6.1). All PVP polymers were dispersed in de-ionized water at a concentration of 1.22 g dL^{-1} and stirred until fully dissolved using a magnetic stirrer. A water/1,2-propylene glycol mixture was prepared at a 50:50 wt/wt ratio. The Carbomer A gel intermediate was first added to the water/glycol mixture and fully mixed, and the PVP solution was then added and fully mixed. The total polymer concentration of polymer was 0.30 g dL^{-1} with different PAA/PVP ratios. The solutions were then neutralized with 5.0M potassium hydroxide solution to attain a pH of 7.0. 5.0M sodium chloride solution was added to adjust the viscosity profile of the solution to give a profile similar to that observed for the Carbomer-thickened solution. The sample compositions can be found in Table 6.2. The solutions were left to stand for at least 72 hours before measurements were undertaken, allowing the systems to achieve a thermodynamic equilibrium.

Table 6.1 PVP Material Information

Sample	M_W **(KDa)**	**Supplier**	**Form**
P1	360	Aldrich (Gillingham, UK)	Powder
P2	700	BDH (Poole, UK)	Powder
P3	1,300	ISP Technologies (Calvert City, US)	Powder
P4	4,000	ISP Technologies (Calvert City, US)	Liquid

Table 6.2 Carbomer A:PVP Composition Data

Sample	PVP M_W (KDa)	PAA/PVP Ratio	NaCl(g)/Soln(g)
AP101	360	50:50	0
AP102	360	50:50	0.015/100
AP103	360	50:50	0.030/100
AP104	360	50:50	0.045/100
AP105	360	50:50	0.061/100
AP111	360	60:40	0
AP112	360	60:40	0.018/100
AP113	360	60:40	0.036/100
AP114	360	60:40	0.054/100
AP115	360	60:40	0.072/100
AP121	360	40:60	0
AP122	360	40:60	0.012/100
AP123	360	40:60	0.024/100
AP124	360	40:60	0.036/100
AP125	360	40:60	0.048/100
AP201	700	50:50	0
AP202	700	50:50	0.015/100
AP203	700	50:50	0.030/100
AP204	700	50:50	0.045/100
AP205	700	50:50	0.061/100
AP211	700	60:40	0
AP212	700	60:40	0.018/100
AP213	700	60:40	0.036/100
AP214	700	60:40	0.054/100
AP215	700	60:40	0.072/100
AP221	700	40:60	0

AP222	700	40:60	0.012/100
AP223	700	40:60	0.024/100
AP224	700	40:60	0.036/100
AP225	700	40:60	0.048/100
AP301	1,300	50:50	0
AP302	1,300	50:50	0.015/100
AP303	1,300	50:50	0.030/100
AP304	1,300	50:50	0.045/100
AP305	1,300	50:50	0.061/100
AP306	1,300	50:50	0.022/100
AP322	1,300	40:60	0.012/100
AP401	4,000	50:50	0
AP402	4,000	50:50	0.015/100
AP403	4,000	50:50	0.030/100
AP406	4,000	50:50	0.022/100
AP422	4,000	40:60	0.012/100

6.2.2. Rheology

Viscosities were measured using both a temperature ramp at fixed stress, and a steady shear stress ramp at various temperatures. These were carried out using a shear stress-controlled Carri-Med CSL²500 rheometer (TA Instruments, Crawley, UK) using a 4-cm parallel plate fitted with a solvent trap. Temperature was controlled by using the Peltier effect and an anti-freezing bath maintained at 0°C, enabling test temperatures between 15°C and –15°C. Temperature ramp tests were carried out at a rate of 1.0°C per two minutes from 15°C to –15°C, and then from –15°C to 15°C, at shear stresses of 5 and 10 Pa. Steady shear stress tests were carried out at 0°C, –5°C, –10°C and –15°C at 0.1 to 100 Pa, with a ten-fold increase in stress per 10 minutes, and subsequent decrease.

6.2.3. BLDT Measurement

Wind tunnel testing was carried out to determine the removal capability of the fluid from a flat surface. The wind tunnel consists of a duct through which temperature-controlled air is blown. The effectiveness of the removal of the fluid is evaluated using pressure sensors to determine the boundary layer displacement thickness (BLDT) which is a measure of the remaining film thickness on the surface during its continuous removal by the increasing flow of air. The acceleration of the air flow mimics the passage of air over the wind during the initial stages of take-off.

Samples of test fluid were initially applied as a coating on the floor of the duct to a thickness of 1.5 mm using a scraper and this simulates the coating which would be deposited by spray application. The temperature of the test facility was thermostatically controlled and tests were carried out at approximately 0°C, -5°C, -10°C and -15°C. At the start of each run, air velocity was increased from stationary at a linear rate to 65 ms^{-1} over a period of 25 seconds.

The BLDT was determined from the measurement of two pressure differences corresponding to the inlet $p_1 - p_2$ and outlet $p_2 - p_3$ of the wind tunnel from

$$\delta^* = \frac{1}{C}\left[A_3 - A_2\sqrt{\frac{p_1 - p_2}{(p_1 - p_2) + (p_2 - p_{3)}}}\right]$$

where A_2 and A_3 are the upstream and downstream areas of the duct, and C is the perimeter of the duct. The BLDT is the average thickness measured between 27 and 33 seconds after the start of the process and once the air has reached its maximum velocity. Each test was repeated in triplicate.

6.3. Results and Discussion

From previous chapters it has been established that for a de-icing fluid to be acceptable

for use, the shear-thinning characteristics over the operational temperature range are critical. In Chapter 5, a commercially available fluid based on a 50:50 mixture of water/1,2-propylene glycol thickened by Carbomer A, a high molecular weight poly(acrylic acid), was characterised rheologically as a reference. A series of sample solutions thickened by Carbomer A with increasing concentration of electrolyte were also examined. The addition of PAA had an obvious effect of reducing the temperature sensitivity of the viscosity of the original water/glycol mixture while creating the desirable shear-thinning profile. It is important to examine whether the PAA/PVP blends are also capable of providing the appropriate thickening properties to the fluids. Four PVP polymers with different molecular weight have been blended with Carbomer A and evaluated using the same conditions as those used for the Carbomer A system. The mixing ratios of PVP/PAA are 40:60, 50:50, and 60:40 for 360k and 700k molecular weight PVP and 40:60 and 50:50 for 1.3M and 4M PVP. Electrolyte, sodium chloride, was also progressively added to the systems and the ratio of which was held constant.

For temperature ramp data of each individual sample not exhibited in this chapter, please refer to Appendix C.

6.3.1. System AP1 (Carbomer A/PVP 360k)

The viscosity variation with temperature for PVP 360k dispersion in 50:50 water/propylene glycol mixture was examined prior to blending with Carbomer A (Figure 6.1). The polymer concentration was 0.30 g dL^{-1} and pH was adjusted to 7.0 at 20°C. Because of the relatively low concentration, PVP 360k did not enhance the viscosity of the solvent by the same extent as Carbomer A. At 5 Pa of shear stress applied, viscosity was 0.012 Pa s at 15°C and 0.074 Pa s, which is negligible compared to Carbomer A solution A1 (at the same polymer concentration). Shear-thinning behaviour was observed; and a lack of hysteresis suggests a shorter relaxation time compared to Carbomer A solution at the same condition. The PVP will not be extensively complexed at these concentrations and the backbone dynamics will be similar to those of a flexible

polymer chain.

Blends of Carbomer A/PVP were then formulated in a 50:50 water/glycol mixture. Holding the total polymer concentration constant at 0.30 g dL^{-1}, the blending ratios of Carbomer A/PVP are 50:50, 60:40, and 40:60, wt/wt.

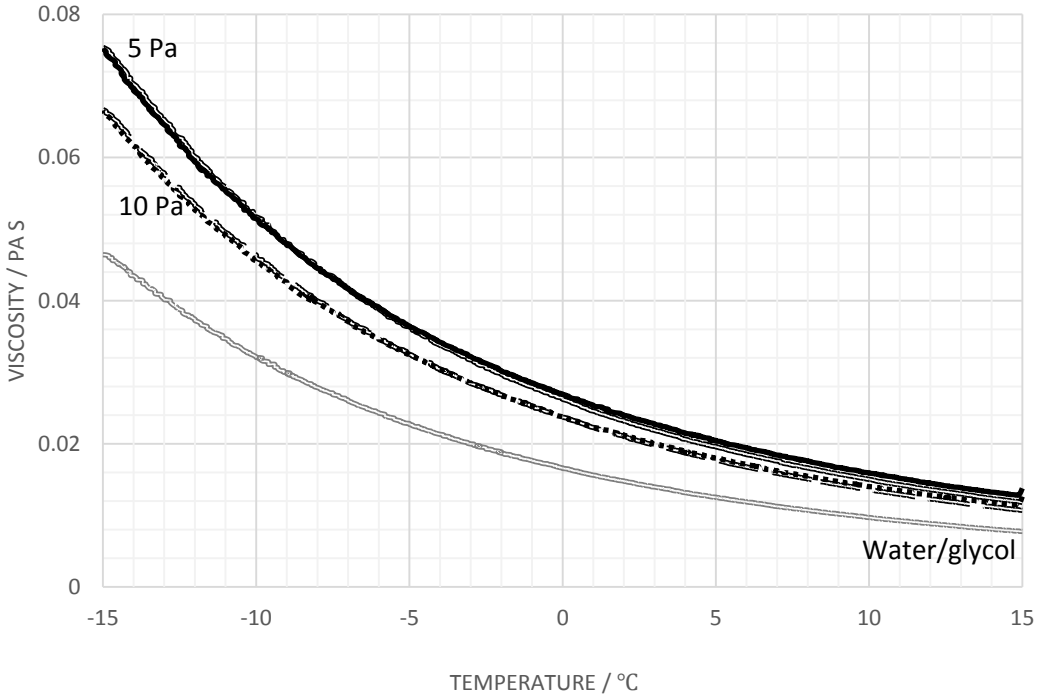

Figure 6.1 Viscosity variation with temperature plots for PVP 360k at concentration of 0.30 g/dL, shear stress 5 and 10 Pa. Water/glycol 50:50 wt/wt.

6.3.1.1. Weight Ratio 50:50 (Carbomer A:PVP 360k)

With increasing electrolyte level, the behaviour of these solutions is similar in form to those observed with corresponding Carbomer A fluids. For fluids without electrolyte addition, Figure 6.2 showed a drop in viscosity for the PVP/PAA-thickening system. The viscosity dropped to 2.68 Pa s at 15°C and 15.24 Pa s at -15°C, compared to 9.37 Pa s at 15°C and 48.64 Pa s at -15°C for A1, the PAA-thickened fluid. Assuming that the viscosity of Carbomer A solution scales with the polymer concentration, viscosity would be expected to reduce with reduced concentration. A theoretical curve was presented in Figure 6.2 to represent half of the original viscosity level. Experimental results exhibited

a larger (approximately 56% across the temperature range) reduction in viscosity than the theoretically predicted values. Reducing the polymer concentration is clearly reducing its ability to undergo polymer-polymer interactions and the chains are adopting a more 'isolated' polymer chain configuration. Although the viscosity level of AP101 is lower compared to A1 it is still considerably higher than the water/glycol mixture. The molecular weight of the PVP polymer is significantly lower than the PAA polymer, which resulted in less entanglements being formed through both intra- and inter-polymer interactions. As the applied shear stress increased to 10 Pa, the viscosity dropped to 1.53 Pa s at 15°C and 10.87 Pa s at -15°C (Figure 6.3), exhibiting shear thinning characteristics. The observation of shear thinning is consistent with their being some form of structure formed through chain entanglement and or hydrogen bonding interactions between carboxylic acid functions.

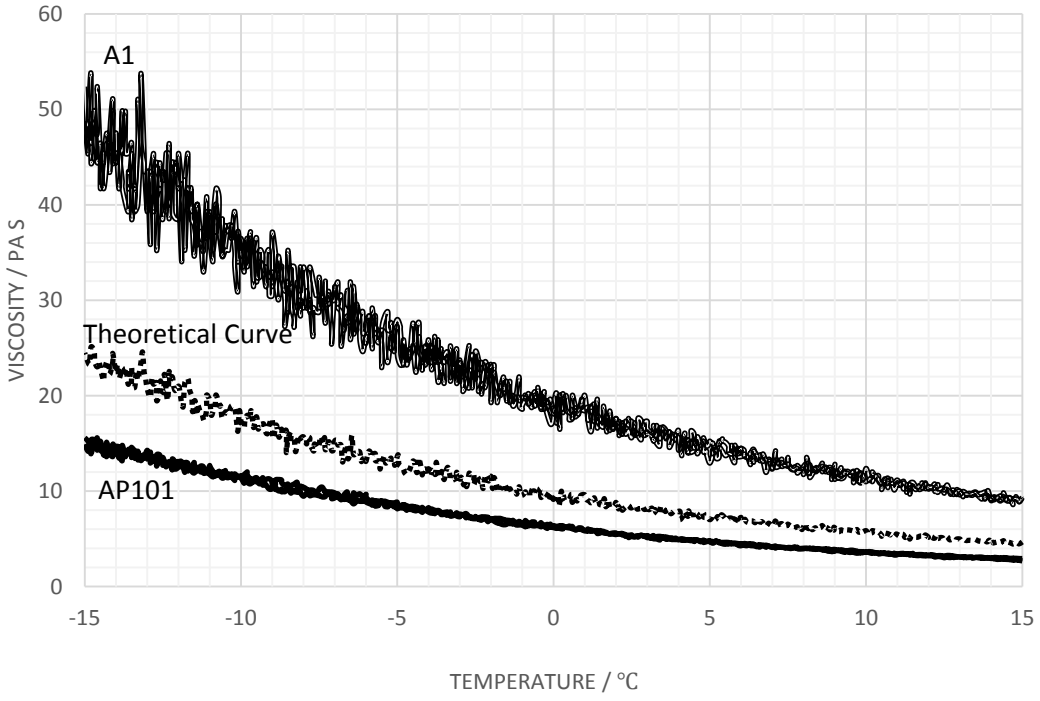

Figure 6.2 Viscosity variation with temperature plots for AP101 and comparison with A1 and theoretical prediction, shear stress 5 Pa. Water/glycol 50:50 wt/wt.

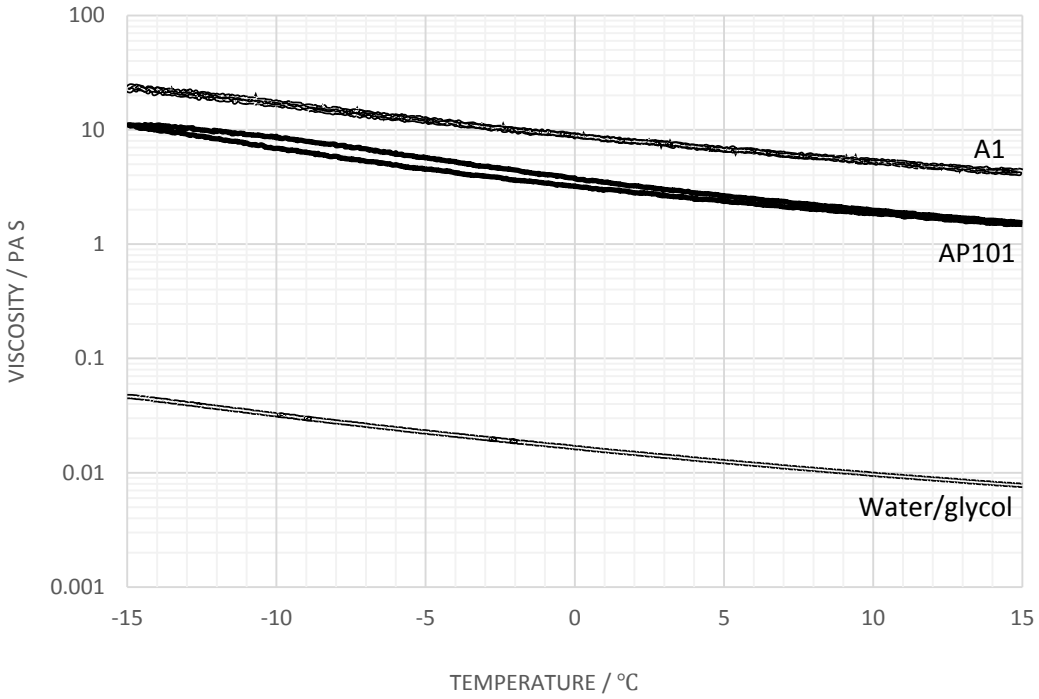

Figure 6.3 Viscosity variation with temperature plots for AP101 and comparison with A1, shear stress 10 Pa. Water/glycol 50:50 wt/wt.

With the addition of sodium chloride electrolyte to the system, the interactions between carboxylic groups are reduced, the sodium cations screening the carboxylic groups and reducing their hydrogen-bonding potential. For example, in Figure 6.4, a blend of 50:50 PAA/PVP was formulated in a 50:50 water/glycol mixture, the electrolyte level being adjusted to 0.015 g (NaCl) per 100 g (solution). At an applied shear stress of 5 Pa, the viscosity measured at 15°C is lower at 0.36 Pa s; however a peak value of 0.9 Pa s is reached between -2°C and -5°C, before the viscosity drops to 0.58 Pa s. The maximum viscosity across this temperature range is very similar to Carbomer A solution A4, which contains 0.061 g (NaCl) per 100 g (solution) and has a maximum viscosity of approximately 0.98 Pa s at around -0.9°C with applied shear stress of 5 Pa. To compare AP102 with A4, the content of PAA was reduced to 50% whereas it requires only 25% of the amount of electrolyte to suppress the viscosity to the same level, suggesting the extent of interactions between carboxylic groups has been reduced. The viscosity curves show hysteresis, the values measured on heating being lower than those on cooling.

Similar behaviour is observed for measurements performed at 10 Pa, the location of the peak being dependent on whether measurements are made on cooling or heating. In comparison with a pure PAA-thickened fluid A2 (Figure 6.5), the viscosity curves of temperature dependence appear to be of the same shape. The 'peak' location of AP102 is at similar temperature of around -5°C compared to A4 indicating similar extent of screening effect of electrolyte. The observation of a peak in the viscosity temperature profile is indicative of the balance on interactions associated with the formation of globular particles ascribed to the behaviour in PAA solutions.

In the mixtures the interaction of the PVP with the PAA will involve hydrogen bonding between the pyrrolidone ring and the carboxylic acid groups on the PAA. The similarity in viscosity behaviour implies that to some extent a similar balance of interactions is being created with the blends to those which exist in the Carbomer A-thickening systems; however the observed differences in behaviour are a reflection of the role of the hydrogen bonding interactions between PVP and PAA. In the pure polymer systems hydrogen bonding will occur between non-screened groups, in the blends these occur where the two polymers can interact. At lower temperatures, a combination of the de-shielding of the carbonyl groups and changes on conformation will lead to a pre-gelation state which gives rise to the hysteresis and the reduction in viscosity below 0°C. The shift in the peak to higher temperatures reflects the fact that the pre-gel form will require time to dissociate on heating leading to an observed lowering of the value of the viscosity and increase in temperature of the peak.

Further increasing the electrolyte level, the general level of viscosity continues to decrease, which is similar to the behaviour of pure Carbomer A-thickened fluids (Figure 6.6). Apart from AP101, which has no electrolyte, all other samples exhibited a certain viscosity 'peak' or 'plateau' across the temperature range and its location is shifted slightly within the range of 0°C to -5°C. Such a characteristic is desirable for the application of these mixtures as de-icing fluids. When the applied shear stress was

increased to 10 Pa (Figure 6.7), the locations of viscosity 'peak' (or 'plateau') have all been slightly shifted to lower temperature by approximately 2 to 3 degrees Celsius. The higher shear stress may be expected to disentangle elements of the interacting PAA chain and change the extent to which interactions occur. The observation of present hysteresis indicates the latency of break-down of pre-gel complex.

Among all the 50:50 PVP/PAA samples, AP102 with 0.015 g (NaCl) per 100 g (solution) electrolyte was of particular interest for its similar viscosity level to the commercial sample ABC-2000. To form a basis of becoming a potential candidate of de-icing fluid, further examinations are required in terms of its aerodynamic performances (Section 6.3.5).

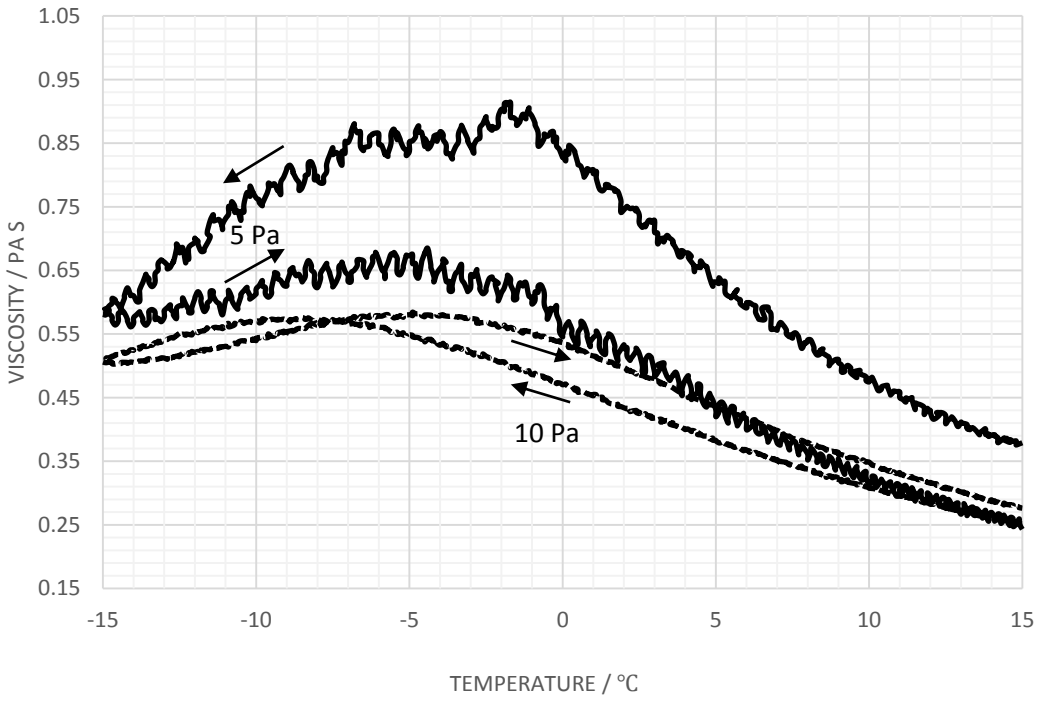

Figure 6.4 Viscosity variation with temperature plots for AP102, applied shear stresses 5 and 10 Pa.

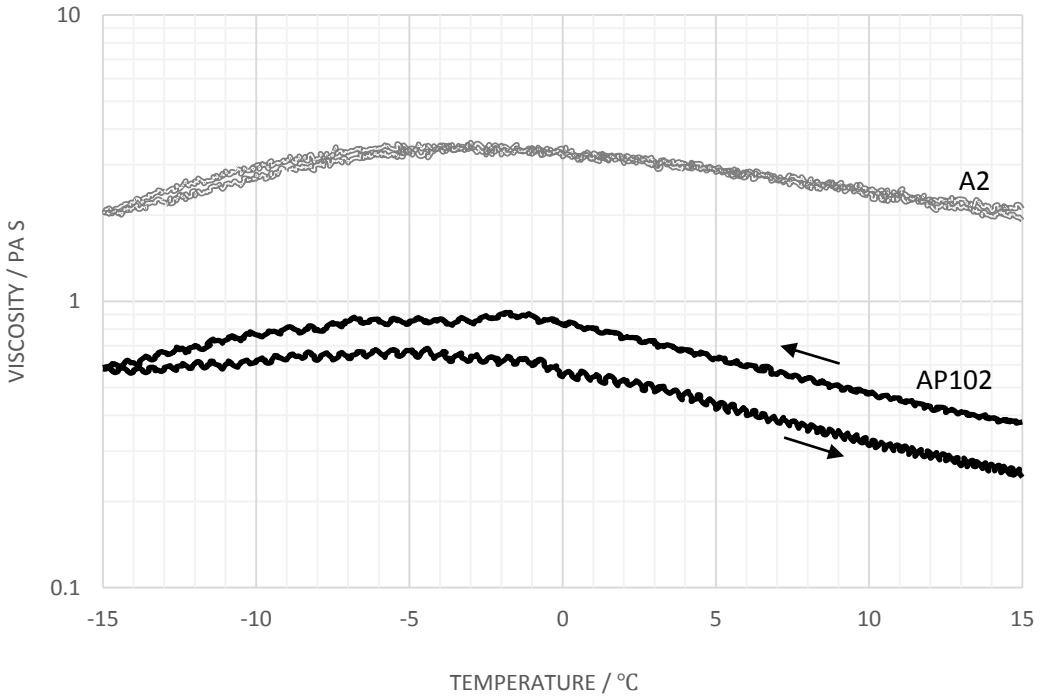

Figure 6.5 Viscosity variation with temperature plots for AP102 and comparison with A2, shear stress 5 Pa.

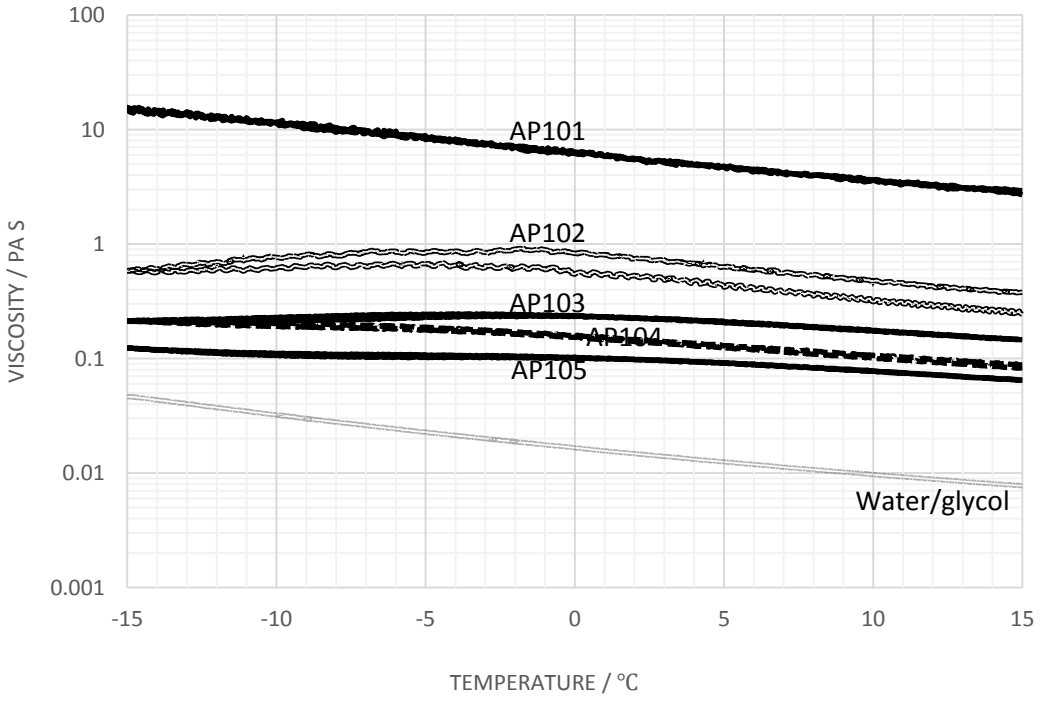

Figure 6.6 Viscosity variation with temperature plots for AP1 series, PVP_{360k}:Carbomer A=50:50 wt/wt, shear stress 5 Pa.

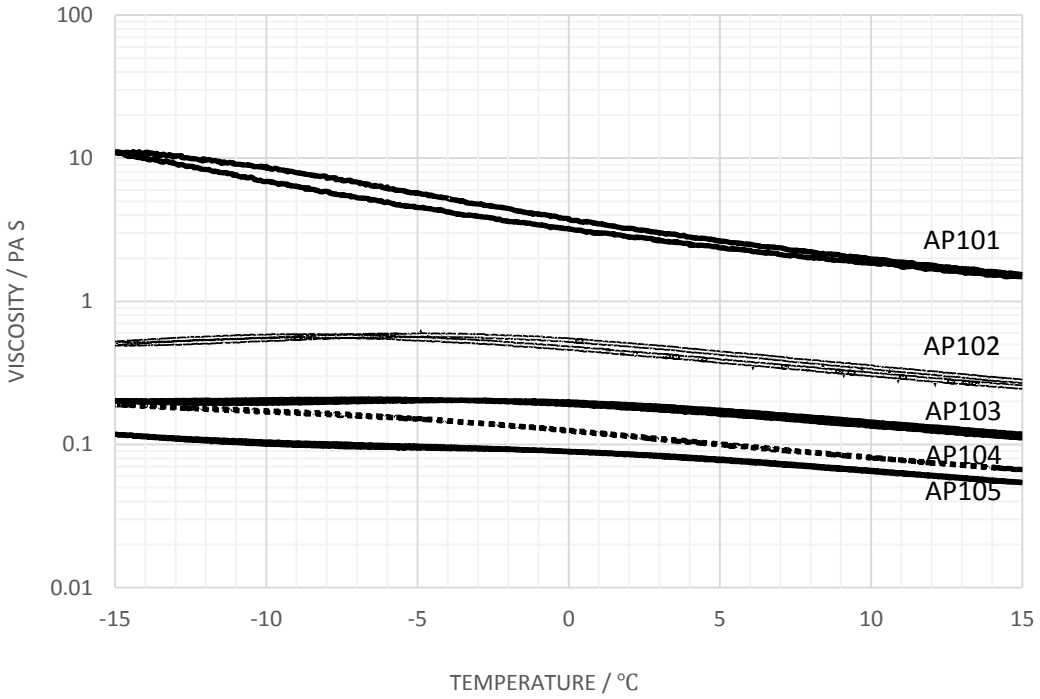

Figure 6.7 Viscosity variation with temperature plots for AP1 series, PVP_{360k}:Carbomer A=50:50 wt/wt, shear stress 10 Pa.

6.3.1.2. Weight Ratio 60:40 (Carbomer A/PVP 360k)

To further explore the nature of the pre-gelation complex the blend of 60:40 PAA/PVP was investigated. With no electrolyte added, AP111 appeared more viscous than the 50:50 blend, AP101, across the temperature range of 15°C to -15°C, but still remained less viscous than the pure Carbomer A fluid, A1. At an applied shear stress of 5 Pa (Figure 6.8), the viscosity of AP111 was approximately 3.78 Pa s at 15°C and continuously rising to approximately 22.45 Pa s at -15°C. Increasing the PAA content leads to a significant increase in viscosity. With electrolyte progressively added to the system, the viscosity decreased continuously (Figure 6.9) suggesting the shielding effect of salt is still a primary factor influencing the hydrodynamic volume exhibited by the polymers in the blend. Assuming the molecular weight of Carbomer A has dropped to 1 MDa after intense shear (Chapter 5), the molar ratio of PAA/PVP increased from 0.36:1 at 50:50 wt/wt mixing ratio to 0.54:1 at 60:40 wt/wt. It appears that in this blend the PAA is playing the

dominant role and its interactions with PVP are not significantly affecting the rheological performances. Presumably the increased sodium concentration is influencing the shielding of the carboxylic acid groups from interacting with themselves and with the pyrrolidone ring protons.

For sample AP112, the electrolyte concentration is 0.018 g (NaCl) per 100 g (solution); the viscosity at 5 Pa of shear stress increased from 0.55 Pa s at 15°C and to approximately 1.41 Pa s at -15°C (Figure 6.10). Unlike the 50:50 blend AP102, no viscosity 'peak' was observed in this blend; however the viscosity appears to level off at -15°C suggesting that a peak value may be being reached. There is also a little hysteresis between the heating and cooling measurements at either 5 Pa or 10 Pa of applied shear stress (Figure 6.11). These suggest that in a 60:40 blend of PAA/PVP, PAA is primarily contributing to the rheological performances. Because of its shorter polymer chains and incapability of intra-polymer entanglement, PVP is effectively suppressing the extent of polymer interactions, resulting in a lower viscosity in comparison with the pure Carbomer A-thickened system, however it is capable of weak interaction with the PAA through hydrogen bonding leading to enhancement of the viscosity.

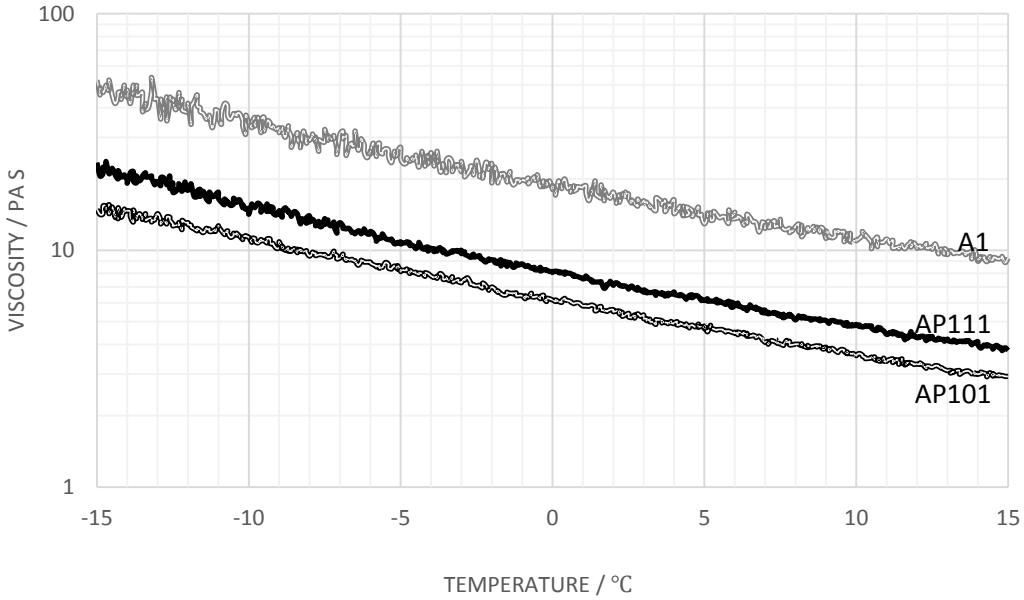

Figure 6.8 Viscosity variation with temperature plots for AP111 and comparison with AP101 and A1, shear stress 5 Pa.

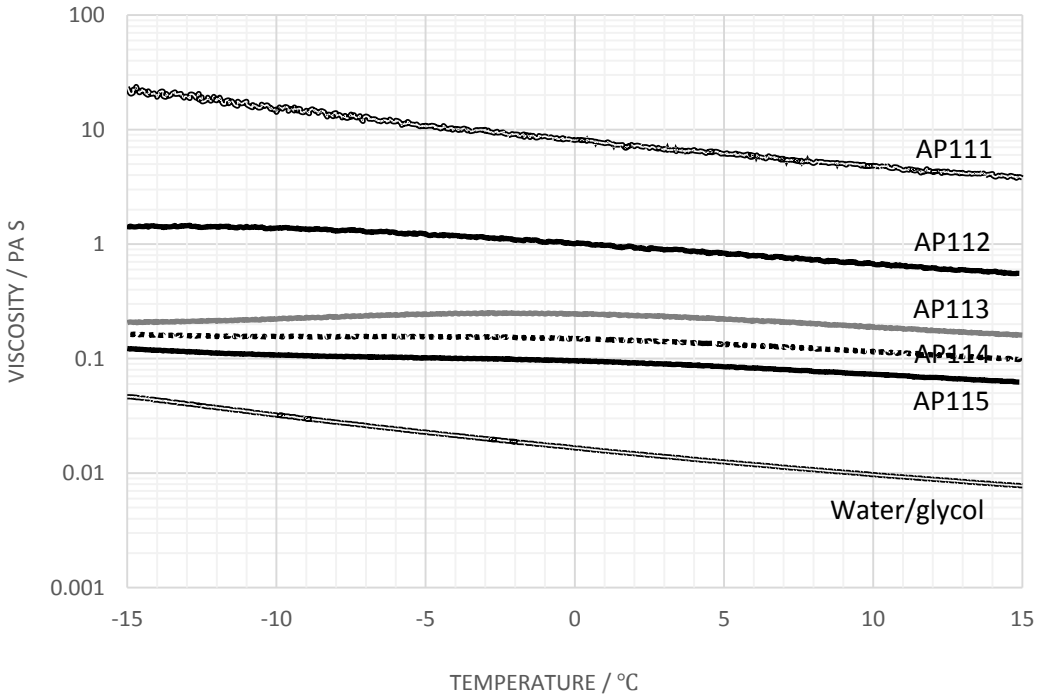

Figure 6.9 Viscosity variation with temperature plots for AP1 series, PVP_{360k}:Carbomer A=40:60 wt/wt, shear stress 5 Pa.

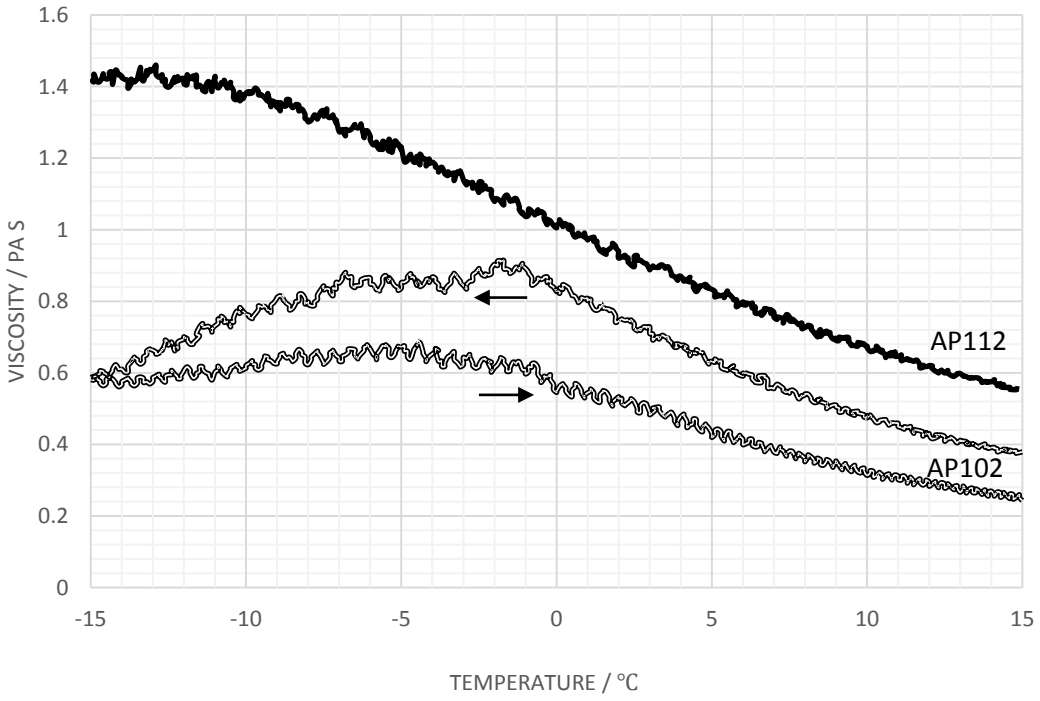

Figure 6.10 Viscosity variation with temperature plots for AP112 and comparison with AP102, shear stress 5 Pa.

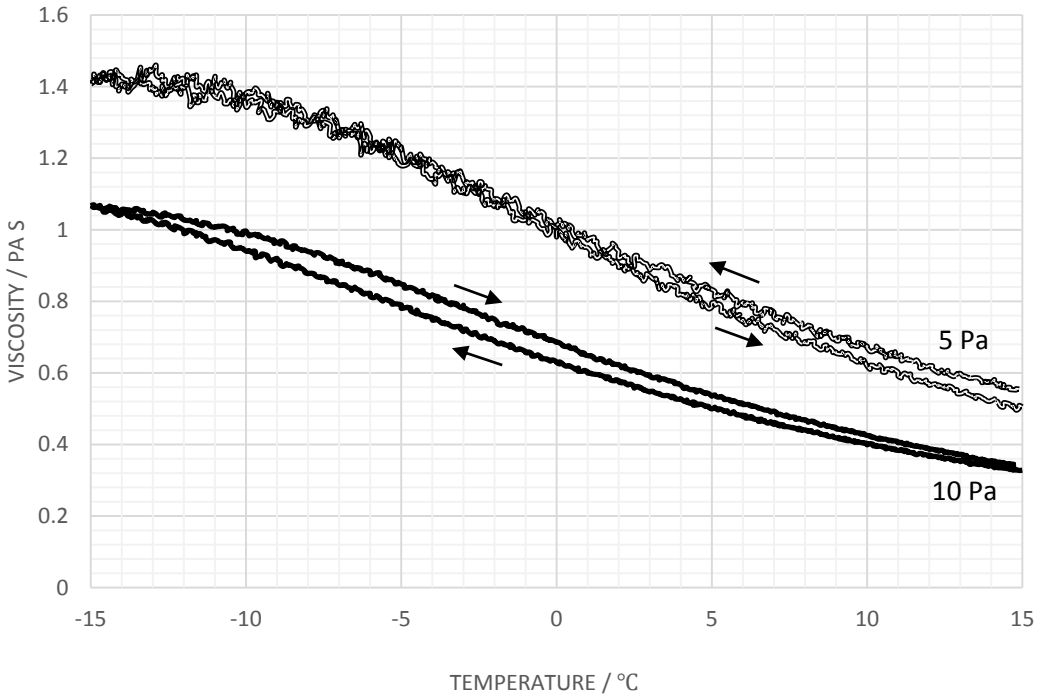

Figure 6.11 Viscosity variation with temperature plots for AP112, shear stresses 5 Pa and 10 Pa.

It has been established previously that the shear-thinning characteristic remains one of the most important features of de-icing fluids. For a de-icing fluid to be acceptable, the viscosity must remain sufficiently high when the aircraft is at standby and taxiing positions. After ground acceleration prior to take-off, the layer of fluid must be shear cleaned to allow the wings to produce sufficient lift. Although the water/glycol mixtures are thickened by PAA/PVP blends instead of pure PAA polymers, the shear-thinning characteristics remain unchanged; and the addition of electrolyte does not change such characteristics. At 0°C (Figure 6.12) and other temperatures, all 5 samples with 60:40 PAA/PVP weight ratio blends exhibited shear-thinning properties. For AP111 at 0°C, -5°C, -10°C, and -15°C (Figure 6.13), it remains shear-thinning which demonstrates the general usability for a de-icing fluid under a wide temperature range, although the viscosity level needs to be adjusted for its removability under high shear.

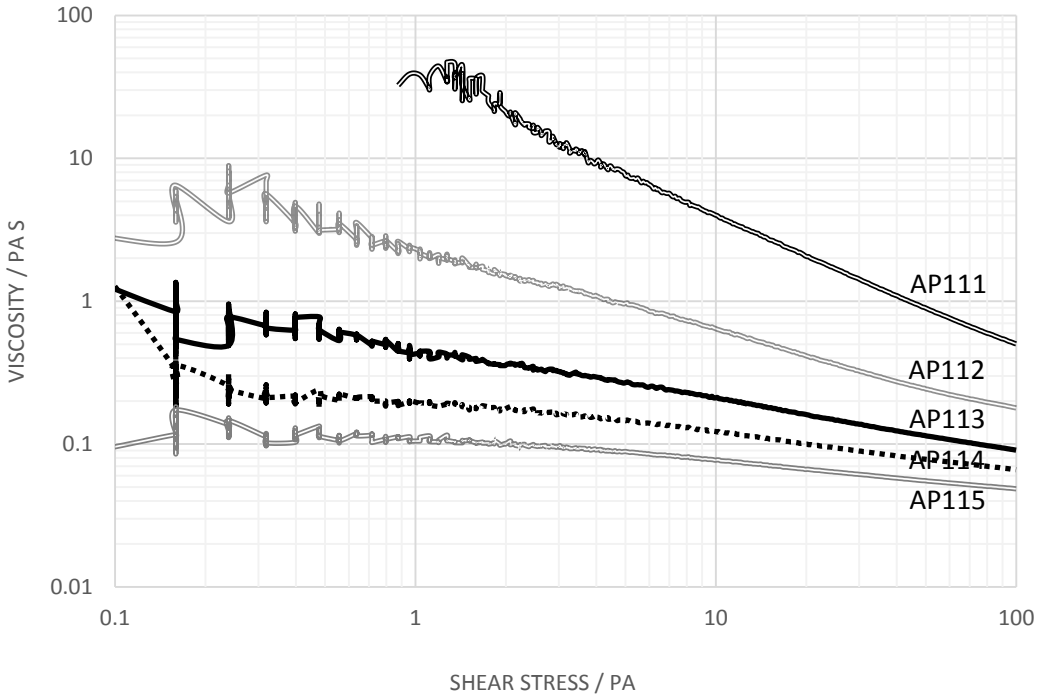

Figure 6.12 Viscosity variation with applied shear stress plots for AP1 series, PVP_{360k}:Carbomer A=40:60 wt/wt, temperature 0°C.

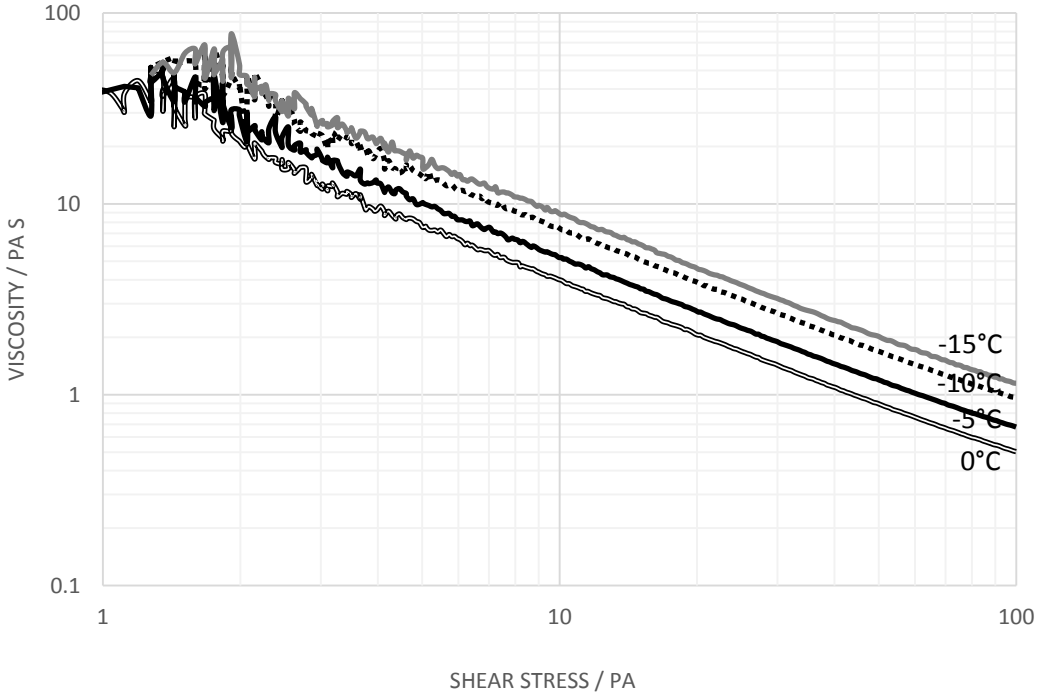

Figure 6.13 Viscosity variation with applied shear stress for AP111.

6.3.1.3. Weight Ratio 40:60 (Carbomer A/PVP 360k)

In previous sections, results suggested that the rheological behaviour of the solutions has been influenced by the content of PVP polymer. It is necessary to explore the effect of increasing PVP concentration to a higher level. Previous studies [8] suggest that PVP and PAA will form a complex when the monomer molar ratio approaches 1:1. Further increasing the weight ratio of PVP/PAA to 60:40 gives a monomer molar ratio of 0.925.

Temperature ramp tests confirms similar rheological behaviours for a PVP/PAA 40:60 wt/wt blend. From Figure 6.14 it is obvious that increasing the content of PVP results in lower viscosity when no electrolyte was added to the system. Because of the significant differences of molecular weights between the two polymers and consequentially their size in solution it is expected that at the higher PVP content there is a tendency to phase separation and less interactions will occur with a consequential lowering of the viscosity. As electrolyte was added to the system, the viscosity level decreased severely (Figure 6.15). Electrolyte is effectively shielding the hydrogen-bonding between the carboxylic group of PAA and pyrrolidone ring of PVP. With the PAA chains screened, the low molecular weight PVP was no longer able to retain hydrogen bonding interactions to form the network and therefore a dramatic decrease in viscosity is observed.

Sample AP122 has 0.012 g (NaCl) per 100 g (solution) electrolyte added to the system. The viscosity profile (Figure 6.16) resembles that of AP102, the 50:50 PVP/PAA blend system. At 15°C and 5 Pa of shear stress, the viscosity was approximately 0.15 Pa s. As temperature decreased, it reached a peak value of 0.30 Pa s at approximately -7°C and then dropped to 0.25 Pa s at -15°C. Similar behaviour was observed when 10 Pa of shear stress was applied. The hysteresis effects were enhanced at both shear stresses when temperature approached the 'peak' location suggesting that the balance between the de-shielding of carbonyl groups and conformational changes leads to a formation of a pre-gelation structure. The fact that the viscosity values measured on heating were lower than those on cooling indicates the break-down of the network structure and the

influence of the chain dynamics on the equilibrium conformation in solution.

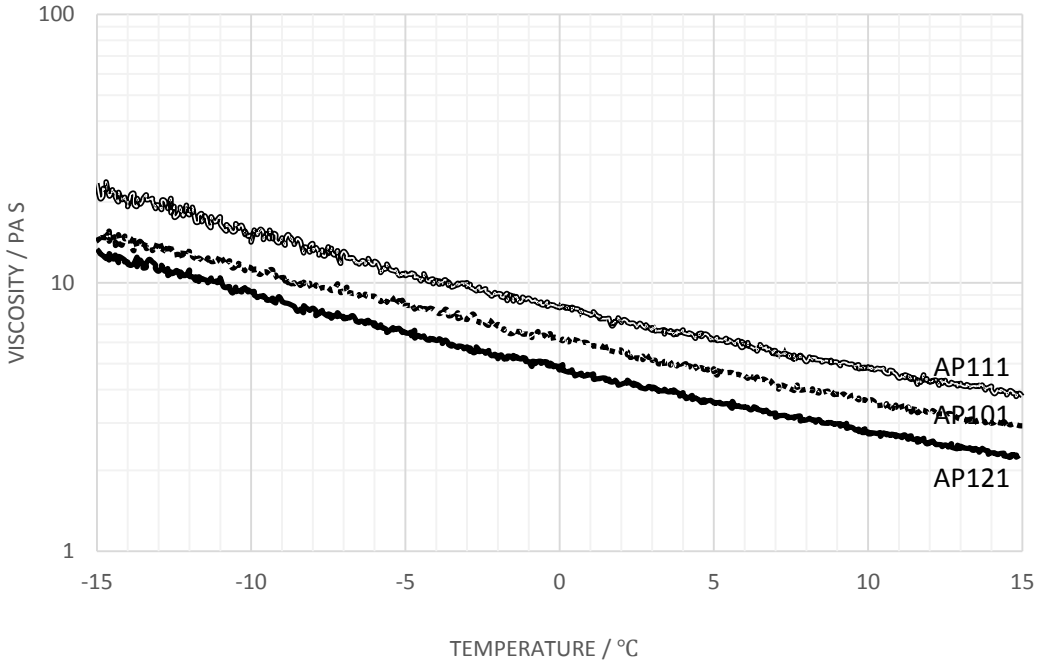

Figure 6.14 Viscosity variation with temperature plots for AP121 and comparison with AP101 and AP111, shear stress 5 Pa.

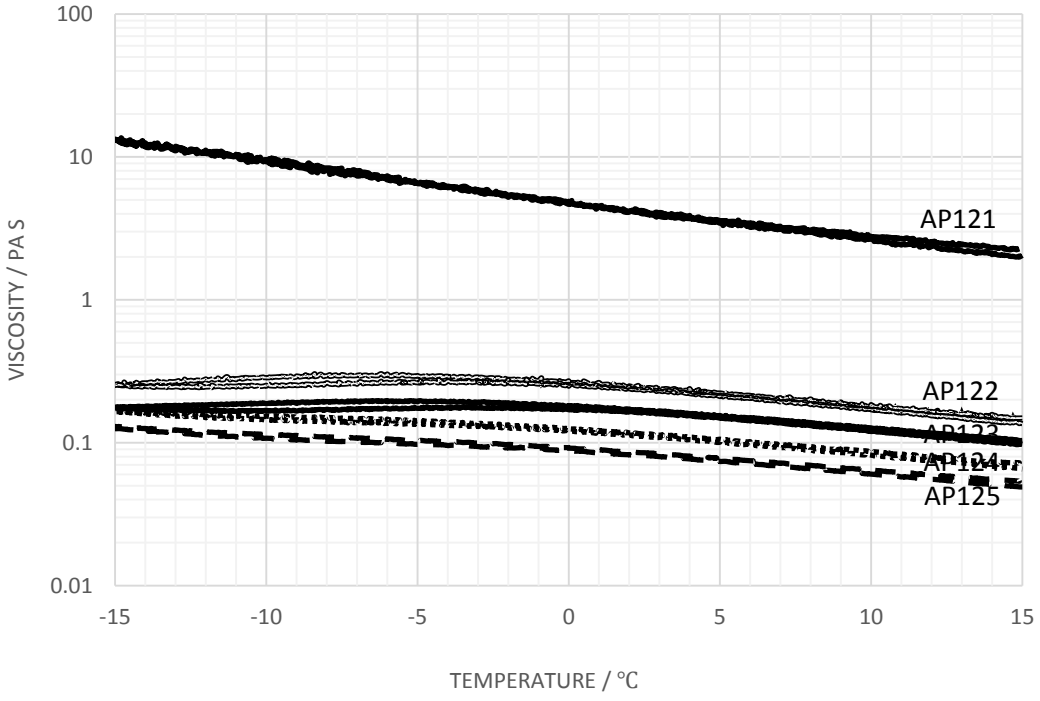

Figure 6.15 Viscosity variation with temperature plots for AP1 series, PVP360k:Carbomer A=60:40 wt/wt, shear stress 5 Pa.

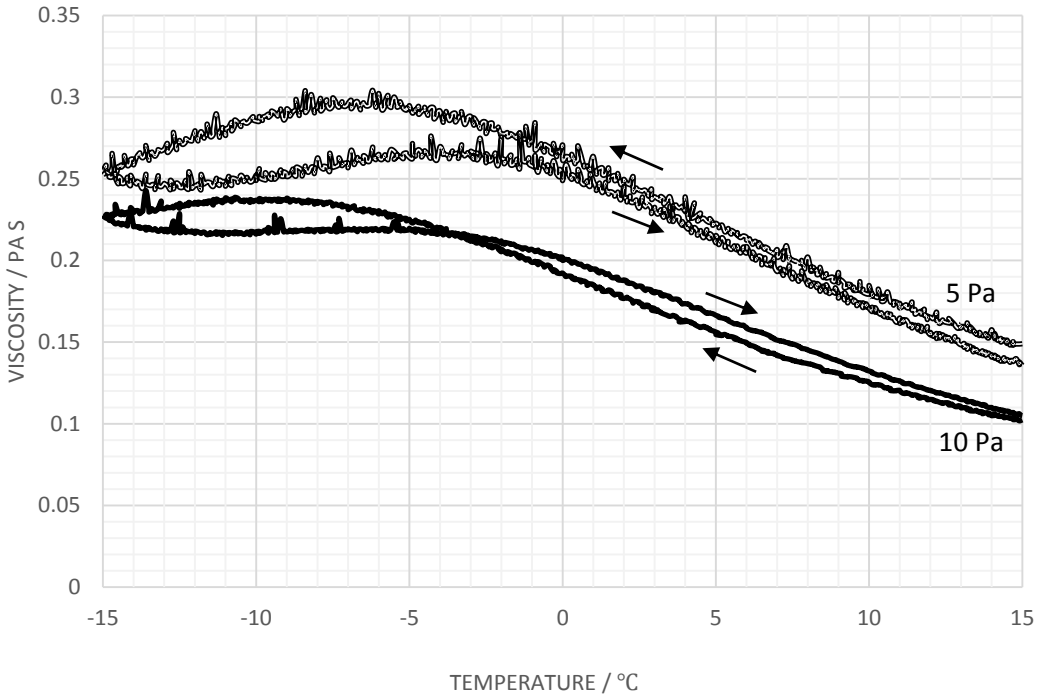

Figure 6.16 Viscosity variation with temperature plots for AP122, shear stresses 5 Pa and 10 Pa.

Steady shear flow tests confirmed that all samples with 60:40 PVP/PAA wt/wt blend exhibited shear-thinning characteristics at 0°C (Figure 6.17) and other temperatures.

The following figure (Figure 6.18) shows a series of viscosity variations with applied shear stress for AP122 at 4 different temperatures. At higher shear stresses, the viscosity tends to increase with decreasing temperature. However as the shear stress is reduced to approximately 10 Pa, the changes in viscosities at temperatures below 0°C are almost identical. As the stress is further decreased to below about 4 Pa, the viscosity at -15°C was lower than at other temperatures. Such an observation is consistent with the idea of a dynamic network in which the extent of interaction between the PVP and PAA is influenced by the extent to which the PAA chain is extended as well as being shielded by the electrolyte.

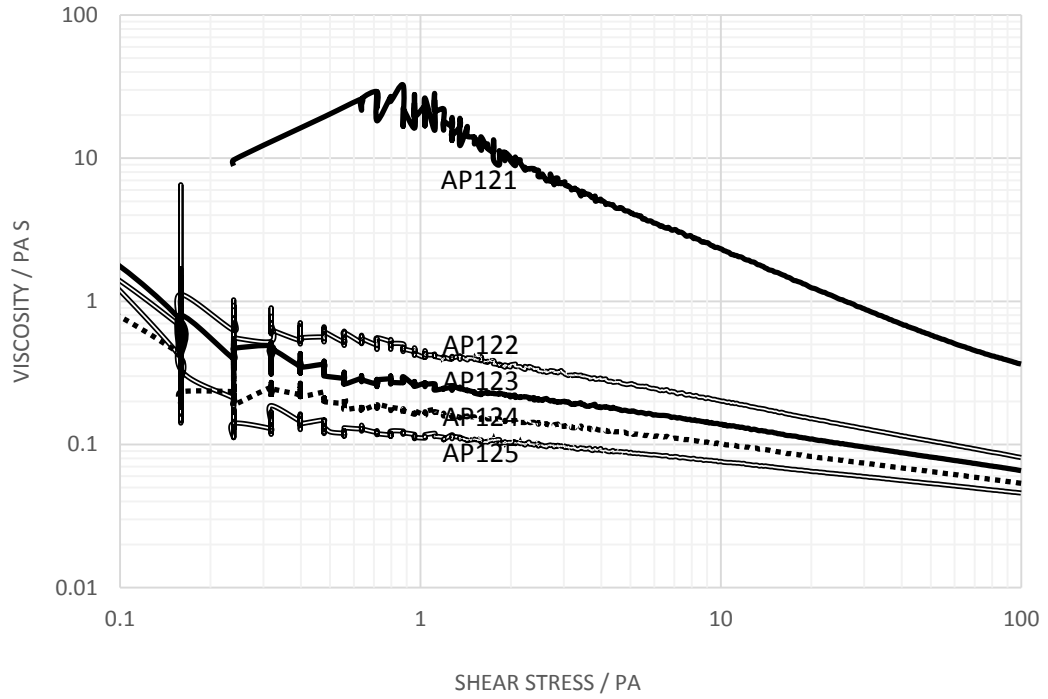

Figure 6.17 Viscosity variation with applied shear stress plots for AP1 series, PVP_{360k}:Carbomer A=60:40 wt/wt, temperature 0°C.

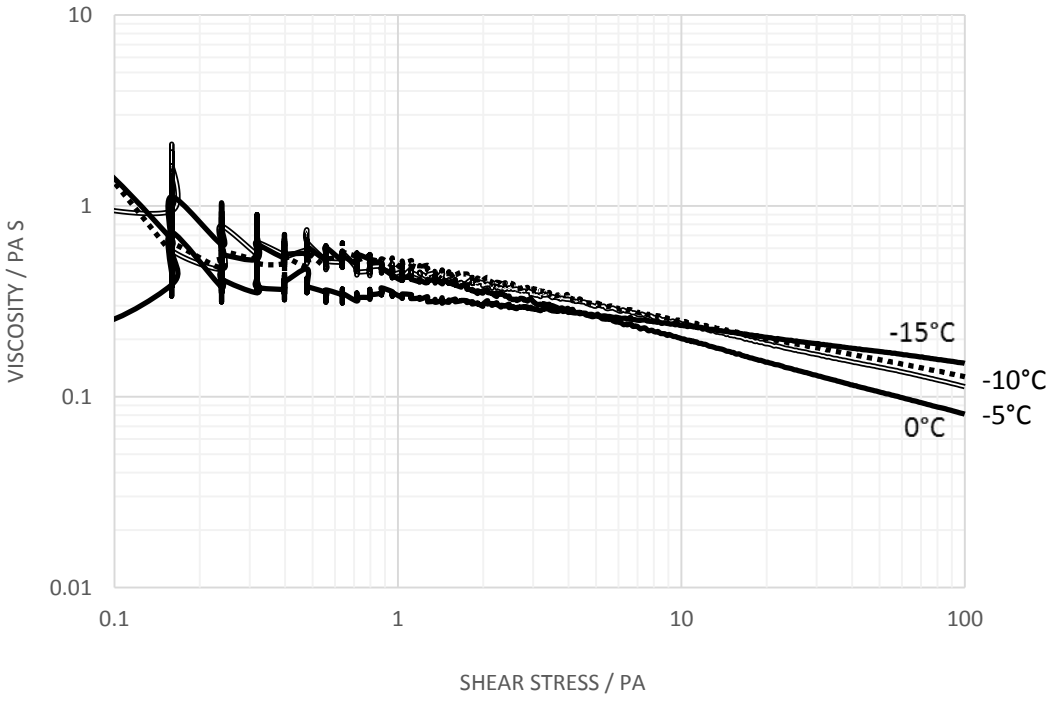

Figure 6.18 Viscosity variation with applied shear stress for AP122.

6.3.2. System AP2 (Carbomer A/PVP 700k)

The rheological characteristics of the deicing fluids are achieved by polymer-polymer interaction creating a virtual polymer with large hydrodynamic volume. From the previous series of experiments it was discovered that the molecular weight of PVP1, which is 360,000, was not achieving as large an enhancement in the viscosity as the PAA it replaced. It was expected that increasing the molecular weight of the PVP from 360k to 700k would allow an increase in the hydrodynamic volume of the polymer in solution which should increase the viscosity and possibly allow it to achieve more interactions with the PAA. A 0.30 g dL^{-1} PVP 700k polymer dispersion in 50:50 water/glycol mixture was formulated and neutralized to pH 7.0. Temperature ramp tests were carried out and the viscosity variation with temperature was plotted in Figure 6.19. The viscosity profile highly resembles the one for PVP 360k; and the viscosity level is similarly negligible compared to Carbomer A. A series of blends of Carbomer A and PVP2 (*Mw* 700k) were formulated in a 50:50 aqueous glycol mixture and rheological experiments were carried out upon the systems.

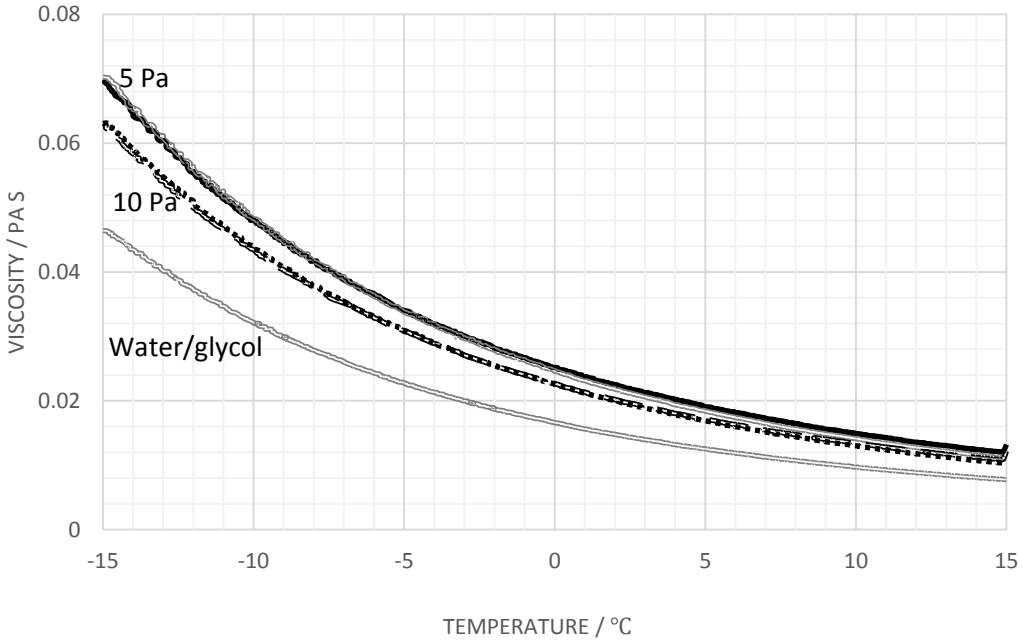

Figure 6.19 Viscosity variation with temperature plots for PVP 700k at concentration of 0.30 g/dL, shear stress 5 and 10 Pa. Water/glycol 50:50 wt/wt.

6.3.2.1. Weight Ratio 50:50 (Carbomer A/PVP 700k)

The temperature dependence of viscosity of this 50:50 blend is presented in Figure 6.20. The theoretical prediction curve is similar to the one used in PVP 360k assuming viscosities linearly additive with each polymer component and their concentration. The viscosity increased from approximately 1.52 Pa s at 15°C to 22.45 Pa s at -15°C. Compared to AP101, the viscosity of AP201 is considerably lower at 15°C and higher at -15°C; compared with theoretical prediction, the viscosity of AP201 is 190% lower at 15°C yet approximately the same at -15°C. Such behaviour suggests the hydrogen bonding formed between the carbonyl group of pyrrolidone ring and carboxylic group of PAA has an increasing influence on the inter- and intra-molecular interactions of PAA polymers as the temperature decreases. At higher temperature less polymer entanglement was formed by PAA chains with a resulting lower viscosity being observed. However at lower temperature, the hydrogen bonding between PVP and PAA effectively prevented the collapse of the PAA forming a globular complex leading to gelation. As the temperature is lowered the interaction between the salt and the carboxylic acid groups is reduced, allowing a higher probability of the creation of hydrogen bonds between PVP and PAA chains and leading to a more extended structure being created and hence a higher viscosity. The difference between AP201 and AP101 is a possible result of different polymer chain size.

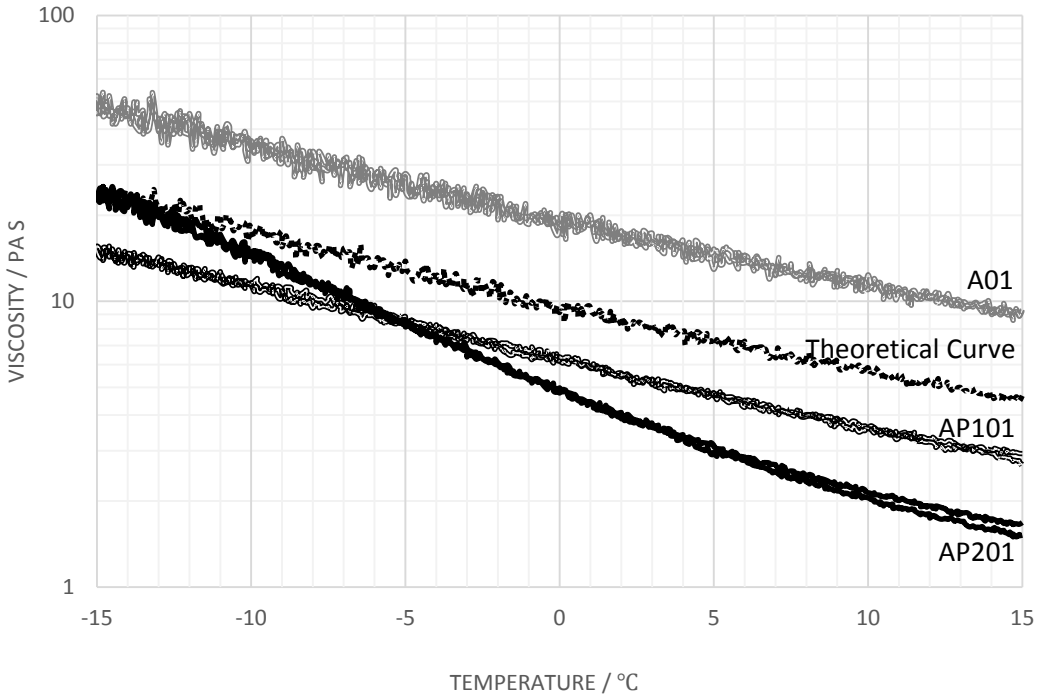

Figure 6.20 Viscosity variation with temperature plots for AP201, in comparison with A01, AP101 and theoretical prediction, shear stresses 5 Pa.

Figure 6.21 showed the viscosity variation of temperature for AP202, which contains 0.015 g (NaCl) per 100 g (solution) of electrolyte. The plots obtained are similar to those for AP112 (Carbomer A:PVP360k in 60:40 mixture) however the peak value for the viscosity at -15°C is lower with this blend which contains higher molecular weight PVP. The effectively lower sodium chloride content will be less effective at screening the carboxylic acid groups and allows with the higher molecular weight PVP the creation of species with an effective large hydrodynamic volume. The lack of hysteresis is also consistent with the increased role of the PVP and the less sensitivity to the effects of stretching of the polymer chain on the pre-gelation structure.

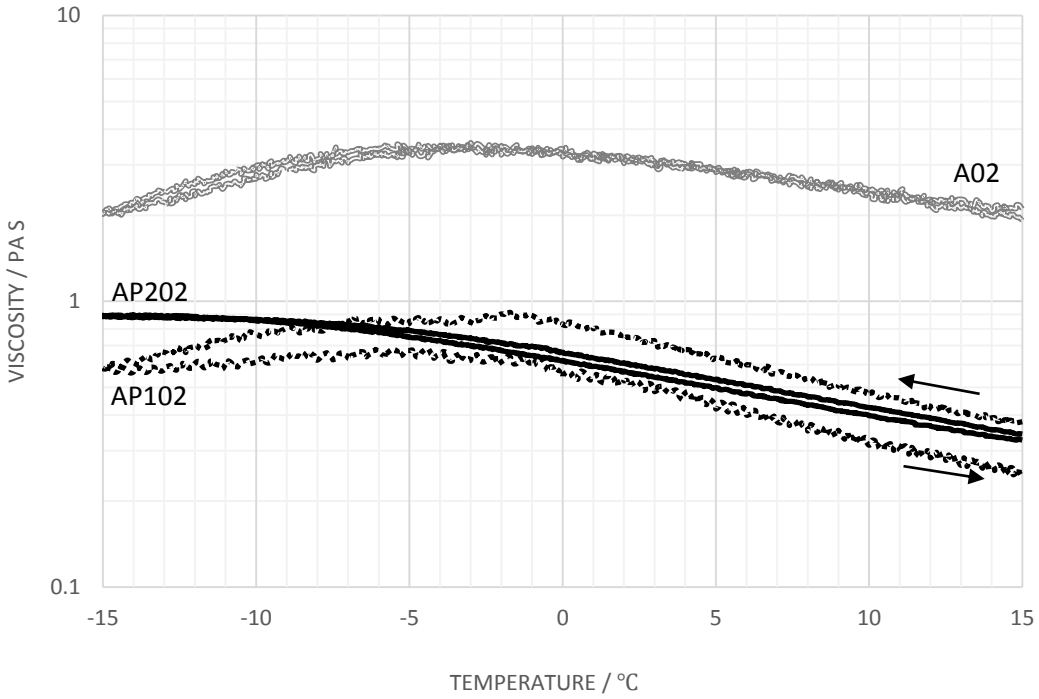

Figure 6.21 Viscosity variation with temperature plots for AP202, in comparison with A02 and AP102, shear stresses 5 Pa.

The following figure (Figure 6.22) showed diminishing viscosity levels with increasing electrolyte concentration. The addition of electrolyte also suppressed the magnitude of viscosity increment on decreasing the temperature as the difference between viscosities at 15°C and -15°C were not as large for the ones without the electrolyte as the one with. Such an observation indicates that the screening effect contributes to the stabilisation of viscosity across the temperature range. With larger molecular weight PVP blended to the polymer system, such effect was depressed which may explain why the tendency of forming a viscosity 'peak' was diminished across the series.

Shear-thinning characteristics remains present in the series of 50:50 blends regardless of the electrolyte concentration.

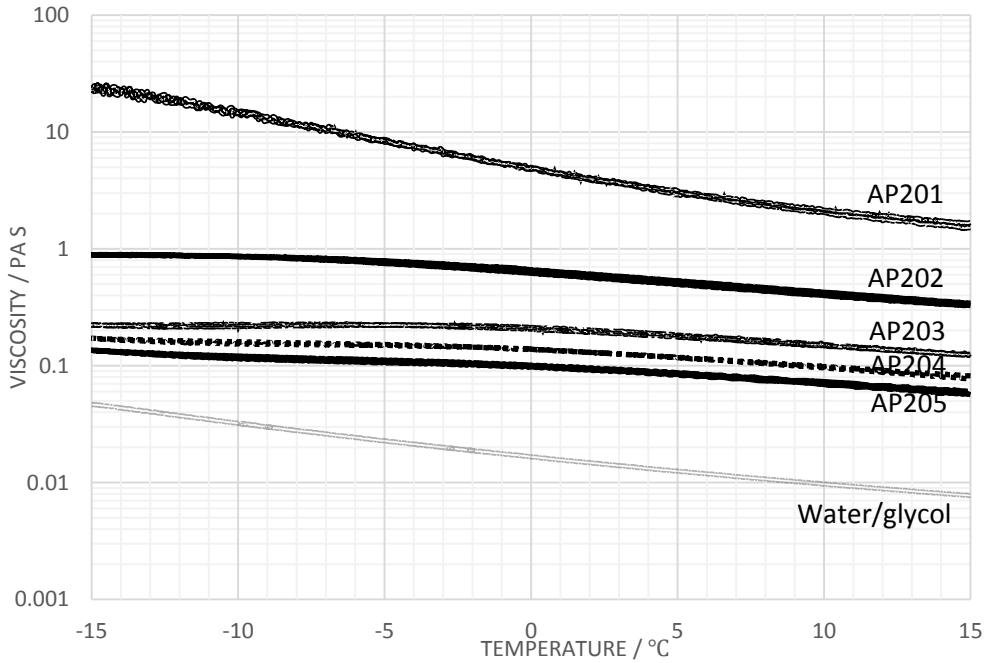

Figure 6.22 Viscosity variation with temperature plots for AP2 series, PVP_{700k}:Carbomer A=50:50 wt/wt, shear stress 5 Pa.

6.3.2.2. Weight Ratio 60:40 (Carbomer A:PVP 700k)

Compared to the molecular weight of PVP of 700,000, the molecular weight of Carbomer A is still considerably larger. Longer polymer chains create larger networks to build up the viscosity of a solution. Therefore it is normal to have observed an increment in viscosity while the content of Carbomer A was increased from 50 wt% to 60 wt% in the blend (Figure 6.23).

Cross-comparison was performed for two blends with different PVP polymers, AP111 and AP211, each having the same overall polymer concentration of 0.30 g dL^{-1} and the same polymer blending ratio of 60:40 wt/wt for Carbomer A to PVP. The viscosity variation with temperature was measured and plotted in Figure 6.24. As shown, the viscosity profiles are very similar; the differences in viscosity level can be attributed to the increased molecular weight of the PVP.

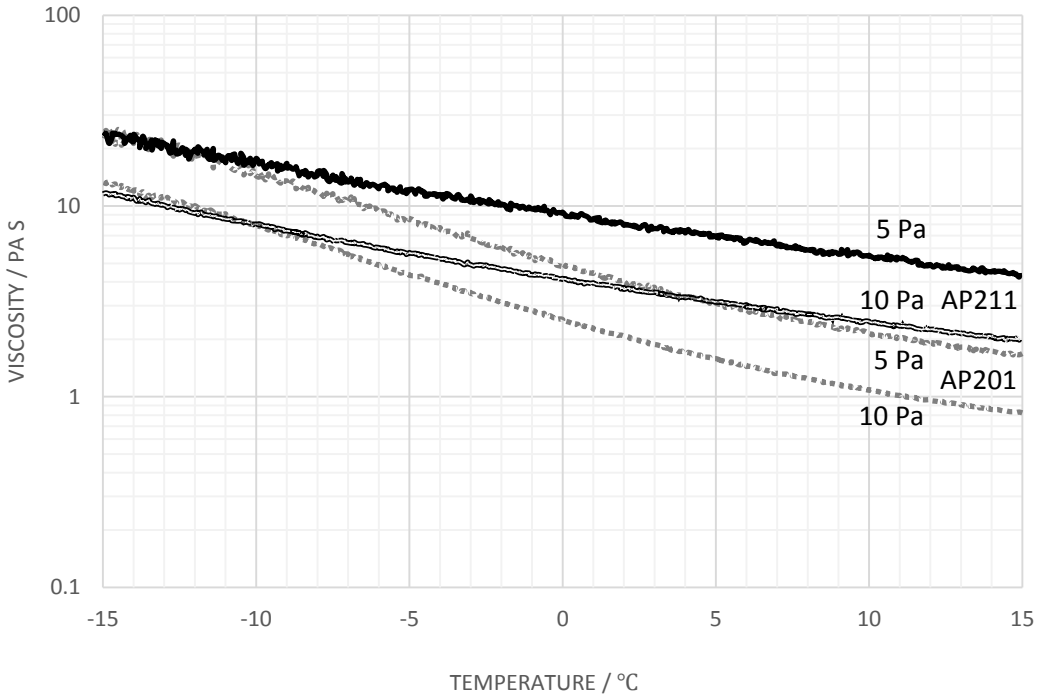

Figure 6.23 Viscosity variation with temperature plots for AP211, in comparison with AP201, shear stresses 5 and 10 Pa.

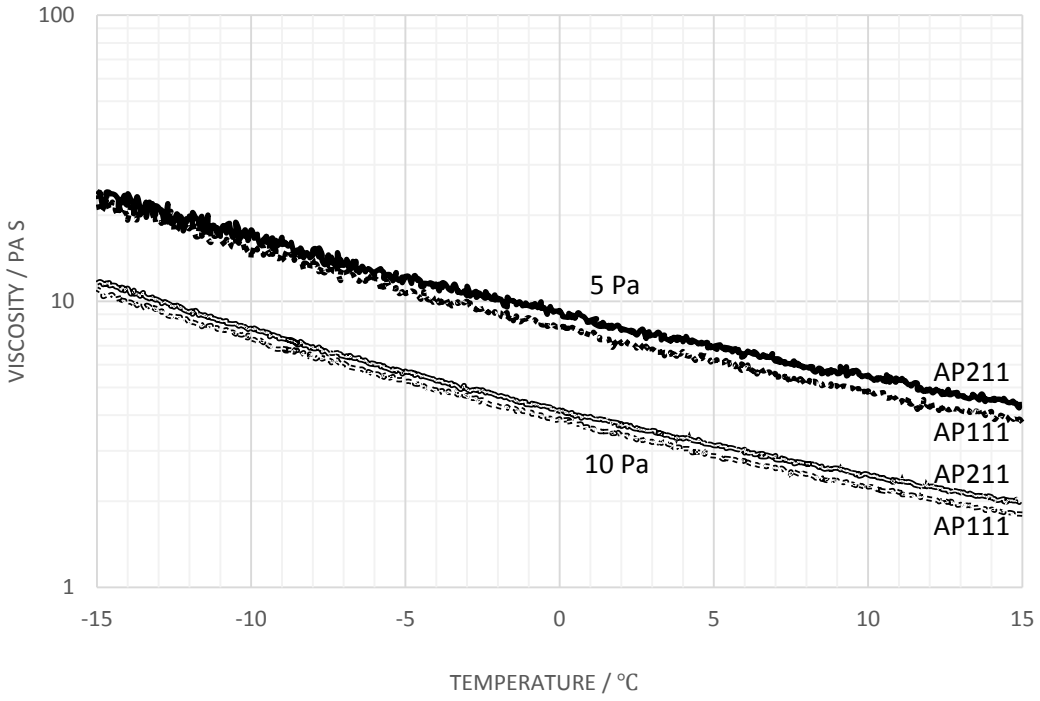

Figure 6.24 Viscosity variation with temperature plots for AP211, in comparison with AP111, shear stresses 5 and 10 Pa.

With added electrolyte, the viscosity of the solution dropped significantly as expected (Figure 6.25). The increased PAA content leads to the greater tendency to form the pre-gelation structure and once more the observation of a peak at approximately -12°C. The viscosities are generally increased as would be expected if the higher molecular weight PVP is able to effectively increase the hydrodynamic volume of the pre-cluster entity. This blend exhibits very little hysteresis and the peak at 10 Pa s is in a similar location to that at 5 Pa s which suggest that the preformed gel structure is exhibiting reversible characteristics. Further increasing the electrolyte level causes a progressive decrease in the viscosity of the solution (Figure 6.26).

Steady shear flow tests confirmed the shear-thinning characteristics at different temperatures for this series of blends. Figure 6.27 is the viscosity variation with shear stress for sample AP212. When approximately 3 Pa to 20 Pa of shear stresses were applied, the measured viscosity values at -10°C and -15°C were very close. Such an observation coincides with the findings of the temperature ramp results suggesting a 'peak' is being approached.

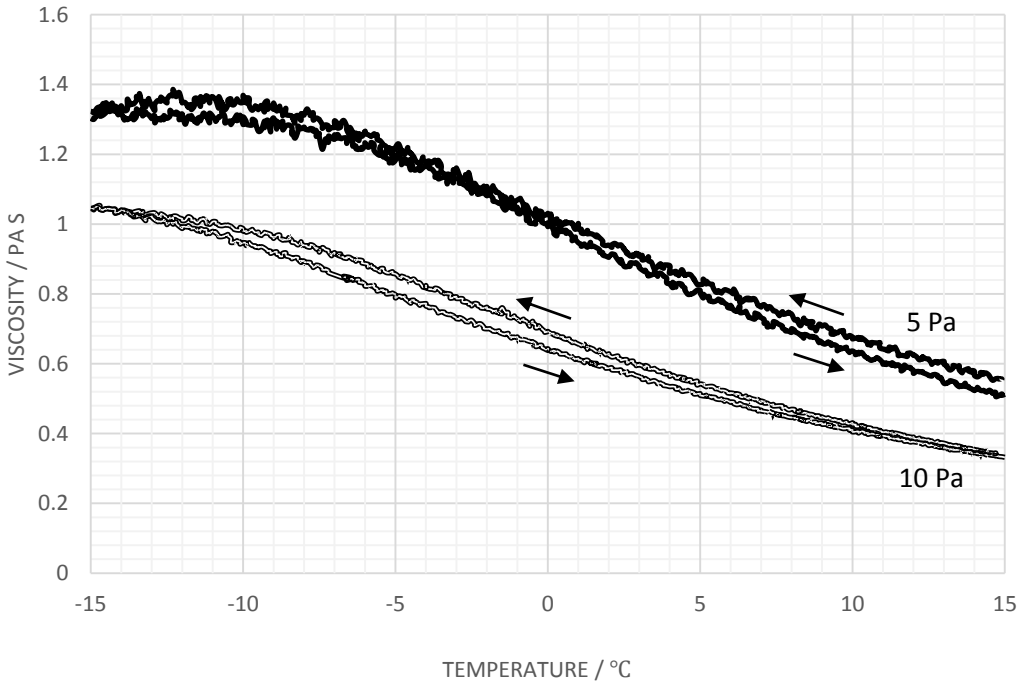

Figure 6.25 Viscosity variation with temperature plots for AP212, shear stresses 5 and 10 Pa.

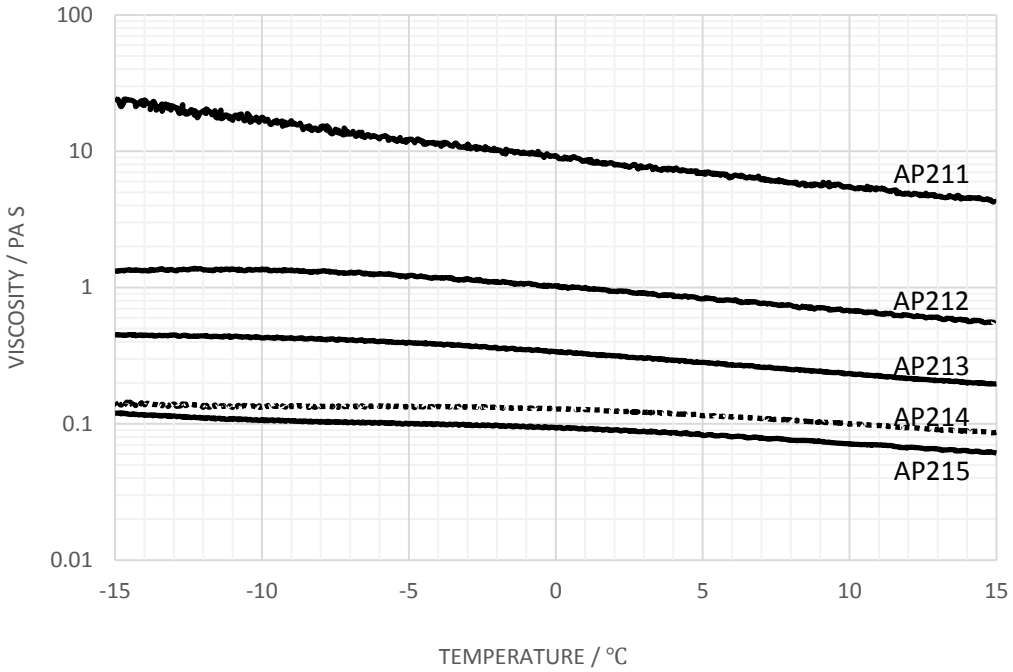

Figure 6.26 Viscosity variation with temperature plots for AP2 series, PVP_{700k}:Carbomer A=40:60 wt/wt, shear stress 5 Pa.

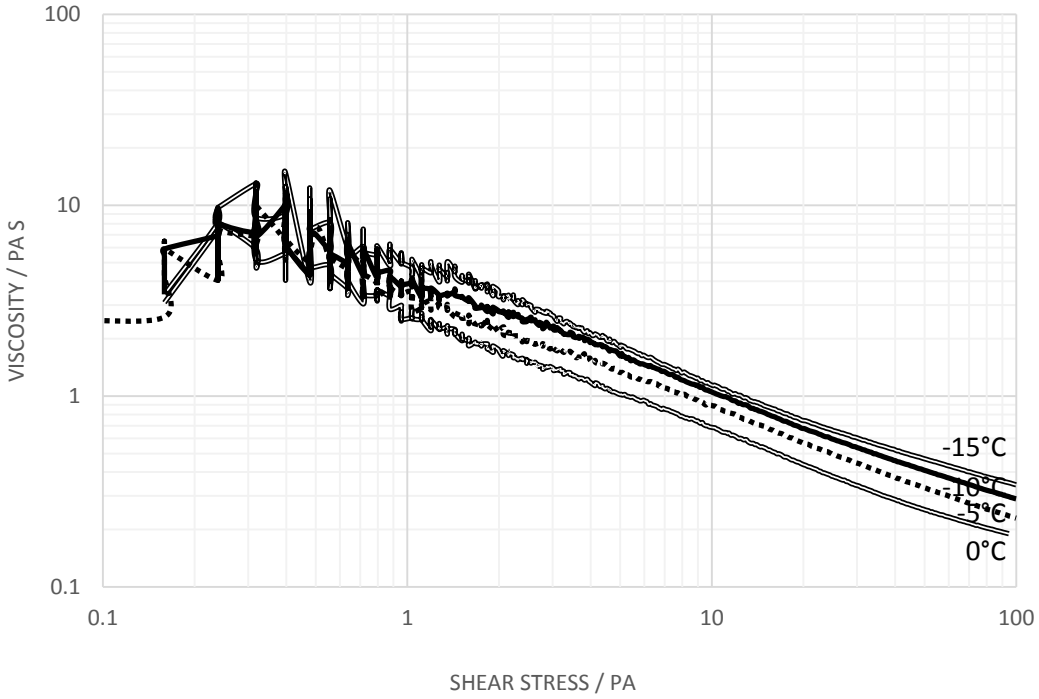

Figure 6.27 Viscosity variation with applied shear stress for AP212.

6.3.2.3. Weight Ratio 40:60 (Carbomer A/PVP 700k)

Increasing the content of PVP to 60 wt% leads to changes in viscosity profile. For blends without electrolyte addition, the viscosities above 0°C are higher for the 60 wt% PVP solutions, however at temperatures below 0°C the 50 wt% PVP blend has higher viscosities at both 5 and 10 Pa of shear stress (Figure 6.28). With 0.012 g (NaCl) per 100 g (solution) of electrolyte added and compared with the blend with 50 wt% PVP 700k (AP202) and the 60 wt% blend with PVP 360k (AP122), at 5 Pa of shear stress the viscosity level of AP222 is lower than AP202 and higher than AP122 (Figure 6.29). Generally, increasing the content of Carbomer A and using the higher molecular weight of PVP provides higher viscosity values, indicating that the viscosity profile is to some extent additive although the changes in temperature dependence indicate that there are interactions between the two polymers.

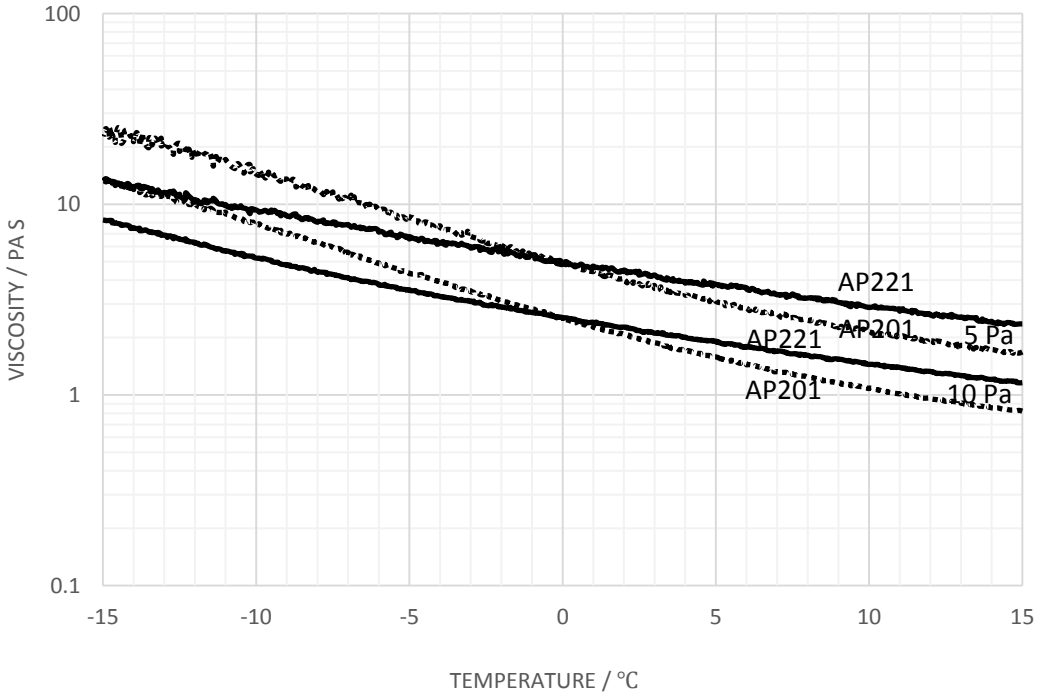

Figure 6.28 Viscosity variation with temperature plots for AP221, in comparison with AP201, shear stresses 5 and 10 Pa.

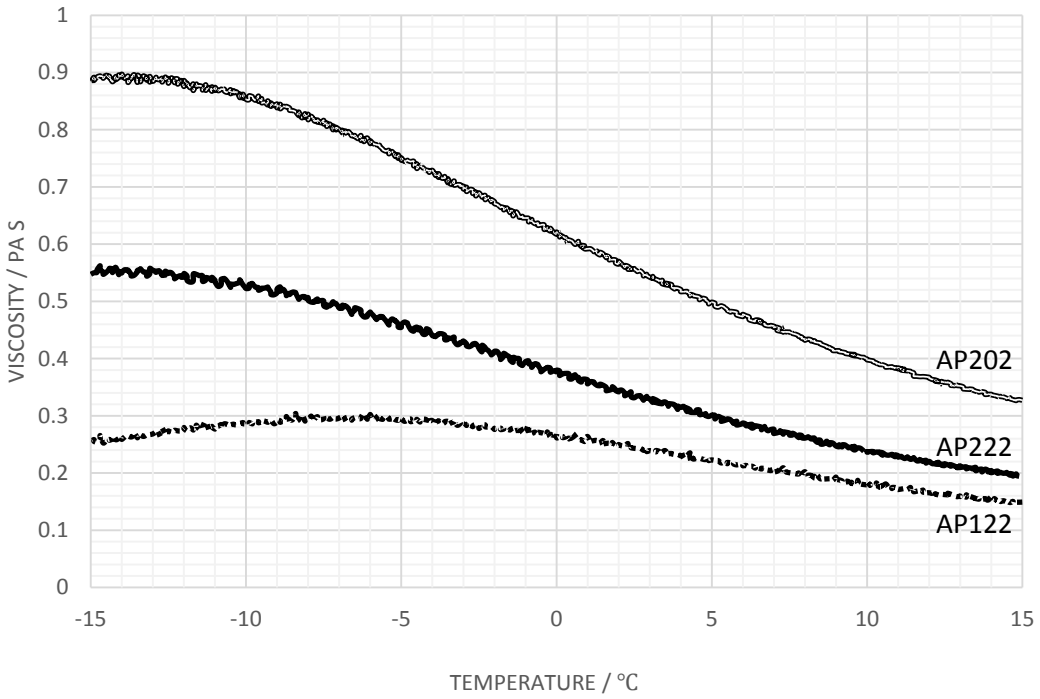

Figure 6.29 Viscosity variation with temperature plots for AP222, in comparison with AP202and AP122, shear stresses 5 Pa.

6.3.3. System AP3 (Carbomer A/PVP 1.3M)

Through a previous series of experiments, it has been demonstrated that it is very difficult to duplicate the rheological profile of the Carbomer A-based de-icing fluid, ABC-2000, using different polymer blends as thickeners. Increasing the molecular weight of PVP generally elevates the viscosity of a solution by a narrow margin and reduces the influence of electrolyte on the system, especially when the temperature is lowered to the critical range below zero. The observations would suggest that it is worth investigating whether further increases in the viscosity might be achieved by using higher molecular weight PVP.

A blend of 50:50 wt/wt Carbomer A:PVP (Mw 1.3M) was formulated and added to the 50:50 water/propylene glycol mixture. From Figure 6.30, at 5 Pa of shear stress, the viscosity profile of AP301 appears to be very similar to that of AP101. However at 10 Pa,

the viscosities differentiate as the temperature is decreased. The difference rose from 7.84 Pa s to over 10.56 Pa s for AP301 compared to AP101 at -15°C.

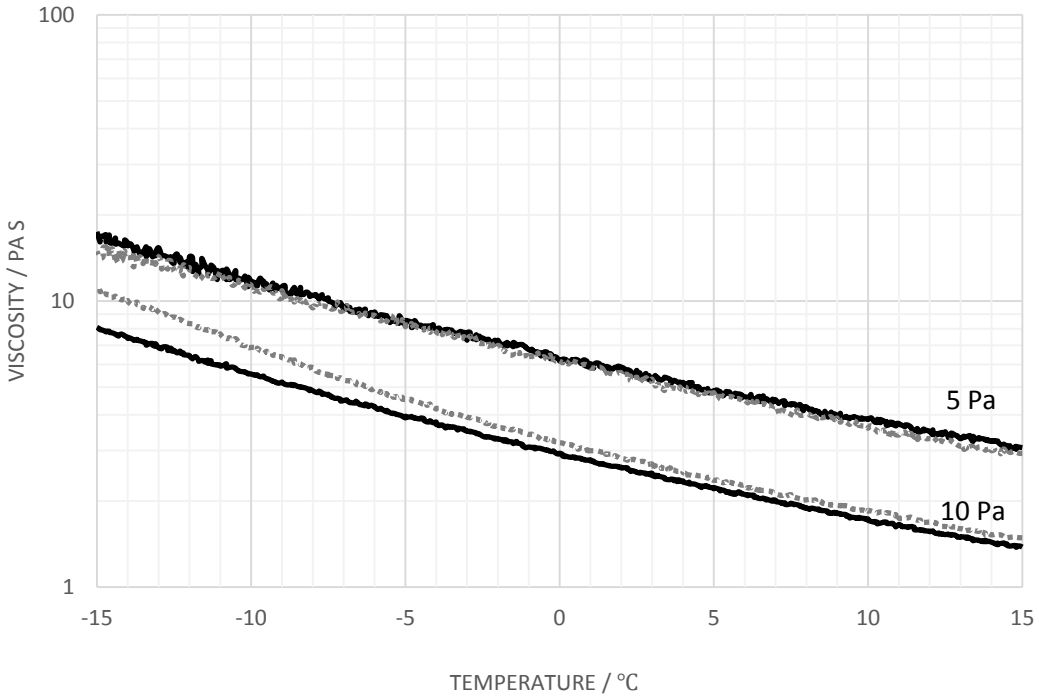

Figure 6.30 Viscosity variation with temperature plots for AP301, in comparison with AP101, shear stresses 5 and 10 Pa. (—) AP301; (...) AP101.

With added electrolyte of 0.015 g (NaCl) per 100 g (solution), unlike the phenomenon observed in the temperature ramp tests for PVP 360k and 700k blends, the viscosity of AP302 continues to rise as the temperature is decreased (Figure 6.31). This suggests the hydrogen bonding between the pyrrolidone ring and the carboxylic group becomes more efficient with the larger PVP molecules and the temperature at which the salting out-screening effect becomes operative and the tendency that polymer molecules adopt extended structures of low energy state starts to balance causing the temperature at which the formation of the pre-gelation structure to be shifted to lower ranges. The hysteresis found in the blends of PVP 360k and Carbomer A was reduced significantly which is consistent with previous findings. The viscosity variations with temperature at 5 Pa of shear stress for this blend with increasing electrolyte levels are plotted in Figure 6.32.

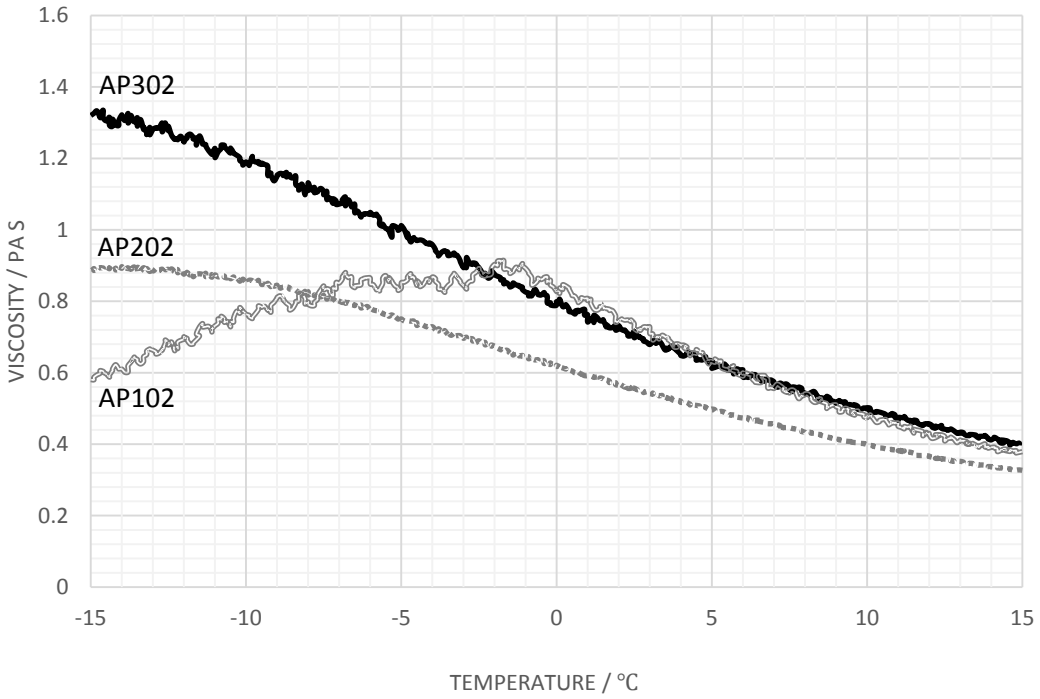

Figure 6.31 Viscosity variation with temperature plots for AP302, in comparison with AP202 and AP102, shear stresses 5 Pa.

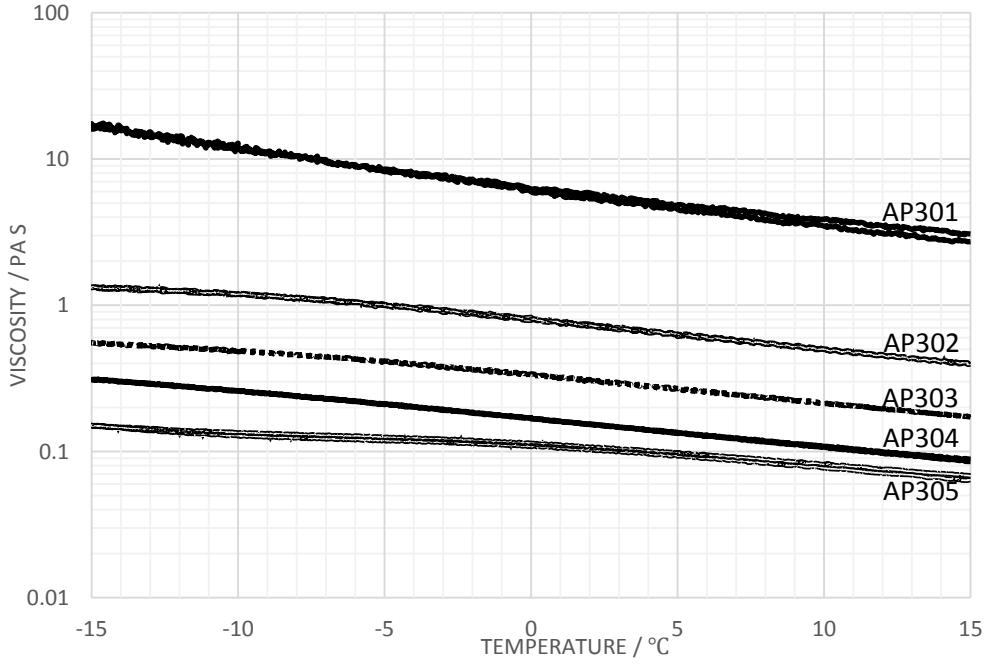

Figure 6.32 Viscosity variation with temperature plots for AP3 series, $_{PVP1.3M}$:Carbomer A=50:50 wt/wt, shear stress 5 Pa.

It was found previously that the commercial material ABC-2000 has a viscosity range of 0.6 Pa s to 0.7 Pa s at the shear stress of 5 Pa between the temperatures of 0°C and -15°C and that the characteristics of maintaining the viscosity of the fluid is desirable for it to be used over a broad temperature range. Previous observations suggest that it is appropriate to use electrolyte to adjust the viscosity level of the solutions. The balance between the de-shielding effect on carbonyl groups and formation of gel-like structures is complicated and will shift with changing electrolyte concentration. From Figure 6.32 it is clear that the viscosity range of between 0.60 and 0.70 Pa s falls between those of AP302 and AP303. Therefore it was decided to create AP306, which has the same polymer composition as the previous samples but a different electrolyte concentration of 0.022 g (NaCl) per 100 g (solution), and to further extend the testing temperature range to below -20°C. The viscosity variation with temperature is plotted in Figure 6.33.

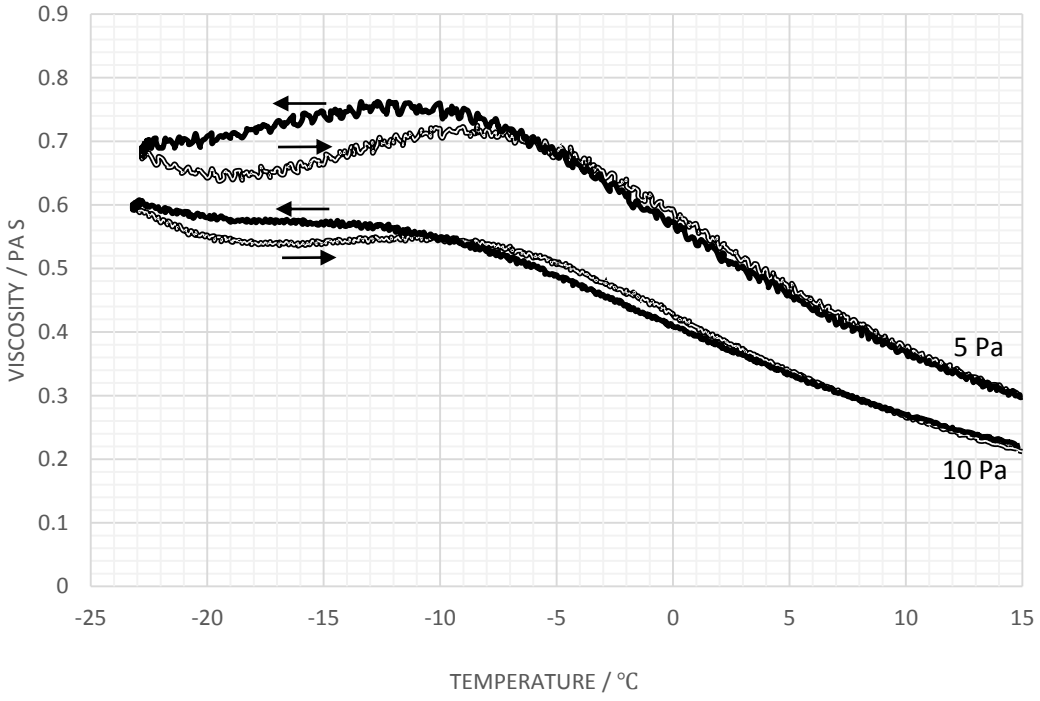

Figure 6.33 Viscosity variation with temperature plots for AP306, shear stresses 5 and 10 Pa.

With adjusted electrolyte level, the viscosity range at 5 Pa of shear stress across the temperature range of 0 to -23 °C was 0.58 Pa s to 0.77 Pa s, which is similar to the commercial product ABC-2000. In this plot it is worth noticing that: (1) at 5 Pa shear stress the viscosity began to 'peak' at approximately -12°C and started to decrease thereafter, however at 10 Pa shear stress it only formed a 'plateau' at a lower temperature of approximately -15°C and continued to rise with decreasing temperature; (2) at 5 Pa shear stress the hysteresis effects began to broaden below -8°C however at 10 Pa shear stress the magnitude of hysteresis was reduced; (3) the viscosity appeared to be at a higher level when the solution was cooled down compared to when it was heated up. All three observations may all be considered as the precursor to the formation of a gel-like complex. Elevating temperature and increasing applied shear stresses increased the system energy which accelerated the breakdown of such pre-gelation structure suggesting such structure are reversible.

Further increasing the content of PVP 1.3M to a 60:40 wt/wt with Carbomer A and adjusting the electrolyte level to 0.012 g (NaCl) per 100 g (solution) produces a sample solution AP322. Temperature ramp test showed that the viscosity 'peak' has been further shifted to the lower temperature ranges (Figure 6.34); at 5 Pa shear stress the peak presented at approximately -15°C and at -18°C when the shear stress was 10 Pa. Such a phenomenon was expected as the increasing content of PVP was able to interact with PAA molecules more effectively causing a lower formation of gel-like structures. Overall viscosity changed from 0.57 Pa s at 0°C to 0.90 Pa s at -15°C at 5 Pa shear stress, suggesting that increasing the content of PVP has reduced the viscosity level, consistent with previous observations.

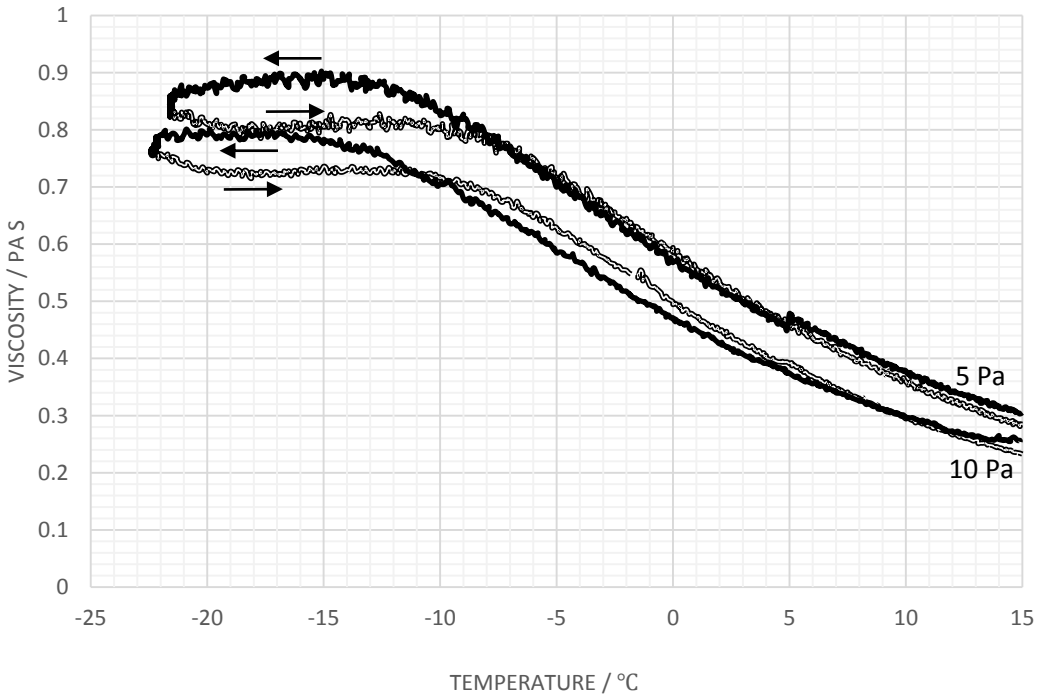

Figure 6.34 Viscosity variation with temperature plots for AP322, shear stresses 5 and 10 Pa.

6.3.4. System AP4 (Carbomer A/PVP 4M)

With studies on blends of Carbomer A and three PVP polymers of different molecular weights, it was clear that changing molecular weight corresponded to changing the size of the polymer molecules and therefore altering the interaction between PVP and PAA molecules. The formation of a gel-like structure causes a viscosity 'peak' and changing the temperature alters the extent to which electrolyte shielding and hydrogen bonding between the carboxylic group of PAA and carbonyl group of PVP occurs. The binding efficiency appears to be critical in the rheological performance. Therefore it was decided to create a series of blends of 50:50 wt/wt Carbomer A and PVP4 (molecular weight 4M). Figure 6.35 showed that at 5 Pa shear stress the viscosity increased from 2.81 Pa s at 15°C to as high as 16 Pa s at approximately -16°C; and at 10 Pa the viscosity level was much lower especially in the lower temperature range indicating desirable shear-thinning characteristics. The presence of hysteresis and shifting viscosity peak location

to higher temperature during heating up suggest potential breakdown and reforming of the gel-like structure.

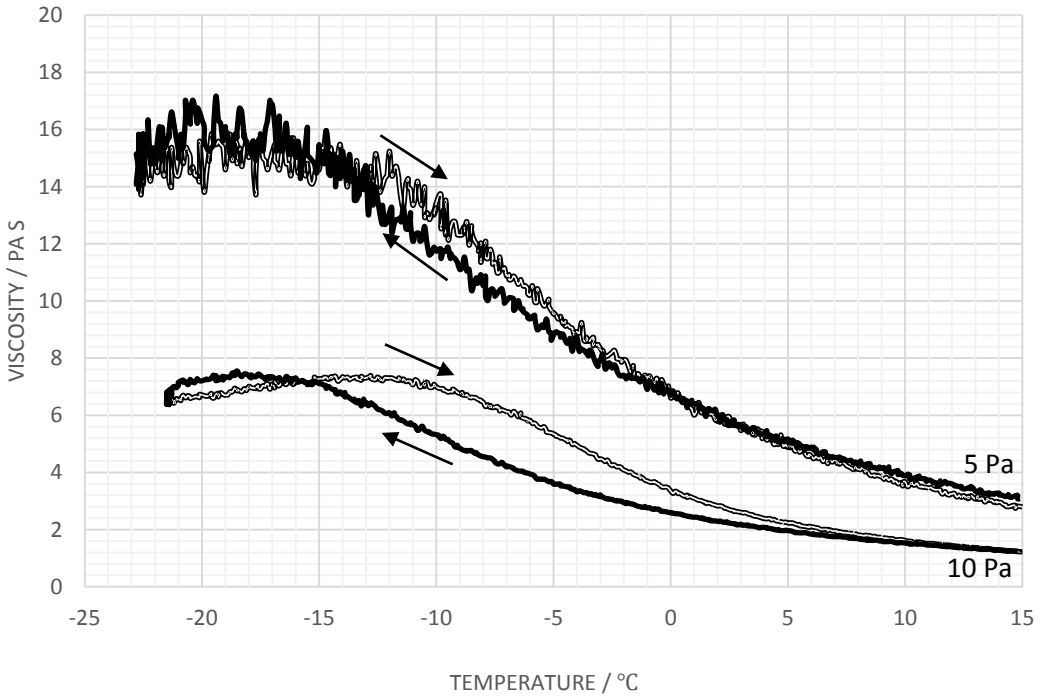

Figure 6.35 Viscosity variation with temperature plots for AP401, shear stresses 5 and 10 Pa.

Figure 6.36 is a comparison of viscosity variation with temperature at 5 Pa shear stress for four different blends of PVP and Carbomer A with the only difference being the molecular weight of PVP. At 15°C, AP402 has the highest viscosity of 0.51 Pa s which is as expected, since it has the largest molecular weight of the PVPs studied. As the temperature decreases, AP402 exhibited a viscosity peak at approximately -3°C and a significant viscosity drop to 0.58 Pa s at -15°C. Such viscosity profile is very similar to the one of Carbomer A thickened fluid A4, and also AP102 (50:50 wt/wt blend of PVP 360k and Carbomer A) including the near identical location of viscosity 'peak' and the viscosity value at -15°C. On the other hand, viscosities of AP202 and AP302 did not peak at such high temperature. This suggests that the binding efficiency of PVP and PAA does not linearly increase as the molecular weight of PVP is increased. At a molecular weight of

4M, it is possible that the phase separation may occur and contribute to the behaviour of the system and hence the interactions between PAA and PVP are not increased to the extent which might be anticipated. The increasing extent of hysteresis (Figure 6.37) is consistent with the observation that the PAA behaves in a similar manner to the way it behaves in the pure solution, but with reduced effect.

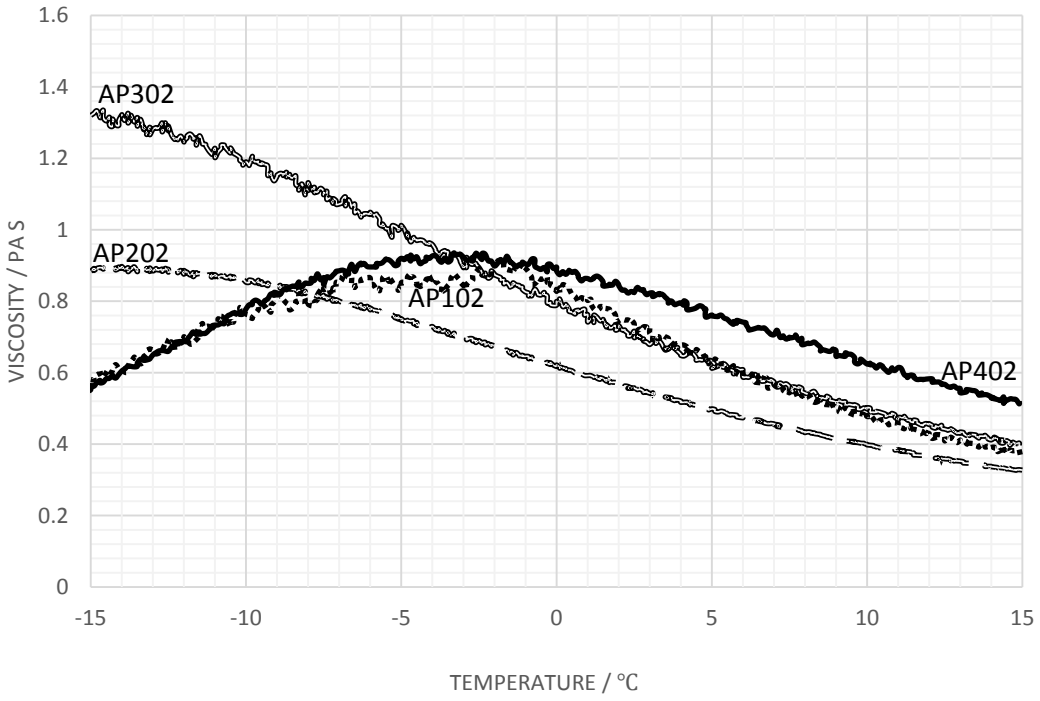

Figure 6.36 Viscosity variation with temperature plots for AP402, in comparison with AP102, AP202, and AP302, shear stresses 5 Pa.

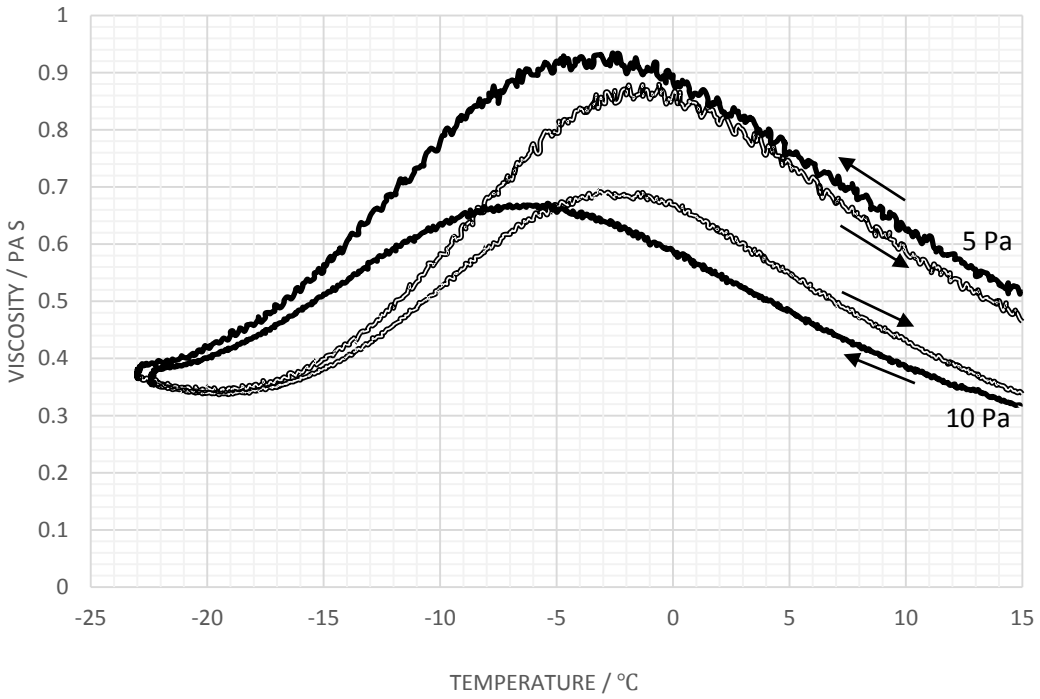

Figure 6.37 Viscosity variation with temperature plots for AP402, shear stresses 5 and 10 Pa.

A similar phenomenon was observed as the electrolyte level was doubled (0.030 g NaCl per 100 g solution, Figure 6.38). AP403 reached a temperature peak earlier than AP203 and AP303, suggesting the formation of a pre-gelation complex at higher temperature.

At 60:40 wt/wt ratio of PVP to PAA, the viscosity variation with temperature exhibited a similar pattern to that found in 50:50 wt/wt blends (Figure 6.39). The general viscosity level of AP422 is lower than AP322, which is similar to that for AP403 and is less viscous than AP303; the viscosity peak of AP422 is observed at higher temperature compared to the temperature at which it occurs in AP322 and AP222. These are all consistent with previous findings.

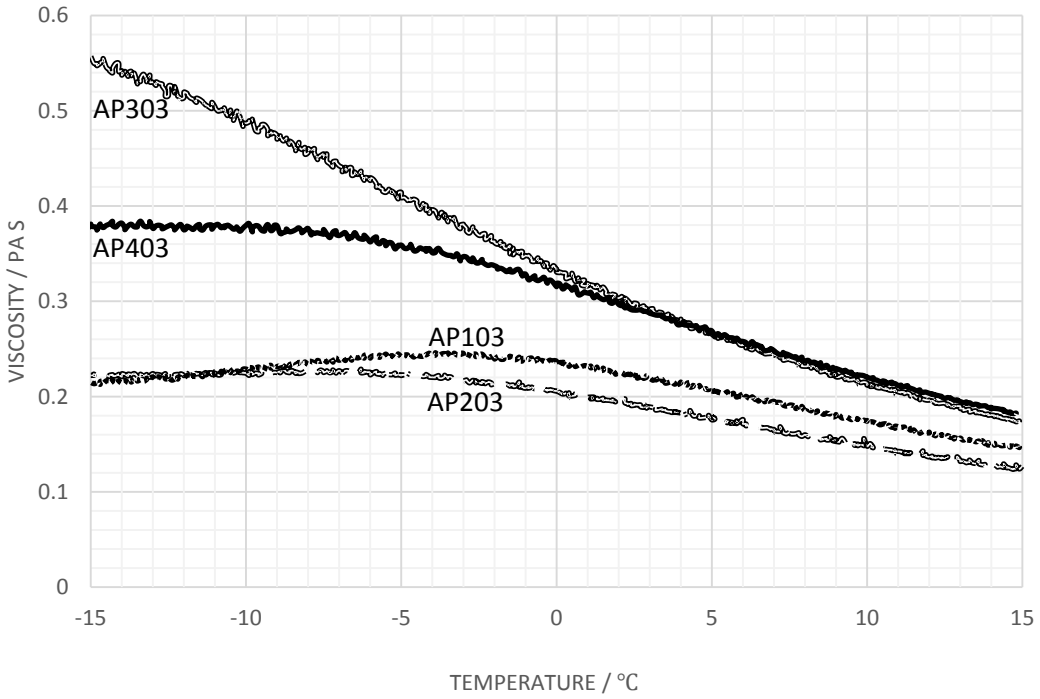

Figure 6.38 Viscosity variation with temperature plots for AP403, in comparison with AP103, AP203, and AP303, shear stresses 5 Pa.

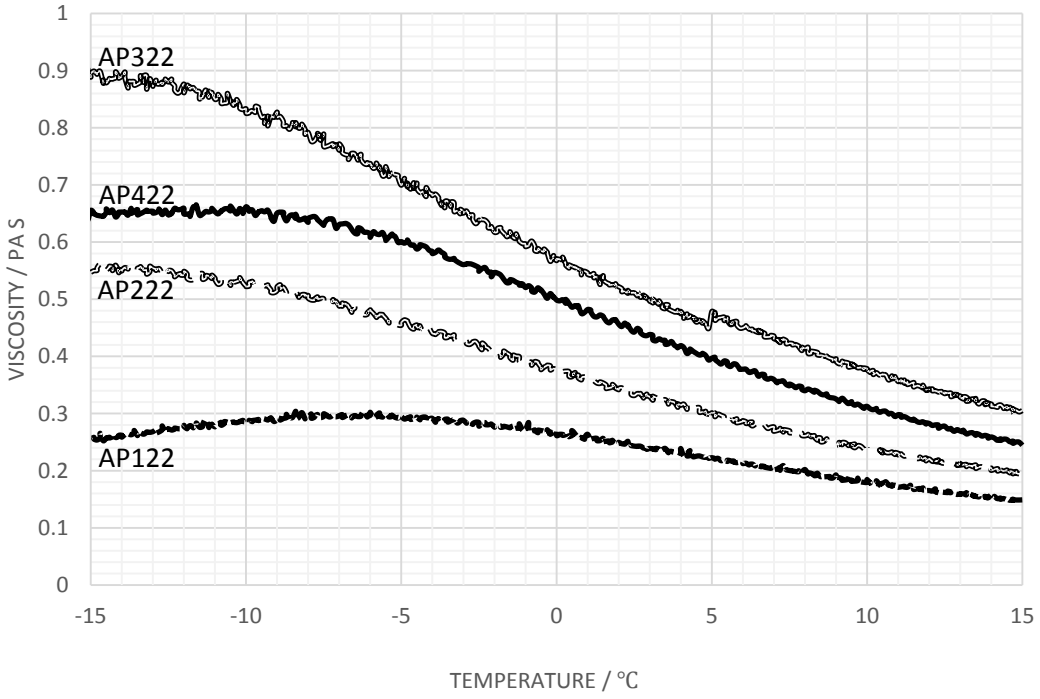

Figure 6.39 Viscosity variation with temperature plots for AP422, in comparison with AP122, AP222, and AP322, shear stresses 5 Pa.

6.3.5. BLDT Measurement

For a fluid to possess suitable characteristics to perform as a type II, III or IV fluid it is important that the film which is created during the deicing process should be removed in the period up to rotation. The behaviour of the model fluid is shown in Figure 6.40.

The values of the BLDT are measured in terms of the film thickness at around 30 sec, which is the rotation time for most small to medium sized aircraft. Acceptable values for fluids are that the BDLT should be lower than 11.3 at -20°C and below 8.75 at 0°C [12-17]. The model system lies approximately on the limiting line. The increased value of the BLDT is in parallel with the increased viscosity as the temperature is lowered. As the solution is diluted with water, the values will decrease, but the lowest usable temperature will also increase. This data can be used as a bench mark to assess the PAA/PVP blends. Identical measurements to those performed on the model system were carried out on the blends.

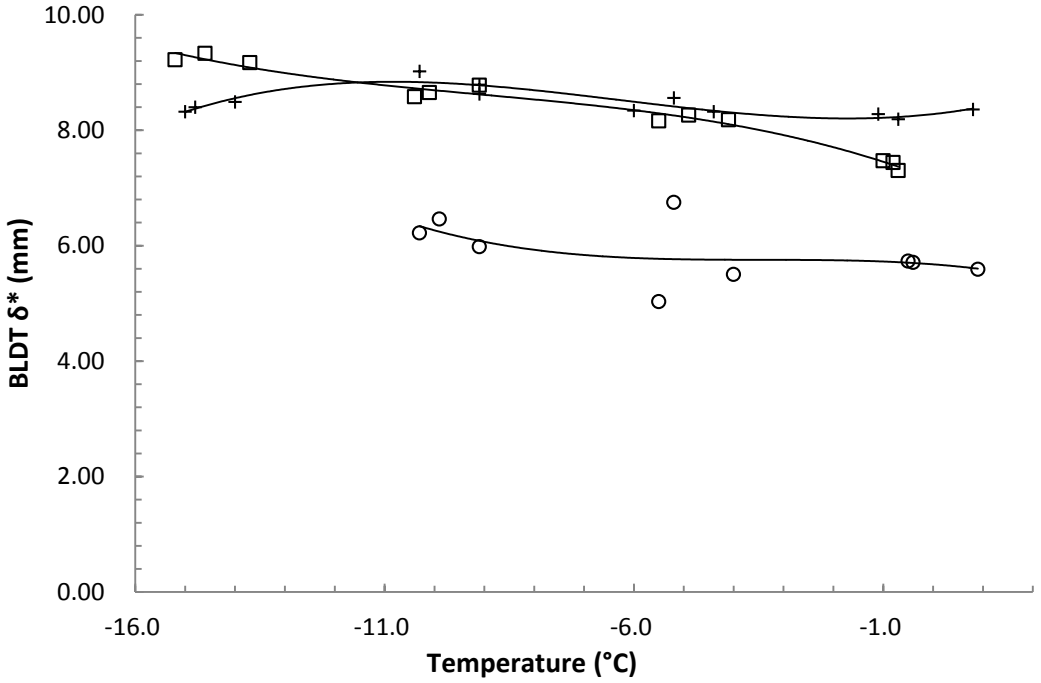

Figure 6.40 BLDT for pure PAA model fluid A4. (+) Undiluted, (□) 75% concentration wt/wt%, (○) 50% concentration wt/wt %.

6.3.5.1. Carbomer A/PVP 360k

The 50:50 wt/wt solution of Carbomer A/PVP (360k), AP102, yielded the results shown in Figure 6.41. The values of the BLDT are comparable to those of the pure Carbomer A model system A4; however the value of the film thickness is retained to a slightly higher value at the highest temperature. On dilution the values fall in line with the reduction in the viscosity and are similar to those found in the model on dilution.

The 60:40 Carbomer A:PVP mixtures, AP112 (Figure 6.42), exhibit values which are higher than those for the 50:50 PAA/PVP blend which is consistent with the higher viscosity values observed with this blend.

On dilution the BLDT is retained at a higher level for the 50:50 blend, but are in line with those observed for the model system.

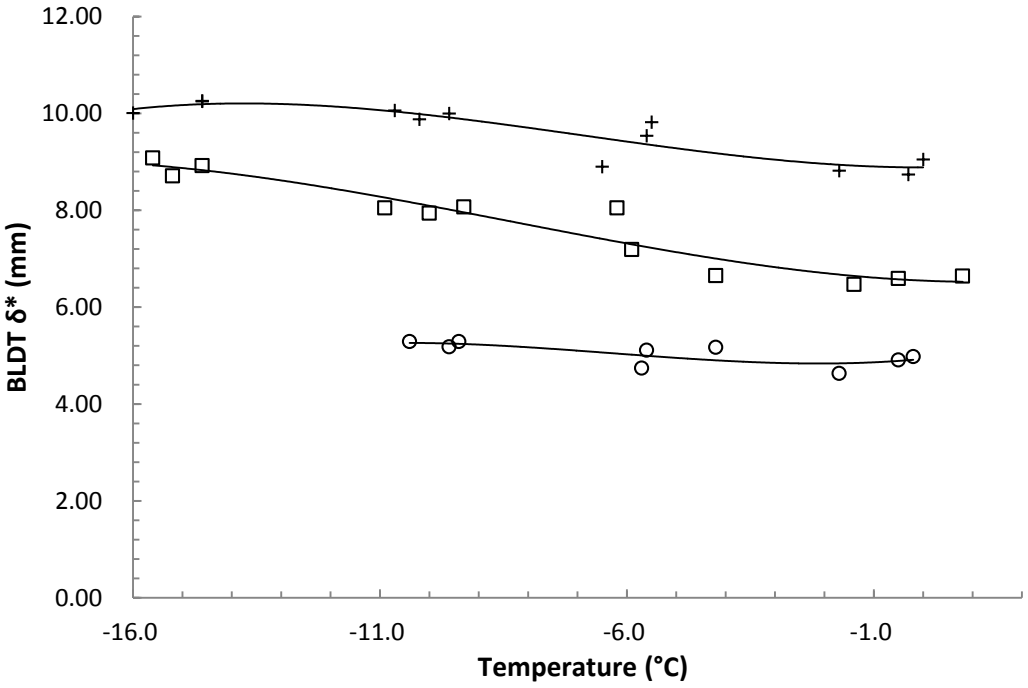

Figure 6.41 BLDT for AP102. (+) Undiluted, (□) 75% concentration wt/wt%, (○) 50% concentration wt/wt %.

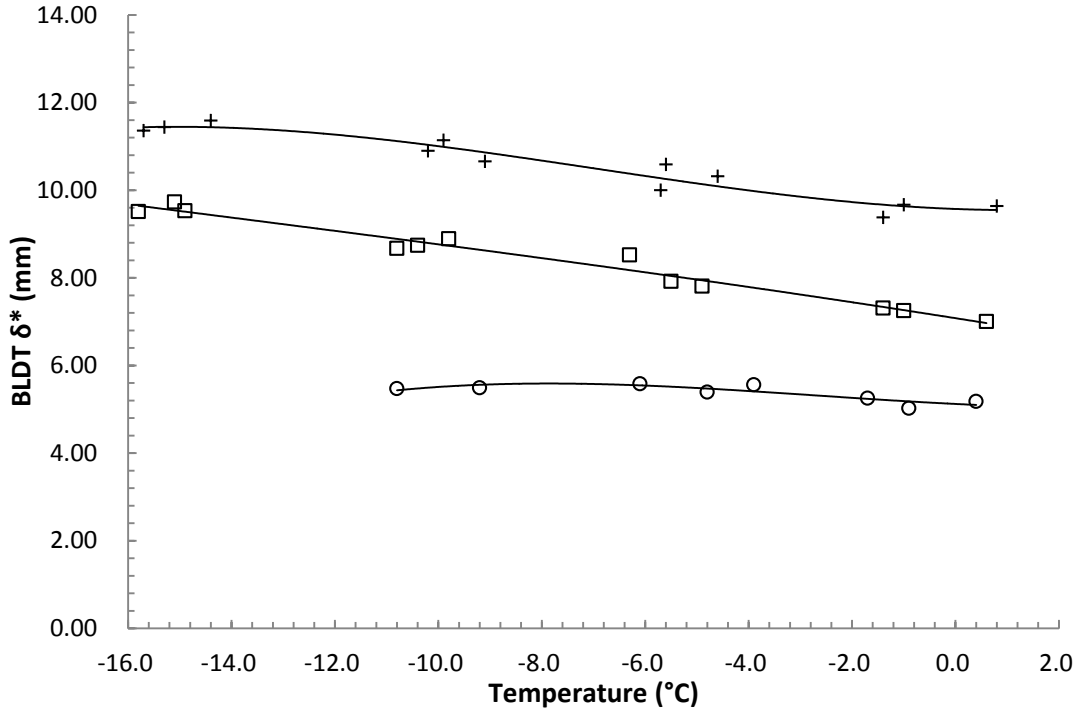

Figure 6.42 BLDT for AP112. (+) Undiluted, (□) 75% concentration wt/wt%, (○) 50% concentration wt/wt %.

6.3.5.2. Carbomer A/PVP 700k

The 50:50% solution of Carbomer A/PVP (700k), AP202, yielded the results shown in Figure 6.43. The values of the BLDT measured at -15°C are similar to those observed with the other systems however there is not the expected decrease as the temperature is increased. On dilution, however, the variation becomes closer to that observed with the other systems. The rheological study on this blend has shown significantly higher values of the viscosity in this system compared with that for the blends produced using the PVP (360k). However the viscosity values had dropped in a similar manner to those for the other polymers. The viscosity measured at 5 Pa s and 10 Pa s does not reflect the total dynamics of these systems and the differences observed are themselves a reflection of the dynamics of the processes encountered by the fluid in the wind tunnel.

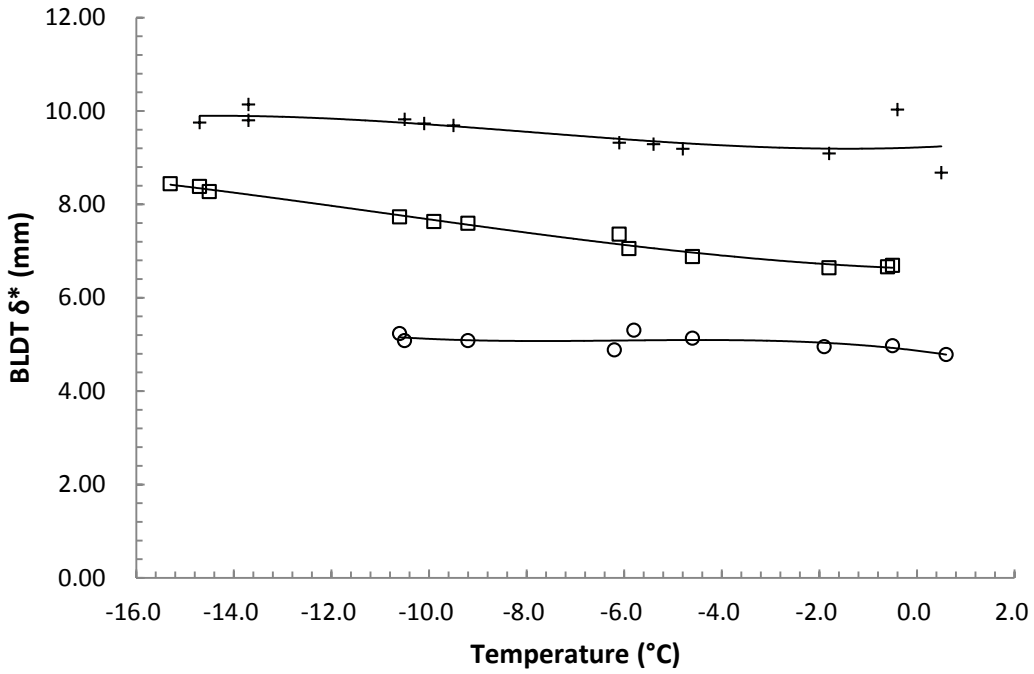

Figure 6.43 BLDT for AP202. (+) Undiluted, (□) 75% concentration wt/wt%, (○) 50% concentration wt/wt %.

Changing the composition of the blend to a 60:40% Carbomer A/PVP blend (AP212) produces the data in Figure 6.44. As with the 50:50 blend the value of the BLDT is surprisingly low when the viscosity profile is considered for this system. Thus although the fluid exhibits a high viscosity at low temperatures the ability to clear the fluid from the aerofoil does not appear to be affected. Both the 700k systems show peaks at lower temperatures than those used in the wind tunnel measurements which implied that the point at which gelation was occurring was lower than that for the model system.

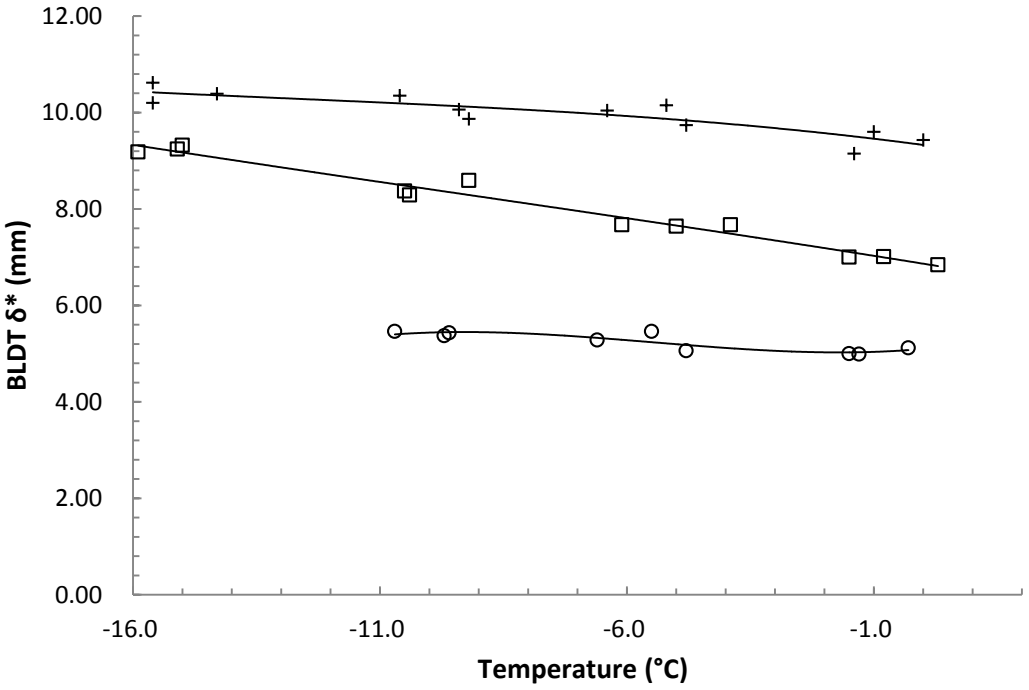

Figure 6.44 BLDT for AP212. (+) Undiluted; (□) 75% concentration wt/wt%, (○) 50% concentration wt/wt %.

The main difference which appears between the Carbomer A model system and the PAA/PVP systems is the difference in the temperature dependence for the 100% solutions. In the case of the PAA system, in which gel forming at about 3°C the BLDT drops with increase in temperature. In these systems where the PVP is adding to the formation of the transient polymer structure the BLDT does not drop as dramatically with increasing temperature. The fluid will experience a spectrum of shear rates during the removal process and the changes in the polymer-polymer interactions will influence the ability of the fluid to be deformed under the action of wind shear.

It is clear that the four fluids studied in this section have the potential of being used as deicing fluids, however all clearly would require to be evaluated further and modified to deliver a commercial product.

6.4. Conclusions

The rheological behaviour of the PAA/PVP mixtures is complex. The factors which influence the viscosity behaviour can be summarised as follows:

1) The blend exhibits many of the characteristics observed in the model PAA polymer solution, however there is evidence that there is interaction to a limited extent between the PAA and the PVP.

2) In the mixture of PVP/PAA, changes in the electrolyte concentration influence the extent to which the carboxylic acid groups are de-shielded, and hence affect the balance between intra- and inter-molecular interactions which define the hydrodynamic volume of the polymer in solution. Changes in the extent to which the PAA is forced into an open structure will be influenced by the pH and this influences the ability of groups on one polymer to interact with those on another polymer. The electrolyte can screen the ionised groups from hydrogen-bonding interactions and control the enhancement in the viscosity which occurs on the addition of PVP.

3) The PVP is able to interact with the PAA however as the molecular weight is increased the tendency to phase separate can increase and although the polymer has a larger hydrodynamic radius it does not produce the expected increase in the extent to which interactions occur with the PAA.

4) The location of the peak in the temperature/viscosity plot arises from a balance between several competing interactions. As the temperature is lowered the ability of the electrolyte to screen the PAA will change and this will influence the equilibrium conformation of the polymer and the balance between intra- and inter-molecular interactions. At very low temperature, the PAA will tend to form gel particles and this collapse of the polymer structure will effectively reduce the viscosity.

5) Changes in temperature will influence the properties of the solution; it will in turn influence the viscosity of the solvent, propylene glycol/water mixtures, and the equilibrium conformation of both the PVP and PAA. The extended polymer chains will be able to interact, however as the chains adopt a more collapsed structure the interactions will be reduced and consequently a lower viscosity.

This study has indicated that by adopting a systematic approach to adjusting the molecular weight of the PVP, the ratio of PVP/PAA, and the electrolyte concentration it is possible to achieve viscosity temperature/shear rate/shear stress characteristics which are similar to those found in PAA de-icing fluid systems. The wind tunnel characteristics are found to associate with the predictions in terms of the rheology measurements.

6.5. References

1. Oechsner, M. and Keipert, S., *Polyacrylic acid polyvinylpyrrolidone bipolymeric systems. I. Rheological and mucoadhesive properties of formulations potentially useful for the treatment of dry-eye-syndrome.* European Journal of Pharmaceutics and Biopharmaceutics, 1999. **47**(2): pp. 113-118.

2. Haaf, F., Sanner, A., and Straub, F., *Polymers of N-Vinylpyrrolidone: Synthesis, Characterization and Uses.* Polymer Journal, 1985. **17**(1): pp. 143-152.

3. Ferguson, J. and Sundar Rajan, V., *The hydrolysis of N-vinylpyrrolidone in the presence of polyacrylic acid and potassium persulphate.* European Polymer Journal, 1979. **15**(7): pp. 627-630.

4. Samuels, W.D., Conkle, H.N., Monzyk, B.F., Simmons, K.L., Frye, J.G., Werpy, T.A., Kuczek, S.F., and Chauhan, S.P., *Deicing/anti-icing fluids* USPTO, Editor 2005: U.S.

5. Nurkeeva, Z.S., Khutoryanskiy, V.V., Mun, G.A., Biktekenova, A.B., Kadlubowski, S., Shilina, Y.A., Ulanski, P., and Rosiak, J.M., *Interpolymer complexes of poly(acrylic acid) nanogels with some non-ionic polymers in aqueous solutions.* Colloids and Surfaces a-Physicochemical and Engineering Aspects, 2004. **236**(1-3): pp. 141-146.

6. Jin, S.P., Liu, M.Z., Chen, S.L., and Chen, Y., *Complexation between poly(acrylic acid) and poly(vinylpyrrolidone): Influence of the molecular weight of poly(acrylic acid) and small molecule salt on the complexation.* European Polymer Journal, 2005. **41**(10): pp. 2406-2415.

7. Pradip, Maltesh, C., Somasundaran, P., Kulkarni, R.A., and Gundiah, S., *Polymer-Polymer Complexation in Dilute Aqueous-Solutions - Poly(acrylic acid)-Poly(ethylene oxide) and Poly(acrylic acid)-Poly(vinylpyrrolidone).* Langmuir, 1991. **7**(10): pp. 2108-2111.

8. Lau, C. and Mi, Y.L., *A study of blending and complexation of poly(acrylic acid)/poly(vinyl pyrrolidone).* Polymer, 2002. **43**(3): pp. 823-829.

9. Henke, A., Kadlubowski, S., Wolszczak, M., Ulanski, P., Boyko, V., Schmidt, T., Arndt, K.F., and Rosiak, J.M., *The Structure and Aggregation of Hydrogen-Bonded Interpolymer Complexes of Poly(acrylic acid) With Poly(N-vinylpyrrolidone) in Dilute Aqueous Solution.* Macromolecular Chemistry and Physics, 2011. **212**(23): pp. 2529-2540.

10. Devine, D.M. and Higginbotham, C.L., *The synthesis of a physically crosslinked NVP based hydrogel.* Polymer, 2003. **44**(26): pp. 7851-7860.

11. Kaczmarek, H., Szalla, A., and Kaminska, A., *Study of poly(acrylic acid)-poly(vinylpyrrolidone) complexes and their photostability.* Polymer, 2001. **42**(14):

pp. 6057-6069.

12. SAE, *SAE AS5900B Standard Test Method for Aerodynamic Acceptance of SAE AMS 1424 and SAE AMS 1428 Aircraft Deicing/Anti-icing Fluids*, 2007, SAE International.

13. Beisswenger, A., Laforte, J.L., Tremblay, M.M., and Perron, J., *Investigation of a New Reference Fluid for Use in Aerodynamic Acceptance Evaluation of Aircraft Ground Deicing and Anti-icing Fluid*, in *prepared for the Federal Aviation Administration*2007.

14. Louchez, P.R., Laforte, J.L., Bouchard, G., and Farzaneh, M., *Laboratory Evaluation of Aircraft Ground De Antiicing Products*, in *Proceedings of the Fourth*, Chung, J.S., Karal, K., and Koteryama, W., Editors. 1994, International Society Offshore& Polar Engineers: Cupertino. pp. 479-483.

15. Louchez, P., Laforte, J.L., and Bouchard, G., *Boundary Layer Evaluation of Anti-Icing Fluids for Commuter Aircraft*, 1994, UQAC.

16. Louchez, P., Laforte, J.L., and Bernardin, S., *A proposal of standard evaluation of aerodynamic performance of de-icing and anti-icing fluids applied on commuter type aircraft*, 1994, Universite du Quebec a Chicoutimi.

17. Renton Division Aerodynamics Engineering, *Aerodynamic Acceptance Test for Aircraft Ground Deicing/Anti-icing Fluids*, 1992, Boeing: Chicago, IL.

Chapter 7. Rheology of Carbomer B – PVP Fluids

7.1. Introduction

In Chapter 6 various blends of PVP polymers with Carbomer A have been studied. It proved that as substitutes for pure Carbomer A, the blends have the capability to deliver the required shear-thinning characteristics while potentially reducing the formation of an irreversible gel complex. Carbomer B is a PAA-based homo-polymer provided by Kilfrost which has a nominal molar mass of 5 MDa. As indicated in Chapters 3 and 5 this polymer is more highly branched than Carbomer A, possibly in a star-shaped pattern, resulting in a high degree of random inter-molecular interactions; although essentially of smaller hydrodynamic volume it may forming larger clusters. Therefore the solution of Carbomer B appeared to be much more viscous than the Carbomer A solution under the same conditions. However electrolyte will provide a shielding effect to the carboxylic acid group interactions and reduce the possibility of forming inter-molecular networks; this has been confirmed with the previous observation of the significant viscosity drop of Carbomer B solutions when electrolyte was added. The behaviour of a viscosity 'peak', which has been discussed repeatedly in previous chapters, was also altered by electrolyte and possibly shifted to lower temperatures. Given such sensitivity towards electrolyte, it was expected that, by blending with PVP and forming hydrogen bonds with the carbonyl group of pyrrolidone rings, the carboxylic groups of PAA will be more tolerant to salts. Therefore in this chapter a series of study of the rheological behaviour of Carbomer B blends with two molecular weight PVP polymers dispersed in propylene glycol/water mixtures are reported. However due to lack of information on the particular type of de-/anti-icing fluids on which Carbomer B is utilized as thickening agents, this part of study will not focus on matching the standard performance of commercial product as did in the previous chapter for Carbomer A/PVP blends.

7.2. Experimental

7.2.1. Materials and Sample Preparation

Carbomer B, a poly(acrylic acid) based homo-polymer, was supplied by Lubrizol (Brussels, Belgium) as flocculated solid particles with nominal molar mass of 5 MDa. Characterisation of this material has been undertaken and has been reported in Chapters 3 and 5, including FTIR and NMR analyses, intrinsic viscosity measurements, acid number determination, and rheological measurements. To achieve quick dissolution, solid polymer was dispersed using a Silverson L4R high shear mixer placed in a 1 L beaker containing 600 g of de-ionized water and operated at 4800 rpm for 5 minutes; on completion the rotation speed was reduced to 3600 rpm and stirring continued for a further 55 minutes. A 'gel-like' dispersion was produced with a polymer concentration of 1.22 g dL^{-1}.

Two PVP polymers used in this study were of nominal molecular weights 360,000 and 700,000 supplied by Aldrich Chemical Company Limited (Gillingham, UK) and BDH (Poole, UK), respectively. Each was prepared by dispersion in de-mineralised water also at a concentration of 1.22 g dL^{-1} and stirred until fully dissolved using a magnetic stirrer. A water/1,2-propylene glycol mixture was prepared at a 50:50 wt/wt ratio. The Carbomer B gel intermediate was first added to the water/glycol mixture and fully mixed; the PVP solution was then added and fully mixed. The total polymer concentration of polymer was 0.30 g dL^{-1} with 50:50 wt/wt mixing ratios of PAA to PVP. The solutions were then neutralized with 5.0M potassium hydroxide solution to attain a pH of 7.0. 5.0M sodium chloride solution was added to adjust the viscosity profile. The sample compositions can be found in Table 7.1.

Table 7.1 Carbomer B:PVP Composition Data

Sample	PVP M_W (KDa)	PAA : PVP Ratio	NaCl(g)/Soln(g)
BP101	360	50:50	0
BP102	360	50:50	0.015/100
BP103	360	50:50	0.030/100
BP104	360	50:50	0.045/100
BP105	360	50:50	0.061/100
BP201	700	50:50	0
BP202	700	50:50	0.015/100
BP203	700	50:50	0.030/100
BP204	700	50:50	0.045/100
BP205	700	50:50	0.061/100

7.2.2. Rheology

Viscosities were measured using a temperature ramp at fixed stress. These were carried out using a shear stress-controlled TA Instruments Carri-Med CSL^{2}500 rheometer (TA Instruments, Crawley, UK) using 4-cm parallel plate fitted with a solvent trap. Temperature was controlled by using Peltier effect and an anti-freezing bath maintained at 0°C, enabling test temperatures between 15°C to -15°C. Temperature ramp tests were carried out at a rate of 1.0°C per two minutes from 15°C to -15°C, and then from -15°C to 15°C, at shear stresses of 5 and 10 Pa.

7.3. Results and Discussion

In Chapter 5 it was determined that there were major differences between Carbomer A and Carbomer B. Despite the fact that both PAA-based polymers exhibited shear-thinning characteristics within a certain range of applied shear stresses regardless of the

electrolyte level, there are major differences between the two in terms of the viscosity level, the viscosity 'peak' behaviour, and rheological change with electrolyte addition. These are likely caused by the structural differences between the two polymers. With more inclusions of highly branched PAA molecules for Carbomer B, larger inter-molecular networks were formed occupying a larger hydrodynamic volume, resulting in higher viscosity generally; however this structure also made the material vulnerable to salt effects which explained the observed significant viscosity drop. Such characteristics made Carbomer B-thickened fluids rather unstable in terms of rheological performance. It is necessary to examine whether the Carbomer B:PVP blends are able to provide desirable thickening properties with a more stable and predictable rheological profile compared to the pure Carbomer B-thickened systems. Two PVP polymers with molecular weight of 360k and 700k were blended with Carbomer B in a 50:50 wt/wt mixing ratio. The electrolyte levels matched the ones of pure Carbomer B systems in the same weight ratio to PAA polymer.

For temperature ramp data of each individual sample not exhibited in this chapter, please refer to Appendix C.

7.3.1. System BP1 (Carbomer B/PVP 360k)

A significant viscosity drop was observed immediately for the 50:50 blend of Carbomer B and PVP 360k (Figure 7.1). At 5 Pa of applied shear stress, the viscosity of the blend system is approximately 0.20 Pa s at 15°C and rises to approximately 1.15 Pa s at -15°C. The values are much lower even compared to the ones observed for Carbomer B sample B1 at 100 Pa of shear stress. The slight hysteresis exhibited between the curves during the processes of cooling-down and heating-up indicates the rheological performance remains influenced by the random inter-molecular interactions between Carbomer B molecules, which is consistent with the behaviour observed in the temperature ramp test data for Carbomer B. These interactions are formed through hydrogen bonding between the carboxylic groups of PAA. Because of the higher degree of branching, as the

temperature decreases it takes longer for the polymer network to equilibrate and this gives generally higher viscosity levels when the fluid was heated up compared to when it was cooled down.

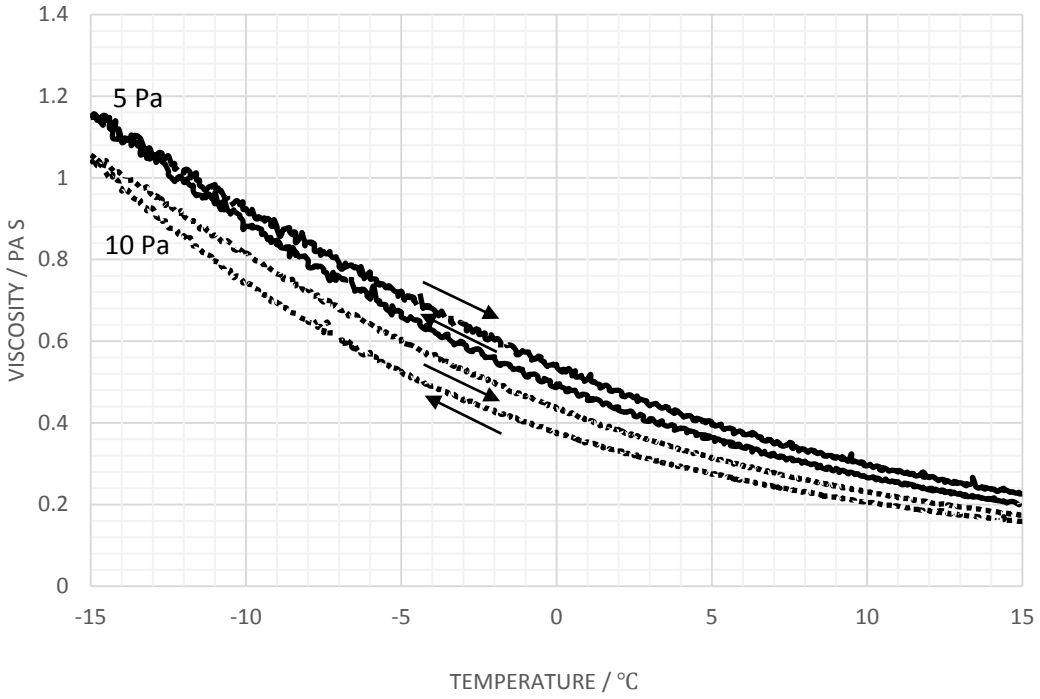

Figure 7.1 Viscosity variation with temperature plots for BP101, applied shear stresses 5 and 10 Pa.

With added electrolyte, significant viscosity drop occurred for situations with both 5 Pa and 10 Pa of shear stresses applied. With electrolyte/PAA ratio adjusted to the same for Carbomer B:PVP 360k sample BP102 and pure Carbomer B sample B2, at 5 Pa of shear stress, the viscosity measured was approximately 0.054 Pa s at15°C and 0.18 Pa s at -15°C for BP102 (Figure 7.2), and 0.26 Pa s at 15°C and 0.45 Pa s at -15°C for B2. It has been established that due to the inclusion of more highly branched molecules Carbomer B-thickened fluids would be much more sensitive to electrolyte addition in terms of viscosity level compared to Carbomer A fluids. Consider the situation similar to that which has been observed with Carbomer A and PVP blends, the inclusion of low molecular PVP will inherently thicken the water/glycol mixture less effectively than the high molecular weight PAA by itself. What is more important is the role of PVP as a

hydrogen bonding agent in these blended thickening agents. Hydrogen bonding can be created between the N-H group of the pyrrolidone ring and the carbonyl of the acid or between the –OH of the carboxylic acid and the carbonyl groups of pyrrolidone rings. The role of hydrogen bonding is expected to reduce the sensitivity towards electrolyte effects.

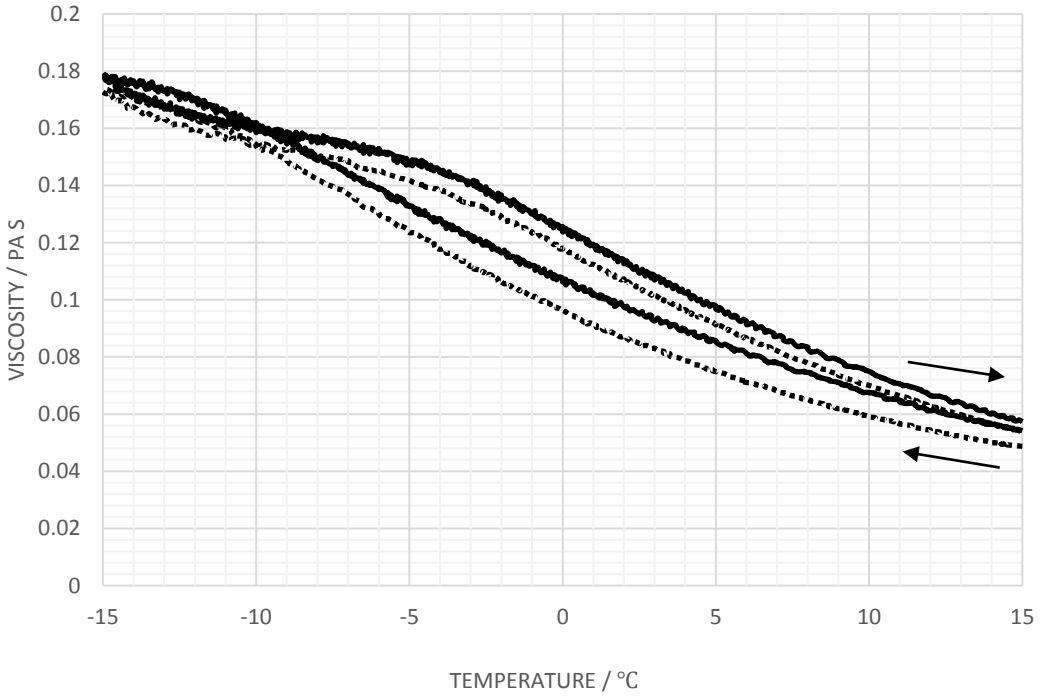

Figure 7.2 Viscosity variation with temperature plots for BP102, applied shear stresses 5 and 10 Pa; (–) 5 Pa, (…) 10 Pa.

Figure 7.3 is the temperature ramp test result for sample BP105, which contains 0.061 g (NaCl) per 100 g (Solution) of sodium chloride. Compared to B5, which is the pure Carbomer B-thickened fluid with equivalent electrolyte level, at 5 Pa of shear stress, the viscosity of BP105 was at 0.053 Pa s at 0°C and increased to 0.11 Pa s at -15°C, which is approximately the same as B5 at 0°C and 25% greater than it at -15°C. Hysteresis, although slightly present, is reduced for BP105. These observations suggest that blending with PVP has provided improvement over the sensitivity issue with Carbomer B towards electrolyte addition.

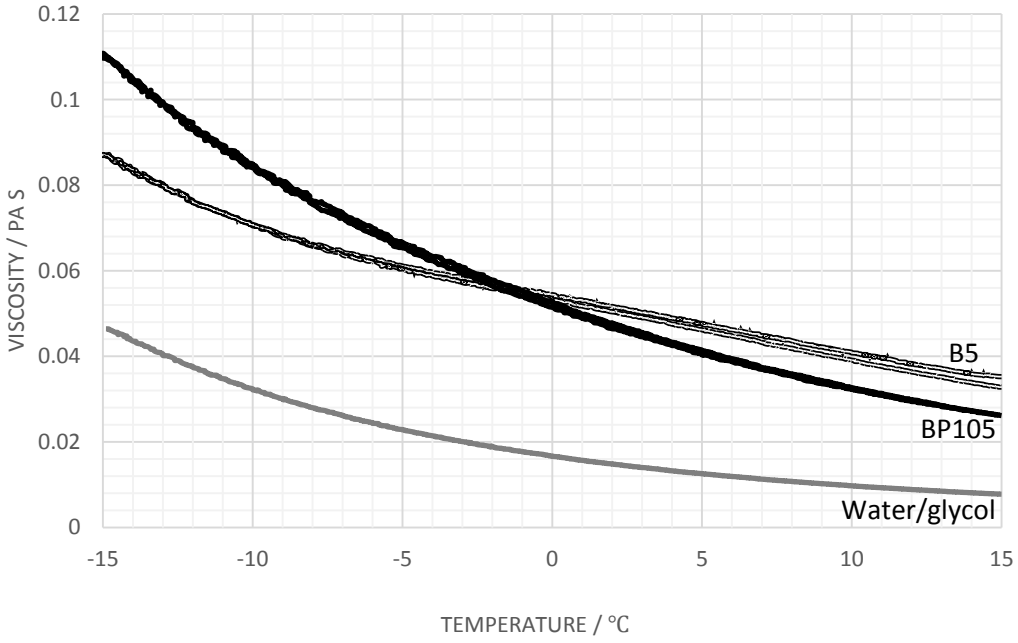

Figure 7.3 Viscosity variation with temperature plots for BP105, in comparison with B5, applied shear stresses 5 Pa.

7.3.2. System BP2 (Carbomer B/PVP 700k)

Increasing molecular weight of PVP from 360k to 700k has reduced the general viscosity level by a large margin (Figure 7.4) which may suggest that the binding between carbonyl and carboxylic groups are significantly influencing the inter-molecular (also intra-molecular) interactions formed between PAA molecules. Such behaviour is similar to the difference observed between AP101 and AP201 in which the high molecular weight PVP blend remained less viscous compared to the lower molecular weight PVP blend at temperatures above -5°C. Given that Carbomer B is a more highly branched polymer than Carbomer A, higher molecular weight PVP can be significantly reducing the magnitude of polymer network formed by Carbomer B, and therefore causing a large drop in viscosity level.

With added electrolyte, viscosity of PVP 700k blends with Carbomer B continued to drop progressively as expected (Figure 7.5). With the same level of electrolyte added to the system, Carbomer B-PVP 700k blend behaves very similarly to the one with PVP 360k

(Figure 7.6 and Figure 7.7).

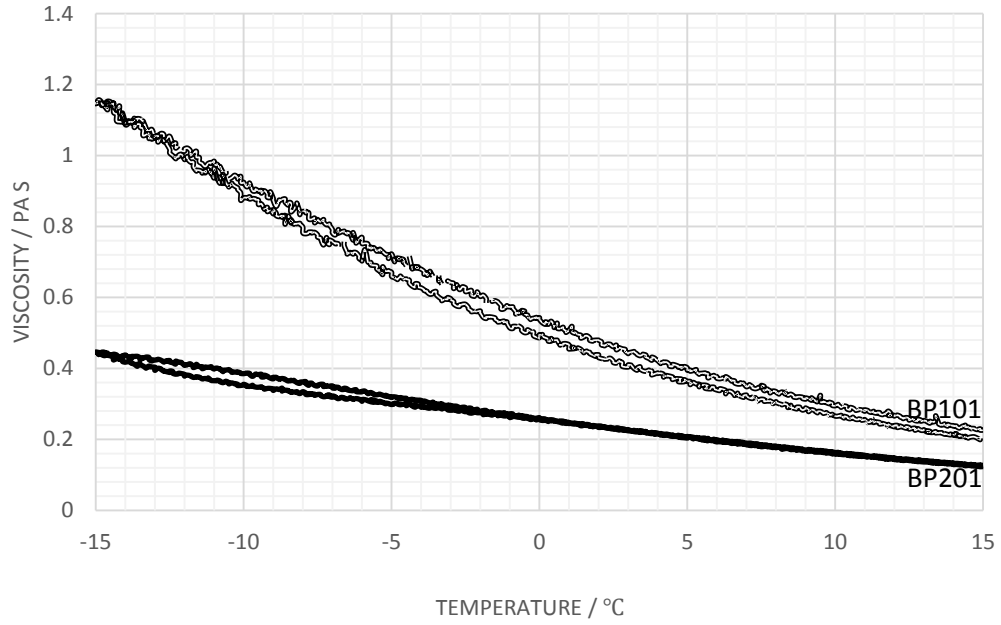

Figure 7.4 Viscosity variation with temperature plots for BP201, in comparison with BP101, applied shear stresses 5 Pa.

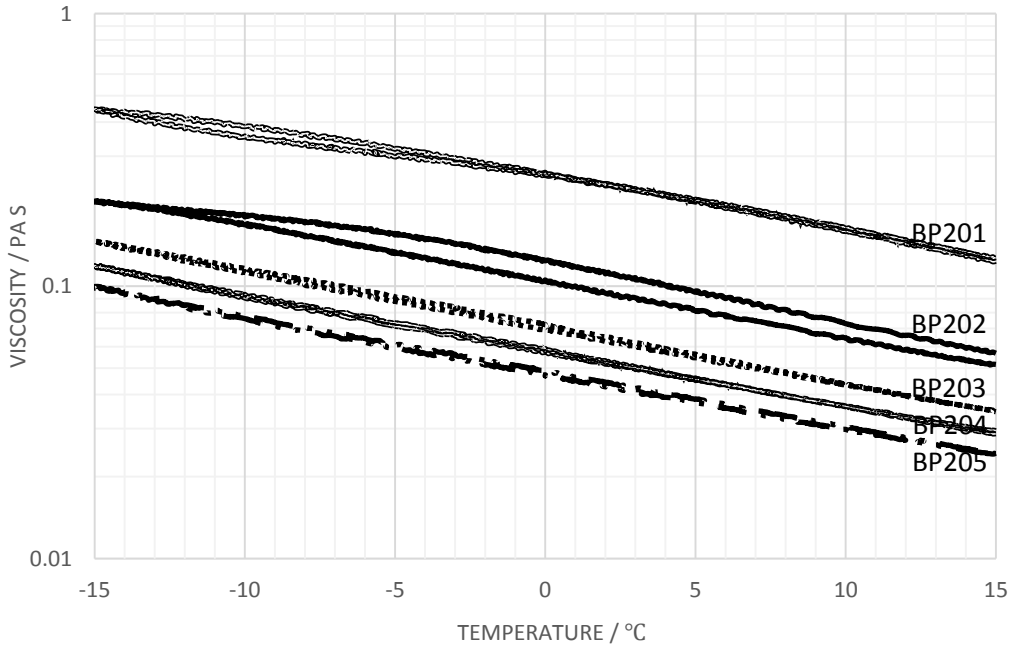

Figure 7.5 Viscosity variation with temperature plots for BP2 series, PVP700k:Carbomer B=50:50 wt/wt, shear stress 5 Pa.

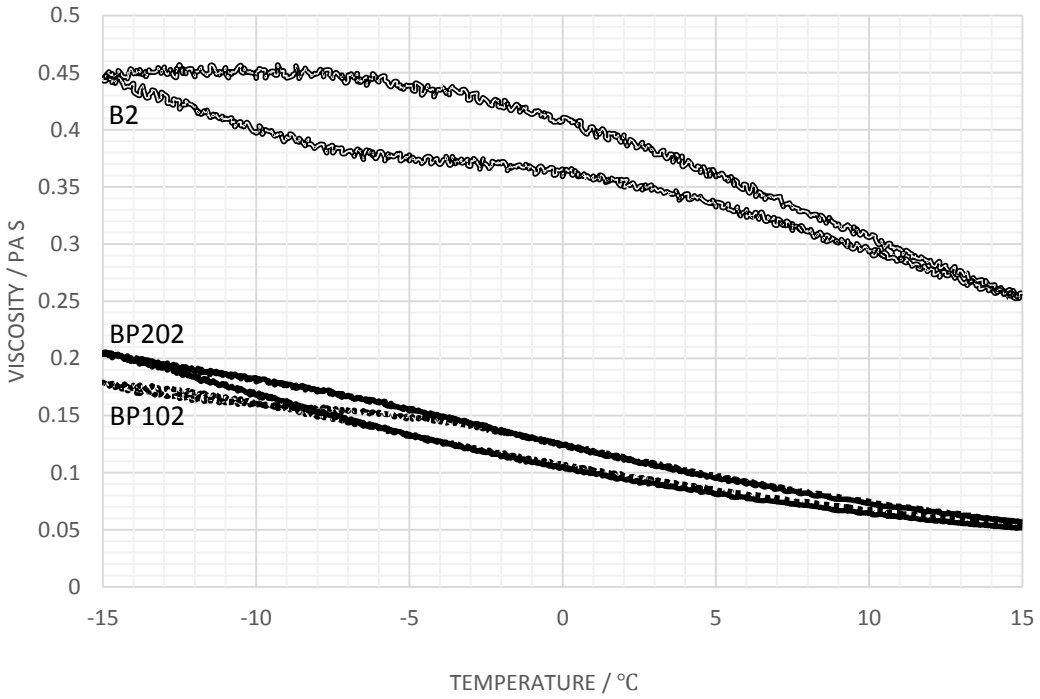

Figure 7.6 Viscosity variation with temperature plots for BP202, in comparison with BP102 and B2, applied shear stresses 5 Pa.

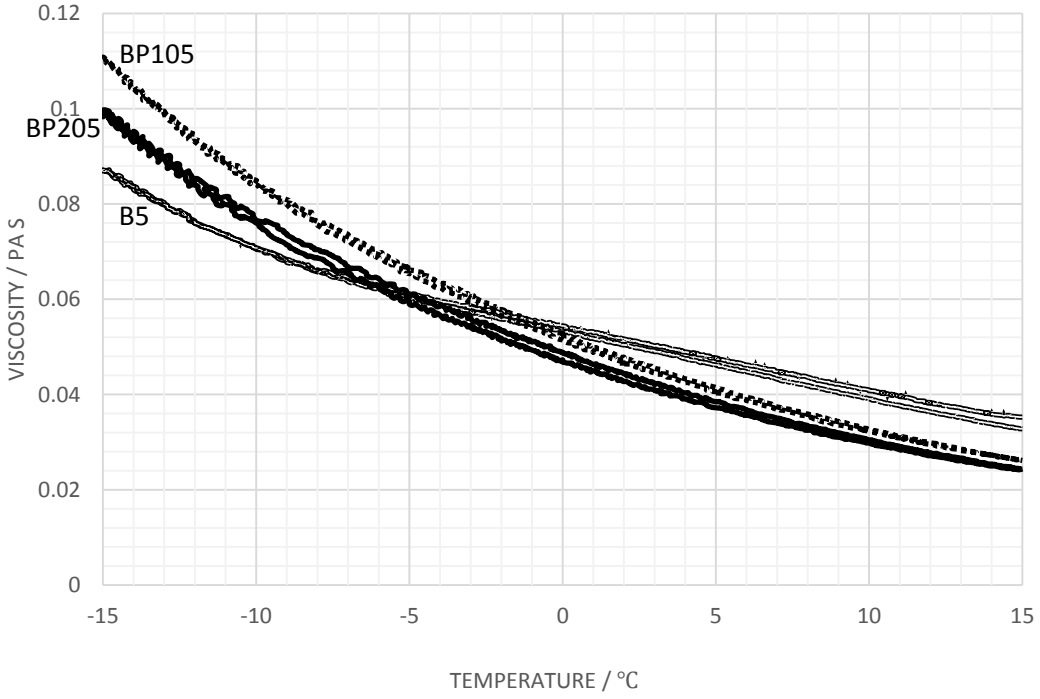

Figure 7.7 Viscosity variation with temperature plots for BP205, in comparison with BP105 and B5, applied shear stresses 5 Pa.

7.4. Conclusions

The studies with Carbomer B do not indicate the presence of a peak in the temperature dependence of the viscosity. The significant temperature dependence exhibited by the pure polymer and the mixtures indicate that it is unlikely to be a candidate for use as a de-icing fluid, the viscosity levels being insufficient for a stable film. The behaviour in terms of the apparent lack of sensitivity to shear stress level implies that the chain branching acts to inhibit the formation of a network structure of the form observed with Carbomer A leading to a more accessible structure for the PVP. The lack of major thickening by the PVP is consistent with the previous observations on Carbomer A solutions where the PVP is only able to form weak interactions with the PAA.

Wind tunnel measurements were not performed on these solutions.

Chapter 8. Evaluation of the Influences of Potassium and Calcium Cations on Thickened Fluids

8.1. Introduction

It is usual in field applications to dilute de-/anti-icing fluids with water when the weather conditions are mild and moderate. Type II and type IV fluids are commonly composed of a 50:50 water/glycol mixture which enables their fluidity to be maintained at temperatures above -39°C [1-3]. As conditions may require, parent fluids can be diluted to 50% or 75% by weight of their original concentration and the process of dilution is usually carried out on site at airports using local water [4-10]. Mono- and bi-valent cations are commonly present in local water, and as previously established, electrolytes are able to influence the rheological behaviours of de-icing fluids to a large extent (Chapter 5-7, [11, 12]). Divalent cations, such as calcium and magnesium, are capable of bridging two carboxylic groups in a poly(acrylic acid) solution, which leads to formation of larger polymeric networks and eventually phase separation. Monovalent cations (such as potassium and sodium), on the other hand, as previously examined, are able to provide screening effect to carboxylic groups and therefore suppress the viscosity level of the fluids. Furthermore, potassium formate has been extensively utilized in run-way de-icing products, in the forms of both granules and solutions [13, 14]; and this makes it more common for aircraft de-icing fluids to be in with monovalent cations. Therefore it was decided to carry out a series of measurements to determine the influence of water dilution on the fluids thickened by both Carbomer A and Carbomer A-PVP blends.

8.1.1. Definition of Hard Water

Hard water is classified according to the total concentration of ions present. The major components of hard water include Ca^{2+} and Mg^{2+}, with other multivalent ions, namely iron, aluminium, and manganese present to varying extents, reflecting the geography of

the water source location. The total water hardness, including both Ca^{2+} and Mg^{2+} ions, is reported in parts per million or mass/volume of calcium carbonate in the water [15].

Because it is the precise mixture of minerals dissolved in the water, together with the water pH and temperature, that determines the behaviour of the hardness, a single-number scale does not adequately describe hardness. Furthermore, the occurrence of Ca^{2+} and Mg^{2+} and other ions varies with location. It is appropriate to simplify the definition of 'hardness' by reference to the Ca^{2+} ionic concentrations or equivalent. Descriptions of hardness correspond roughly with ranges of Ca^{2+} concentrations are presented in the following table (Table 8.1).

Table 8.1 Water quality designation

Water Quality Designation	**Ca^{2+} Concentration (mg/L)**
Soft	0 – 60
Moderately Hard	61 – 120
Hard	121 – 180
Very Hard	≥ 181

8.1.2. Global Water Hardness Variation

In defining the study of the effects of hard water on the potential for gelation of de-icing fluids, it is appropriate to survey the variations which are found around the world [15-17].

a) Australia

Analysis of water hardness in major Australian cities by the Australian Water Association shows a range from very soft (Melbourne) to very hard (Adelaide). Total hardness levels of calcium carbonate in ppm are presented in Table 8.2.

Table 8.2 Water hardness in Australia

Location	Calcium Carbonate Level (ppm)
Canberra	40
Melbourne	10 – 26
Sydney	39.4 – 60.1
Perth	29 – 226
Brisbane	100
Adelaide	134 – 148
Hobart	5.8 – 34.4
Darwin	31

b) Canada

Prairie Provinces (mainly Saskatchewan and Manitoba) contain high quantities of calcium and magnesium, often as dolomite, which are readily soluble in the ground water that contains high concentrations of trapped carbon dioxide from the last glaciation. In these parts of Canada, the total hardness (in ppm of calcium carbonate equivalent) frequently exceeds 200, when ground water is the only source of potable water. The west coast, by contrast, has unusually soft water, derived mainly from mountain lakes fed by glaciers and snowmelt. Some typical values are in Table 8.3.

Table 8.3 Water hardness in Canada

Location	Calcium Carbonate Level (ppm)
Montreal	116
Calgary	165
Regina	202
Saskatoon	< 140

Winnipeg	77
Toronto	121
Vancouver	< 3
Charlottetown	140 – 150

c) England and Wales

Information from the British Drinking Water Inspectorate shows that drinking water in England is generally considered to be 'very hard', with most areas of England, particularly east of a line between the Severn and Tees estuaries, exhibiting above 200 ppm for the calcium carbonate equivalent. Wales, Devon, Cornwall and parts of North-West England are softer water areas, and range from 0 to 200 ppm. Water in Manchester in England is soft because it comes from Thirlmere and Haweswater reservoirs in the Lake District, and in their headwaters there is no exposure to limestone or chalk. Similarly, tap water in Birmingham is also soft as it is sourced from the Elan Valley reservoirs in Wales.

d) The United States

More than 85% of American homes have hard water. The location of hardness in the United States is shown in the map below (Figure 8.1). The softest water is to be found in New England, the South Atlantic-Gulf States, the Pacific Northwest, and Hawaii. Moderately hard waters were common in many rivers of Alaska and Tennessee, in the Great Lakes region, and the Pacific Northwest. Hardest waters (≥ 1000 mg L^{-1}) were measured in streams in Texas, New Mexico, Kansa, Arizona, and southern California.

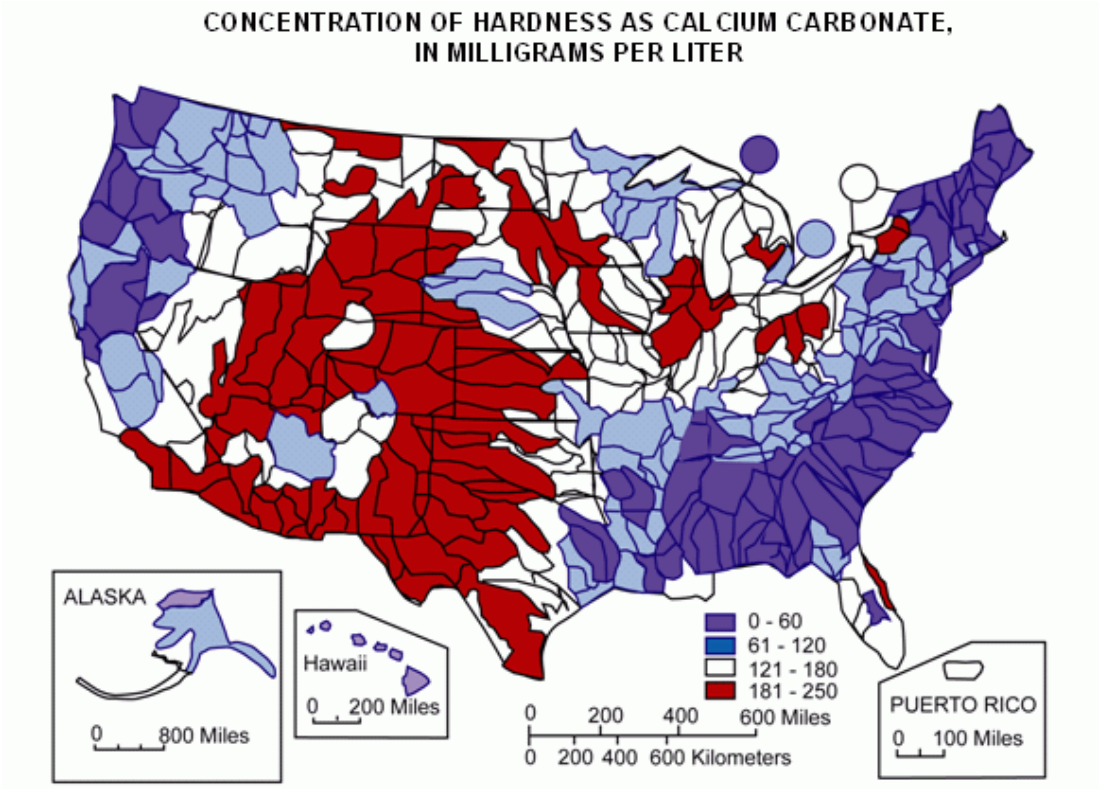

Figure 8.1 Concentration of Hardness as Calcium Carbonate in the US, mg/L.[1]

e) Turkey

The concentrations of Ca^{2+} and Mg^{2+} in the area of southern Anatolia vary between 40.1 and 72.1 mg L^{-1} (Ca^{2+}) and 11.6 to 18.2 mg L^{-1} (Mg^{2+}). The Na^{+} level being typically between 0 and 31.1 mg L^{-1} in which places the water is moderately hard.

f) Norway

The concentrations depend on area but range from 16.6 to 17.3 mg L^{-1} for the mafic rocks, to values of 15.6 mg L^{-1} for Precambrian granite and 40.2 mg L^{-1} for late Precambrian placing these areas in the lower end of the harness scale. Whilst a definite linear

[1] http://water.usgs.gov/owq/images/HardnessMap.gif

correlation does not hold there is an approximate scaling of the Na^+ level with the increased level of Ca^{2+} in the analysis; the scaling is approximately 10 : 1 (Na^+ : Ca^{2+}).

g) China

As with other areas the Ca^{2+} concentrations vary with the underlying geological structure and values vary from 10 to over 240 mg L^{-1}. The variation is the Ca^{2+} appears to be mirrored by changes in the Na^+ and K^+ levels which with the lower Ca^{2+} concentrations have values of 84 mg/L and rise to a value of 250 mg L^{-1} with the highest Ca^{2+} level.

The general ranges in terms of water hardness map well on the likely areas where airports might through adding water to the de-icing fluids experience gelation problems. It is, however, important also to note that in general an increase in the hardness of the water also appears to correlate with an increase in the combined sodium and potassium levels, the former being often at a level of 100:1 in the analysis. Local variations reflect a number of factors, influence of volcanic activity on the ground water in Japan, variations in the geology from the point of view of Russia, etc. Looking at various papers it is possible to find that changing the calcium level will also change the sodium level. Whilst this is not always the case, the values indicated below (Table 8.4) correspond to values found in various global locations.

Table 8.4 Global water hardness in calcium and sodium ion levels

Water Quality Designation	**Ca^{2+} (mg/L)**	**Na^+ (mg/L)**
Soft	60	80
Moderately Hard	120	160
Hard	180	230
Very Hard	230	560

8.1.3. Background on the Influences of Potassium Formate

Alkali cation binding events and hydration have been drawing quite a lot of attentions in biology [18]. Potassium and sodium are the major ionic components of intra- and extracellular fluids, and their function is critical to various biological activities. Both of them are in the same chemical group and have the same properties. The presence of both potassium and sodium ions will influence the ionic strength of the de-icing fluid [19, 20]. However, it has been found that Na^+ and K^+ have various degrees of binding affinities with the carboxylic acid head groups of fatty acid. Furthermore, the number of cation-anion contacts is different for Na^+ and K^+, which depends on the different ionic radius. Previous study has demonstrated that the Carbomer-based aqueous solutions are sensitive to sodium addition (Chapter 3 and Chapter 5), in terms of viscosity and visco-staticity. This set of experiments aimed to test the influence of potassium formate on fluid viscosities. Potassium formate is used for deicing runways and hence there is a high probability of it becoming mixed with the de-icing fluids and forming the gel precipitate.

8.2. Experimental

8.2.1. Materials and Sample Preparation

8.2.1.1. Hard Water Dilution for Carbomer A Fluid

Carbomer A-thickened solution A4 (preparation detail in Section 5.2.1), which is a 0.30 g dL^{-1} of Carbomer A dispersion in a 50:50 mono-propylene glycol/water mixture with 0.060 wt% NaCl addition, was selected as the parent fluid for dilution. Various diluting agents (artificial hard water) were formulated by dissolving solid calcium acetate and sodium chloride in de-ionized water. The cation concentration of these artificial hard water samples is listed below (Table 8.5). The parent fluid was diluted with de-ionized water and the diluting agents by 75 wt% of its original concentration.

Table 8.5 Artificial hard water cation concentration

Sample No.	Water Quality	Ca^{2+} (mg/L)	Na^{+} (mg/L)
1	Soft	50	0
2	Moderately Hard	100	0
3	Hard	150	0
4	Very Hard	200	0
5	Soft	50	100
6	Soft	50	200

8.2.1.2. Hard Water Dilution for Carbomer A/PVP Fluids

Six Carbomer A/PVP blend thickened fluids were selected as parent fluids. Fluids were all based on 50:50 wt/wt mono-propylene glycol/water mixture. Total polymer concentrations were maintained at 0.30 g dL^{-1} and polymer compositions are available in the following table (Table 8.6). Various levels of sodium chloride were added to the fluids to adjust the viscosity level. All samples were diluted with 'AEA-designated' hard water (which contains Ca^{2+} 400±5 mg L^{-1} and Mg^{2+} 280±5 mg L^{-1} by specification, [10]) by 75 wt% and 50% of their original concentrations.

Table 8.6 Carbomer A:PVP composition data

Sample	PVP M_W (KDa)	PAA/PVP Ratio	NaCl(g)/Soln(g)
AP102	360	50:50	0.015/100
AP112	360	60:40	0.018/100
AP202	700	50:50	0.015/100
AP212	700	60:40	0.018/100
AP302	1,300	50:50	0.015/100
AP402	4,000	50:50	0.015/100

8.2.1.3. Influence of Potassium Formate

Carbomer A-thickened fluid with 0.30 g dL^{-1} PAA was prepared using the standard procedure (Section 5.2.1). Electrolyte, potassium formate, was added to the system to replace sodium chloride (partially or totally) which was originally used in all Carbomer and PAA/PVP blends thickened fluids in order to establish comparison; and the concentrations of electrolyte were maintained at the same levels and listed below (Table 8.7).

Table 8.7 Electrolyte level of sample solutions with potassium addition

Sample No.	**Electrolyte and Concentration (% wt)**
A2K	K^+ 0.030
A4K	K^+ 0.060
A5K	Na^+ 0.030 + K^+ 0.045

8.2.2. Rheology

Viscosities were measured using a temperature ramp at fixed stress. These were carried out using a shear stress-controlled TA Instruments Carri-Med $CSL^2$500 rheometer (TA Instruments, Crawley, UK) using 4-cm parallel plate fitted with a solvent trap. Temperature was controlled by using Peltier effect and an anti-freezing bath maintained at 0°C, enabling test temperatures between 15°C to -15°C. For samples diluted by 75 wt% of their original concentration, temperature ramp tests were carried out at a rate of 1.0°C per two minutes from 15°C to -15°C, and then from -15°C to 15°C, at shear stresses of 5 and 10 Pa; for those diluted by 50 wt%, because of the -10.6°C freezing point, temperature ramp tests were carried out between 15°C and -10°C.

8.2.3. WSET Measurement

For experiment detail refer to Section 2.2.7.

8.3. Results and Discussion

8.3.1. Influence of Hard Water on Carbomer A-Thickened Fluids

Figure 8.3 is the viscosity variation with temperature for sample fluid A4 (0.30 g dL^{-1} of Carbomer A and 0.060 wt% of sodium chloride) and its 75 wt% dilution. At 5 Pa of shear stress, the viscosity of 75% dilution continuously increased from approximately 0.43 Pa s at 15°C to 1.27 Pa s at -15°C. Such a viscosity profile is different from the one of the parent fluid in two major aspects: 1) at 15°C the 75% dilution has a 60% lower viscosity while at -15°C the viscosity is approximately twice that of its parent fluid; 2) the 75% dilution did not exhibit a viscosity 'peak' within the temperature range whilst the viscosity of its parent fluid reached peak value (although still lower than the maximum viscosity of the 75% dilution which was present at -15°C) at around 0°C. Such observations indicate that while the process of dilution effectively reduced the polymer concentration resulting in a lower probability of polymer entanglement it also lowered the electrolyte level which lead to changes in balancing factors of viscosity variation with decreasing temperature and hence the 'peak' shifting to lower temperature (Section 5.3.1). Previous studies also suggested that the polymer may swell by absorbing water when diluted with de-ionized water [21-23] causing an increment in viscosity. This may contribute to maintaining (or 'stabilizing') the overall viscosity level and reduce the impact of water dilution.

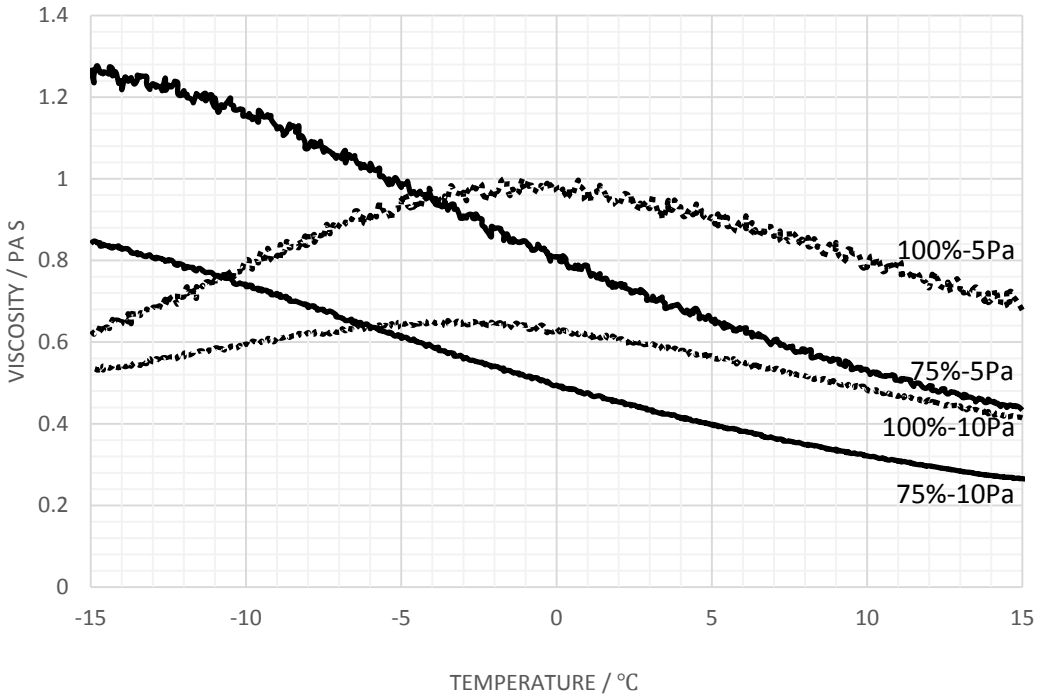

Figure 8.2 Viscosity variation with temperature for A4, 100% and 75 wt% dilution; shear stress 5 and 10 Pa.

Figure 8.3 showed a generally decreasing viscosity level with increasing calcium concentration. The influence of divalent cations, unlike monovalent cations, was not limited in reducing the overall charge repulsion along the polymer backbone but also promoting phase separation by bridging polymer chains. This may explain the shift of viscosity 'peak' to higher temperature with increasing electrolyte concentration. Compared to the parent fluid, for 75% dilution with 200 mg/L Ca^{2+} addition the viscosity dropped from 0.97 Pa s to 0.39 Pa s at 0°C, and from 0.62 Pa s to 0.40 Pa s at -15°C. The drop in the viscosity reflects the formation of the globular form which exists pre-gelation. The viscosity level of this dilution changed insignificantly across the temperature range, which can be considered desirable, however the general viscosity level is considerably lower compared to its parent fluid.

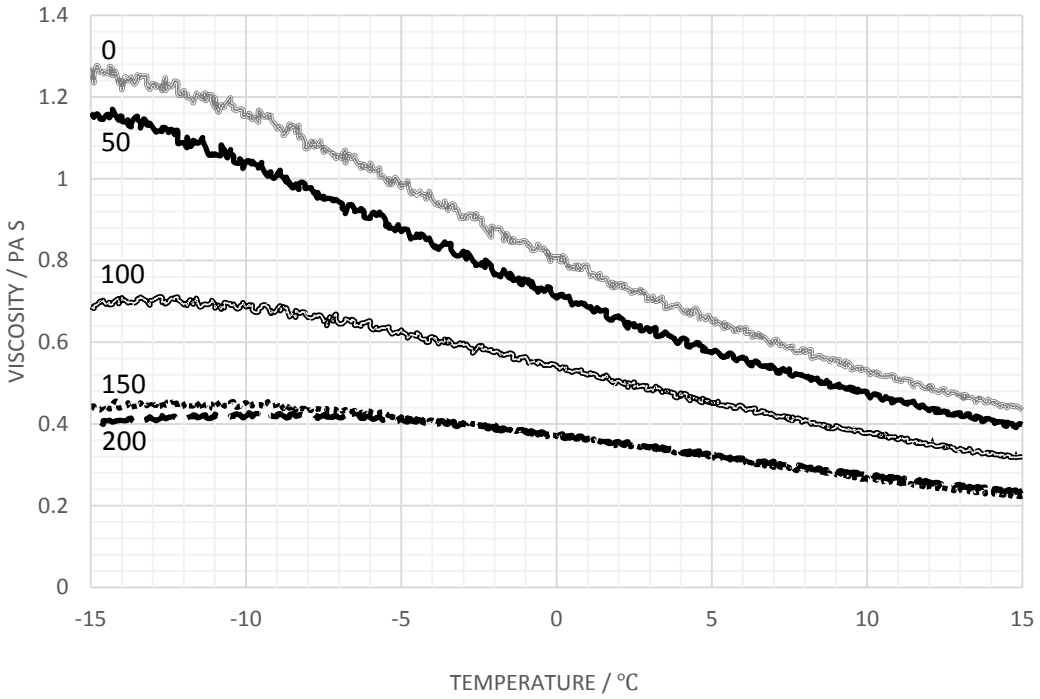

Figure 8.3 Viscosity variation with temperature for 75 wt% dilution of A4 with increasing Ca^{2+} level (in mg/L); shear stress 5 Pa.

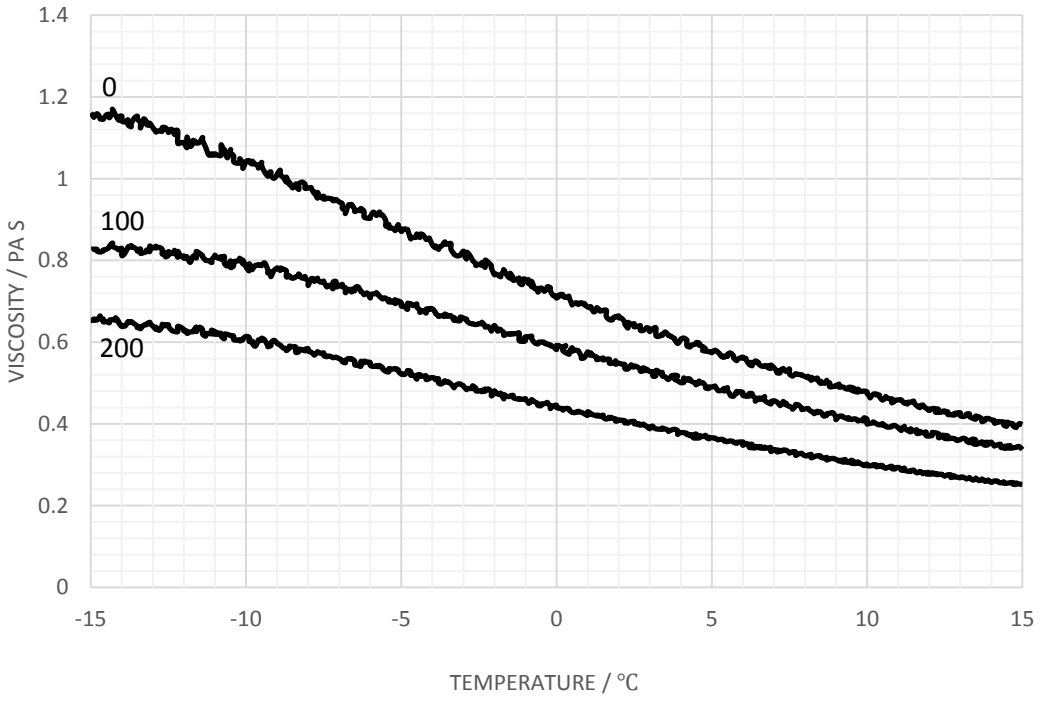

Figure 8.4 Viscosity variation with temperature for 75 wt% dilution of sample A4; diluting agents contain 50 mg/L Ca^{2+} and various level of Na^{+} in mg/L; shear stress 5 Pa.

While maintaining the calcium level at 50 mg L^{-1} and progressively increasing the sodium concentration to 100 mg L^{-1} and 200 mg L^{-1}, the viscosity of the fluid continued to drop (Figure 8.4). Such observation was expected.

Previous study suggests that in addition to reducing the thickening effect of Carbomer A in a aqueous system, divalent or trivalent ionisable salts are also capable of producing insoluble precipitate at sufficiently high levels [12]. A series of titration tests were carried out to determine the critical concentration of calcium to induce precipitates using 0.2M calcium acetate aqueous solution. As calcium ion content gradually increased, the appearance of the fluid changed from clear (phase I) to slight cloudy without visible precipitates (phase II), and then to cloudy liquid with visible precipitates at the bottom of the container (phase III), until total phase separation with clear layer of liquid on top of the precipitates layer (phase IV) (Figure 8.5). The critical concentrations of fluid A4 to transit from phase I to phase IV after calcium addition were listed below (Table 8.8). In the experiments of hard water dilution, the maximum calcium ion concentration was approximately 50 mg L^{-1} and no visible precipitate was formed during the dilution process.

Table 8.8 Critical concentration of phase transition for A4 after calcium ion addition

Phase Transition	**I to II**	**II to III**	**III to IV**
Ca^{2+} (mg/L)	103.9	152.0	430.8

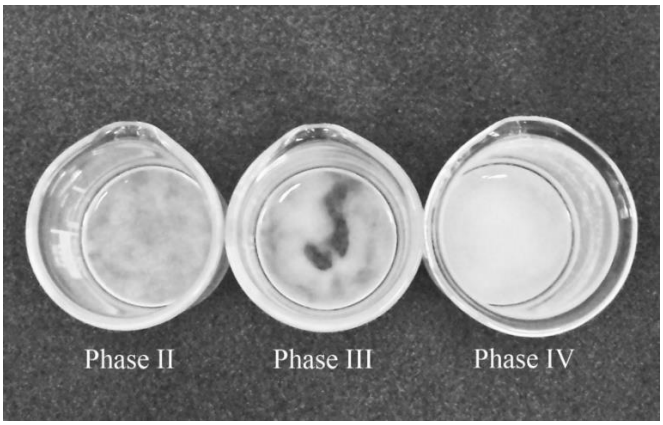

Figure 8.5 Phase transition of A4 after calcium ion addition.

8.3.2. Influence of Hard Water on Carbomer A:PVP Thickened Fluids

Previous study (Chapter 6) has examined the rheological properties of the Carbomer A/PVP thickened water/glycol mixtures. It has been established that, in terms of viscosity and aerodynamic performance, Carbomer A-PVP blends are capable of forming thickening agents for the purpose of de-/anti-icing fluid applications. In this set of experiments 6 samples were selected and diluted with AEA hard water, which contains Ca^{2+} 400±5 mg L^{-1} and Mg^{2+} 280±5 mg L^{-1}, by 75% and 50% wt/wt of its original concentration. Due to such high level of divalent cation content, Carbomer A-PVP blends thickened systems exhibited significant drop in viscosity (Figure 8.6) indicating loss in polymer molecule interactions. For a 50:50 wt/wt blend of Carbomer A and PVP 360k, AP102, the viscosity dropped approximately 80% on average between 15°C and -15°C when diluted by 75 wt% and even further when diluted to 50 wt%. As previously established (Chapter 6), PVP molecules interact with PAA molecules by a limited extent and the contribution of PVP towards overall viscosity is considered negligible. When high levels of divalent cations are introduced to the system a PAA molecules loses partial interactions due to reduced charge repulsion and is no longer able to retain the polymer network to thicken the water/glycol solution. By increasing the PAA content in the polymer thickening system from 50 wt% to 60 wt%, the ability of the fluid to maintain viscosities after dilution has been improved (Figure 8.7) however there is also an increased probability of forming insoluble precipitates which may eventually contribute to the gel residue after evaporation of solvent.

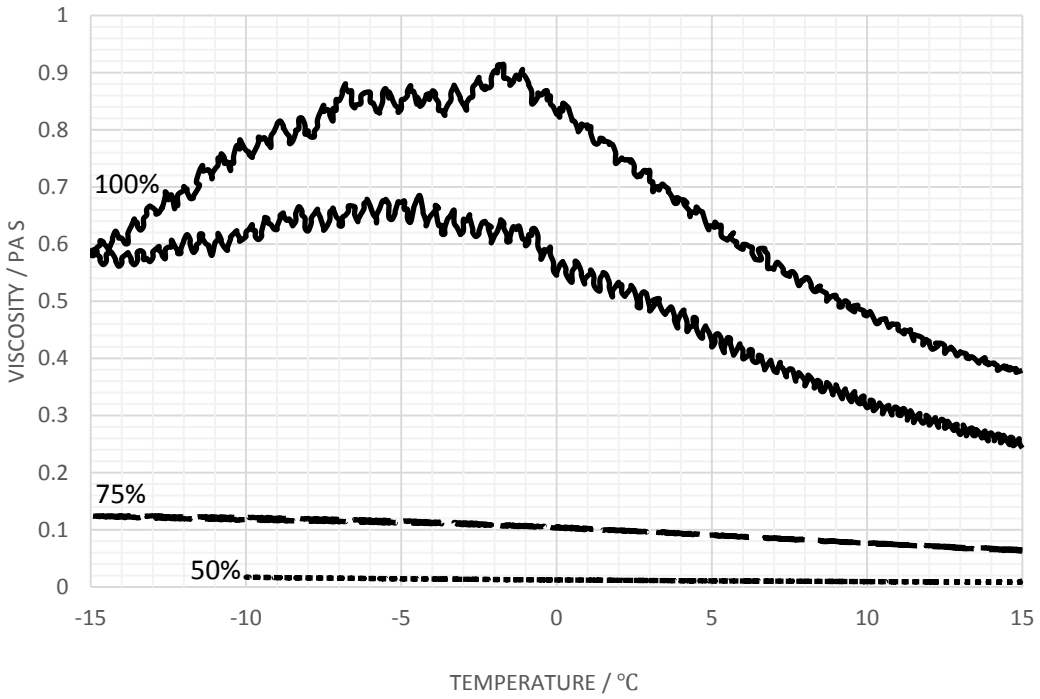

Figure 8.6 Viscosity variation with temperature for AP102, 100% with 75% and 50% wt/wt dilution with AEA hard water; shear stress 5 Pa.

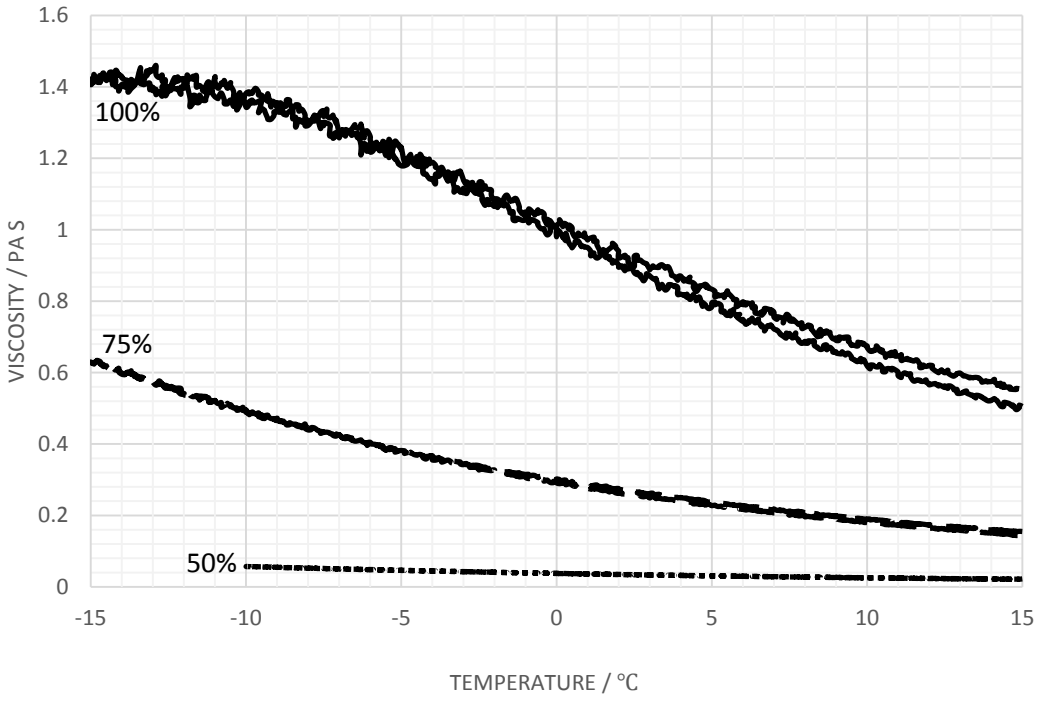

Figure 8.7 Viscosity variation with temperature for AP112, 100% with 75% and 50% wt/wt dilution with AEA hard water; shear stress 5 Pa.

Increasing the molecular weight of PVP to 700k while maintaining the weight ratio at 50:50 resulted in slight improvements in preserving viscosity after dilution (Figure 8.8) however compared to the pure Carbomer A thickened fluid the viscosity drop is significant which may greatly impact on the fluid holdover time. By increasing the content of PAA from 50 wt% to 60 wt% the viscosity was approximately 50% higher for both dilutions (for 75% dilution, 0.126 Pa s to 0.083 Pa s at 15°C and 0.358 Pa s to 0.234 Pa s at -15°C; for 50% dilution, 0.017 Pa s to 0.011 Pa s at 15°C and 0.037 Pa s to 0.024 Pa s at -15°C) (Figure 8.9). Such an observation was consistent with Carbomer A and PVP 360k blends.

WSET measurements were carried out for the four sample fluids and the results are shown in Table 8.9. After shearing process in the lab, which was intended to simulate the shear experienced by fluids when ejected through a nozzle, slight hold-over time reductions occurred. When diluted with AEA hard water, the hold-over time for each sample fluid was significantly shortened. Such observations remain consistent with the results from rheology measurements. Despite the fact that during WSET measurements fluid experiences lower levels of shear stress and continuous dilution processes compared to rheology measurements, the thickening efficiencies of Carbomer A-PVP blends were significantly influenced by hard water dilution.

Table 8.9 Hold-over time of four Carbomer A:PVP samples

Sample No.		AP102	AP112	AP202	AP212
Composition		PAA/PVP_{360K} 50:50	PAA/PVP_{360K} 60:40	PAA/PVP_{700K} 50:50	PAA/PVP_{700K} 60:40
Hold-over Time	100%	32m 21s	37m 36s	22m 15s	31m 36s
	100% Shear	29m 45s	35m 32s	20m 25s	29m 24s
	75% Shear	10m 18s	15m 29s	5m 23s	11m 19s
	50% Shear	1m 51s	2m 39s	N/A	0m 49s

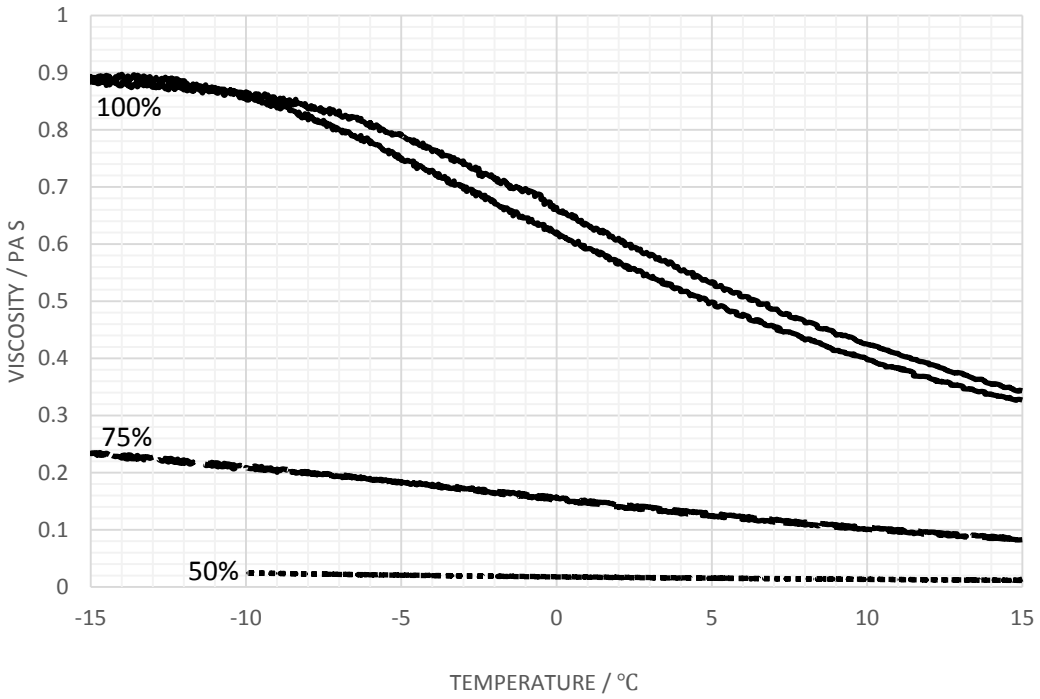

Figure 8.8 Viscosity variation with temperature for AP202, 100% with 75% and 50% wt/wt dilution with AEA hard water; shear stress 5 Pa.

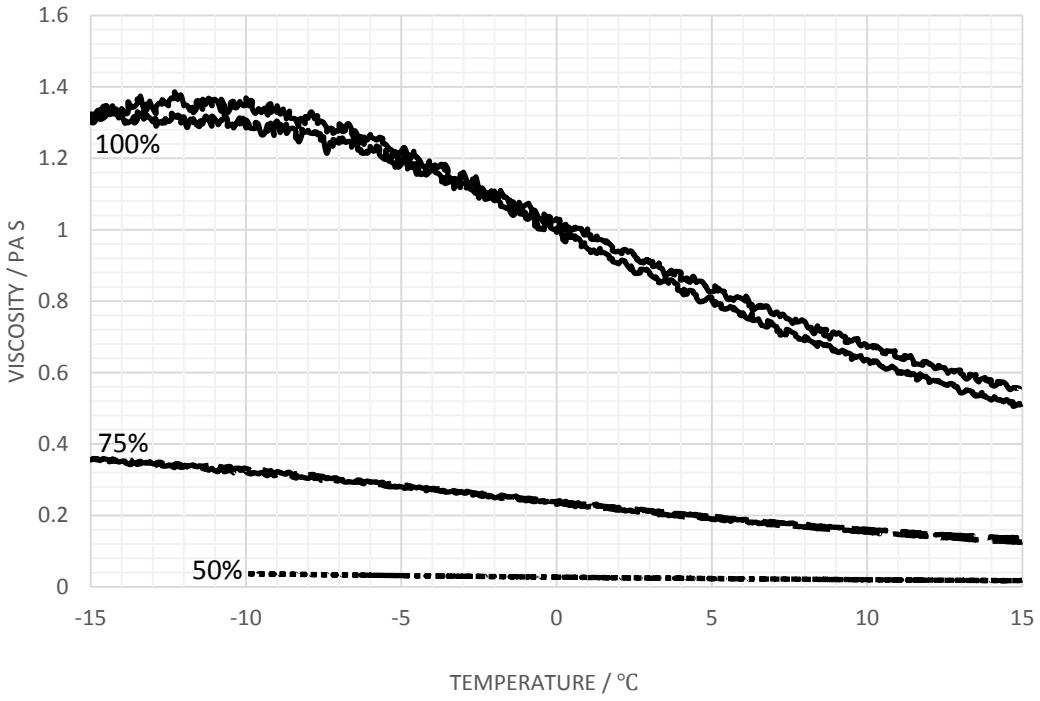

Figure 8.9 Viscosity variation with temperature for AP212, 100% with 75% and 50% wt/wt dilution with AEA hard water; shear stress 5 Pa.

Increasing the molecular weight of PVP polymer further does not promote a linear viscosity increment in the fluid. Figure 8.10 is the viscosity variation with temperature for 75 wt% dilutions of all four PVP polymers blended with Carbomer A by 50:50 wt/wt. As molecular weight of PVP polymer increases from 360k, the viscosity level also increased for 700k and 1,300k PVP however for PVP polymer with 4,000k molecular weight the viscosity level decreased indicating a lower extent of binding between carboxylic groups of PAA and carbonyl groups of PVP. This observation was consistent with the result of rheology experiments with 100% fluids which were presented in Chapter 6.

Table 8.10 shows the critical concentration of phase transitions after calcium ion addition to sample AP102 (50:50 Carbomer A/PVP 360k blend with 0.015 wt% NaCl). Compared to pure Carbomer A-thickened fluid, the tolerance of Carbomer A-PVP blend against insoluble precipitate formation has been increased. In this section of hard water dilution tests, at this concentration of divalent cations, no visible precipitates were formed in dilutions.

Table 8.10 Critical concentration of phase transition for AP102 after calcium ion addition

Phase Transition	I to II	II to III	III to IV
Ca^{2+} (mg L^{-1})	40.54	248.32	506.77

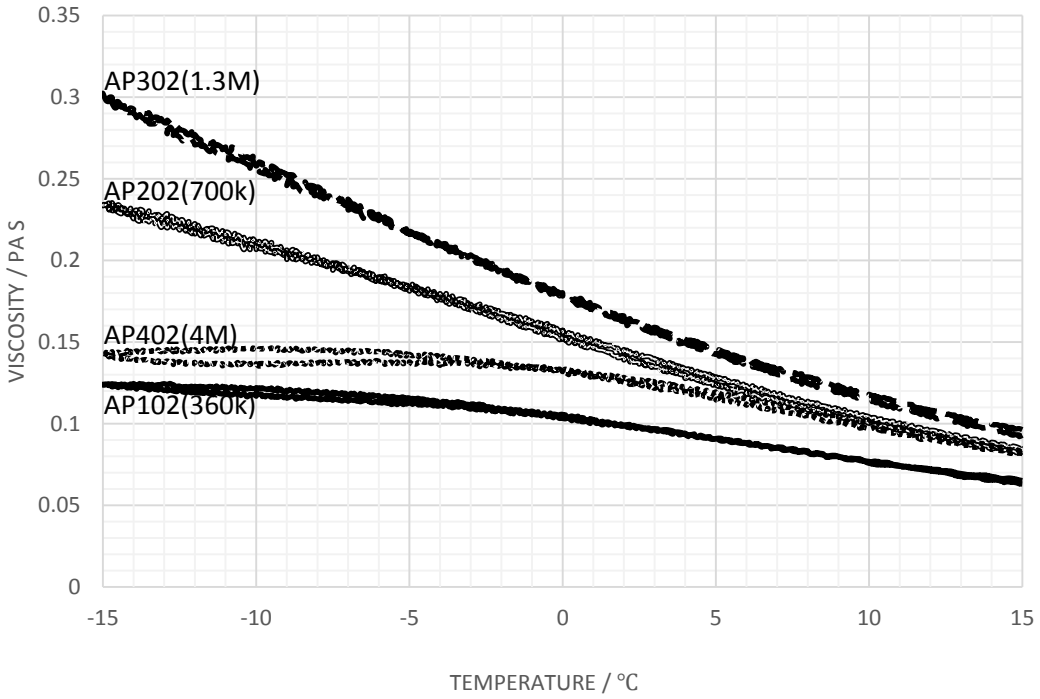

Figure 8.10 Viscosity variation with temperature for 75 wt% dilution of 50:50 wt/wt PVP:Carbomer A blend series; shear stress 5 Pa.

8.3.3. Influence of Potassium Formate

Figure 8.11 shows the viscosity variation with temperature for sample fluids with the same electrolyte concentration, 0.030 wt%, at 5 Pa and 10 Pa of applied shear stress. At 5 Pa of shear stress, the viscosity of A2K (with potassium formate) increased from approximately 1.15 Pa s at 15°C to a peak value of 1.97 Pa s at -3.1°C and then decreased to 1.45 Pa s at -15°C. The viscosity is considerably lower than the same Carbomer A-thickened fluid with sodium addition however the 'peak' location for both fluids appeared at nearly identical temperature. The same phenomenon was observed when the applied shear stress was increased to 10 Pa. Similar behaviour was also exhibited for samples with 0.060 wt% electrolyte addition (Figure 8.12). Since potassium belongs to the same main group as sodium, it was expected that it would contribute to reduction in the thickening effect of Carbomer A similar to sodium; and due to the larger ionic radius

of K^+ and binding power, potassium formate has greater ability to suppress the viscosity level compared to sodium chloride. If sodium chloride was partially replaced by potassium formate, for example, the sample A5K which contains 0.030 wt% of Na^+ and 0.045 wt% of K^+ compared to A5 which contains 0.075 wt% of Na^+ (Figure 8.13), the Carbomer thickened fluid continued to exhibit the same rheological characteristics in terms of shear-thinning behaviour and viscosity 'peak' under steady shear. No evidence was found which indicated that potassium formate is able to alter the rheological behaviour of the fluid in major aspects other than its enhanced ability to generally suppress the viscosity level.

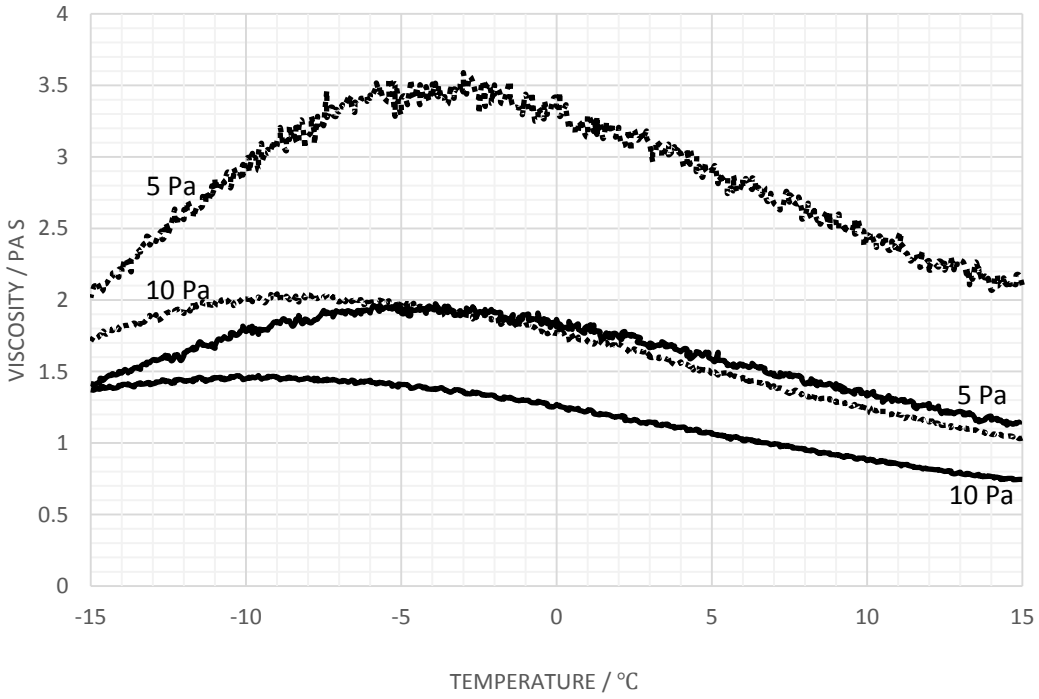

Figure 8.11 Viscosity variation with temperature for sample A2K (–), in comparison with A2 (…); shear stresses 5 Pa and 10 Pa.

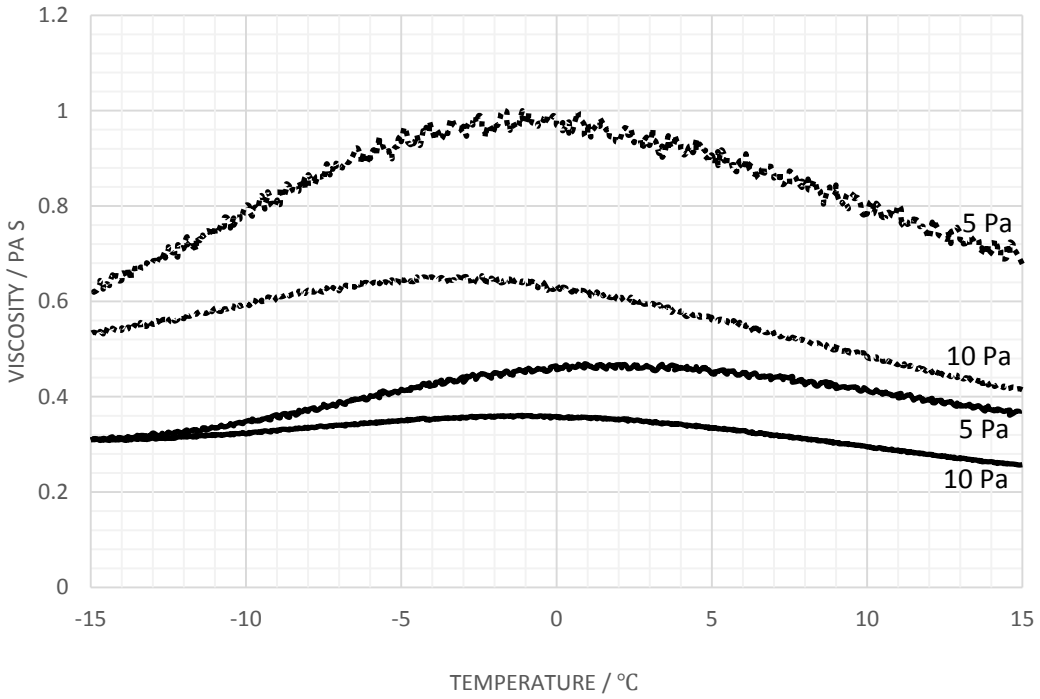

Figure 8.12 Viscosity variation with temperature for sample A4K (–), in comparison with A4 (…); shear stresses 5 Pa and 10 Pa.

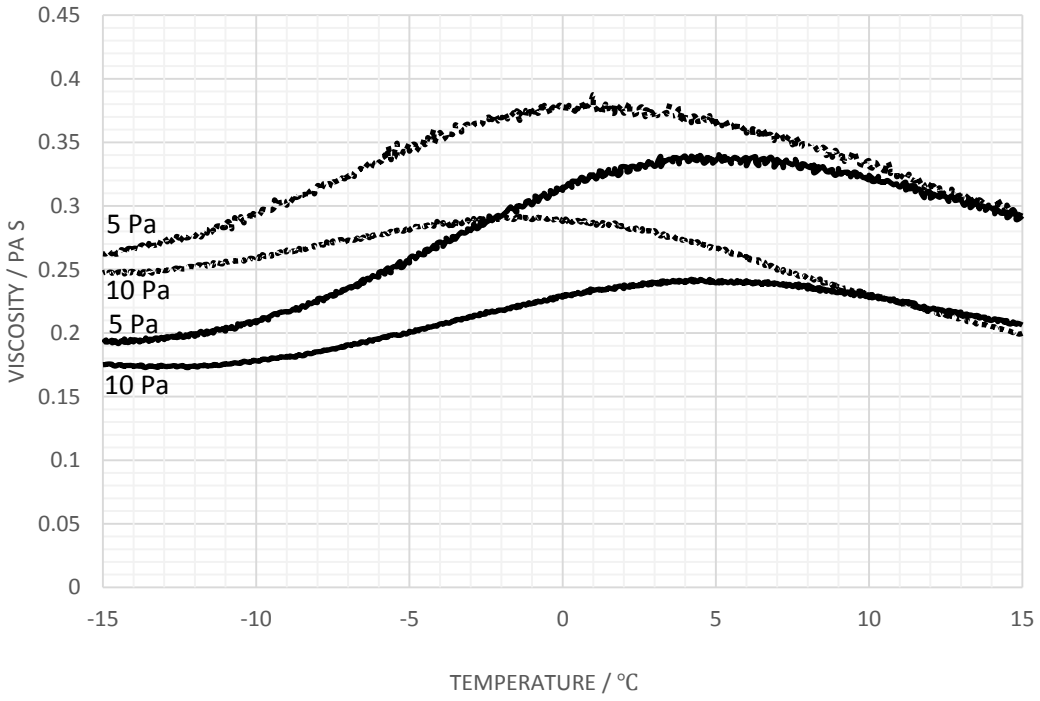

Figure 8.13 Viscosity variation with temperature for sample A5K (–), in comparison with A5 (…); shear stresses 5 Pa and 10 Pa.

8.4. Conclusions

Various measurements were carried out to investigate the influence of potassium and calcium cations on de-/anti-icing fluids, particularly in terms of rheological behaviour.

1) Diluting fluids with hard water will alter the rheological properties of the fluids. Divalent ionisable salts will cause loss of interactions within or between polymer molecules and hence the diminished viscosity level. Through bridging carboxylic groups divalent cations, such as Ca^{2+} and Mg^{2+}, promote phase separation and formation of a gel-like structure, although no visible precipitates or solid gels were observed in the measurements.

2) Addition of PVP reduced the probability of forming insoluble precipitates when thickened fluids were diluted with hard water, however due to limited extent of interaction with PAA and lower viscosity, Carbomer A-PVP blends, compared to pure Carbomer A thickeners, appeared to be more vulnerable to hard water in terms of retaining the extent of the polymer network and maintaining fluid viscosity.

3) Potassium cations appear to have higher binding power than sodium cations. Therefore the ability of potassium to suppress fluid viscosities is stronger at the same weight concentration. However no evidence suggests that potassium formate is capable of inducing gel-like structures formed in thickened fluids.

8.5. References

1. Ross, F., *Aircraft De-/Anti-Icer*, USPTO, Editor 2011, Kilfrost Limited: U.S.
2. Jenkins, R.D., Bassett, D.R., Lightfoot, R.H., and Boluk, M.Y., *Aircraft anti-icing fluids*, USPTO, Editor 1995, Union Carbide Chemicals & Plastics Technology Corporation: U.S.
3. Joseph Zhen Hu, John Wakelin, and Wiesenfeld, A., *Deicing and anti-icing composition for aircraft*, USPTO, Editor 1998, Octagon Process Inc.: U.S.
4. Kotker, D., *Deicing/Anti-Icing Fluids*, in *Aero*1999, Boeing Commercial Airplanes Group: Seattle, WA, USA.
5. Laforte, J.L., Louchez, P., Bouchard, G., and Ma, F., *A Facility to Evaluate Performance of Aircraft Ground De-Antiicing Fluids Subjected to Freezing Rain.* Cold Regions Science and Technology, 1990. **18**(2): pp. 161-171.
6. Laforte, J.L., Louchez, P.R., and Bouchard, G., *Cold and Humid Environment Simulation for De-Anti-Icing Fluids Evaluation.* Cold Regions Science and Technology, 1992. **20**(2): pp. 195-206.
7. Laforte, J.L., Louchez, P., and Bernardin, S., *Experimental Holdover Time Evaluation and Prediction of Type III Anti-Icing Fluid*, 1994, Federal Aviation Administration Technical Center: US Department of Transportation.
8. Louchez, P.R., Laforte, J.L., Bouchard, G., and Farzaneh, M., *Laboratory Evaluation of Aircraft Ground De Antiicing Products*, in *Proceedings of the Fourth*, Chung, J.S., Karal, K., and Koteryama, W., Editors. 1994, International Society Offshore& Polar Engineers: Cupertino. pp. 479-483.
9. SAE, *SAE AMS1428 Fluid, Aircraft Deicing/Anti-Icing, Non-Newtonian (Pseudoplastic), SAE Types II, III, and IV*, 2010, SAE International.
10. SAE, *SAE AS5901B Water Spray and High Humidity Endurance Test Methods for SAE AMS1424 and SAE AMS1428 Aircraft Deicing/Anti-icing Fluids*, 2010, SAE International.
11. Ikegami, A. and Imai, N., *Precipitation of polyelectrolytes by salts.* Journal of Polymer Science, 1962. **56**(163): pp. 133-152.
12. Lubrizol Advanced Materials, I., *Minimizing Influence of Salts In Presence of Carbopol Polymers*, in *TDS-54*2002: Cleveland, Ohio.
13. Hassan, Y., El Halim, A.O.A., Razaqpur, A.G., Bekheet, W., and Farha, M.H., *Effects of runway deicers on pavement materials and mixes: Comparison with road salt.* Journal of Transportation Engineering-Asce, 2002. **128**(4): pp. 385-391.

14. Switzenbaum, M.S., Veltman, S., Mericas, D., Wagoner, B., and Schoenberg, T., *Best management practices for airport deicing stormwater.* Chemosphere, 2001. **43**(8): pp. 1051-1062.

15. van der Aa, M., *Classification of mineral water types and comparison with drinking water standards.* Environmental Geology, 2003. **44**(5): pp. 554-563.

16. Kožíšek, F., *Health significance of drinking water calcium and magnesium.* National Institute of Public Health Czech Republic (http://wwwszucz/chzp/voda/pdf/hardness.pdf), 2003.

17. Tang, K.-w., Hou, J., and Tang, Y., *Assessment of groundwater quality in China: I . Hydrochemical characteristics of groundwater in plain area.* Water Resources Protection, 2006. **22**(2): pp. 5.

18. Hess, B. and van der Vegt, N.F.A., *Cation specific binding with protein surface charges.* Proceedings of the National Academy of Sciences, 2009. **106**(32): pp. 13296-13300.

19. Tang, C.Y. and Allen, H.C., *Ionic Binding of Na+ versus K+ to the Carboxylic Acid Headgroup of Palmitic Acid Monolayers Studied by Vibrational Sum Frequency Generation Spectroscopy†.* The Journal of Physical Chemistry A, 2009. **113**(26): pp. 7383-7393.

20. Mancinelli, R., Botti, A., Bruni, F., Ricci, M.A., and Soper, A.K., *Hydration of Sodium, Potassium, and Chloride Ions in Solution and the Concept of Structure Maker/Breaker.* The Journal of Physical Chemistry B, 2007. **111**(48): pp. 13570-13577.

21. Bromberg, L., Temchenko, M., Moeser, G.D., and Hatton, T.A., *Thermodynamics of temperature-sensitive polyether-modified poly(acrylic acid) microgels.* Langmuir, 2004. **20**(14): pp. 5683-5692.

22. Dobrynin, A.V., *Phase Diagram of Solutions of Associative Polymers.* Macromolecules, 2004. **37**(10): pp. 3881-3893.

23. Miquelard-Garnier, G., Demoures, S., Creton, C., and Hourdet, D., *Synthesis and rheological behavior of new hydrophobically modified hydrogels with tunable properties.* Macromolecules, 2006. **39**(23): pp. 8128-8139

Chapter 9. Conclusion and Future Works

9.1. General Conclusions

This study aimed to investigate the potential of utilizing improved formulae of thickening agents for ground aircraft de-/anti-icing fluids to reduce the gel residue issue of the conventional fluids. Given that poly(acrylic acid) based co-polymers and homo-polymers have been widely used in aviation industry as polymer thickeners specifically for Type II and Type IV fluids for many years and have proved successful, the primary target of this study has been to understand the relationship between the polymer structures of PAA and the rheological properties of the fluids it is used to thicken.

After a general literature review on de-icing operation, analysis of the de-icing fluid specifications, and particularly the rheological characteristics of general PAA polymer, the study on two specific PAA based polymers, namely Carbomer A and Carbomer B, began with characterisation of both polymers using various techniques. With FTIR and FT-NMR analyses, the compositions and structures of both polymers have been investigated. The intrinsic viscosity measurements provided information on polymer sizes and respective molecular masses. Rheological profiles of both polymers were obtained by different types of rheology measurements on polymer aqueous solutions.

Derived from a combined reptation model, relaxation of the chains by slippage or loop relaxation, and normal Rouse dynamics, a mathematical model was developed using the background information obtained from previous experiments of characterisation and rheology. This model was then utilized to predict the rheological behaviours of Carbomer A thickened water/glycol mixtures at different temperatures.

Extensive rheology experiments were carried out to investigate the influences of electrolyte addition on Carbomer thickened water/glycol mixtures in terms of the rheological properties. The effect of electrolyte suppressing fluid viscosity has been

important to de-icing operation given the specific requirements on the fluids, and is significant due to its ability to block the bonding of neighbouring carboxylic acid groups. Wind tunnel tests, aiming to measure the boundary layer displacement thickness which reflects the aerodynamic fluidity of the fluid, were also conducted to confirm the consistency between the BLDT and viscosity values. A series of criteria to evaluate the performance of a polymer-thickened fluid have been established.

Studies have confirmed that electrolyte additions are able to induce conformation and structure changes of the PAA polymer chains which could potentially cause the formation of gel-like structures; and the addition is not only performed intentionally during fluid production, but also occasionally happens during field use through local water dilution. It had been expected that PVP, as a widely used, environmentally neutral polymer material, when blended with PAA, could effectively block the interactions between PAA molecules and divalent cations and thus reduce the possibility of forming insoluble gel while achieving desirable pseudoplastic characteristics and performing adequately as thickening agents of de-/anti-icing fluids. Therefore a series of rheological experiments were carried out on blends of different molecular weight PVP polymers with PAA polymers in different mixing ratios.

The rheological behaviour of PVP/PAA mixtures is complex. Various factors influence the viscosity of the thickened fluid, including the blending ratio of both polymers, the size of the polymer chains, and the concentration of electrolyte, which all together contribute to the pattern of interactions between polymer molecules within the fluid system. This study has indicated that by adopting a systematic approach to adjusting the defining parameters, it is possible to achieve the desirable rheological properties found in PAA thickened fluids while reducing the possibility of forming insoluble gel.

9.2. Suggestion on Future Work

1) To further investigate the hysteresis observed in certain systems and their sensitivities to thermal history.

2) To further investigate the interactions between PVP and PAA molecules and the relationships between polymer interactions and the rheological behaviours of the fluids, with the purpose of developing a systematic approach to adjust the formulating of thickening agents.

3) To further study the polymer interaction with the solvent system and adapt the mathematical model to a broader range of application.

4) A high level of shear commonly occurs during the production and application of the fluids and has significant impact on them in various ways. Quantitative analyses would be helpful in predicting the rheological behaviour of the fluids.

Appendix A. Modelling Program

The following program was composed using Parametric Technology Corporation (PTC) Mathcad® 15.0.

Frequency Sweep Calculation (with expanded frequency range)

Define parameters:

Start frequency..... $\omega_1 := 10^{-5}$ rad/s $\log(\omega_1) = -5$

End frequency..... $\omega_2 := 10^{8}$ rad/s $\log(\omega_2) = 8$

Fraction interal..... $n_1 := 0.1$

Logarithmic frequency step..... $f_\omega := \log(\omega_1), \log(\omega_1) + n_1 .. \log(\omega_2) =$

-5
-4.9
-4.8
-4.7
-4.6
-4.5
-4.4
-4.3
-4.2
-4.1
-4
-3.9
-3.8
-3.7
-3.6
...

Sweep frequency step..... $\omega := 10^{f_\omega}$

Molecular Weight Distribution

Define parameters:

Molecular weight at the peak of the molar frequency distribution.....

$$M_g := 1 \cdot 10^3 \quad \text{kg/mol}$$

Standard deviation of log-normal MWD..... $\sigma := 0.316$

Mean value of log-normal MWD of molar frequency.....

$$\mu := \log(M_g)$$

Fraction intervel for MWD..... $n_2 := 0.1$

Integral factor for MWD.....

$$N_2 := \frac{2}{n_2}$$

So that the molar frequencies can be evenly distributed through two decades.....

$\mu_f := \mu - 1, \mu - 1 + n_2 .. \mu + 1 =$

2
2.1
2.2
2.3
2.4
2.5
2.6
2.7
2.8
2.9
3
3.1
3.2
3.3
3.4
...

Hence the MW in the *i*th fraction of distribution.....

$$M_i := 10^{\mu_f}$$

And the molar frequency in the *i*th fraction of distribution.....

$$f_i := \frac{1}{\sigma \cdot \sqrt{2\pi}} \cdot e^{\frac{-(\mu - \mu_f)^2}{2\sigma^2}}$$

The number-average molecular weight is.....

$$M_n := \frac{\sum_{i=0}^{N_2} \left(f_{i_i} \cdot M_{i_i} \right)}{\sum_{i=0}^{N_2} f_{i_i}}$$

Input variables

Conditions - water/glycol based solution at -10 degree Celsius

Critical molecular weight of entanglement..... $M_c := 30$ kg/mol

Molar mass of a rigid entity..... $M_d := 5 \cdot M_c$ kg /mol

Molecular weight of a monomer unit..... $M_{mon} := 72 \cdot 10^{-3}$ kg/mol

Molar mass of a Kuhn unit..... $M_k := 12 \cdot M_{mon}$ kg/mol

Total mode number..... $N := \text{floor}\left(\frac{M_n}{M_k}\right)$

Number of entanglement units in a molecule..... $N_c := \text{floor}\left(\frac{M_n}{M_c}\right)$

Number of rigid units in a molecule..... $N_d := \text{floor}\left(\frac{M_n}{M_d}\right)$

Number of segments between entanglement points.....

$N_e := \text{floor}\left(\frac{M_c}{M_k}\right)$

Monomer length..... $b := 1.54 \cdot 10^{-10}$ m

Kuhn segment length..... $l_k := 12 \cdot b$

Tube diameter..... $a := b \cdot \frac{M_d}{M_{mon}}$

Mode number (initial)..... $p := 1$

Solvent viscosity..... $\eta_s := 0.0315$ Pa s

Zero shear rate viscosity of solution..... $\eta_0 := 0.72$ Pa s

Equilibrium viscosity of solution..... $\eta_e := 1500$ Pa s

Solution density..... $\rho := 1050$ kg/m^3

Temperature..... $T := 263.15$ K

Universal gas constant..... $R := 8.314$ J mol^{-1} K^{-1}

Boltzmann constant..... $k := 1.3806503 \cdot 10^{-23}$ m^2 kg s^{-2} K^{-1}

Avogadro's number..... $N_A := 6.0221415 \cdot 10^{23}$ mol^{-1}

Bead friction coefficient for Rouse motion..... $\zeta_r := \frac{36 \cdot \eta_s \cdot M_k^{\,2}}{\rho \cdot M_c \cdot N_A \cdot l_k^{\,2}}$

Bead friction coefficient for reptation motion..... $\zeta_d := \frac{36 \cdot \eta_s \cdot M_c^{\,2}}{\rho \cdot M_n \cdot N_A \cdot a^2}$

Scaling factors.....

Rouse motion - $c_r := 6600$

Slip-coil motion - $z_1 := 0.016$

Reptation - $z_2 := 1 - z_1$

Complexation - $h_1 := 0.9$ $h_2 := 1 - h_1$

Relaxation times.....

Rouse - $\tau_r := \frac{6 \cdot \eta_0 \cdot M_c}{\pi^2 \cdot \rho \cdot R \cdot T} \cdot c_r$

Slip-coil motion - $\tau_b := \frac{\zeta_r \cdot l_k^{\,2} \cdot N_e^{\,2}}{3 \cdot \pi^2 \cdot k \cdot T} \cdot N^2$

Complexed reptation motion - $\tau_{d1} := \frac{1}{\pi^2} \cdot \frac{\zeta_d \cdot a^2 \cdot N_e}{k \cdot T} \cdot \left[N \cdot \left(1 + h_1\right)\right]^3$

Un-complexed reptation motion - $\tau_{d2} := \frac{1}{\pi^2} \cdot \frac{\zeta_d \cdot a^2 \cdot N_e}{k \cdot T} \cdot N^3$

Viscosity.....

$$\eta_1(\omega) := \eta_s + \frac{6(\eta_0 - \eta_s)}{\pi^2} \cdot \sum_{p=1}^{N_c} \frac{p^2}{p^4 + \omega^2 \cdot \tau_r^2} + \frac{1}{2} \cdot z_1 \cdot \frac{8(\eta_e - \eta_0)}{\pi^2} \cdot \sum_{p=1}^{N_e} \frac{p^2}{p^4 + \omega^2 \cdot \tau_b^2}$$
$$+ \frac{1}{2} \cdot z_2 \cdot \left[\frac{8(\eta_e - \eta_0) \cdot h_1}{\pi^2} \cdot \sum_{p=1}^{N_d} \frac{p^2}{p^4 + \omega^2 \cdot \tau_{d1}^2} + \frac{8(\eta_e - \eta_0) \cdot h_2}{\pi^2} \cdot \sum_{p=1}^{N_e} \frac{p^2}{p^4 + \omega^2 \cdot \tau_{d2}^2} \right]$$

Program parameters are adjusted accordingly to fit the conditions specified in Section 5.3.3. The fluid sample for simulation is pure Carbomer A-thickened propylene glycol/water mixture with 0.30 g dL^{-1} of polymer concentration and 0.060 wt% of NaCl addition, and was measured at -10°C. The model-fitting result is shown in Figure 5.17.

As stated in Chapter 4 and Chapter 5, the model is very sensitive to the interaction scaling parameters, z_1 and h_1, which indicates the contribution of 'slip-coil' motion and degree of complexation, respectively. Figure 5.17 showed that in order to fit the experiment data, the scaling factors had to be adjusted to the values of 0.016 for z_1 and 0.9 for h_1.

In the following figure (A-Fig 1), the degree of complexation, h_1, remains unchanged at 0.9, by changing the value of the scaling factor of 'slip-coil' from 0.016 to 0.032 and 0.16, the viscosity response at frequency range between 10^{-2} and 10^{2} rad s^{-1} changed significantly. Similarly, the change in h_1 also influenced the viscosity response (A-Fig 2). When z_1 remains at 0.016, changing h_1 from 0.9 to 0.8 and 0.5 resulted significant viscosity change at frequency range between 10^{-2} and 1 rad s^{-1}.

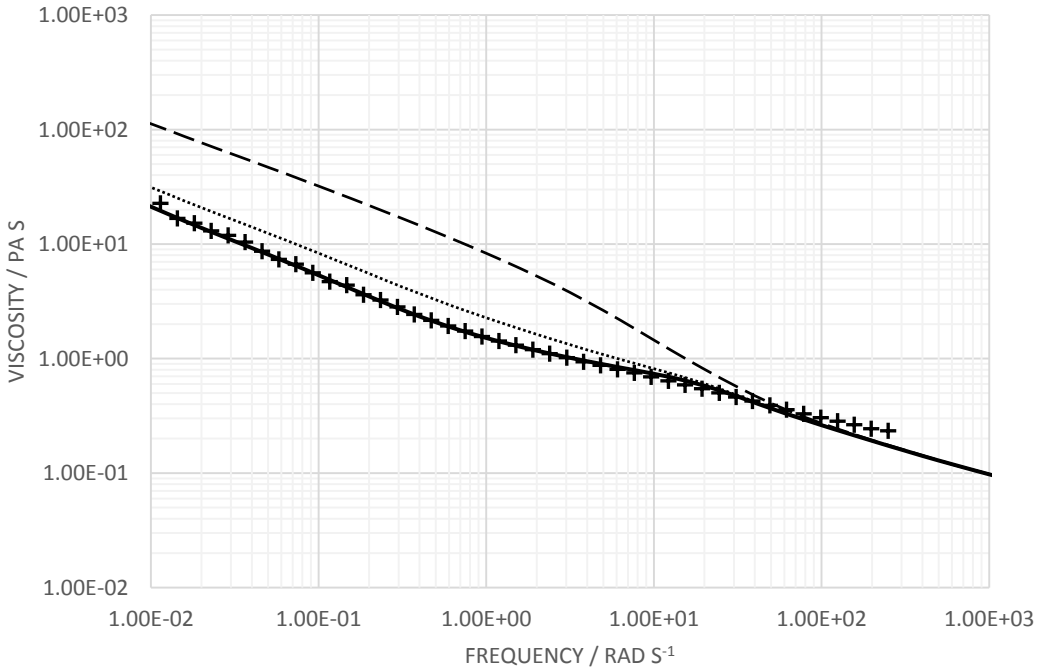

A-Fig 1 Model fitting for Carbomer A solution A4 at -10°C, h_1=0.9. Lines are (+) experimental; (—) z_1=0.016; (...) z_1=0.032; (––) z_1=0.16.

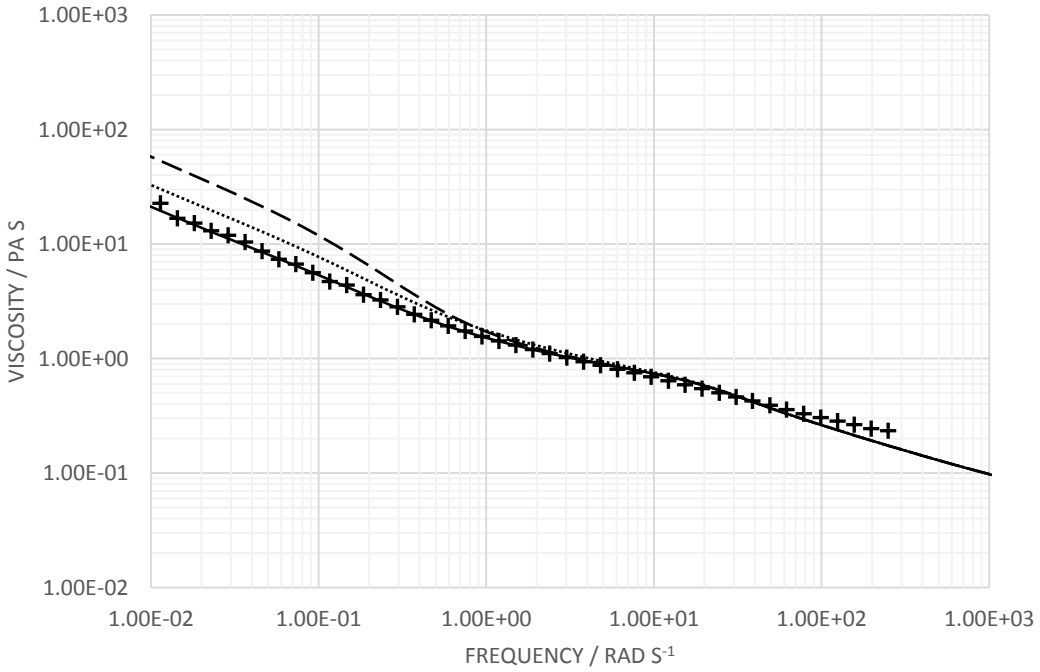

A-Fig 2 Model fitting for Carbomer A solution A4 at -10°C, z_1=0.16. Lines are (+) experimental; (—) h_1=0.9; (...) h_1=0.8; (––) h_1=0.5.

Appendix B. Supplementary Data for Chapter 5

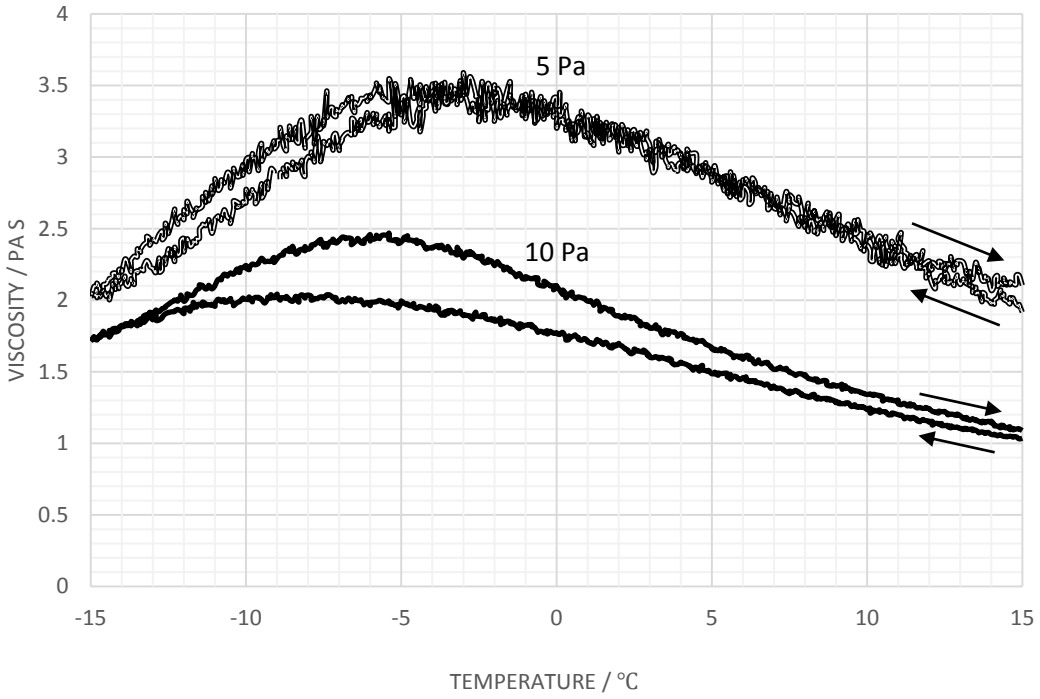

B-Fig 1 Viscosity variation with temperature plots for A2, applied shear stresses 5 and 10 Pa.

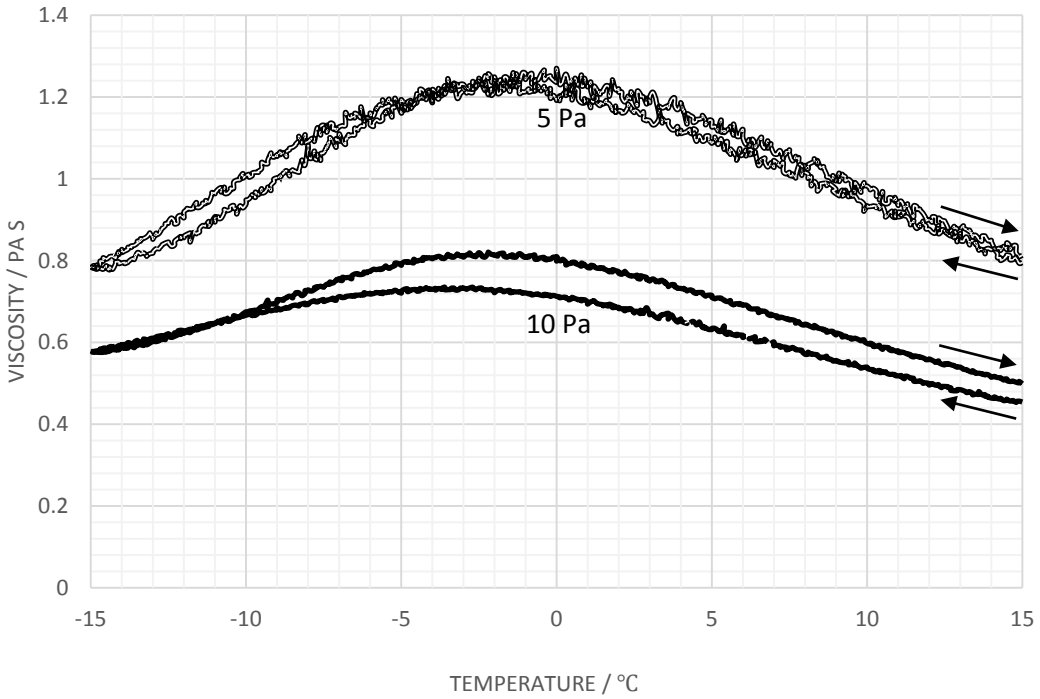

B-Fig 2 Viscosity variation with temperature plots for A3, applied shear stresses 5 and 10 Pa.

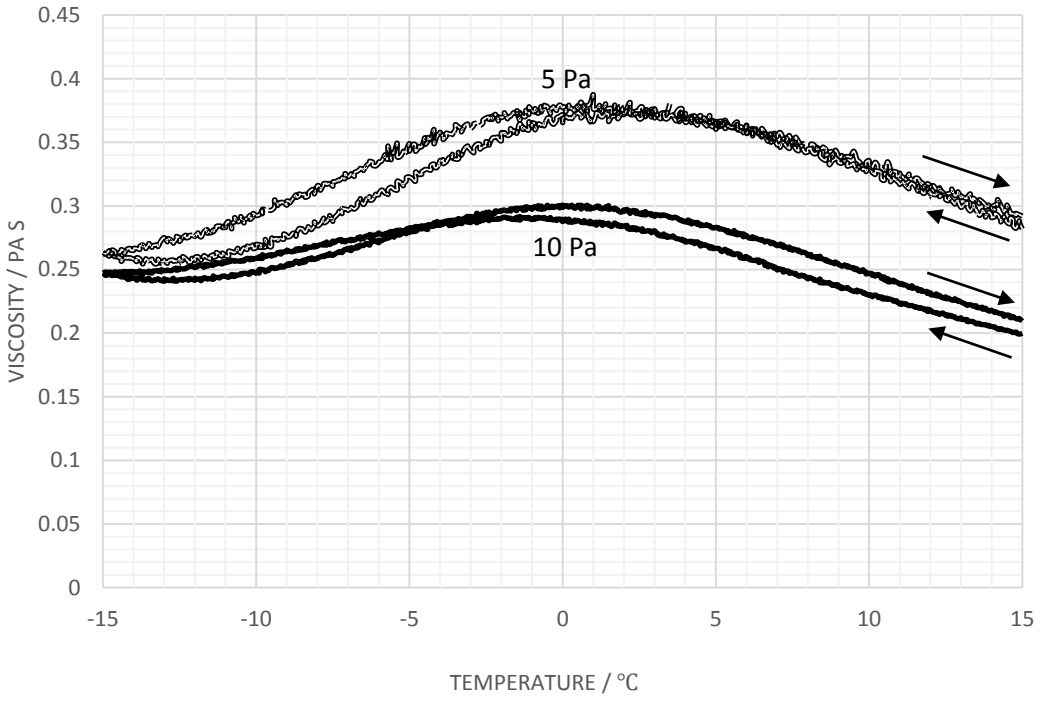

B-Fig 3 Viscosity variation with temperature plots for A5, applied shear stresses 5 and 10 Pa.

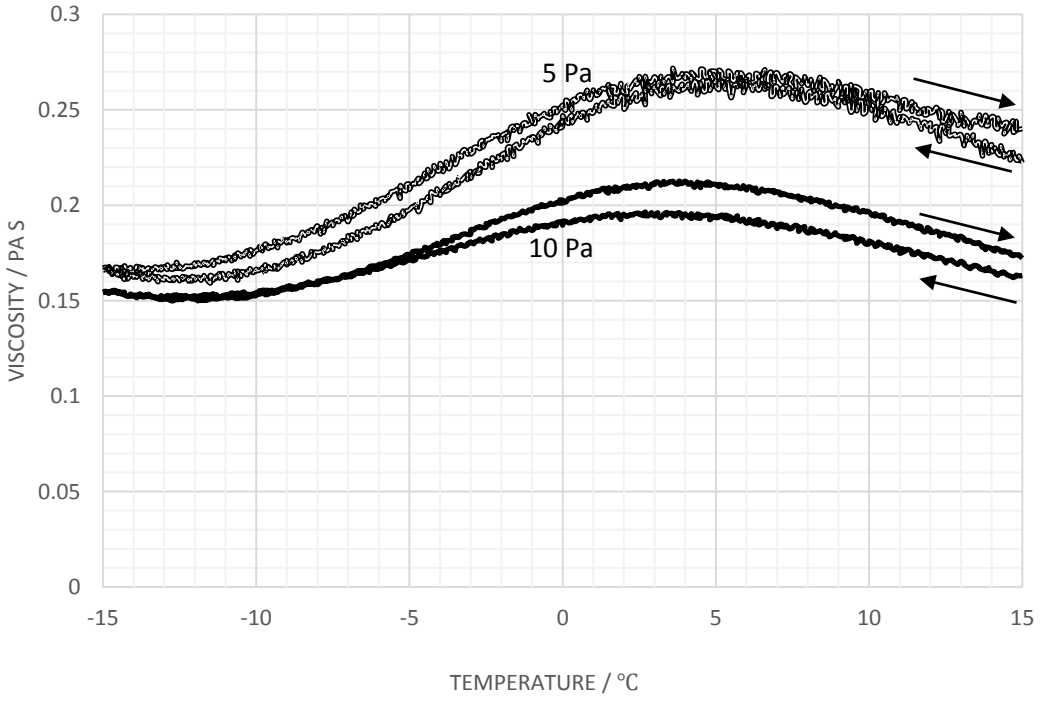

B-Fig 4 Viscosity variation with temperature plots for A6, applied shear stresses 5 and 10 Pa.

Appendix C. Supplementary Data for Chapter 6

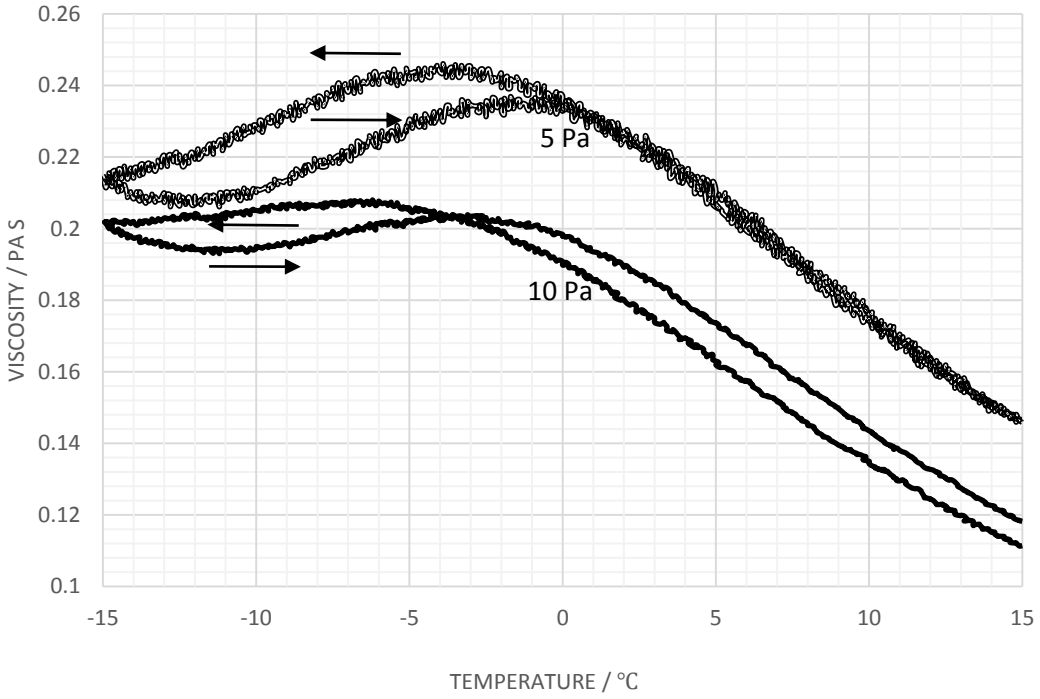

C-Fig 1 Viscosity variation with temperature plots for AP103, applied shear stresses 5 and 10 Pa.

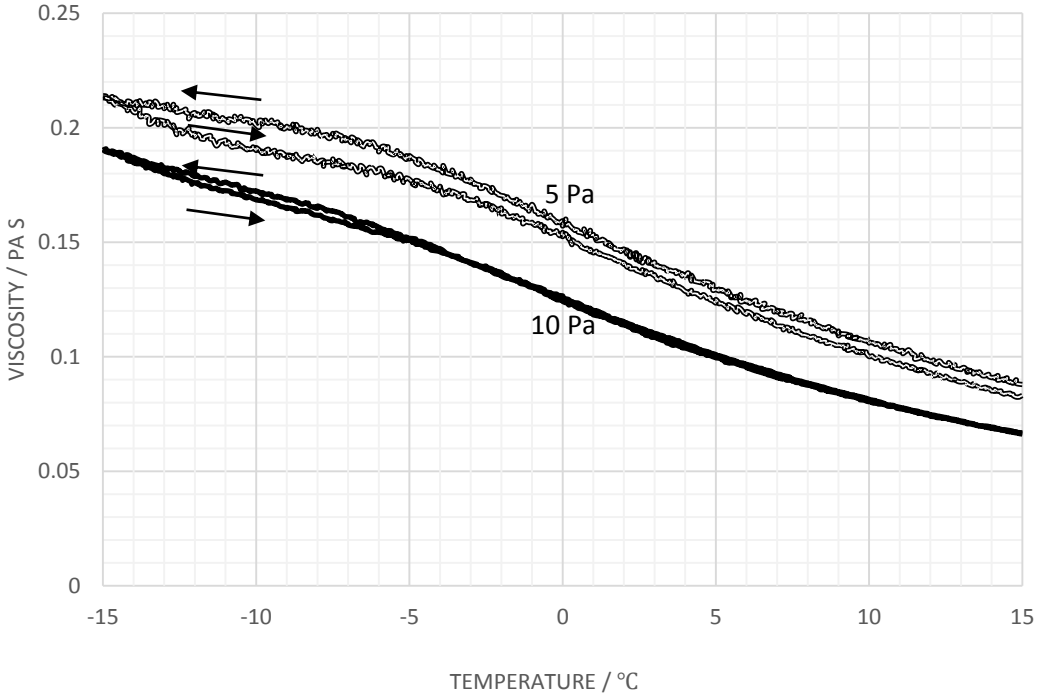

C-Fig 2 Viscosity variation with temperature plots for AP104, applied shear stresses 5 and 10 Pa.

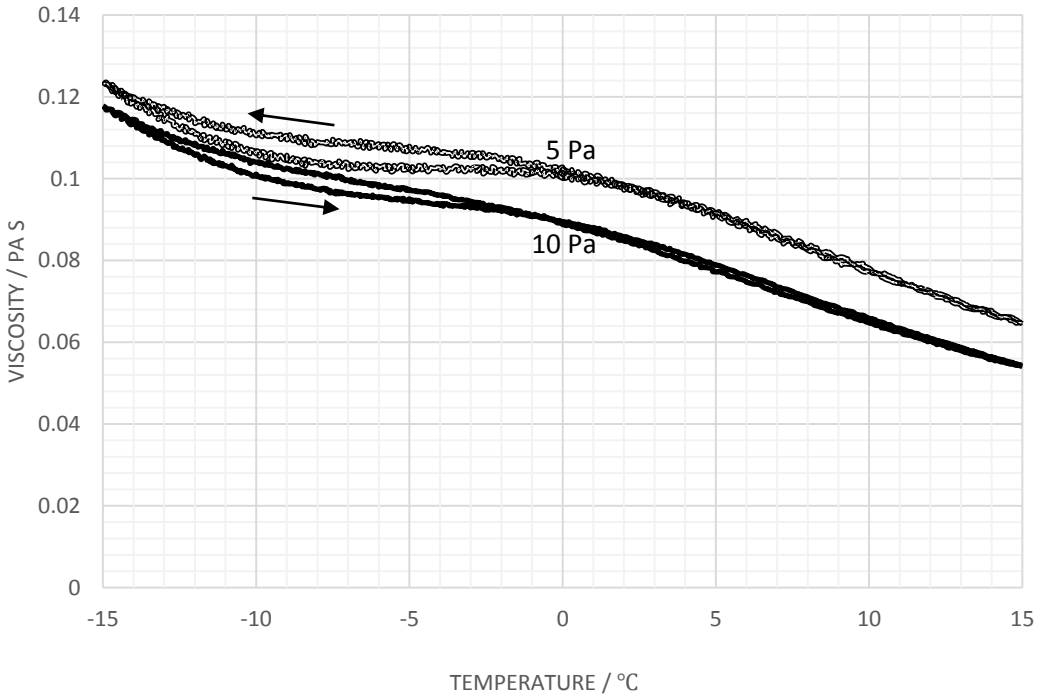

C-Fig 3 Viscosity variation with temperature plots for AP105, applied shear stresses 5 and 10 Pa.

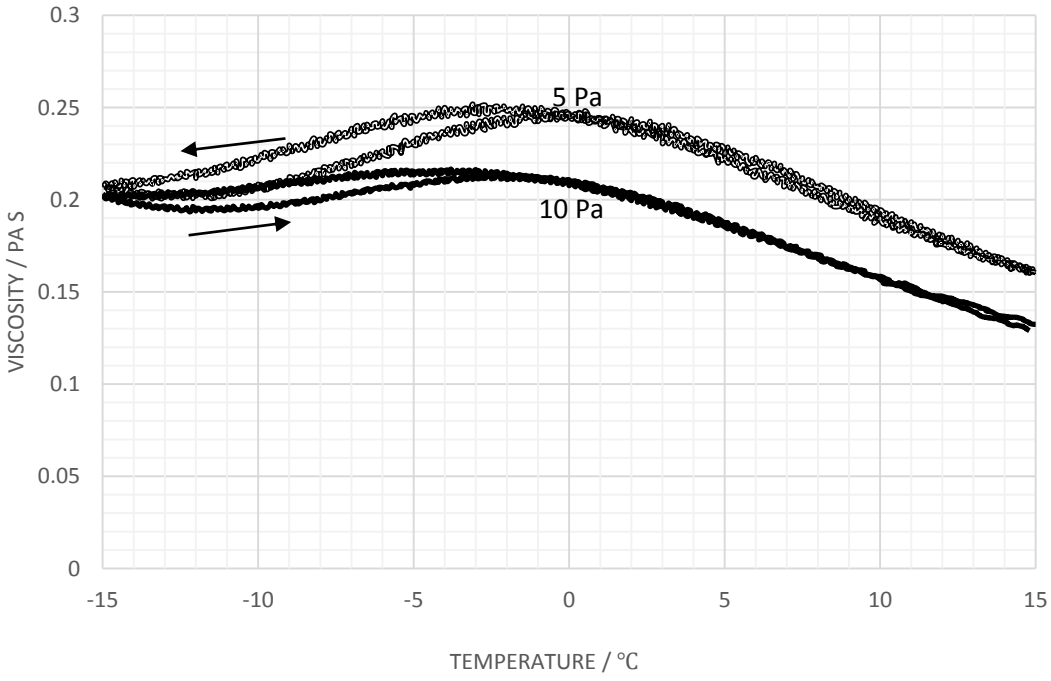

C-Fig 4 Viscosity variation with temperature plots for AP113, applied shear stresses 5 and 10 Pa.

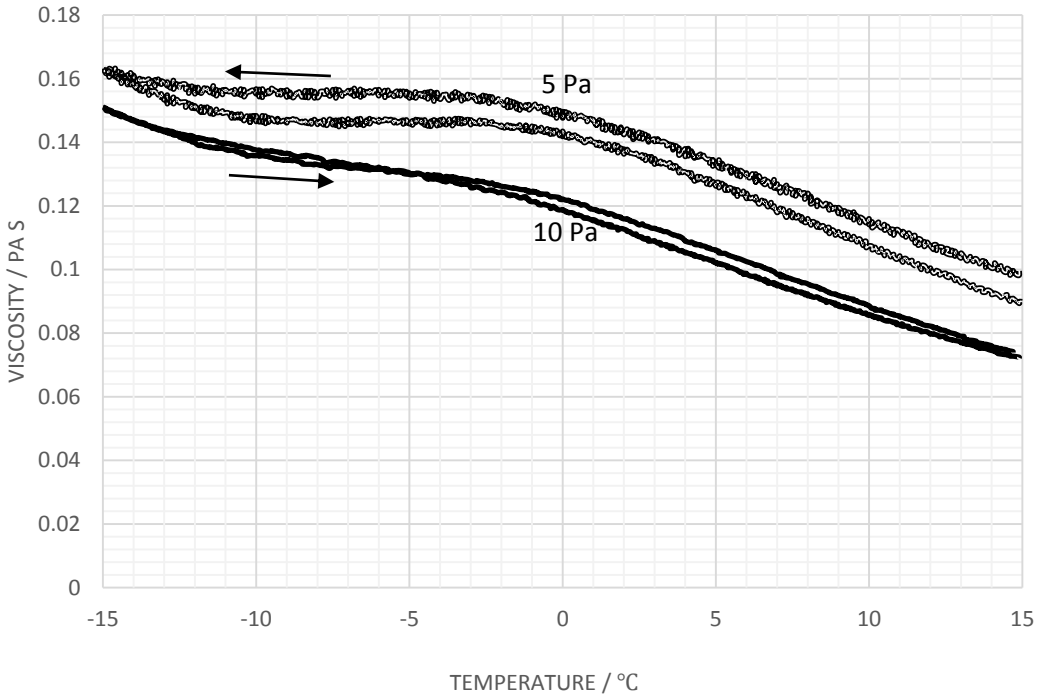

C-Fig 5 Viscosity variation with temperature plots for AP114, applied shear stresses 5 and 10 Pa.

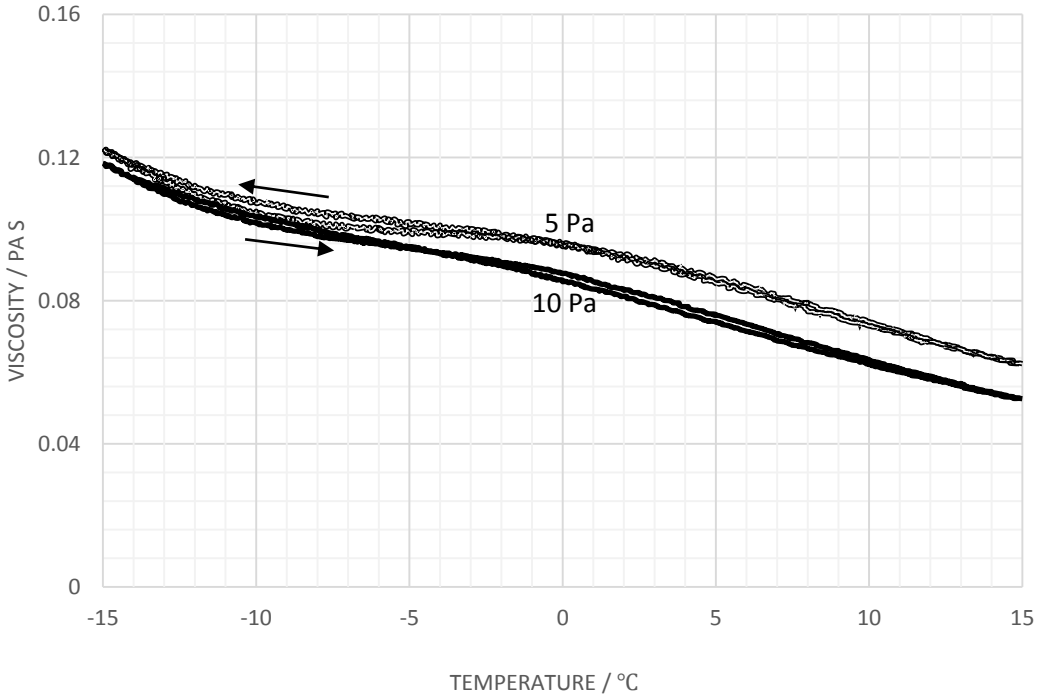

C-Fig 6 Viscosity variation with temperature plots for AP115, applied shear stresses 5 and 10 Pa.

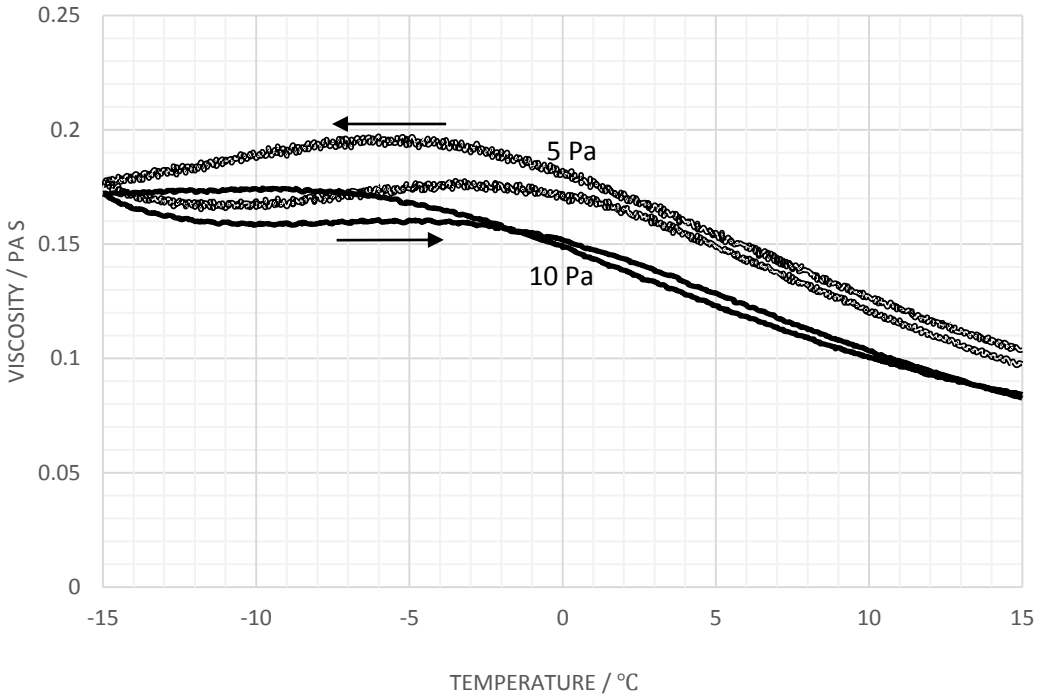

C-Fig 7 Viscosity variation with temperature plots for AP123, applied shear stresses 5 and 10 Pa.

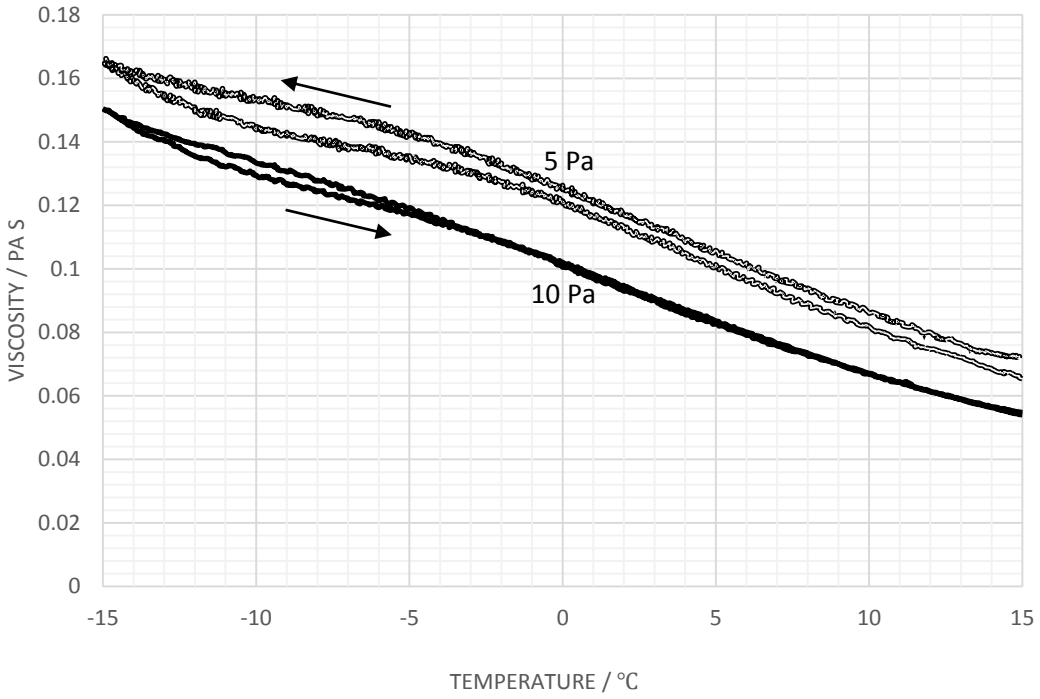

C-Fig 8 Viscosity variation with temperature plots for AP124, applied shear stresses 5 and 10 Pa.

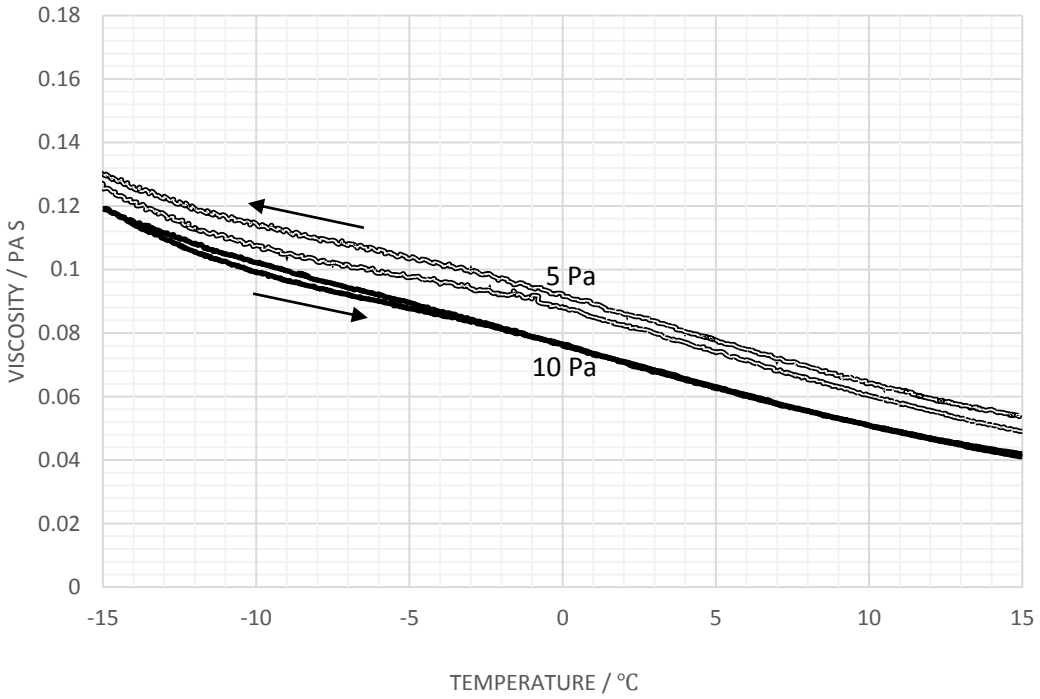

C-Fig 9 Viscosity variation with temperature plots for AP125, applied shear stresses 5 and 10 Pa.

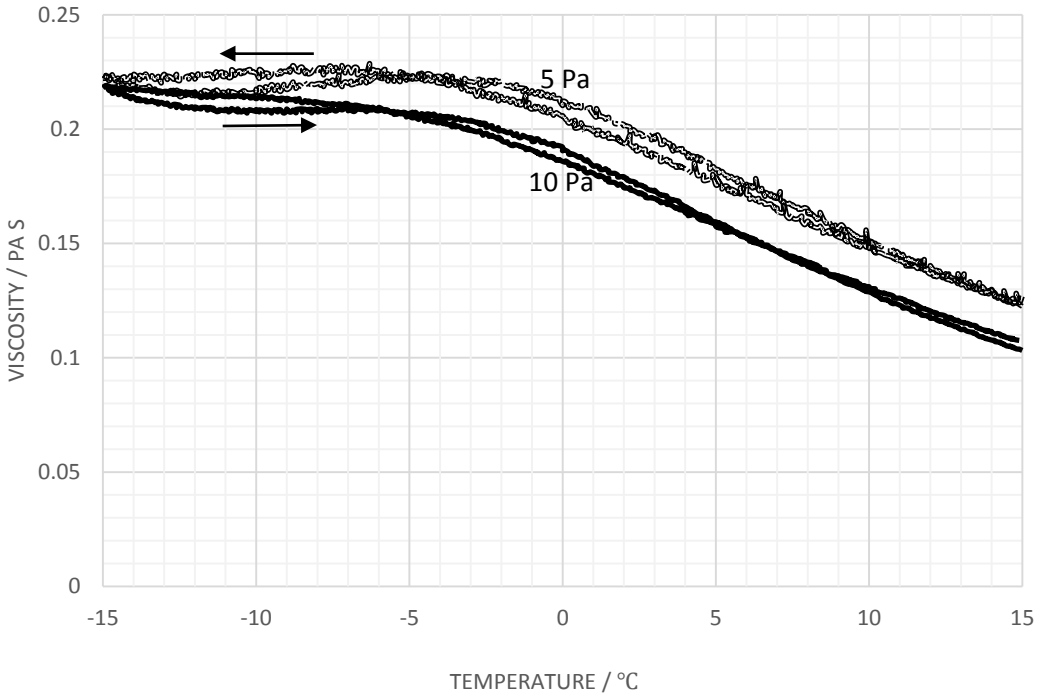

C-Fig 10 Viscosity variation with temperature plots for AP203, applied shear stresses 5 and 10 Pa.

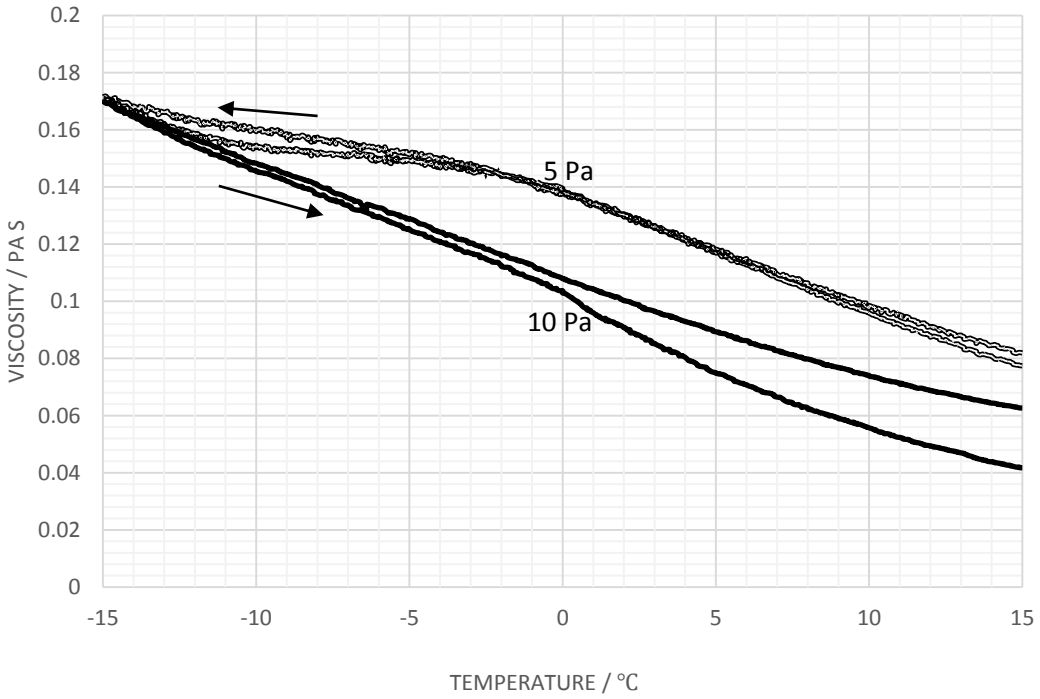

C-Fig 11 Viscosity variation with temperature plots for AP204, applied shear stresses 5 and 10 Pa.

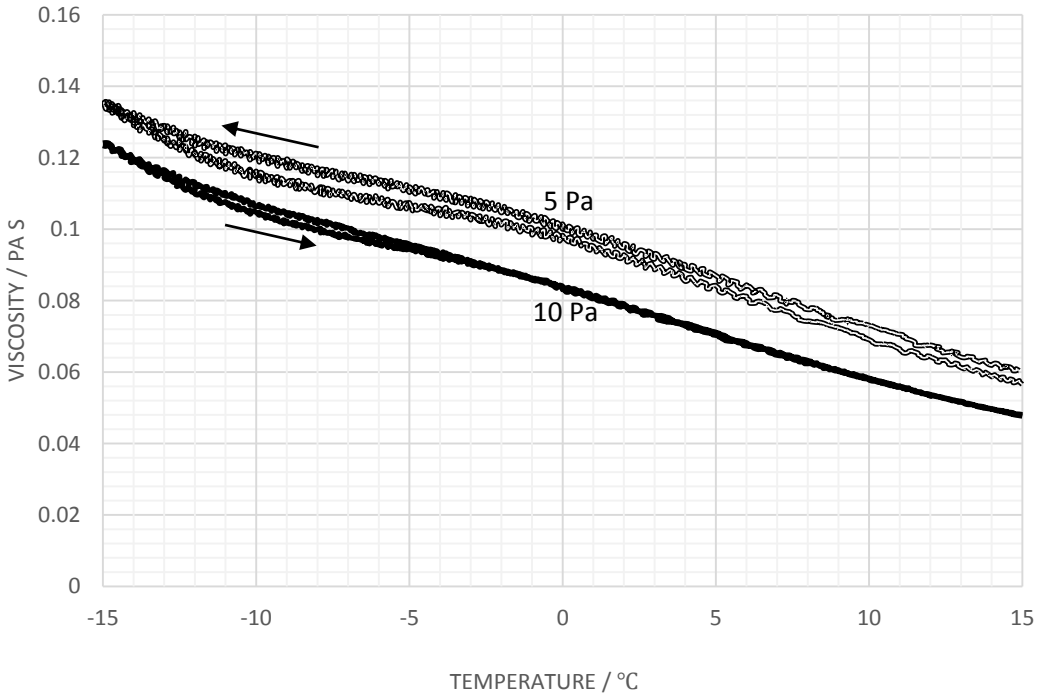

C-Fig 12 Viscosity variation with temperature plots for AP205, applied shear stresses 5 and 10 Pa.

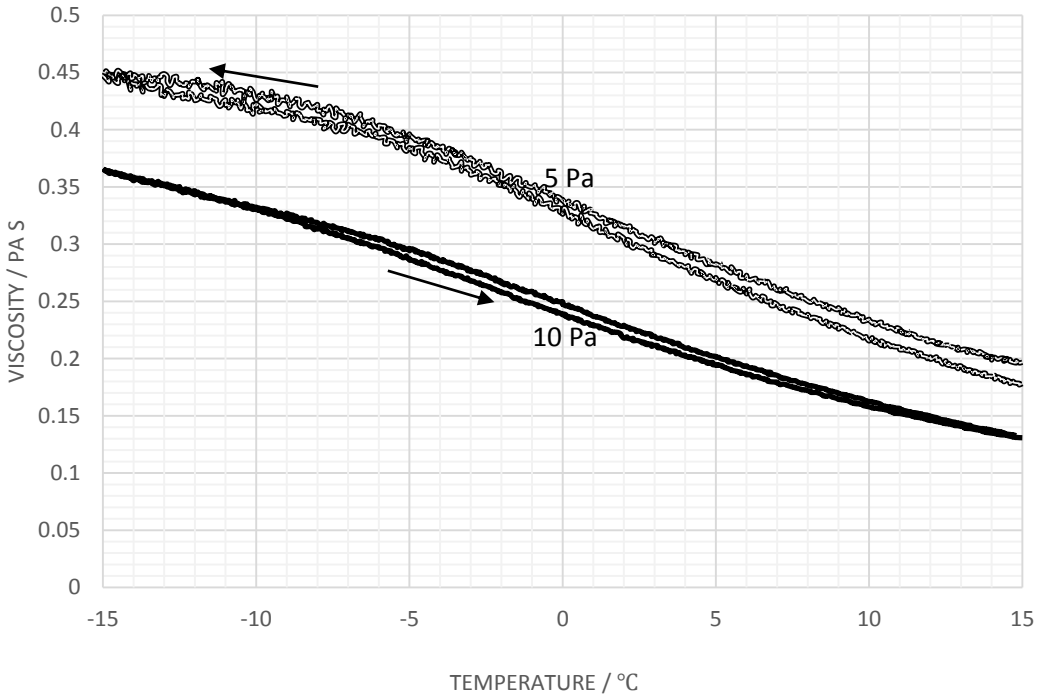

C-Fig 13 Viscosity variation with temperature plots for AP213, applied shear stresses 5 and 10 Pa.

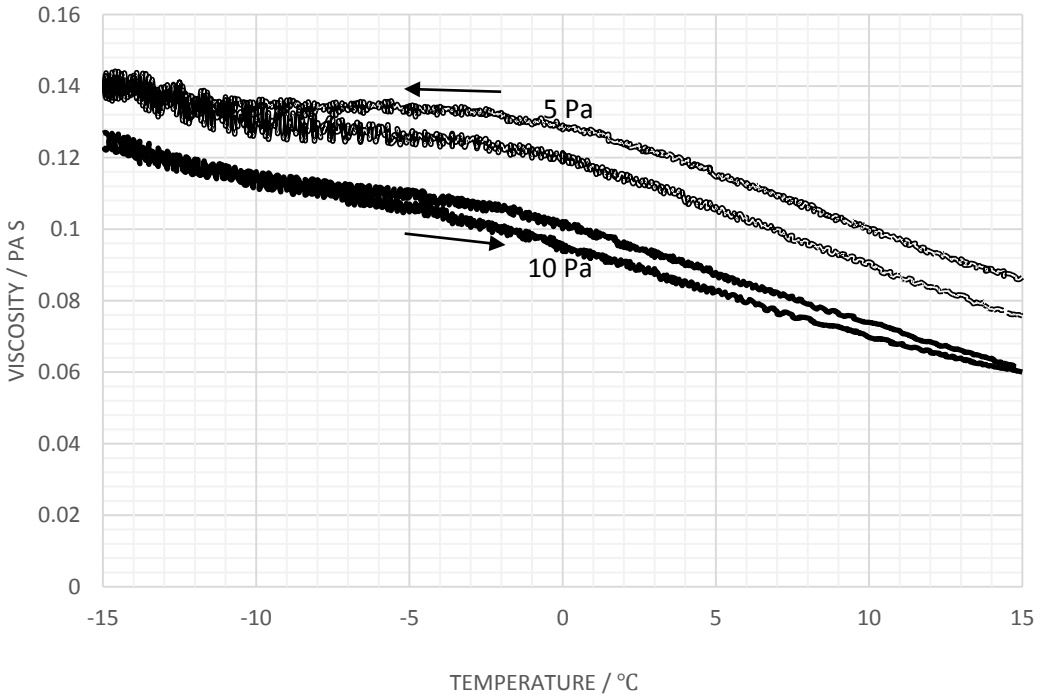

C-Fig 14 Viscosity variation with temperature plots for AP214, applied shear stresses 5 and 10 Pa.

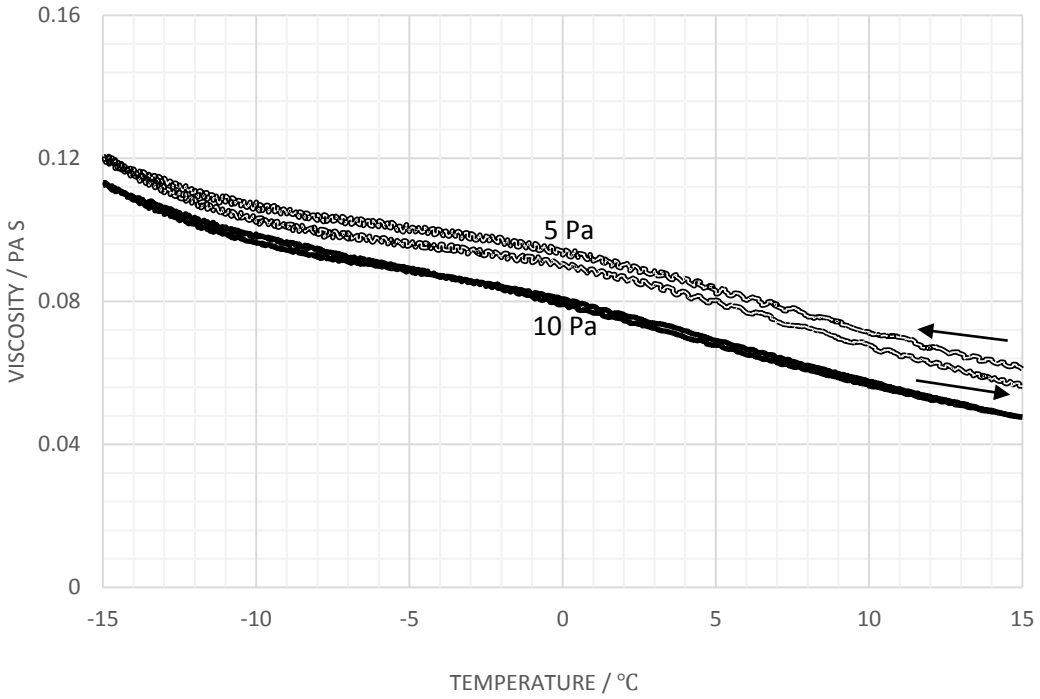

C-Fig 15 Viscosity variation with temperature plots for AP215, applied shear stresses 5 and 10 Pa.

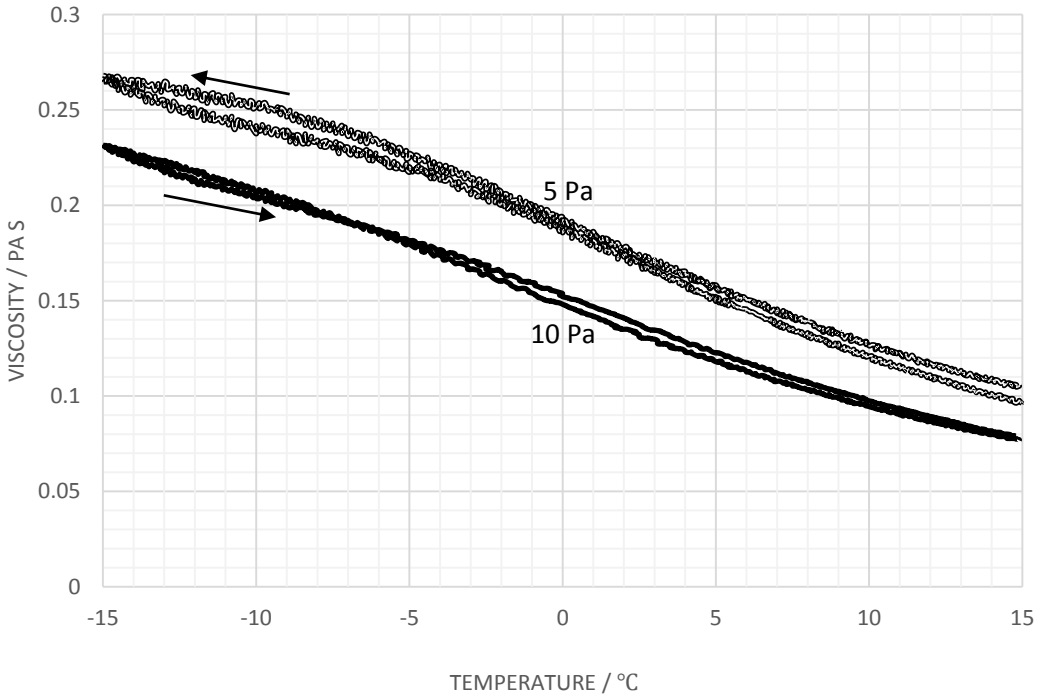

C-Fig 16 Viscosity variation with temperature plots for AP223, applied shear stresses 5 and 10 Pa.

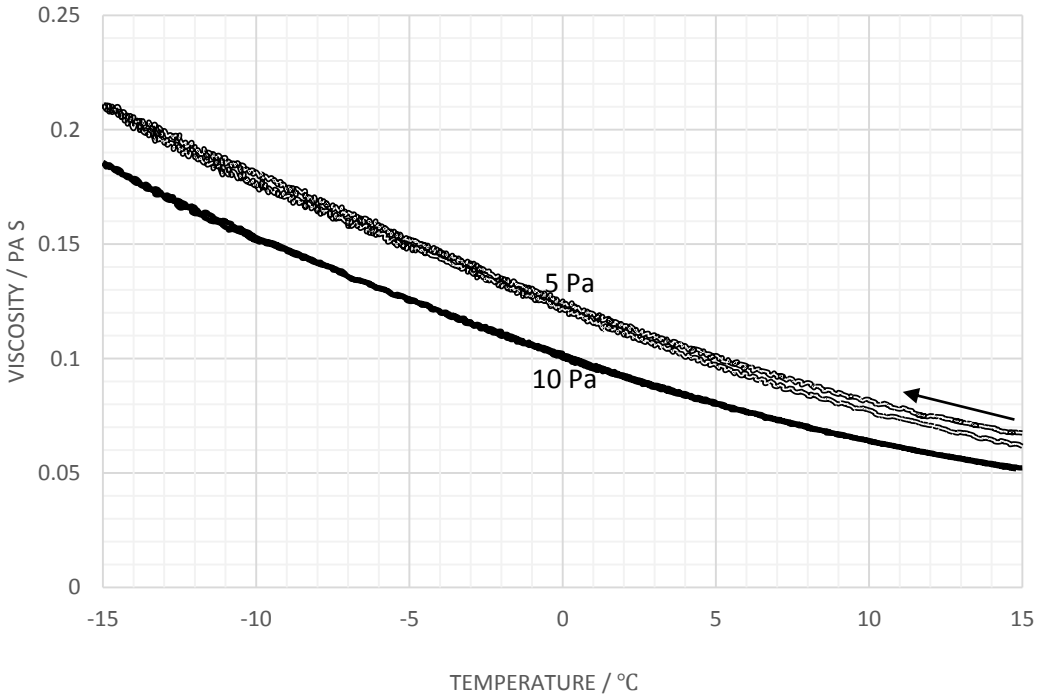

C-Fig 17 Viscosity variation with temperature plots for AP224, applied shear stresses 5 and 10 Pa.

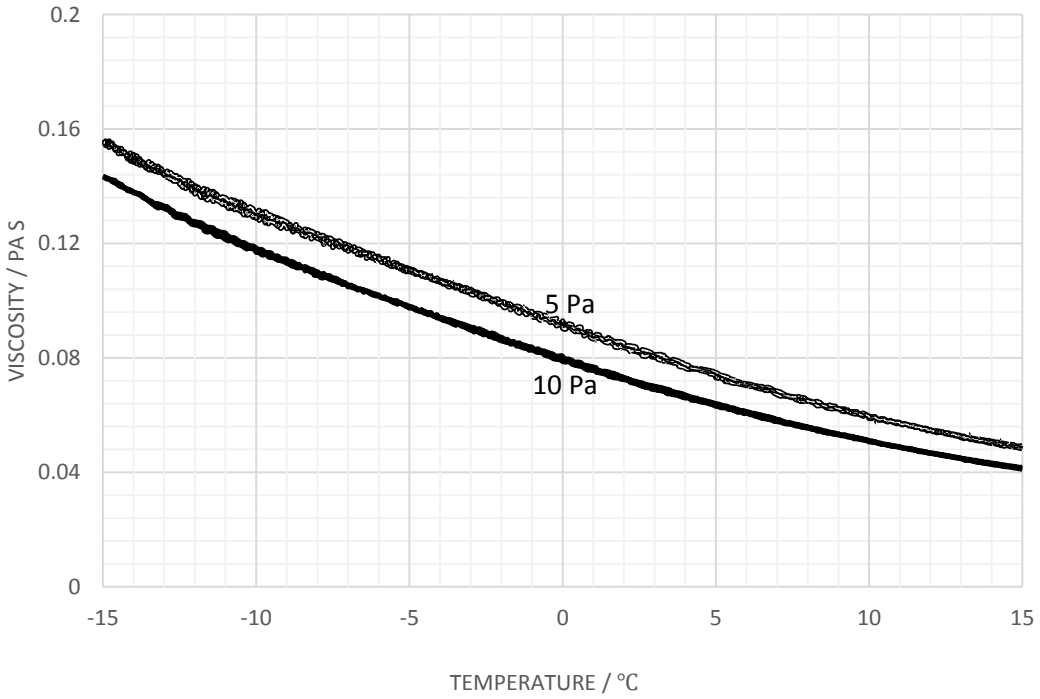

C-Fig 18 Viscosity variation with temperature plots for AP225, applied shear stresses 5 and 10 Pa.

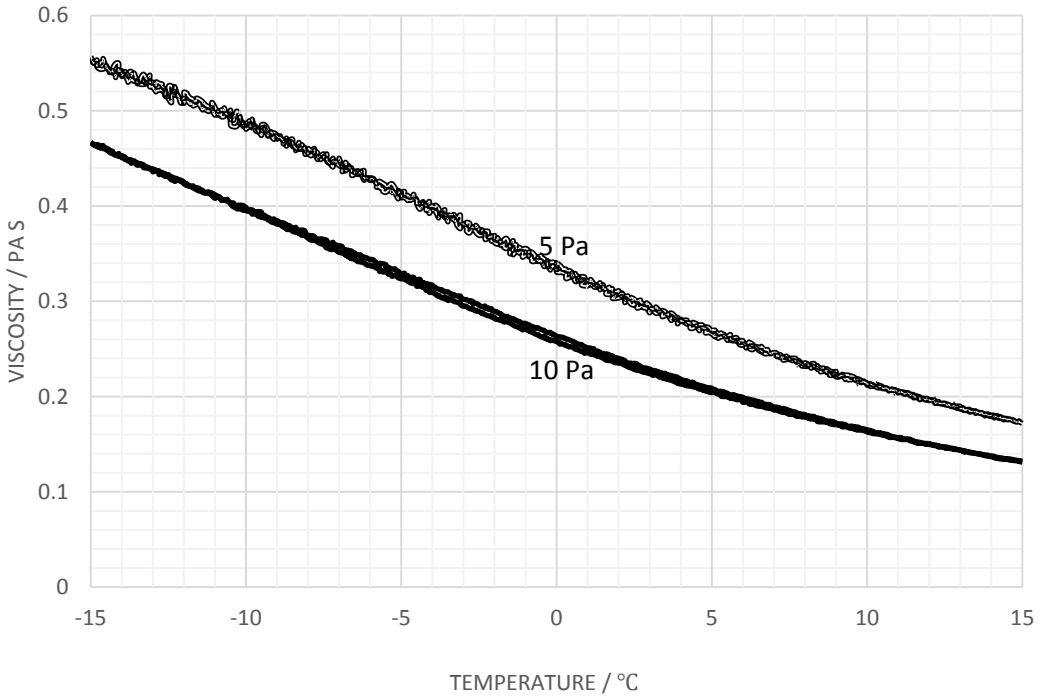

C-Fig 19 Viscosity variation with temperature plots for AP303, applied shear stresses 5 and 10 Pa.

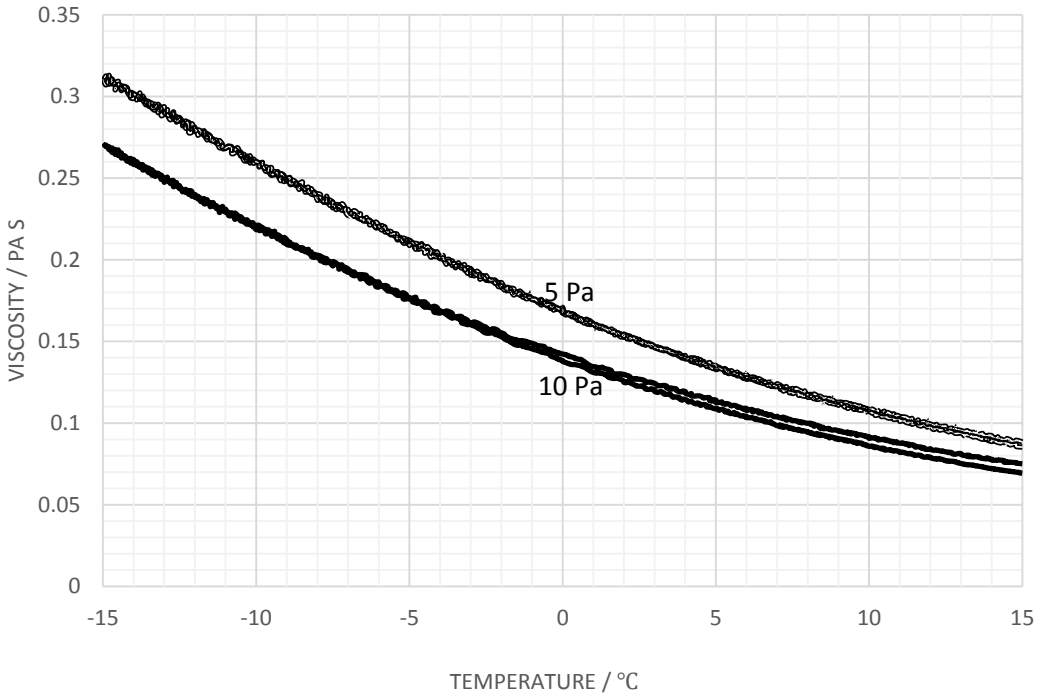

C-Fig 20 Viscosity variation with temperature plots for AP304, applied shear stresses 5 and 10 Pa.

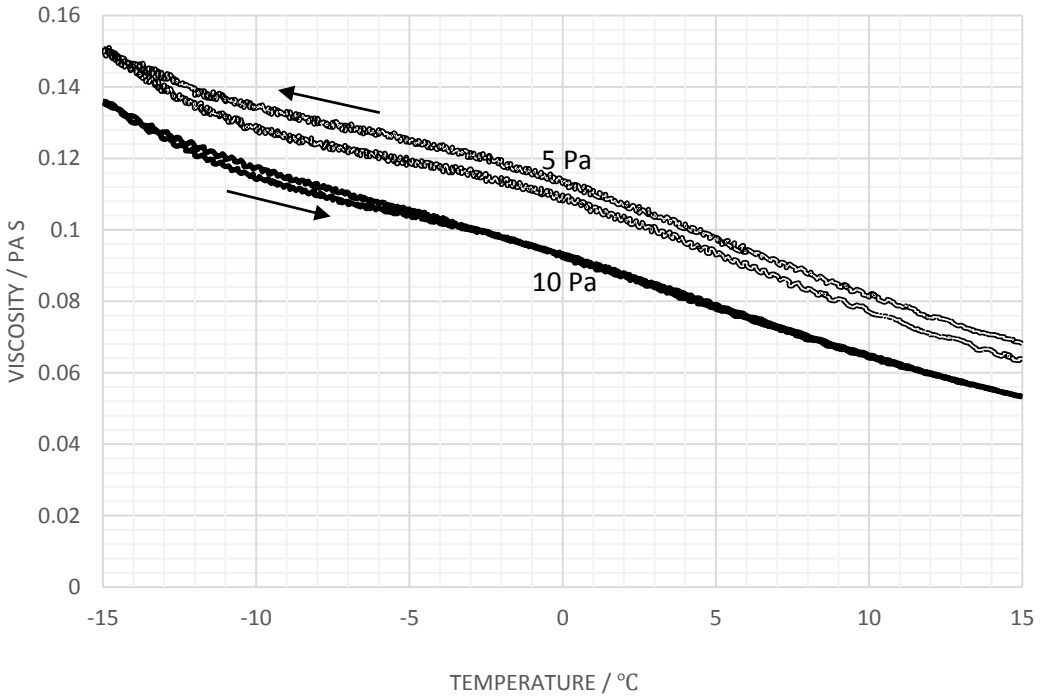

C-Fig 21 Viscosity variation with temperature plots for AP305, applied shear stresses 5 and 10 Pa.

Appendix D. Supplementary Data for Chapter 7

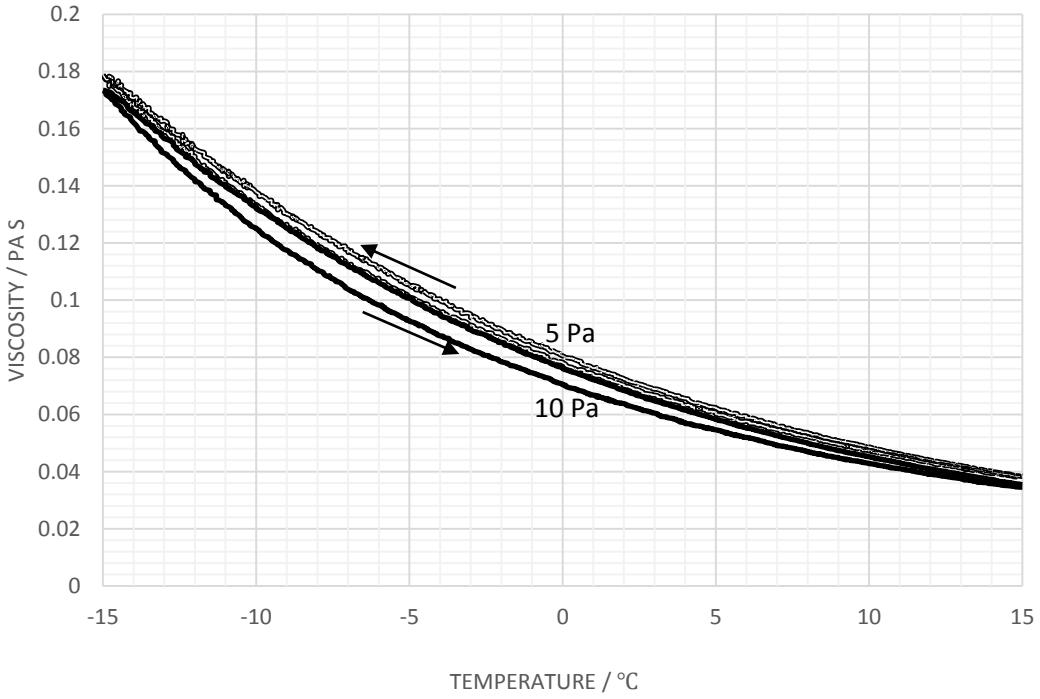

D-Fig 1 Viscosity variation with temperature plots for BP103, applied shear stresses 5 and 10 Pa.

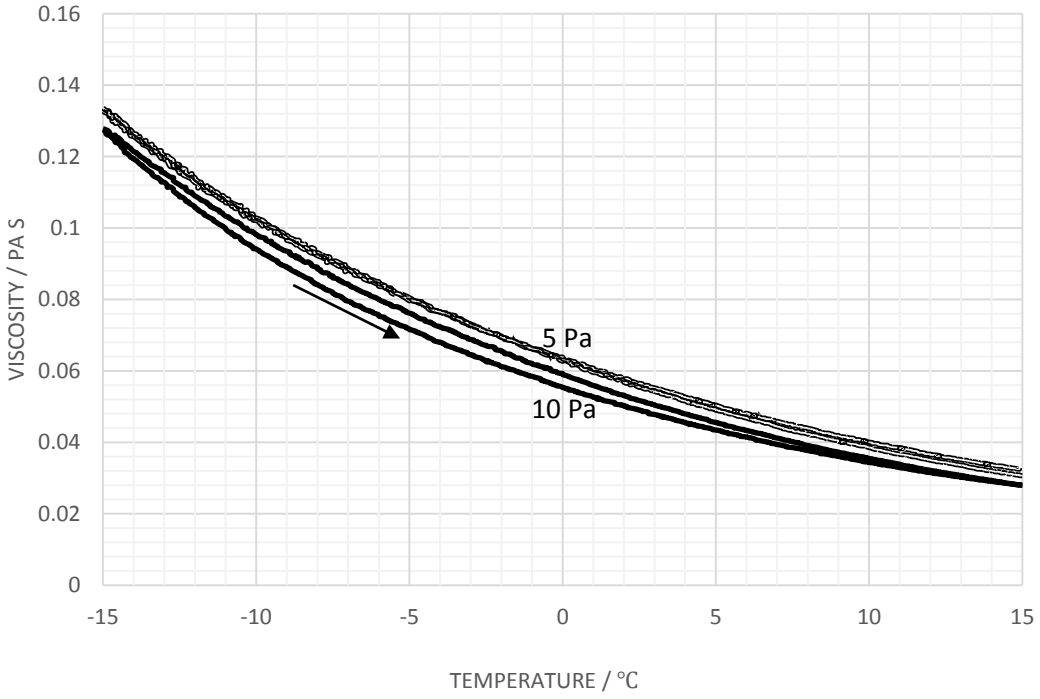

D-Fig 2 Viscosity variation with temperature plots for BP104, applied shear stresses 5 and 10 Pa.

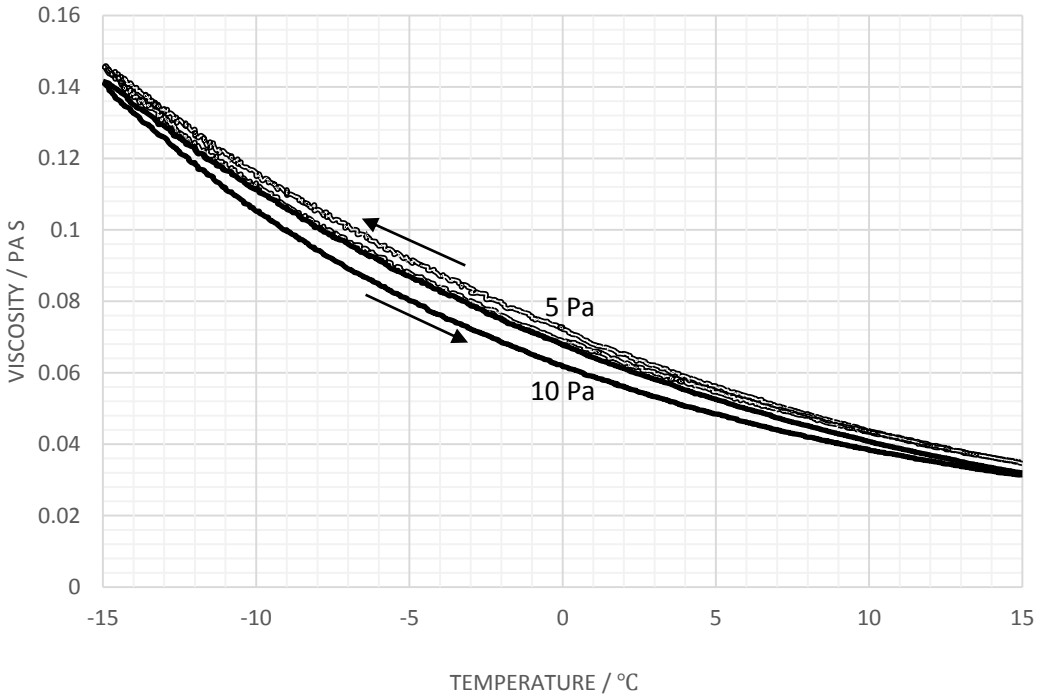

D-Fig 3 Viscosity variation with temperature plots for BP203, applied shear stresses 5 and 10 Pa.

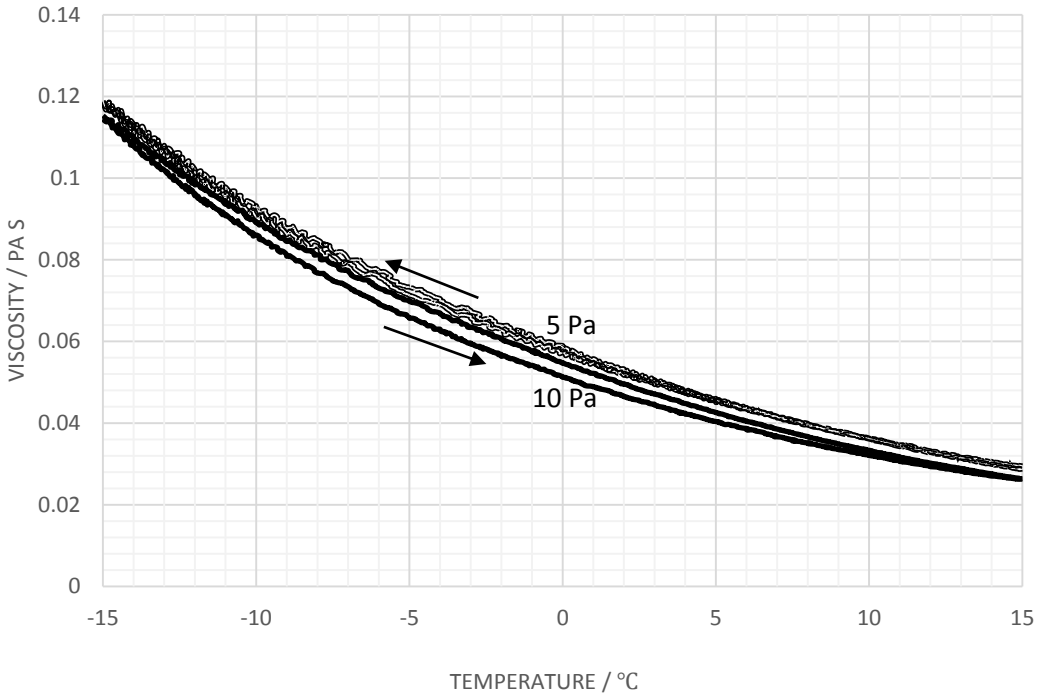

D-Fig 4 Viscosity variation with temperature plots for BP203, applied shear stresses 5 and 10 Pa.

Appendix E. Publications from the Study

1) **Rheology of Poly(acrylic acid): A Model Study**

   Yuchen Wang, Richard A. Pethrick, Nicholas E. Hudson, and Carl J. Schaschke

   Ind. Eng. Chem. Res., 2012, 51 (50), pp. 16196–16208

   Publication Date (Web): November 8, 2012 (Article)

   DOI: 10.1021/ie302313a

2) **Rheology of poly(acrylic acid) in water/glycol/salt mixtures**

   Yuchen Wang, Richard Arthur Pethrick, Nicholas E Hudson, and Carl J Schaschke

   Ind. Eng. Chem. Res., 2013, 52 (2), pp. 594–602

   Publication Date (Web): December 12, 2012 (Article)

   DOI: 10.1021/ie302765j

3) **Polyacrylic Acid-Polyvinylpyrrolidone Thickened Water-Glycol Fluids**

   Yuchen Wang, Richard A Pethrick, Nicholas E Hudson, and Carl J Schaschke

   Submitted to *Chem. Eng. Res. Des.*

   Date submitted: 12 October 2012

4) **Electrolyte Effects on Poly(acrylic acid)-Polyvinylpyrrolidone Aqueous Glycol Mixtures for Use as De-Icing Fluids**

   Yuchen Wang, Richard A Pethrick, Nicholas E Hudson, and Carl J Schaschke

   Submitted to *Ind. Eng. Chem. Res.*

   Date submitted: 9 March 2013